Microbial Hazards in Changing Coastal Environments

Nathan L R. Williams

BSc Hons

Thesis submitted for the degree of Doctor of Philosophy

27th October 2022

Ocean Microbiology Group & Climate Change Cluster

Faculty of Science, University of Technology Sydney

Sydney, Australia

Certificate of Original Authorship

I, Nathan Lloyd Robert WILLIAMS declare that this thesis is submitted in fulfilment of the requirements for the award of Doctor of Philosophy, in the Faculty of Science at the University of Technology Sydney.

This thesis is wholly my own work unless otherwise referenced or acknowledged. In addition, I certify that all information sources and literature used are indicated in the thesis.

This document has not been submitted for qualifications at any other academic institution.

This research is supported by the Australian Government Research Training Program.

Nathan L R WILLIAMS

Production Note:
Signature removed prior to publication.

Date: 25th October 2022

Student Certification

I certify that this thesis has not already been submitted for any degree and is not being submitted as part of candidature for any other degree. I also certify that the thesis has been written by me and that any help that I have received in preparing this thesis, and all sources used, have been acknowledged in the thesis.

I also consent for one copy of the thesis to be held in the UTS library.

Final word count: 63,552 (References not included)

Signature of candidate:

Production Note:
Signature removed prior to publication.

Date: 27/11/2022

Supervisor Certification

Student name: Nathan L R Williams

Student ID: [redacted]

Thesis title: *Microbial Hazards in Changing Coastal Environments*

The undersigned hereby states that the above student's thesis meets the requirements for submission and is hence ready for examination.

Principal supervisor name: Professor Justin R. Seymour

Principal supervisor's signature:

Production Note:
Signature removed prior to publication.

Date: 27 / 10/ 2022

Acknowledgments

First, I wish to acknowledge the Gadigal people of the Eora Nation upon whose ancestral lands the University of Technology is built. I would also like to pay respect to the Elders both past and present, acknowledging them as the traditional custodians of knowledge for these lands.

I wish to express my deepest thanks to my principal supervisor, Professor Justin Seymour. It has been an absolute privilege to learn from Justin, and I thank him for shaping me into the scientist that I am today. His input and expertise on project design, academic writing, and creative ideas has been invaluable. I look up to Justin as both a mentor and as a researcher. I will be forever grateful to have had him as my supervisor.

To my co-supervisor Dr. Nachshon Siboni, I express my sincere gratitude for your guidance, and all of your technical help and advice. Nachshon, your help has been invaluable, and I would not have survived in the field or have my current knowledge on qPCR and sequencing data analysis without your help and guidance. Thank you for always providing a good laugh.

A huge thank you to Dr. Anna Bramucci, and Dr. Martin Ostrowski for teaching me to code. You have both helped me so much and increased my knowledge beyond what I thought I'd ever have in this area and sparked a new interest in which I wish to pursue in science career.

To Dr. Peter Scanes, Dr. Jaimie Potts, and Dr. Colin Johnson from DPE, thank you all for your help sampling and in the field. In particular, thank you Jaimie for offering up your house on the Central Coast as a sampling base, and thank you to your mother for allowing us to process sample in her back yard, and for the many sandwiches and cuppas on hard days of fieldwork. Thank you, Jaimie, for always being available for a chat regarding data, and for all of your hard work setting up sampling in both Rose Bay and Terrigal. I also thank Dr. Meredith Campey for all of your hard work in planning the sampling at Rose Bay.

I would also like to thank everyone from the OMG lab group of whom I have not yet mentioned, including Nine Le Ruen, James O'brien, Abeeha Kahlil, and Oscar Creasy for your support and friendship. I would also like to thank Dr. JB Raina for his critical feedback on all of my talks, pushing them to the next level, and for being an inspiring scientist that I have looked up to throughout my PhD.

I would also like to thank my desk quad, Kieran Young, Amanda Grima, and Dr. Kirsty Milner for all of your moral support as I have been writing my thesis. In particular, thank you Kieran for the many walks to get treats, the parties, and for being a good friend throughout my PhD.

Thank you, Dr. William King, for all of your support throughout my career as a scientist. You were my first inspiration to do research, and I appreciate the long talks on the phone and via zoom. Even though for most of my PhD you were halfway around the world, you are still a dear friend and a great mentor.

I would like to thank my friends and family for all their help throughout my PhD. Thank you to my mum and dad, Lloyd, and Yvonne, and to my sisters, Monique and Madalyne, for supporting my decision to become a scientist, and always taking an interest in what I do in my research. You have supported me immensely throughout my degrees and put up with my many university related mood swings. Thank you, Michelle, and Graeme Stainlay, for your support, particularly during my final thesis writing days. Thank you to my good friends Lachlan Draper and Thomas O'Sullivan for good times at the pub which have kept me sane through the hard days, and to Brandon McNally and Troy Fenton, and the Cronulla crew, for the morning ritual surfs, which kept me grounded for four years. Finally, thank you Hannah Stainlay for all of your love and support throughout my PhD. I would not have been able to get through it without you.

Statement indicating the format of thesis

This thesis is being submitted in the format of *Thesis by compilation*.

List of Publications

Williams, N. L. R., Siboni, N., King, W. L., Balaraju, V., Bramucci, A., & Seymour, J. R. (2022). Latitudinal Dynamics of Vibrio along the Eastern Coastline of Australia. Water.

Williams, N.L.R., Siboni, N., Potts, J., Campey, M., Johnson, C., Rao, S., Bramucci, A., Scanes, P., Seymour, J.R. (2022). Molecular microbiological approaches reduce ambiguity about the sources of faecal pollution and identify microbial hazards within an urbanised coastal environment. Water Research.

Williams, N.L.R., Siboni, N., McLellan, S., Potts, J., Scanes, P., Johnson, C., James, M., McCann, V., Seymour, J.R. (2022) Rainfall leads to elevated levels of antibiotic resistance genes within seawater at an Australian beach, Environmental Pollution.

Williams, N.L.R., Siboni, N., Potts, J., Scanes, P., Johnson, C., James, M., McCann, Le Reun, N., King, W.L., V., Seymour, J.R., Defining the importance of natural environmental variability and anthropogenic impacts on bacterial assemblages within intermittently opened and closed lagoons. Water Research. (submitted).

Statement of contribution of authors

Research fundings:

Chapter 2 was supported by an Australian Research Council grant (DP210101610) to JRS.

Supervision:

Professor. Justin R. Seymour, UTS (C3)

Dr. Nachshon Siboni, UTS (C3)

Dr. Maurizio Labbate, UTS

Chapter 1:

NLR. Williams wrote the chapter and JR. Seymour and N. Siboni edited it.

Chapter 2:

JR. Seymour, N. Siboni. and V. Balaraju designed the study. NLR. Williams and V. Balaraju took all samples. qPCR was performed by NLR. Williams. ddPCR and *hsp60* PCR were performed by NLR. Williams. and N. Siboni A. Bramucci and NLR. Williams performed the 16S rRNA gene sequencing analysis. N.L.R.W. and WL. King performed the *hsp60* gene sequencing analysis. NLR. Williams. and JR. Seymour prepared and wrote the manuscript. All authors read and agreed to the published version of the manuscript.

Chapter 3:

NLR. Williams, N Siboni, M Campey, C Johnson, J Potts, P Scanes, JR. Seymour contributed to experimental design, NLR. Williams, N Siboni and C Johnson were responsible for sampling. NLR. Williams and N Siboni were responsible for sample processing and qPCR analysis, while NLR. Williams, N Siboni and A Bramucci, were responsible for 16S analysis. NLR. Williams, N Siboni and JR. Seymour contributed to writing the manuscript.

Chapter 4:

NLR. Williams, N. Siboni, S. McLellan, J. Potts, P. Scanes, C. Johnson, M. James, and JR. Seymour planned sampling locations and designed experiments. NLR. Williams, N. Siboni, and C. Johnson collected and processed samples. NLR. Williams performed qPCR, 16S analysis, MIC tools analysis and designed all figures. NLR. Williams analysed data and wrote the manuscript, and all authors contributed to editing it.

Chapter 5:

NLR. Williams, N. Siboni, S. McLellan, J. Potts, P. Scanes, C. Johnson, M. James, and JR. Seymour planned sampling locations and designed experiments. NLR. Williams, N. Siboni, W. King, N. Le Reun, and C. Johnson took and processed samples. NLR. Williams performed qPCR, 16S analysis, MIC tools analysis and designed all figures. NLR. Williams analysed data and wrote the manuscript, and all authors contributed to editing it.

Chapter 6:

NLR. Williams wrote the chapter and JR. Seymour and N. Siboni edited it.

Table of Contents

List of Tables and Figures

Appendix 1 - Latitudinal dynamics of Vibrio spp. along the Australian East Coast

Appendix 2 - Molecular microbiological approaches reduce ambiguity about the sources of faecal pollution and identify microbial hazards within an urbanised coastal environment

Appendix 3 – Rainfall leads to elevated levels of Antibiotic Resistance Genes within seawater at an Australian beach

Appendix 4 – Defining the importance of natural environmental variability and anthropogenic impacts on bacterial assemblages within intermittently opened and closed lagoons

Table 1. Site latitude and longitude.

Table 2. Primers used in study.

Figure 1. Alpha and Beta diversity of bacterial communities within each ICOLL.

Figure 2. Stacked bar graph of the relative abundance of the top 20 indicator taxa at the family level.

Figure 3. Heatmaps showing the levels of the antibiotic resistance genes.

Thesis Abstract

Coastal environments deliver many crucial ecosystem services, such as maintenance of biodiversity, and are used widely for recreation by human populations. While microbial communities within these environments underpin ecosystem services, they often incorporate pathogenic microbes (e.g., *Vibrio* species) that can proliferate under beneficial environmental conditions. Furthermore, pathogens and antimicrobial resistant bacteria (ARB), enter coastal environments via sewage contamination or animal faeces. Many processes which underpin the dynamics of endemic microbial hazards and anthropogenically introduced microbial hazards are not well defined, which hinders remediation efforts. Therefore, I aimed to increase our understanding of these processes. In Chapter 1, I introduce coastal environments, their microbial ecology, and their associated microbial hazards. In Chapter 2, I analysed the latitudinal dynamics of *Vibrio* along the eastern coast of Australia, where I defined their patterns in the abundance and diversity to reveal new insights into the distribution of potential human pathogens within a region experiencing significant ecological shifts due to climate change, along a latitudinal gradient which, in many locations have had no assessment of *Vibrio* ecology. In Chapter 3, I used Microbial Source Tracking (MST) to specify sources of faecal pollution and their impact on an urban beach, which helped to identify remediation targets. In this chapter, I applied the Bayesian statistical package *Source Tracker* to both track the spatiotemporal dynamics of specific bacterial signatures for individual stormwater drains and to quantify the relative strength of the microbial signature from different stormwater drains. To the best of my knowledge, this is the first time *Source Tracker* has been applied in this way. In Chapter 4, I investigated how rainfall leads to elevated levels of AmR bacteria at a recreationally used coastal beach. To do this, I applied the *indicspecies* statistical R package to 16S amplicon data and ran a correlation analysis between the bacteria which were indicators of sewage, with both faecal markers, and ARB. This is the first time this type of analysis has been applied in this context and it revealed strong positive correlations between faecal contamination, bacteria from storm water drains, ARB, and potential human pathogens. In this chapter In Chapter 5, I aimed to define the relative importance of natural environmental perturbations and anthropogenic impacts on bacterial assemblages within intermittently opened and closed lagoons (ICOLLs). This is the first study to provide a detailed spatial and temporal analysis of the microbial communities within ICOLL environments. In this study, I observed that sewage was a principal driver of shifts in the microbiology of ICOLLs exposed to stormwater, while natural seasonal shifts in the physio-chemical parameters controlled

microbial communities at other times. Finally in Chapter 6, I synthesise the results and conclusions of this thesis. Overall, the findings of this project have brought a new understanding to how microbial hazards can proliferate in, and enter, coastal environments. This project has also informed the water quality strategies of government agencies, and in some cases highlighted significant health risks to recreational users of coastal environments.

Chapter 1 - General Introduction

Microbial Threats in Changing Coastal Environments

1.1 - The Importance and State of Australia's Coastal Environments

Coastal environments consist of a variety of crucial ecosystems, which are important for mediating many biogeochemical processes (Testa et al., 2013), supporting biodiversity (Danovaro and Pusceddu, 2007), and primary productivity (Wang et al., 1997), which all influence the health and function of marine environments (Alongi, 1998). Whilst these habitats account for a small portion (7 %) of all oceanic environments, they have a disproportionate influence on oceanic function, whereby they are responsible for 90 % of nutrient decomposition and transformation in sediments, 80 % of organic matter burial, and 19 % of primary production (Alongi and McKinnon, 2005; Azam, 1998; Teeling et al., 2012). These environments also consist of an assortment of habitats including coral reefs (Polak and Shashar, 2013), seagrasses (de Troch et al., 2008), mangroves (Carugati et al., 2018), intermittently opened and closed lagoons (Jones et al., 2018), salt marshes (Lefeuvre et al., 2003), and sand beaches (Dugan and Hubbard, 2010), which all foster biodiversity, the key to ecosystem function. However, while these coastal environments are clearly crucial to marine ecosystem function, they also provide numerous ecosystem services which are valuable to society.

Coastal environments provide substantial societal benefit. Australia's population, in particular, heavily relies on its coasts, with more than 85% of the population living within 50 km of the coast (Clark and Johnston, 2017). Coastal environments foster social and cultural wellbeing (Lau et al., 2019). These environments are sentimental to many people including those who use these them for recreational activities including surfing (Blum and Orbach, 2021; Evers, 2009), as well as those who are tied to the land culturally and spiritually, such as Indigenous Australians (Thurstan et al., 2018). In addition to cultural wellbeing, coastal environments also provide food security (Sala et al., 2021).

Coastal environments in Australia support a substantial fisheries and aquaculture industry, which in turn delivers a significant food supply. The global consumption of seafood per person globally has increased from 9 kg per person in 1961 to 20 kg per person in 2017 (FAO, 2018) and, in Australia, the aquaculture industry is worth over $3.5 billion each year (Mobsby and Curtotti, 2018). While Australia's fishery exports account for less than 1 % of the global demands, Australia supplies the most southern bluefin tuna to Japan, and is also the leading supplier of live lobster and abalone products to Hong Kong, China, and Vietnam (ABARES, 2018).

Australia's coastal environments are also heavily used for recreation and tourism, which are some of the nation's largest sources of income, worth over $60.8 billion GDP in 2019 (TourismAustralia, 2019). Coastal environments in Australia are used for activities such as surfing at national surf reserves, and for snorkelling and diving at locations such as the Great Barrier Reef. These industries alone are worth $130 billion (O'Brien and Eddie, 2013) and $3.6 billion (Deloitte, 2016) respectively. Aquatic and coastal tourism contributed $38.2 billion AUD in 2016 (TourismAustralia, 2019), with Sydney's beaches contributing over $1.6 billion (Deloitte, 2016).

It is clear that coastal environments are invaluable resources which are important to the environment, the economy, and society; however, the value of coastal ecosystems is currently under threat. The world's coastal environments are currently threatened by a number of anthropogenic influenced factors such as urban development, waste dumping, shipping, and port operations (Kennish, 2002). Furthermore, there is strong evidence that climate change, driven by human carbon emissions, is having among the most severe negative impacts on these environments (Halpern et al., 2008). One example of a negative impact caused by climate change is a dramatic increase in sea surface temperature (SST) (Lima and Wethey, 2012). SST has risen 0.88 °C in the period between 1901 – 2022 and is predicted to rise a further 2.01 – 4.07 °C by 2100 (Cooley et al., 2022). In addition to rising SST, the frequency and intensity of marine heatwaves (MHWs) are increasing (Frolicher et al., 2018; Oliver et al., 2018). MWHs are periods of extremely high SST, relative to the average seasonal temperature. This high SST can last for periods of days to months (Hobday et al., 2016) and can span thousands of kilometres (Lima and Wethey, 2012). MHWs have had a dramatic impact on economies and society (Mills et al., 2013) whereby they have been responsible for extreme mortality events of commercially important fish species (Caputi et al., 2016), inducing toxic algal blooms (Cavole et al., 2016), and coral bleaching (Hughes et al., 2017). While it's clear that climate change is impacting SST and in turn many coastal environments and their ecosystems, climate change is also increasing the intensity and frequency of heavy rainfall events (Madakumbura et al., 2021).

Heavy rainfall events have a significant impact on coastal environments because they amplify levels of anthropogenic runoff. Harmful runoff can originate from multiple sources such as industry, agriculture, urban areas, construction, mining, septic systems, landfills, and sewage overflows (Kennish, 2002). These runoff sources can transport pollutants, including heightened levels of nutrients (Balls et al., 1995) and toxic chemicals such as petroleum

hydrocarbons, polycyclic aromatic hydrocarbons, sewage (McLellan et al., 2015), and heavy metals (Kennish, 2002; Turner, 2000) into coastal environments. Increases in nutrients can cause eutrophication of aquatic environments (Dederen, 1990), while inputs of toxic chemicals can be lethal to biotic organisms, degrading both biodiversity and coastal ecosystem health (Kennish, 2017). Contamination of aquatic environments by sewage can not only introduce nutrients and harmful chemicals (McLellan et al., 2015), but also import multiple microorganisms into the environment, many of which are human pathogens (McLellan et al., 2015). Recently, in NSW Australia, water pollution has been highlighted as a major threat to coastal environments (Craik and Grafton, 2018), with input from community-based surveys highlighting coastal water quality to be of very high importance to the community.

1.2 - Microbiology of coastal environments

The majority of microorganisms in coastal environments play important beneficial roles in maintaining coastal ecosystems (Coelho et al., 2013). Marine environments harbour the largest biome on earth, which consists of viruses, phytoplankton, archaea, and bacteria, which together account for the 10^{29} microbial cells in these environments (Curtis et al., 2002). Microbes play pivotal roles in coastal ecosystems, whereby they are responsible for a large amount of metabolic activity (Curtis and Sloan, 2004), are the foundation of aquatic food webs (Kirchman and Gasol, 2018), and underpin nutrient recycling and re-mineralisation (Anderson and Ducklow, 2001). Marine microbes are also crucial to ecosystem productivity (Kirchman and Gasol, 2018), whereby they contribute up to 50 % of Earth's photosynthesis (Sarmiento and Gruber, 2007) and are key to the decomposition of organic matter (Arnosti, 2011). All of these processes are crucial to coastal ecosystem function.

The spatiotemporal and diversity patterns of microbial assemblages are governed by a suite of both anthropogenic and natural determinants. These determinants include seasonal and shorter-term shifts in water temperature, salinity, pH, dissolved oxygen, nutrients, and the availability of organic matter (Fuhrman et al., 2006; Gilbert et al., 2012; Hu et al., 2014; Staley et al., 2015) and interactions with other organisms (Steele et al., 2011). However, given that coastal environments are at the terrestrial and aquatic interface, they are often subject to urban terrestrial runoff. This can often introduce microbes from various sources, which include urban surfaces such as roads, roofs, and parks (Herve et al., 2018), stormwater infrastructure (McLellan et al., 2015) or sewage outfalls and overflows (Feng and McLellan, 2019; Williams

et al., 2022a). While in some cases severe fluctuations in natural environmental factors can cause spikes in the abundance of microbes that are human pathogens such as *Vibrio* bacteria (Semenza et al., 2017), in other cases microbes entering via sewage outfalls and overflows within stormwater infrastructure can also be human pathogens (Carney et al., 2020; Williams et al., 2022a; Williams et al., 2022b), both of which indicate serious microbial hazards within coastal environments.

1.3 - Microbiological Threats in Coastal Habitats from Endemic Organisms

Some microbes that naturally occur in coastal environments can be hazardous to humans and other biota. Harmful algal blooms (HABs) pose a significant health threat (Anderson et al., 2012), with the micro-algae *Karenia brevis* (Ryan and Campbell, 2016), *Alexandrium fundyense* (Sehein et al., 2016), and *Prorocentrum donghaiense* (Yan et al., 2022), being a few examples of micro-algae that are responsible for HABs. These dinoflagellates are responsible for 'red tides' that have been responsible for over $81 million in losses to tourism and human health, and over $39 million in losses to aquaculture in China alone (Yan et al., 2022).

Cyanobacteria blooms can also sometimes be a significant health threat. *Cyanobacteria* can form destructive blooms in all aquatic environments (O'Neil et al., 2012). Species including *Microcystis*, *Anabaena*, and *Cylindrospermopsis* within freshwater environments, *Nodularia*, *Aphanizomenon* within estuarine environments, and *Lyngbya*, *Synechococcus*, and *Trichodesmium* within marine environments all excrete toxins which can cause a variety of human health issues, including liver disease, and skin irritations (Chorus and Welker, 2021; Codd et al., 2022; Codd et al., 2005; Humpage, 2008; Klisch and Häder, 2008; Li et al., 2001; Smith et al., 2011). These organisms generally occur in low abundances, but environmental perturbations can cause them to become dominant members of the microbial community (SjÖStedt et al., 2012).

Cyanobacteria blooms can occur as a result of high levels of inorganic nutrients entering the environment, or an increase in water temperature (Paerl et al., 2016; Paerl et al., 2011). These blooms can dramatically change the physio-chemical state the environment and lead to the release of toxins, which are harmful to both humans and marine organisms (Gobler et al., 2017). Algal blooms can also provide resources to other harmful microbes, including heterotrophic bacteria, such as members of the *Vibrio* genus.

The *Vibrio* genus of bacteria contains a variety of known pathogens of humans and marine organisms. The most notable *Vibrio* human pathogens are *V. cholerae*, *V. parahaemolyticus* and *V. vulnificus* (Baker-Austin et al., 2018), with infections from these species causing $30 million in losses to the US economy each year (Ralston et al., 2011). *V. cholerae* causes the gastrointestinal disease cholera (Howardjones, 1984). Worldwide, more than 3 million people contract cholera yearly (WHO, 2016), with ~100,000 of these cases fatal (WHO, 2016). *V. parahaemolyticus* is mostly contracted via consumption of undercooked or raw seafood (Baker-Austin et al., 2017), with a reported 30,000 cases of *V. parahaemolyticus* in the USA during 2011 (Scallan et al., 2011). *V. vulnificus* infections, which can also be contracted from contaminated seafood consumption, can also be contracted from exposure of wounds to seawater, resulting in wound infections and secondary septicaemia (Baker-Austin et al., 2018). *V. vulnificus* infections are particularly concerning as they have a mortality rate greater than 50 % (Rippey, 1994). The *Vibrio* genus also includes species that are pathogens of marine organisms, such as *V. coralliilyticus* , which is an infectious coral pathogen that causes lysis of the coral tissue (Ben-Haim and Rosenberg, 2002), and *V. harveyi* which causes disease in oysters, fish, and shrimp (Defoirdt and Sorgeloos, 2012; Green et al., 2019b). These bacteria are ubiquitous in the environment, and generally exist at low levels, however, changes to environmental factors can result in spikes in their abundances, resulting in a heightened human health risk.

While the abundance patterns of *Vibrio* bacteria can be governed by the aforementioned algal blooms (Asplund et al., 2011), they are often governed by perturbations in the physio-chemical properties of their habitat. Increases in nutrients such as phosphate have been recorded to influence increases in *Vibrio* abundance (Eiler et al., 2006) and in contrast increases in levels of nitrogen have been recorded to decrease *Vibrio* abundance (Blackwell and Oliver, 2008). *Vibrio* abundances have also been recorded to correlate with levels of dissolved oxygen and pH (Blackwell and Oliver, 2008). However, the strongest recorded determinants of *Vibrio* abundance, are salinity, temperature, and chlorophyll (Eiler et al., 2006; Froelich et al., 2013; Heidelberg et al., 2002; Nigro et al., 2011; Oberbeckmann et al., 2012; Turner et al., 2009; Wetz et al., 2008), with a combination of moderate salinity levels and elevated temperatures often leading to increased *Vibrio* abundances (Oberbeckmann et al., 2012; Takemura et al., 2014). The environmental determinants and optimum conditions vary across *Vibrio* species (Takemura et al., 2014). For instance, *V. cholerae*, *V. vulnificus*, and *V. parahaemolyticus* are

generally more abundant within warm waters where the temperature exceeds 20 °C and salinity is below 10 ppt (Takemura et al., 2014).

Currently, the warming ocean has been linked an increase in *Vibrio* populations and infections in various parts of the world including Spain, the Baltic Sea, Israel, the USA, Chile, and Peru (Baker-Austin et al., 2010; Baker-Austin et al., 2012; CDC, 1998; González-Escalona et al., 2005; Martinez-Urtaza et al., 2008; Paz et al., 2007). In Australia, high levels of *Vibrio* bacteria have been reported in Sydney Harbour (Siboni et al., 2016), as well as in the tropical north at Darwin (Padovan et al., 2021), raising the possibility that *Vibrio* bacteria may be dangerously abundant at many more sites along Australia's eastern coast, where they largely remain uncharacterised. Climate change is driving extreme weather events on a global scale, and particularly concerning for coastal environments are climate change induced marine heatwaves (Doney et al., 2012) that increase SST, and heavy rain events (Madakumbura et al., 2021) that reduce salinity. These changing environmental conditions have the potential to create a "perfect storm" scenario for increases in the abundance and impact of coastal marine pathogens.

1.4 - Microbiological Threats in Coastal Habitats from Anthropogenic pollution

While some microbiological hazards in coastal environments are related to endemic marine species, others can also be introduced to the environment via urban runoff (Olds et al., 2018; Wen et al., 2017; Yang and Toor, 2018) (Figure 1, A). Heavy rain events wash microbes from urban surfaces, such as exposed buildings and roads, and from plants, soils, and animals within the natural environment (McLellan et al., 2015). Often, this results in faeces from domestic animals such as dogs, and wildlife such as birds entering the environment, however in some cases, sewage can also enter the environment through stormwater pipes (Sauer et al., 2011; Sercu et al., 2009)

Often, stormwater pipes which drain into coastal environments, are contiguous to sewage infrastructure. When sewage infrastructure is blocked, cracked via intrusions such as tree roots, or there is a heavy rain event, sewage can enter the stormwater pipes, resulting in raw sewage entering coastal environments (Olds et al., 2018). Sewage entering coastal environments is a major public health concern as it is enriched in pathogens, including protistan parasites such as *Giardia duodenalis* and *Cryptosporidium* (Efstratiou et al., 2017), bacteria such as *Escherichia coli* (Anastasi et al., 2012) and *Arcobacter* species, including *A. butzleri*

and *A. defluvii* (Fisher et al., 2014), and viruses such as *Rotavirus, Norovirus* and *Adenovirus* (Strubbia et al., 2019). These pathogens all have a significant impact on society, with the global economic impact of human illness linked to faecal contamination of coastal waters estimated to exceed $12 billion a year, with over 50 million gastrointestinal illnesses linked to coastal recreation annually (Shuval, 2003).

In addition to pathogens, sewage and impacted water infrastructure also contains other microbiological hazards, including high levels of antimicrobial resistant bacteria (ARB) (Karkman et al., 2019). Widespread use of antibiotics in medicine and agricultural settings (Kunin, 1993) results in large quantities of these chemicals in wastewater, which are often not removed during wastewater treatment (Ahmed et al., 2015a). As a result, microbial assemblages inhabiting human waste-streams are exposed to consistently high levels of antibiotics (Michael et al., 2013), resulting in selection for antibiotic resistance (Figure 1, C) (Bougnom et al., 2019). In addition, ARB can also accumulate in the guts of medicated patients, who then shed resistant bacteria into sewage (Steinbakk et al., 1992). These resistant bacteria can be introduced into coastal environments during stormwater and sewage overflows (Carney et al., 2019) . A recent study has shown that recreational use of sewage impacted waterways increases the likelihood of contracting an ARB pathogen (Leonard et al., 2018), highlighting this as a significant human health threat.

Animal faeces can also harbour both human pathogens and ARB. Animal faeces from cattle, chickens, and pigs can harbour pathogens such as *E. coli* O157 (Ateba and Bezuidenhout, 2008) and *Salmonella* (Topalcengiz et al., 2020). Meanwhile, animals more common to urban areas such as dogs and birds also harbour pathogens such as *Salmonella* (Topalcengiz et al., 2020), *E. coli* (Foster et al., 2006; Yuri et al., 1999), and *Arcobacter* (Celik and Otlu, 2020; Houf et al., 2008). Moreover, these animals have also been recorded to harbour pathogenic *E. coli* that are resistant to the quinolone and tetracycline antibiotics (Bryan et al., 2004; Vredenburg et al., 2014).

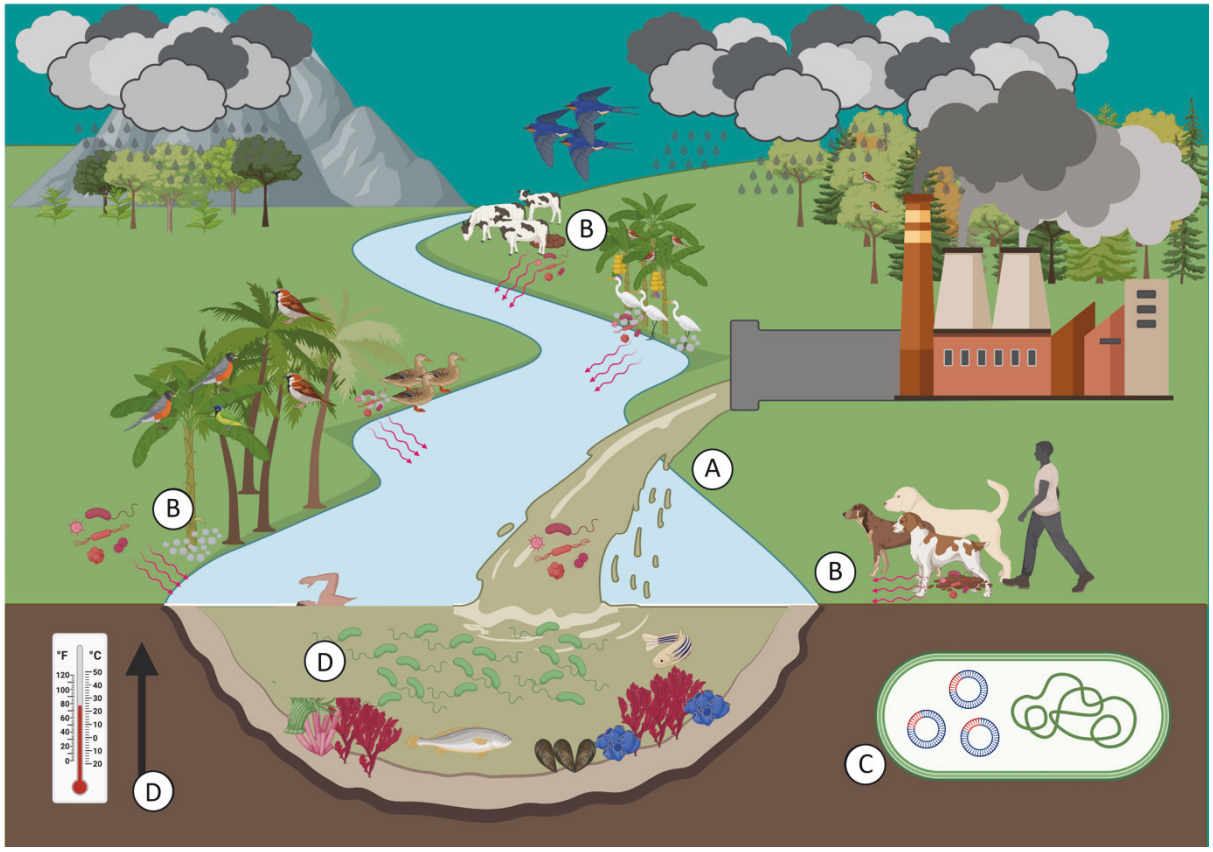

Figure 1. Diagram of microbial hazard sources relevant to this introduction. These include A) Input from urban runoff and sewage overflow, B) Runoff from animal faeces such as livestock, domestic pets, and wildlife, C) Bacteria entering from stormwater infrastructure within sewage contamination and animal faeces can possess ARGs and D) Endemic microbes existing in nature and blooming as a result of climate change induced environmental perturbations such as heavy rainfall and heatwaves.

1.5 - Monitoring for Microbiological Threats in Coastal Habitats

Both endemic pathogens and anthropogenically introduced microbes can pose a human health risk. Currently, there are over 50 million cases of gastro-intestinal illness linked to recreation in coastal environments, amounting to a global economic impact of over $12 billion a year (Shuval, 2003). Therefore, adequate monitoring and management of water quality are key elements in maintaining environmental and human health within coastal ecosystems. The current world health organisation guidelines state that enumeration of faecal indicator organisms (FIO) such as the faecal indicator bacteria (FIB) *E. coli* (Tallon et al., 2005), or the culturable human enteric viruses, Enteroviruses (Costán-Longares et al., 2008) and Reoviruses (Betancourt et al., 2018) are all adequate indictors of faecal contamination, which can be used

to monitor for faecal contamination in coastal environments. However, these guidelines recommend enumeration of the FIB enterococci, using the International Organization for Standardization – ISO or American Society for Testing and Materials – ASTM methods, carried out by an accredited laboratory (WHO, 2021). FIO such as enterococci reside in faeces of many animals (Hammerum, 2012) and rarely exist in unpolluted waters, making them a good tool for faecal contamination in coastal environments. Whilst these methods are currently in line with the global standard, are easy to perform, and are also relatively cheap, FIO enumeration methods are limited in two significant ways. The first limitation of this method is the inability to precisely determine the source of the FIO. As well as being an indicator of human faeces (sewage), many FIO such as enterococci are also present in the faeces of other warm-blooded animal species, including wild, agricultural, and domestic animals (Hammerum, 2012). Therefore, it is often difficult to directly link high FIO levels solely to sewage contamination. The second flaw of FIO approaches is that these techniques fail to detect microbial hazards in the environment, including other microbial pathogens and ARB. The lack of specificity of FIO assays limits capacity to manage impacted environments, beyond closing beaches during periods when high FIO levels are recorded. Of more concern, these standard approaches may miss important threats within coastal habitats, meaning that swimmers are exposed to dangerous microbiological elements without warning. These shortcomings are recognised by the World Health Organisation, and so their current recommendation states that when FIO levels reach unacceptable levels, it is important to discriminate the faecal source using molecular microbial source tracking (MST) techniques (WHO, 2021).

The most widely used MST technique is qPCR. qPCR assays are designed to target genes that are indicators of specific fecal material in the environment, with the main benefit of these assays being that they are able to discriminate between human and animal faeces. Currently, there are numerous markers which are indicative of human sewage within the environment. One marker for human sewage, the HF183 marker (Green et al., 2014a; Templar et al., 2016), which detects human specific *Bacteriodales*, has proven useful in detecting sewage in the environment (Sauer et al., 2011; Sercu et al., 2011). However, in some cases, *Bacteriodales* markers are not abundant in human hosts due to the diet people have in particular regions of the world (Ahmed et al., 2016; Koskey et al., 2014; Okabe and Shimazu, 2007). In addition, human associated *Bacteriodales* have been shown to be detected in cat, dog, chicken, turkey, and racoon faeces (Ahmed et al., 2010; Green et al., 2014b; Haugland et al., 2010; Newton et al., 2015), and therefore, new markers have been developed, such as the Lachno3

assay (Feng et al., 2018), which targets human specific *Lachnospiraceae*, a family of bacteria that is abundant in human faeces and rarely found in other animals (Feng et al., 2018). Whilst this marker is being used more frequently in MST studies, it is recommended that a weight of evidence approach be implemented, incorporating multiple markers to gain the most resolution when attempting to identify sources of faecal contamination (Codello et al., 2021), as well as including pathogen assessment, including human specific pathogens, into MST.

Importantly, in addition to detecting sewage, specific MST qPCR markers can also be used to detect faeces from a range of animals. In many cases where FIO methods are unable to discriminate from agriculture faeces or sewage, the broad-spectrum ruminant assay that targets ruminant specific *Bacteroidetes* can be implemented (Reischer et al., 2006). This assay detects faeces from cattle, deer, chamois, roe deer, sheep, and goats (Reischer et al., 2006). Additionally, agricultural animal faeces can be more specifically discriminated using the CowM2 and CowM3 assay, which detect *Bacteriodales* specific to cow faeces (Shanks et al., 2008), the Pig-Bac-2 assay, which detects *Bacteriodales* specific to pig faeces (Dick et al., 2005), or LA35 assay which detects *Brevibacterium* specific to poultry faeces (Weidhaas and Lipscomb, 2013). In addition to agricultural animals, there are also assays to detect faeces animals that are abundant in urban areas such as the DG3 assay, which detects *Bacteriodales* specific to dog faeces (Green et al., 2014b), and the GFD assay which detects *Heliobacter* specific to bird faeces (Green et al., 2012). While many animal MST markers have been detected at low quantities (<10 copies/reaction) within the faeces of other animals (Green et al., 2014b), the GFD (Green et al., 2012) and DG3 assays (Green et al., 2014b) were chosen for this study as they had 100% specificity when tested against a variety of animal faeces. When used together, a suite of MST markers can be applied to accurately discriminate the sources faecal contamination within aquatic environments.

1.6 - Knowledge Gaps and Aims

The primary focus of this thesis was to identify the extent, and causes, of microbial hazards to recreational users of eastern Australian coastal environments. Chapter 2 of this thesis (first data chapter) examined the occurrence, distribution, and environmental determinants of endemic coastal pathogens within the *Vibrio* genus, with a particular focus on how their patterns of abundance and diversity are distributed along large latitudinal gradients. In Chapter 3, I explored the utility of MST approaches in defining the causes and consequences of water

contamination within a coastal environment exposed to a complex assortment of potential sources of faecal contamination. These sources included sewage overflow within stormwater drains, canine faeces from the surrounding dog beach, and avian faeces from the surrounding bird life. This chapter also investigated bacterial pathogens and ARB entering the environment via anthropogenic waste streams. The fourth chapter of this thesis examined the impact that rainfall has on sewage overflow in a coastal ecosystem, with a central goal of defining the microbial hazards which enter coastal environments with sewage contamination, focusing on bacterial pathogens and ARB. Finally, the fifth chapter of this thesis aimed to define the environmental and anthropogenic perturbations that govern microbial communities in intermittently opened and closed lagoons, with a focus on the microbial hazards which proliferate when microbial communities in these environments are governed by sewage contamination. Across these studies, I hypothesised that significant rainfall would amplify microbial hazards within coastal environments, and the findings of this thesis have identified numerous microbial hazards that proliferate during rainfall induced reductions in salinity, as well as rainfall induced faecal contamination (mainly sewage) within coastal environments, highlighting the health threats associated with wet weather events, as well as emphasising the need for remediation where sewage contamination persists. To accomplish the objectives of each chapter, four separate field and laboratory-based studies were executed, integrating the following aims:

1. **To define the Latitudinal Dynamics of pathogenic *Vibrio* along the Eastern Coastline of Australia**.

Several bacterial species within the *Vibrio* genus are significant human pathogens, which can proliferate during periods of abnormally high SST, as well as periods of low salinity, such as during a significant rainfall event. Whilst these natural driving factors of *Vibrio* abundance are well characterised, their patterns of abundance and diversity along large latitudinal gradients, such as along the East Coast of Australia, have not been clearly defined. Therefore, I aimed to determine the patterns of abundance and diversity of the *Vibrio* community during the Australian summer using the high throughput *hsp60* gene amplicon sequencing assay to characterise the *Vibrio* community across a large latitudinal transect spanning the entire eastern coastline of Australia, one of the largest latitudinal *Vibrio* ecology gradients studied to date. Determining the patterns of abundance and diversity the *Vibrio*

bacteria is essential, as these patterns are anticipated to change with varying temperatures and salinity (Takemura et al., 2014). This is important, because patterns in these two environmental parameters are predicted to shift as a consequence of climate change.

This chapter was published in *Water* on the 15th of August 2022:

Williams, N. L. R., Siboni, N., King, W. L., Balaraju, V., Bramucci, A., & Seymour, J. R. *Water* (2022). Latitudinal Dynamics of Vibrio along the Eastern Coastline of Australia. https://doi.org/10.3390/w14162510

2. Investigate molecular microbiological approaches to reduce ambiguity about the sources of faecal pollution and identify microbial hazards within an urbanised coastal environment.

Urban coastal environments are often impacted by fecal contamination (McLellan et al., 2015), which can contain a number of microbiological hazards including pathogens (Anastasi et al., 2012; Collado et al., 2011; Garcia-Aljaro et al., 2019) and AbR bacteria (Akiyama and Savin, 2010). Current water quality monitoring techniques include enumeration of FIO, but this method does not define the cause or point source of contamination, nor does it detect the associated microbial hazards. At Rose Bay, a densely urban beach in Sydney, Australia, there are long lasting records of high FIB, however it was unknown if these FIB originated from a sewage leak within one of the nine stormwater drains contiguous to Rose Bay, from canine faeces on the beach, as Rose Bay is a dog friendly beach, or from avian faeces, as a variety of avian species live in the surrounding parks and trees. It was also unknown to what extent the faecal contamination spread throughout Rose Bay. Therefore, my principal aim was to determine the source and location of input of fecal contamination using a combination of FIB and MST qPCR techniques, and then to detail the spatial and temporal distribution of contamination using 16S rRNA amplicon sequencing. Moreover, it was also unknown if the FIB within Rose Bay were associated with any microbial hazards such as human pathogens and antibiotic resistant bacteria. Therefore, I also aimed to better define pathogens and antibiotic resistant bacteria associated with faecal contamination within Rose Bay with both 16S rRNA gene amplicon sequencing and qPCR to identify pathogens, as well as qPCR to investigate levels of a suite of antibiotic resistance genes including *sulI*, *tetA*, *qnrS*,

dfrA1, and *vanB*. Understanding the spatial and temporal distribution of fecal contamination and its associated microbial hazards is important because illness caused by pathogens and antibiotic resistant microbes are a significant human health threat and economic (Ralston et al., 2011).

This chapter was published in *Water Research* on the 30th of June 2022:

Williams, N.L.R., Siboni, N., Potts, J., Campey, M., Johnson, C., Rao, S., Bramucci, A., Scanes, P., Seymour, J.R., 2022. Molecular microbiological approaches reduce ambiguity about the sources of faecal pollution and identify microbial hazards within an urbanised coastal environment. Water Res. 218, 118534. https://doi.org/10.1016/j.watres.2022.118534

3. Investigating how rainfall leads to elevated levels of antibiotic resistance genes within seawater at an Australian beach.

Antibiotic resistant bacteria have recently been identified in coastal environments, with links to sewage inputs via stormwater infrastructure (Carney et al., 2019; Karkman et al., 2019), yet our knowledge of the spatial and temporal dynamics of ARB at beaches where there are multiple input points is incomplete. Additionally, recent work has illustrated correlations between pathogens and ARGs in urbanised coastal settings (Carney et al., 2020), but links between ARGs and pathogens due to particular sources – e.g., sewage leaks within stormwater drains - are yet to be clearly defined. Therefore, in this chapter, I aimed to determine the extent of ARB pollution within a coastal environment and if this pollution is linked to sewage contamination. Furthermore, I also aimed to determine if sewage contamination had the potential to transmit ARB pathogens into coastal environments. To do this, I used MST assays to detect sewage contamination, along with qPCR assays to detect levels of a suite of ARGs including *sulI*, *tetA*, *qnrS*, *dfrA1*, and *vanB*. I combined this qPCR data with 16S rRNA sequencing data to determine if these markers were linked to bacterial pathogens entering the environment, and if these pathogens were linked to ARGs. Determining how ARB are distributed and spreading within natural ecosystems is of rising global concern (Finley et al., 2013), and represents a potentially significant human health threat (Leonard et al., 2015; Leonard et al., 2018).

This chapter was published in *Environmental Pollution* on the 30th of June 2022:

Williams, N.L.R., Siboni, N., McLellan, S., Potts, J., Scanes, P., Johnson, C., James, M., McCann, V., Seymour, J.R., Rainfall leads to elevated levels of antibiotic resistance genes within seawater at an Australian beach, Environmental Pollution (2022). https://doi.org/10.1016/j.envpol.2022.119456.

4. Investigating how runoff alters bacterial communities within intermittently opened and closed lagoons (ICOLLS).

Intermittently closed and open lakes and lagoons (ICOLLs) are a type of lagoonal estuary that is episodically open to the ocean, and are relatively common, making up between 8-13% of the total global coastline (McSweeney et al., 2017). These environments are used recreationally and provide a suite of important ecosystem services (Basset et al., 2013), but given their variable connection to the ocean, they are subject to dramatic environmental perturbations, and are extremely sensitive to anthropogenic disturbances (Haines et al., 2006; Sadat-Noori et al., 2016; Schallenberg et al., 2010). While the relative influence of natural environmental variability and anthropogenic impacts on the microbiology of other aquatic ecosystems has been widely studied (Danovaro and Pusceddu, 2007; Savio et al., 2015; Staley et al., 2015), examinations of these impacts on the ecology of ICOLLs have been largely restricted to sediment communities (Filippini et al., 2019), chlorophyll a or zooplankton levels (Everett et al., 2007; Gamito et al., 2019). Consequently, the impact of anthropogenic contamination, and natural physio-chemical properties on the bacterial communities within ICOLLs is not yet well defined. Therefore, in this chapter I aimed to examine the relative importance of natural environmental determinants *vs* faecal contamination, from both sewage and animals, in shaping bacterial composition within ICOLLs. To achieve this, I sampled four ICOLLs on the east coast of Australia on a monthly basis over a period of one year, and linked changes in bacterial composition to environmental determinants, including faecal contamination, using a combination of DNA sequencing and MST techniques. It is important to know how these bacterial communities are shaped, as they provide important ecosystem services to ICOLL environments and in some cases can be harmful to recreational users of these environments.

This chapter is currently in review at *Water Research*:

Williams, N.L.R., Siboni, N., Potts, J., Scanes, P., Johnson, C., James, M., McCann, Le Reun, N., King, W.L., V., Seymour, J.R., Runoff alters bacterial communities within intermittently opened and closed lagoons (ICOLLS), *Water Research* (submitted).

Chapter 2 - Latitudinal dynamics of *Vibrio* along the eastern coastline of Australia

Author Signatures:

Author's state that author contributions are correct, and that the student has completed the work stated in the author contributions.

Author	Signature	Date
Nathan L.R. Williams	Production Note: Signature removed prior to publication.	11/08/2022
Nachshon Siboni	Production Note: Signature removed prior to publication.	11/08/2022
William L. King	Production Note: Signature removed prior to publication.	11/08/2022
Varunan Balaraju	Production Note: Signature removed prior to publication.	11/08/2022
Anna Bramucci	Production Note: Signature removed prior to publication.	11/08/2022
Justin R. Seymour	Production Note: Signature removed prior to publication.	11/08/2022

This chapter has been published: Williams, N. L. R., Siboni, N., King, W. L., Balaraju, V., Bramucci, A., & Seymour, J. R. (2022). Latitudinal Dynamics of *Vibrio* along the Eastern Coastline of Australia. Water. https://doi.org/10.3390/w14162510

2.0 - Abstract

The marine genus of bacteria, *Vibrio,* includes several significant human and animal pathogens, highlighting the importance of defining the factors that govern their occurrence in the environment. To determine what controls large scale spatial patterns among this genus, the abundance and diversity of *Vibrio* communities along a 4000 km latitudinal gradient spanning the Australian coast were examined. A *Vibrio*-specific amplicon sequencing assay was used to define *Vibrio* community diversity, as well as quantitative PCR and droplet digital PCR to identify patterns in the abundances of the human pathogens *V. cholera*, *V. parahaemolyticus* and *V. vulnificus*. The *hsp60* amplicon sequencing analysis revealed significant differences in the composition of tropical and temperate *Vibrio* communities. Over 50% of *Vibrio* species detected, including human pathogens *V. parahaemolyticus* and *V. vulnificus*, displayed significant correlations with either temperature, salinity, or both, as well as different species of phytoplankton. High levels of *V. parahaemolyticus* and *V. vulnificus* were detected in the tropical site at Darwin and the subtropical Gold Coast site, along with high levels of *V. parahaemolyticus* at the subtropical Sydney site. This study has revealed the key ecological determinants and latitudinal patterns in the abundance and diversity of coastal *Vibrio* communities, including insights into the distribution of *Vibrio* pathogens *V. cholerae, V. parahaemolyticus, and V. vulnificus*, within a region experiencing significant ecological shifts due to climate change.

2.1 - Introduction

Understanding the distributional dynamics of a species or a community of organisms is pivotal to understanding their ecology, and how they may respond to environmental perturbations (Chapin Iii et al., 2000). Across a wide range of organisms, species diversity and abundance patterns have been shown to be variable across latitudinal gradients, with many terrestrial and aquatic organisms displaying highest diversity levels at low latitudes (Fischer, 1960; Hillebrand, 2004; Pianka, 1966). Importantly, there is also growing evidence showing that latitudinal range shifts in multiple species are occurring as a consequence of climate change (Sunday et al., 2012).

Latitudinal gradients have been shown to exist among microorganisms in both terrestrial (Bahram et al., 2018) and aquatic environments (Raes et al., 2018; Roy et al., 1998), with two ecological processes often used to explain these patterns. The first of these is that diversity and productivity increase together because larger numbers of organisms are supported by larger rates of resource supply (Brown, 1981). The second is that temperature and diversity increase together, as temperature impacts biological kinetics and therefore the rate of ecological processes such as speciation, ultimately resulting in an increase in diversity (Allen et al., 2002; Brown et al., 2004). Previous studies e.g., (Fuhrman et al., 2008; Pommier et al., 2007) have demonstrated that marine bacterial species richness is correlated with temperature and inversely correlated with latitude. In addition to shaping the diversity of entire bacterial communities, latitude and temperature have been shown to be critical determinants of the distributions of keystone marine bacteria, including numerically abundant groups such as the SAR11 clade (Brown et al., 2012) and dominant primary producers, including the cyanobacteria genera *Synechococcus* and *Prochlorococcus* (Flombaum et al., 2013).

Within coastal and estuarine ecosystems, members of the *Vibrio* genus, which can be particle associated (Liang et al., 2019), or free-living (Li et al., 2020), are notable members of natural bacterial assemblages because of their often-important ecological relationships with marine animals, which can span mutualistic (Nyholm and McFall-Ngai, 2021) to parasitic interactions with a wide diversity of species, including fish (Istiqomah et al., 2020), corals (Kushmaro et al., 2001), and shellfish (Bruto et al., 2018). In addition to impacting natural marine communities, diseases caused by *Vibrio* species are also particularly detrimental to the aquaculture sector, where they globally cause hundreds of millions of dollars in losses across a broad range of industries such as a $44 billion USD production loss to the shrimp industry between 2010 and 2016 (Tang and Bondad-Reantaso, 2019), a $7.4 million USD production

loss to the Malaysian seabass industry in the 1990s and substantial impact on the salmon industry in the 1990s (Lafferty et al., 2015).

In addition to impacting marine species and ecosystems, several *Vibrio* species are notable human pathogens. For example, *V. cholerae* causes the severe gastrointestinal disease cholera, which globally results in over 2.8 million cases and up to 95,000 deaths per year (Ali et al., 2015). *V. parahaemolyticus* is a major cause of seafood poisoning, causing severe and sometimes fatal gastrointestinal disease in up to 30,000 people per year (Daniels et al., 2000). Infections by *V. vulnificus* can follow consumption of seafood as well, but can also result from direct exposure to seawater, and can be particularly dangerous, with up to a 50% mortality rate among infected individuals (Rippey, 1994). Notably, there are indications that the global distributions and seasonal dynamics of some of these pathogenic *Vibrio* species are shifting as a consequence of climate change (Trinanes and Martinez-Urtaza, 2021; Vezzulli et al., 2013), with evidence for poleward latitudinal range shifts (Trinanes and Martinez-Urtaza, 2021).

A suite of environmental factors have been demonstrated to influence *Vibrio* abundance and diversity. *Vibrio* abundance has been shown to increase with nutrients such as phosphate (Eiler et al., 2006), but in contrast decrease with increasing levels of nitrogen, dissolved oxygen, and pH (Blackwell and Oliver, 2008). The most widely observed determinants of *Vibrio* abundance, however, are salinity, temperature, and chlorophyll (Eiler et al., 2006; Froelich et al., 2013; Heidelberg et al., 2002; Nigro et al., 2011; Oberbeckmann et al., 2012; Turner et al., 2009; Vezzulli et al., 2009; Wetz et al., 2008), with moderate salinity levels and elevated temperatures often leading to increased *Vibrio* abundances (Froelich et al., 2013; Hsieh et al., 2008; Oberbeckmann et al., 2012; Randa et al., 2004; Takemura et al., 2014). However, the environmental determinants and optimum conditions vary across *Vibrio* species (Takemura et al., 2014). For instance, *V. cholerae*, *V. vulnificus*, and *V. parahaemolyticus* are generally more abundant within warm waters where the temperature exceeds 20 °C and salinity is below 10 ppt (Takemura et al., 2014). This is particularly relevant as climate change is increasing sea surface temperatures (SST), as well as increasing the frequency of severe rainfall events (Madakumbura et al., 2021), which can result in decreased salinity in coastal environments. Together, these shifting environmental conditions have the potential to create ideal conditions for *Vibrio* blooms in the environment.

In light of the substantial environmental and human health importance of *Vibrio* species, the aim of this study was to determine the patterns of abundance and diversity of the *Vibrio* community during the Australian summer using the high throughput *hsp60* gene

amplicon sequencing assay to characterise the *Vibrio* community across a large latitudinal transect spanning the entire eastern coastline of Australia, one of the largest latitudinal *Vibrio* ecology gradients studied to date. Previous studies have detected high levels of *Vibrio*, including the human pathogens *V. cholerae*, *V. vulnificus*, and *V. parahaemolyticus* in tropical (Padovan et al., 2021) and subtropical (Siboni et al., 2016) Australian environments during summer months when water temperature is highest, but neither of these studies have investigated *Vibrio* ecology on such a large scale. This is particularly relevant within Australia, where there is evidence that climate change is increasing seawater temperatures more rapidly than in any other part of the southern hemisphere (Hobday and Lough, 2011), making this region a climate change hotspot, and a potential location for substantial increases in the abundance of pathogenic *Vibrio* species.

2.2 - Methods

2.2.1 - Sampling Locations and Protocol

Water samples were collected once each from 28 coastal sites along a latitudinal gradient spanning Australia's eastern coast, from Darwin (12° 22' 42.8" S, 130° 50' 30.8" E) to Hobart (42° 51' 05.7" S, 147° 31' 16.2" E) (Figure 1, Appendix 1 Table 1) in a sampling campaign conducted during the Australian summer (December 2017 - January 2018) over a period of 48 days. To consider the impacts of salinity and the common occurrence of *Vibrio* in estuarine environments, at each location, both a river (R-Site) and a beach (B-Site) sample were collected, except for at Rockhampton (23° 15' 17.8" S, 150° 49' 44.5" E), where both samples were taken from the beach due to a lack of river access at the time of sampling, and Bundaberg (24° 45' 41.8" S, 152° 23' 14.6" E), where both samples were taken from the river due to no beach access at the time of sampling.

At each sampling site, 10 L of water was collected from the surface (top 50 cm) in tinted, plastic drums, which had been pre-rinsed with bleach and then miliQ water and then rinsed three times on site prior to sampling. Physiochemical parameters including temperature, dissolved oxygen, salinity, and pH were measured *in situ* using a WTW multiprobe meter (Multi3430, Germany). Triplicate water samples were filtered through 0.22 µm pore size, 47 mm diameter filters (Millipore, DURAPORE PVDF .22UM WH PL) using a peristaltic pump within 3 hrs of collection, with the volume of sample filtered recorded (between 500 ml and 2000 ml) to allow for normalisation of gene copy numbers. Filters were placed in cryotubes and then immediately in dry ice, where they remained for the duration of the sampling trip. Upon returning to the laboratory, samples were stored at -80 °C for 6 months until processing.

2.2.2 - DNA Extraction

Filters were removed from Eppendorf tubes with pre-bleached forceps and transferred open and face-in to a 5 ml bead tube. DNA extraction was then performed using the PowerWater DNA isolation Kit (QIAGEN) in accordance with the manufacturer's instructions. DNA quantity and purity were then evaluated using a Nanodrop-1000 Spectrophotometer, with each sample having between 5 – 50 ng/µl DNA.

2.2.3 - Quantitative PCR (qPCR)

Total bacterial community abundance, as well as the abundance of the total *Vibrio* community were measured using quantitative PCR (qPCR). Total bacterial abundance was quantified using the BACT1369F and PROK1492R 16S primer pair (Suzuki et al., 2000), while total *Vibrio* community abundance was quantified using the primer pair Vib1-f and Vib2-r (Thompson et al., 2004), which targets the *Vibrio*-specific 16S rRNA gene. To quantify levels of *V. parahaemolyticus,* the thermostable direct hemolysin (*tdhS*) gene (Rizvi and Bej, 2010) was targeted, and to quantify levels of *V. vulnificus*, the *V. vulnificus* hemolysin (*vvhA*) gene (Siboni et al., 2016) was targeted. To quantify *V. cholerae*, the outer-membrane protein *ompW* gene (Gubala and Proll, 2006) was targeted. Additionally, toxigenic *V. cholerae* was also tested for, targeting the enterotoxin gene *ctxA* (Blackstone et al., 2007). For further qPCR assay details see Appendix 1 Table 2.

All qPCR analyses were performed on the BIO-RAD CFX384 Touch™ Real-Time PCR Detection System™, with gene copies calculated within each sample by plotting against their respective standard curve using BIO-RAD's CFX MAESTRO™ software version 1.1. Each qPCR analysis was run in triplicate, with all assays set-up in 5 µl reaction volumes that consisted of 2.5 µl BIO-RAD iTaq Universal SYBR® Green Supermix, 1.1 µl nuclease free water, 0.2 µl of each forward and reverse primer, and 1 µl of diluted (1:20) DNA template, with the exception of the *ctxA* assay, which consisted of 2.5 µl BIO-RAD iTaq Universal PROBES Supermix, 1 µl nuclease free water, 0.2 µl of each forward and reverse primer, 0.1 µl of probe, and 1 µl of diluted (1:20) DNA template. Calibration curves were run with every plate and for each SYBR-based assay specificity was confirmed with a melt curve. The process for limit of detection and quantification of each sample goes as follows: In each case, gene copies were calculated for each target, using a (6-7 point) standard curve using BIO-RAD's CFX MAESTROTM software version 1.1. Standard curves were generated from known concentrations of a synthesised DNA fragment of each targeted gene, with a standard curve run with each plate. Samples outside of the calibration curve were considered below the limit of detection and included in the analysis as 0. Each DNA fragment for the standard curve was checked using MEGA7 to ensure they matched both primers, the probe (if applicable) and target gene and blasted in the NCBI database to ensure it was from the correct target gene. Along with standard curves, a no template control (NTC) was added to each qPCR run. To remove inhibitors, a dilution test was performed using the 16S qPCR assay as the 16S gene would be detected in every sample. First, the 16S qPCR was performed on all samples. Next,

samples with high, medium, and low levels of the 16S gene were selected for a dilution series, incorporating dilution factors of 1:2, 1:5, 1:10, 1:20, 1:50 and 1:100, with 16S rRNA qPCR performed on all dilutions. The copies of the 16S gene per 100 ml in each sample were then calculated, which revealed identical copy numbers in the 1:10, 1:20, 1:50 and 1:100 dilutions for all sample types tested. Based on these results, samples were diluted to 1:20 as this would preserve the amount of DNA that could be used throughout the study. Plate preparation was conducted using an epMotion® 5075 I Automated Liquid Handling System.

2.2.4 - Droplet digital Analysis

The abundance of *V. cholerae, V. parahaemolyticus* and *V. vulnificus* was initially determined via qPCR. While no *V. cholerae* was detected, *V. parahaemolyticus* and *V. vulnificus* were detected, but the levels of these organisms were very low, and significant variation between technical replicates was observed. Droplet digital PCR (ddPCR) has increased precision when quantifying low copy numbers of a gene (Hindson et al., 2013), and so, to quantify *V. parahaemolyticus* and *V. vulnificus* more precisely ddPCR was used. All ddPCR analyses were performed using the Bio-Rad QX200 droplet digital PCR instrument. For assay details see Appendix 2 Table 2. The ddPCR mix used comprised of 12.5 µl of EvaGreen Supermix (Bio-Rad), 0.2 µl of forward and reverse primers, 1 µl of diluted DNA template and nuclease free water up to 25 µl, with 20 µl then being used for droplet generation. The PCR reaction was performed on a C1000 Touch Thermal Cycler with 96-Deep Well reaction module (Bio-Rad) using the evergreen protocol with a single modification of the annealing/extension step, which was adjusted to 56 °C for *V. vulnificus vvhA* to suit the Tm of this primer set. The droplets were read with a QX200 Droplet Reader and QuantaSoft software version 1.7.4 (Bio-Rad). A single threshold was applied on all samples and negative controls were used, with the absolute number of gene copies converted to gene copies per litre.

2.2.5 - 16S rRNA gene sequencing

To characterise the total bacterial community composition in samples, the V3–V4 region of the bacterial 16S rRNA gene was amplified using the 341f/805r primer pair (Takahashi et al., 2014), with the following cycling conditions: 95°C for 3 minutes followed by 25 cycles of: 95°C for 30 seconds, 55°C for 30 seconds, 72°C for 30 seconds, and then 72°C for 5 minutes with a final hold at 4°C (Pichler et al., 2018). PCR amplicons were then

sequenced using the Illumina MiSeq platform (300 bp paired-end analysis at the Ramaciotti Institute of Genomics, University of New South Wales).

The DADA2 pipeline (Callahan et al., 2016) was used to process the paired R1 and R2 fastq reads. Reads with 'N' bases were removed and primers were truncated using cutadapt (Martin, 2011). Low quality terminal ends were removed by trimming reads (trunc (R1= 280; R2= 250)). To produce the highest number of merged reads after learning error rate and removing chimeric sequences, the dada2 removeBimeraDenovo program was used at the default threshold stringent minFoldParentOverAbundance=1. Amplicon sequencing variants (ASVs) were annotated against the SILVA v138 database with a 50% probability cut-off. The ASV table was subsequently filtered to remove ASVs not assigned as kingdom bacteria, as well as any ASVs classified as chloroplast or mitochondria. The chloroplast data was removed and then ASVs were annotated using the PR2 version 4.14.0 (Guillou et al., 2013) database with a 50% probability cut-off and then joined back to the bacteria dataset. Finally, the dataset was rarefied to 30,000 reads using vegan (Dixon, 2003). Sequences are available in the NCBI database (ID-PRJNA776096). For 16S pipeline script please see: (https://github.com/Nwilliams96/Australian_Vibrio_Latitude_Project.git).

2.2.6 - hsp60 Sequencing

To quantify the *Vibrio* community with greater species-level precision than is delivered by 16S rRNA gene amplicon sequencing, the *Vibrio*-specific *hsp60* gene amplicon sequencing assay was employed, using the Vib-shpF3-23 and Vib-hspR401-422 primer pairing (King et al., 2019). DNA was diluted 1:10 and 3 µl was used in a 30 µl PCR reaction volume comprising of 6 µl of 5 x Hi-Fi Buffer (Bioline), 3 µl of 10 mM dNTPs, 0.5 µl of high-fidelity velocity polymerase, 3 µl of 10 µM forward primer (Vib-shpF3-23), and 3 µl of 10 µM reverse primer (Vib-hspR401-422). Amplification was performed using the following PCR cycling conditions: one cycle of 98°C for 2 min, 5 cycles of 98°C for 30 s, 60°C for 30 s, and 72°C for 45 s, 21 cycles of 98°C for 30 s, 60°C for 30 s with a reduction of 0.5°C per cycle (60°C to 50°C), and 72°C for 45 s, 16 cycles of 98°C for 30 s, 50°C for 30 s, and 72°C for 45 s, and a final extension time of 72°C for 10 min. Amplicons were subsequently sequenced using the Illumina MiSeq platform (300 bp paired-end analysis at the Ramaciotti Institute of Genomics, University of New South Wales).

As described in King et al. (2019), paired-end sequences were joined using FLASH (Magoc and Salzberg, 2011) and trimmed using Mothur (Schloss et al., 2009). These fragments were then clustered, and chimeric sequences were removed using vsearch (Rognes et al., 2016). Cleaned sequences were BLASTed against a *Vibrio-hsp60* reference dataset, discarding non-*Vibrio* sequences. The fasta file obtained was used to assign operational taxonomic units (OTUs) against the custom *Vibrio-hsp60* reference dataset with the RDP classifier. As there was a large spread of sequences per sample, the data was not rarefied, but the sequences were normalised to the number of sequences per sample to provide the relative abundance for each taxa for each sample. For *hsp60* pipeline script please see (https://github.com/Nwilliams96/Australian_Vibrio_Latitude_Project.git).

2.2.7 - Statistical Analysis

To test for differences in abiotic variables, qPCR, and ddPCR data, between sampling sites and climatic zones, Kruskal-Wallis tests were used, followed by Mann-Whitney pairwise comparisons with Bonferroni corrected p-values. Correlations between qPCR data, ddPCR data and abiotic variables were determined using Spearman's RS, with Bonferroni corrected p values. These statistics were performed in Past Version 4 (Hammer et al., 2001).

To test for differences in microbial community composition (16S rRNA data) and *Vibrio* community composition (*hsp60* data) between samples, as well as differences in the Shannon, Simpson, and Chao1 diversity measures in both data sets, the adonis function from Vegan (Dixon, 2003) was used, as well as the pairwise.adonis function from the PairwiseAdonis (Martinez Arbizu, 2020) R package. To determine how each sample within the 16S rRNA dataset were related to each other, the similarity profile routine test (SIMPROF) in the r package 'clustsig' (Whitaker and Christman, 2010) was used. For the 16S rRNA gene sequencing dataset, it was discovered that the samples clustered into two significantly different groups and so the multipatt function in the indicspecies r package (De Caceres and Jansen, 2018) was run to determine indicator ASVs within each group. Additionally, the correlation analysis package MicTools (Albanese et al., 2018) was used to test for potential correlations between chloroplasts, the *Vibrio* community, and abiotic variables, only accepting p-values < 0.05 and using Spearmans r_s values for analysis.

2.3 - Results

2.3.1 Environmental Conditions

Across the latitudinal gradient examined in this study, water temperatures (Figure 1 B) varied significantly [$p < 0.01$] between tropical (12° 22' 42.8" S - 19° 16' 29.3" S) , subtropical (21° 06' 37. 6" S - 33° 91' 00" S) , and temperate (35° 00' 46.0" S - 42° 53' 20.9" S) climatic zones (mean: 31.25 ± 1.85 °C, 26 ± 2.38 °C, and 21 ± 2.61°C respectively). In contrast, salinity (Figure 1 C) remained statistically indistinguishable between these zones (average 30.53 ± 9.36 ppt, 32.79 ± 6.40 ppt, and 35.70 ± 1.07 ppt respectively). Of note however, four sites had significantly lower [$p < 0.01$] salinity than the mean salinity of the dataset (Darwin river: 22.54 ppt, Darwin beach: 10.30 ppt, Bundaberg river site 2: 19.26 ppt and Gold Coast river: 17.90 ppt), which coincided with rainfall events in the 3 days prior to sampling (Darwin: 24 mm, Bundaberg: 3.2 mm and Gold Coast:17.4 mm). The Hobart sites had significantly lower [$p < 0.01$] dissolved oxygen levels than the other sites (Hobart beach: 9.48% , Hobart river: 10.01%), and were in fact 10-times lower than the mean dissolved oxygen observed along the latitudinal gradient. The pH within samples did not vary significantly between climatic zones.

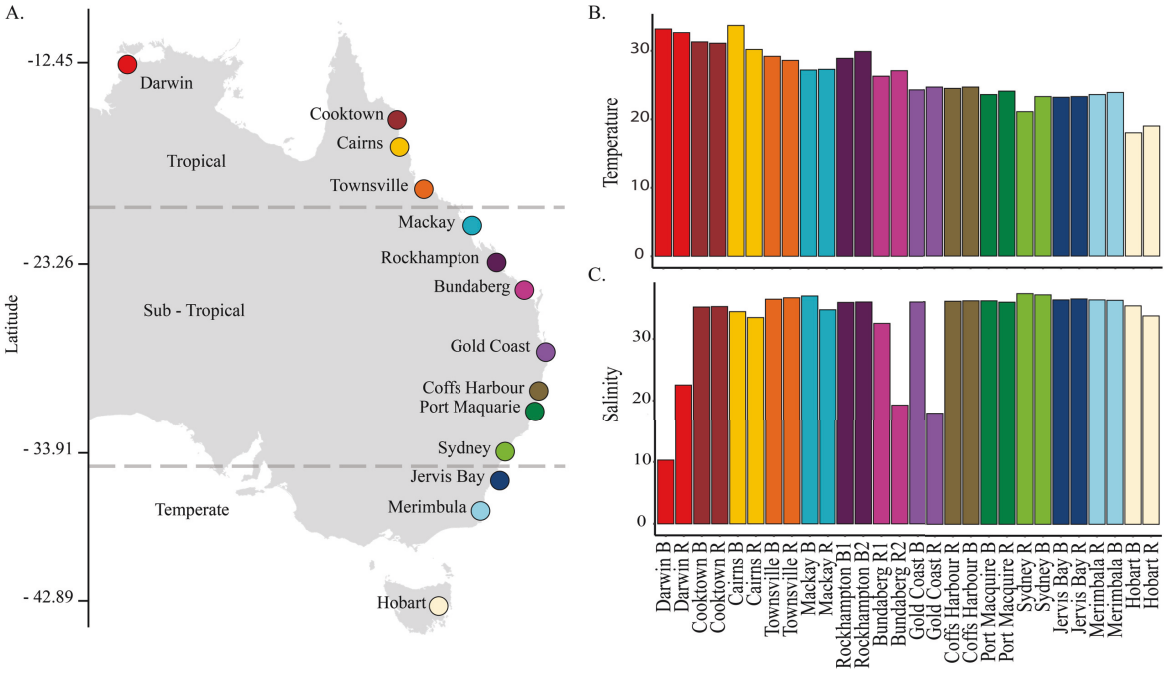

Figure 1. Map of sampling locations, along with temperature and salinity at each location. A) Map of sampling locations. At each location, a sample was taken at the beach and in the river with the exception of Rockhampton where both samples were beach sites and Bundaberg where

both sites were river sites. B) Water temperature at each site in °C. C) Salinity at each site in ppt.

2.3.2 - Quantification of the total bacterial community

Along the Eastern Coast of Australia, there were no correlations observed between levels of the 16S rRNA gene, used here as a proxy measure for bacterial biomass, and any of the environmental variables measured. The highest levels of 16S rRNA gene copies were observed within the subtropical region [mean: $1.69 \times 10^{11} \pm 1.24 \times 10^{11}$ copies/L, n = 24], where levels were 61- and 68-times higher than levels detected within the tropical [mean: $1.05 \times 10^{11} \pm 7.55 \times 10^{10}$ copies/L, n = 43] and temperate [mean: $1.00 \times 10^{11} \pm 5.58 \times 10^{10}$ copies/L, n = 18] regions. Average levels of the 16S rRNA gene did not statistically differ [$p > 0.05$] between beach [mean: $1.39 \times 10^{11} \pm 1.12 \times 10^{11}$ copies/L, n = 42] and river [mean: $1.56 \times 10^{11} \pm 1.40 \times 10^{11}$ copies/L, n = 42] sites along the latitudinal gradient. However, the beach sites within the subtropical region displayed significantly higher [$p < 0.01$] levels of the 16S rRNA gene than the beach sites within the tropical and temperate regions. This pattern was not true of river sites, whereby across regions there was no statistically distinguishable difference.

2.3.3 - Bacterial Community Analysis

Across the dataset, the 16S rRNA gene amplicon sequencing analysis revealed a total of 67, 218 unique bacterial ASVs. Both alpha diversity [$F = 93.63$, $p < 0.01$] and community composition [$F = 104.7$, $p < 0.01$] were significantly different between sites across the entire dataset. When beach and river sites were pooled, the most diverse climatic zone was the temperate zone, with both Shannon [$F = 6.6$, $p < 0.05$] and Simpson diversity [$F = 16.9$, $p < 0.01$] indexes within this zone being significantly higher than within the tropical zone. Simpson diversity index was also significantly higher [$F = 6.2$, $p < 0.05$] within the temperate climatic zone than within the subtropical zone. When dividing the samples into river and beach sites, diversity did not differ significantly between the river sites within any of the climatic zones along the latitudinal gradient, with no significant difference in Chao1, Simpson or Shannon diversity index. In contrast, within the beach sites, Chao1 was significantly lower within the temperate climatic zone compared to the subtropical climatic zone [$F= 8.39$, $p < 0.01$].

To identify patterns in similarity among bacterial assemblages, a SIMPROF analysis was performed, which revealed a bifurcation of samples into two major groups that were significantly different [$F = 21.472$, $p < 0.01$] (Figure 2). The first group contained samples from only above a latitude of 30.29 °S (the Sydney Beach site was an exception to this and clustered with these northern samples) and the second group contained samples from only below 30.29°S.

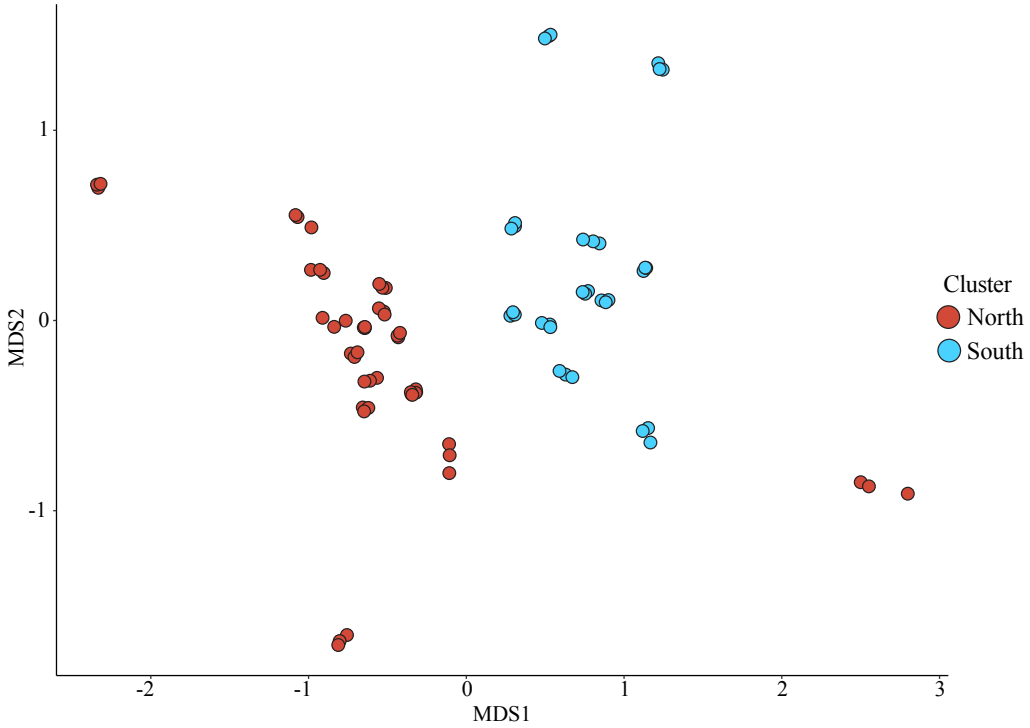

Figure 2. NMDS showing the results of SIMPROF and the bacterial community composition similarities between locations. NMDS (stress = 0.1269098) This cut-off occurred at latitude 30.29° S.

To determine what bacterial ASVs may be indicators of both the northern and southern communities, the *multipatt* function within the *indicspecies* R package was used. This analysis revealed 663 ASVs as indicators of the southern community, with the most abundant of these including a *Rubritaleaceae* ASV, a *Flavobacteriaceae* ASV and a *Cyanobiaceae* ASV, which contributed to 2.8 %, 2.4 % and 2.3 % to the relative abundance of the southern community, respectively. There were also 464 ASVs identified as indicators of the northern community, with the most abundant of these consisting of a *Rhodobacteraceae* ASV and two *Actinomarinaceae* ASVs, contributing 1.4 %, 1.6 % and 0.8 % to the relative abundance of the northern community, respectively. Of note, within the northern community indicator ASVs, 11

Vibrio spp. were identified. These *Vibrio* spp. included seven unassigned *Vibrio* spp., *V. brasiliensis*, *V. maritimus*, *V. harveyi* and *V. sinaloensis*.

2.3.4 - Quantification of the total Vibrio community

Vibrio were detected via qPCR at all 28 sites sampled along the Australian eastern coastline (Figure 3 A, B). Along the latitudinal gradient no correlations between total *Vibrio* levels and any of the environmental variables were observed. The highest levels of total *Vibrio* occurred within the subtropical climatic zone [mean: $1.00 \times 10^7 \pm 9.29 \times 10^6$ copies/L, n = 41], where levels were 14-times higher than those detected within the tropical climatic zone [mean: $8.81 \times 10^6 \pm 1.13 \times 10^7$ copies/L, n = 22] and 184-times higher than the temperate climatic zone [mean: $3.54 \times 10^6 \pm 2.33 \times 10^6$ copies/L, n = 17]. However, in contrast to this overall pattern, the highest levels of *Vibrio* were detected within the Darwin river [mean: $3.05 \times 10^7 \pm 8.93 \times 10^6$ copies/L, n = 3] and Darwin beach [mean: $2.47 \times 10^7 \pm 1.30 \times 10^7$ copies/L] sites, where levels were significantly higher [$p < 0.01$] than any other site. Also of note, there were only three other regions (Rockhampton, Gold Coast and Sydney) (Figure 3 A, B), which had total *Vibrio* levels exceeding 1×10^7 copies/L. The sites within these regions included the Rockhampton beach site 1 [mean: $2.13 \times 10^7 \pm 2.40 \times 10^6$ copies/L, n = 3], Rockhampton beach site 2 [mean: $1.25 \times 10^7 \pm 4.81 \times 10^5$ copies/L, n = 3], the Gold Coast beach, Gold Coast river, Sydney beach and Sydney river sites, all of which were significantly higher [$p < 0.05$] than any other site (excluding the Darwin sites) along the latitudinal gradient.

Across the entire dataset, average *Vibrio* levels were 37 times higher at the beach [mean: $9.57 \times 10^6 \pm 9.31 \times 10^6$ copies/L, n = 41] sites compared to river sites [mean: $7.01 \times 10^6 \pm 9.11 \times 10^6$ copies/L, n = 31], which was also true within the subtropical and temperate climatic zones, [subtropical beach mean: $1.25 \times 10^7 \pm 8.53 \times 10^6$ copies/L, n = 21; temperate beach mean: $3.41 \times 10^6 \pm 2.42 \times 10^6$ copies/L, n = 9], which were characterised by significantly higher [$p < 0.01$] *Vibrio* abundances than the river sites [subtropical mean: $7.46 \times 10^6 \pm 9.55 \times 10^6$ copies/L, n = 20, temperate mean: $3.67 \times 10^6 \pm 2.39 \times 10^6$ copies/L, n = 8].

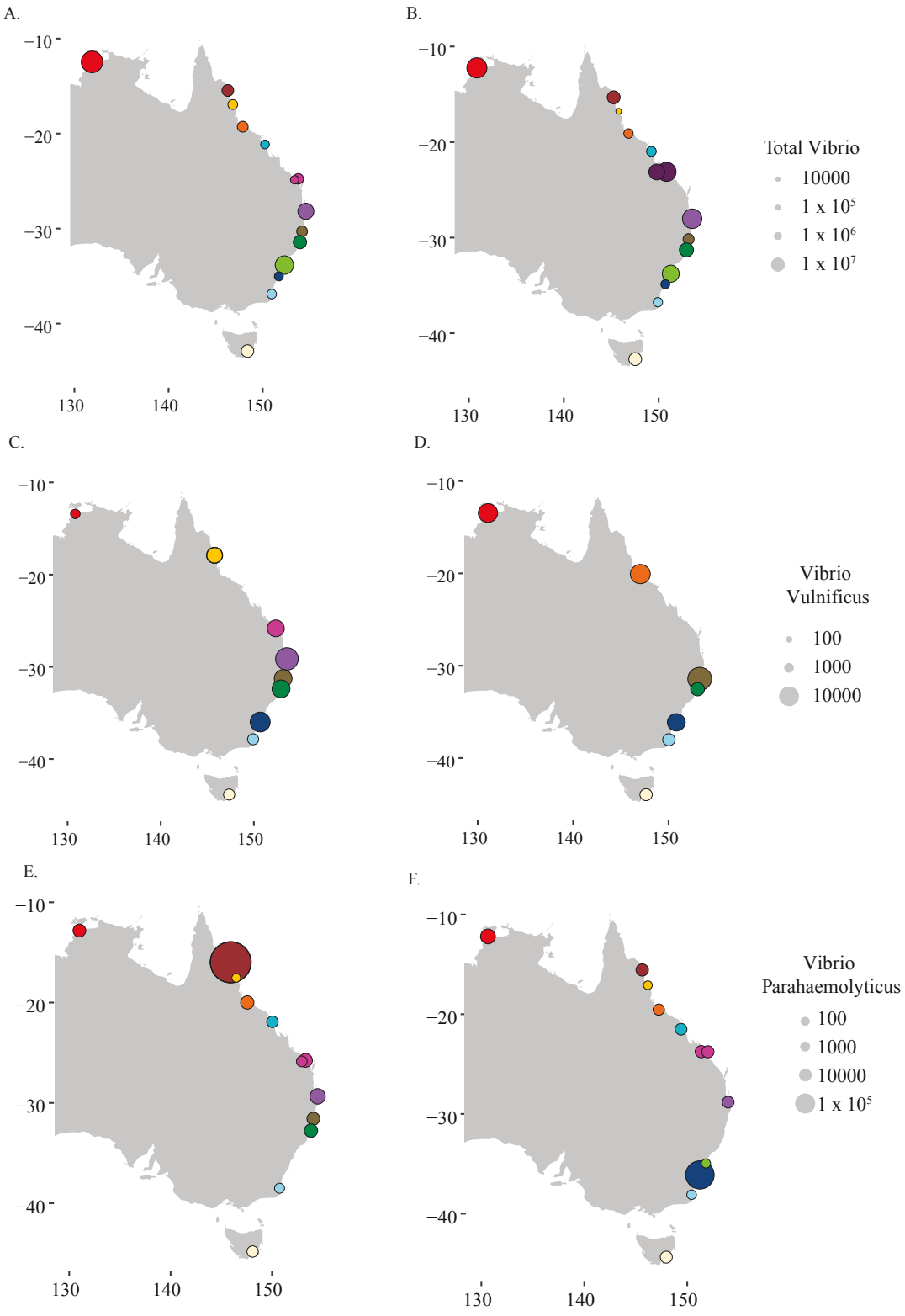

Figure 3. Total *Vibrio* qPCR, *Vibrio vulnificus*, and *Vibrio parahaemolyticus* ddPCR. Results from A and B Total *Vibrio* qPCR, C and D *V. vulnificus* ddPCR, E and F *V. parahaemolyticus* ddPCR. A, C and E are river sites, while B, D, and F are beach sites. Size scale represents copies/L of each assay.

2.3.5 - Vibrio Diversity

Vibrio-specific *hsp60* gene amplicon sequencing identified the occurrence of 59 unique *Vibrio* species across the entire dataset, with the most abundant species including *V. campbellii* and *V. harveyi*, which were detected in 93% and 89% of samples respectively (Figure 4). All sites had a significantly different [$F = 7.5$, $p < 0.001$] Shannon's diversity and a significantly different [$F = 7.15$, $p < 0.001$] community composition. No significant differences were observed in *Vibrio* diversity between tropical, subtropical, and temperate zones, nor did any of the diversity indices correlate with environmental variables. There was, however, a significant difference [$F = 4.5$, $p < 0.01$] in *Vibrio* community composition between the tropical and temperate climatic zones, which was driven by *V. campbellii* and *V. harveyi*, accounting for 24% and 6% of the dissimilarity between these two regions respectively. *Vibrio* community composition did not differ between river and beach sites, nor was there a significant difference between tropical and subtropical, or subtropical and temperate climatic zones.

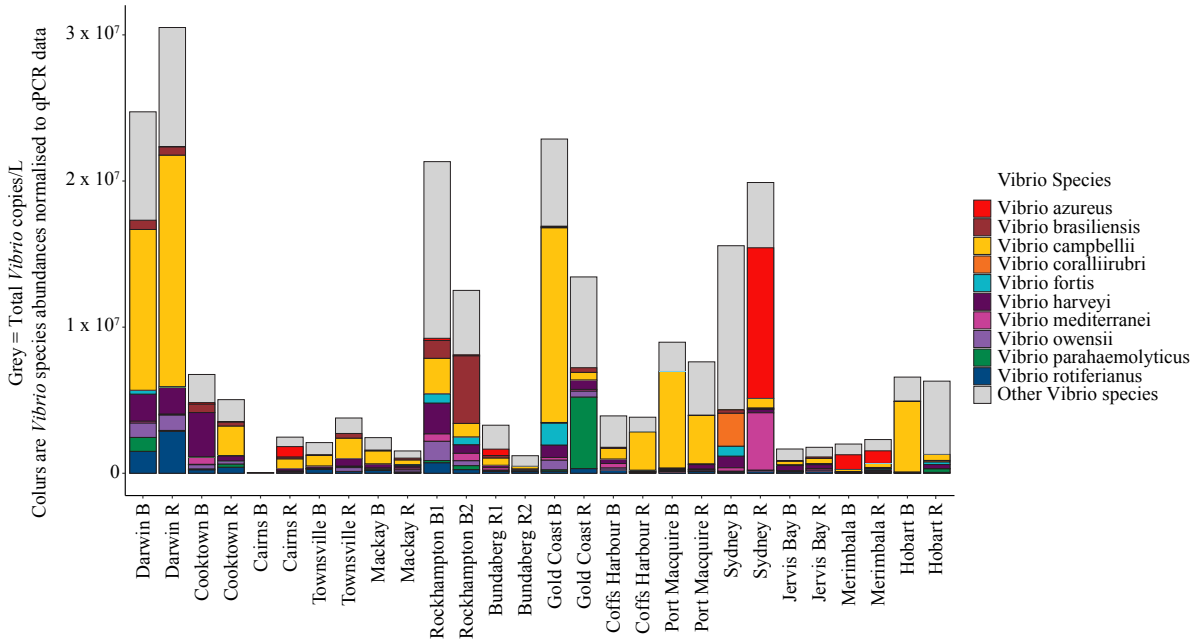

Figure 4. Stacked bar-plot of the top 10 most abundant *Vibrio* species from the *hsp60* gene amplicon sequencing. Data is normalised to the total *Vibrio* qPCR data (grey).

Among the most abundant *Vibrio* species, the relative abundance of *V. harveyi* (mean relative abundance = 7.69%, n = 78) was positively correlated with temperature, DO% and latitude [$r_s = 0.38$, 0.08 and 0.38, $p < 0.01$], and negatively correlated with salinity and pH [$r_s = -0.43$ and -0.54, $p < 0.01$]. The relative abundance of *V. harveyi* was also positively correlated

[r_s = 0.03, $p < 0.05$] with the relative abundance of one phytoplankton ASV belonging to the genus *Tetraselmis*. The relative abundance of *V. campbellii* (mean relative abundance = 34.94%, n = 78) was positively correlated with temperature and latitude [r_s = 0.18 and 0.10, $p < 0.01$] and negatively correlated with DO%, salinity and pH [r_s = -0.10. -0.32 and -0.46, $p < 0.01$]. *V. campbellii* relative abundance was also positively correlated with 17 phytoplankton ASVs, which were mostly members of the *Bacillariophyta* family. The strongest correlation [r_s = 0.1] with an ASV from the *Phaeocystis* genera.

Among known human pathogens, *V. parahaemolyticus* OTUs were detected in 78 % (n = 22/24) of samples, with their relative abundance positively correlated with latitude [r_s = 0.26, $p < 0.01$] and negatively correlated with salinity and pH [r_s = -0.71 and -0.52, $p < 0.01$] (Figure 5). *V. parahaemolyticus* relative abundance was also significantly correlated with two *Raphid-Pennate* ASVs [r_s = 0.28 and 0.12, $p < 0.05$], an *Arcocellulus* ASV [r_s = 0.09, $p < 0.05$], two *Olisthodiscus* ASVs [r_s = 0.09 and 0.02, $p < 0.05$], a *Teleaulax* ASV [r_s = 0.09, $p < 0.05$] and a *Marsupiomonas* ASV [r_s = 0.09, $p < 0.05$]. *V. vulnificus* OTUs were recorded at three sites, namely the tropical environments at Bundaberg R2 , Darwin B and Darwin R, where the relative abundance of this pathogen displayed a positive correlation to temperature, latitude and DO% [r_s = 0.06, 0.06 and 0.07, $p < 0.01$] while displaying a negative correlation to salinity [r_s = -0.47, $p < 0.01$].

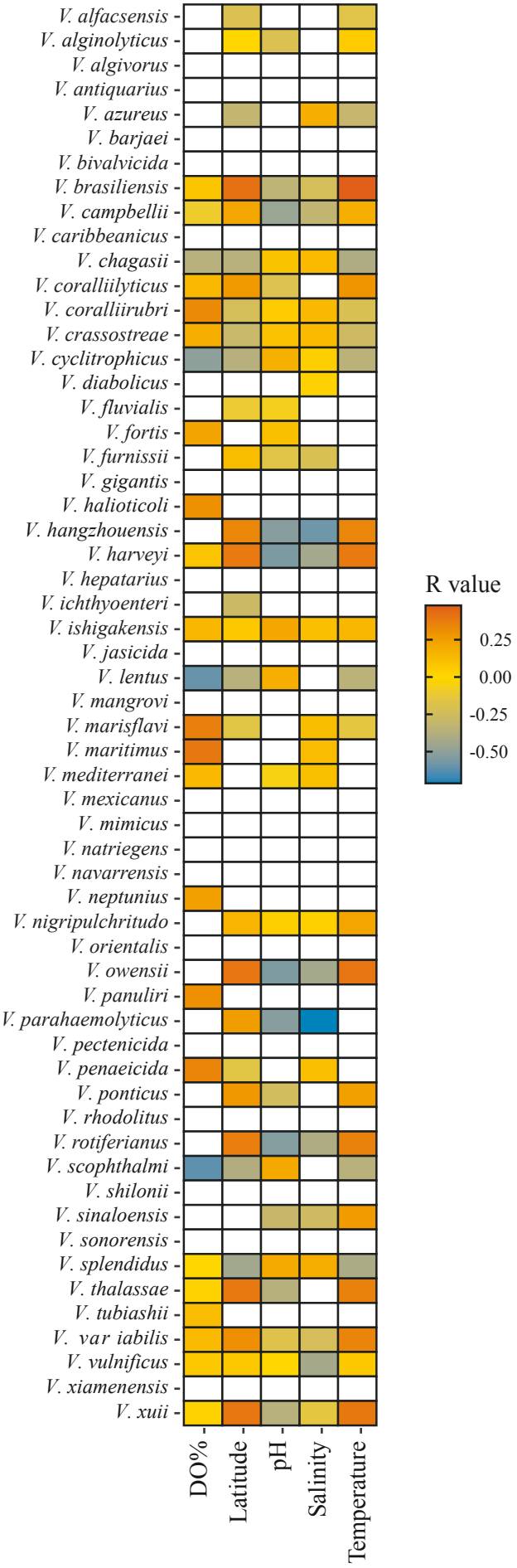

Figure 5. Heatmap displaying the correlations from MicTools analysis between environmental variables and *Vibrio* species from HSP60 dataset. Each cell is either coloured or white, with coloured cells representing pearsonR R value and white cells representing no significant correlation.

2.3.6 - Potentially Pathogenic Vibrio species: Vibrio Cholerae, Vibrio Parahaemolyticus and Vibrio Vulnificus

V. cholerae was not detected in any sample, which is consistent with the results from the *hsp60* sequencing analyses where this species was also not detected. *V. parahaemolyticus* was detected in 79% (22/28) of samples, with the highest levels detected at the Cooktown river site (15° 27' 37.8" S, 145° 14' 57.6" E) [mean: $2.56 \times 10^5 \pm 4.43 \times 10^5$ copies/L, n = 3] and the Jervis Bay beach site (35° 00' 46.0" S, 150° 41' 38.5" E) [mean: $9.5 \times 10^4 \pm 1.65 \times 10^5$ copies/L, n = 3]. On average, the tropical climatic zone had the highest levels of *V. parahaemolyticus* [mean: $4.59 \times 10^4 \pm 1.66 \times 10^5$ copies/L, n = 21], where they were 310-times higher than levels within the subtropical climatic zone and 1,814-times and significantly [$p < 0.05$] higher than levels within the temperate climate zone (Figure 3 E and F). *V. vulnificus* was detected in 57 % (16/28) of samples, with the highest levels detected at the Coffs Harbour beach site [mean: $1.34 \times 10^4 \pm 2.61 \times 10^3$ copies/L, n = 2] and the Gold Coast river site [mean: $1.26 \times 10^4 \pm 1.60 \times 10^4$ copies/L, n = 3]. On average, the subtropical climatic zone had the highest levels of *V. vulnificus* [mean: $3.65 \times 10^3 \pm 6.22 \times 10^3$ copies/L, n = 34], where they were 26-times higher than levels within the tropical climatic zone [mean: $2.90 \times 10^3 \pm 4.13 \times 10^3$ copies/L, n = 22] and 44 times higher than levels within the temperate climatic zone [mean: $2.54 \times 10^3 \pm 3.03 \times 10^3$ copies/L, n = 23] (Figure 3 C and D). In contrast to the patterns seen in the *hsp60* gene amplicon sequencing data, no significant correlations were observed between *V. vulnificus* or *V. parahaemolyticus* and any measured environmental variables. However, this may be due to the limited proportion of samples that these organisms were detected in, and it is notable that both organisms occurred in greatest abundance in warm water tropical and subtropical environments, such as Cooktown and the Gold Coast.

2.4 - Discussion

The principal goal of this study was to characterise patterns in the diversity and abundance of *Vibrio* species, along a large latitudinal gradient spanning the eastern coastline of Australia, which is a region that has been identified as a climate change hotspot (Hobday and Loug, 2011). Along this transect, it was observed that the highest levels of *Vibrio* bacteria were in Darwin, the northern most, and warmest site sampled, as well as positive correlations between both pathogenic and non-pathogenic *Vibrio* species with temperature, salinity, and phytoplankton ASVs.

Bacterial communities are often governed by differing environmental variables such as temperature (Gilbert et al., 2012) along latitudinal gradients. Previous studies have demonstrated that some bacterial populations change with latitude along the eastern coastline of Australia, including poleward increases in the abundance of members of the *Marine Roseobacter Group* (O'Brien et al., 2022), and latitudinal shifts in the abundance of aerobic anoxygenic phototrophic bacteria (Bibiloni-Isaksson et al., 2016). In this study, I observed a notable bifurcation of the total bacterial community into two significantly different groups that separated at approximately 30°S, into a northern and southern group of samples. Upon examination of the taxa responsible for this split, 11 *Vibrio* ASVs were defined as indicators of the northern community, which is consistent with prior observations that many *Vibrio* species show a preference for warmer waters (Eiler et al., 2006; Froelich et al., 2013; Heidelberg et al., 2002; Nigro et al., 2011; Oberbeckmann et al., 2012; Turner et al., 2009; Vezzulli et al., 2009; Wetz et al., 2008).

2.4.1 - Latitudinal trends in Vibrio abundance and diversity

Vibrio often exist in a higher abundance at low latitudes where water temperature is high (Padovan et al., 2021; Wong et al., 2019). I observed the greatest levels of *Vibrio* spp. in Darwin, the lowest latitude at which I sampled, as well as high levels in Rockhampton, the Gold Coast, and in Sydney. Not only were these sites amongst the sites with the warmest temperatures (Figure 1 B), but two of these sites, Darwin, and the Gold Coast River site, also had the lowest salinities. This finding aligns with other studies (Johnson et al., 2010; Oberbeckmann et al., 2012; Randa et al., 2004), which have also found a higher abundance of *Vibrio* bacteria at low salinities and high temperatures. While not examined in this study, in a recent study, *Vibrio* spp. were discovered to form biofilms on microplastic particles and, their

occurrence on these microplastics was correlated to proximity to major cities (Kesy et al., 2020), which may explain high levels of *Vibrio* bacteria at these locations, which are all highly urbanised. Another potential reason for these differences may be due to temporal changes, which were not accounted for in this study, with each site being sampled once within a period of 48 days during the Australian summer, and indeed, further studies comparing seasonality, and within season variation in *Vibrio* communities would provide further valuable insights into the major drivers of *Vibrio spp.* abundance patterns.

I observed a significant difference in community composition between all sites and between the tropical and temperate regions of the coastline. These differences were largely driven by heterogeneity in the relative abundance of *V. campbellii*, *V. azureus*, and *V. harveyi* OTUs, whereby *V. campbellii* and *V. harveyi* OTUs were more abundant in the tropical sites and *V. azureus* OTUs were more abundant at the temperate sites. Notably, strains of all of these species are known marine pathogens, infecting shrimp (Defoirdt and Sorgeloos, 2012), oysters (Green et al., 2019) and fish species (Istiqomah et al., 2020). These patterns show some similarities to those observed in other large-scale examinations of *Vibrio* diversity, where *V. campbellii* and *V. harveyi* were also amongst the most abundant *Vibrio* species isolated from corals, fireworms, soil, and water, along the tropical coast of Brazil (Chimetto Tonon et al., 2015). Additionally, *V. campbellii*, *V. azureus* and *V. harveyi* OTUs displayed positive correlations with specific phytoplankton groups identified in the 16S rRNA gene amplicon sequencing analysis. These observations point towards a potentially important role of phytoplankton in defining the abundance of some *Vibrio* species, which is consistent with previous observations (e.g., Turner et al. 2009) that have observed strong correlations between *Vibrio* and chlorophyll *a*. In this case, it is possible that species specific relationships underpin this pattern, which has been observed before during a yearlong time-series, where an unknown *Vibrio* species increased from baseline relative abundance of 0 - 2% up to 54%, closely following an increase in the relative abundance of the diatom *Chaetoceros compressus* (Gilbert et al., 2012).

Of the human pathogens detected within the community data, a *V. vulnificus* OTU was detected at the northern most sampling location Darwin, where water temperatures were < 32°C, as well as the Bundaberg river 2 site. *V. parahaemolyticus* OTUs occurred within 78% (22/28) of sites but were also most abundant in Darwin. *V. vulnificus* OTUs levels displayed a significant, albeit weak, correlation with temperature across the transect, but a much stronger negative correlation to salinity, which is consistent with previous observations (Blackwell and

Oliver, 2008; Oberbeckmann et al., 2012). *V. parahaemolyticus* was correlated positively with phytoplankton ASVs including a *Raphid-Pennate* ASV, an *Arcocellulus* ASV, two *Olisthodiscus* ASVs, a *Teleaulax* ASV and a *Marsupiomonas* ASV. Whilst *V. parahaemolyticus* has previously been shown to display ecological interactions with phytoplankton (Hartwick et al., 2021), to our knowledge this is the first evidence for links between *V. parahaemolyticus* and these specific phytoplankton taxa.

2.4.2 - Latitudinal patterns in Vibrio pathogens

Some strains of *V. cholerae* cause cholera, a disease responsible for ~100,000 deaths annually (Ali et al., 2015). However, non-cholera causing *V. cholerae* have also been implicated in milder forms of gastroenteritis, otitis, and life-threatening necrotizing fasciitis (Vezzulli et al., 2020). However, neither environmental nor toxigenic strains of *V. cholerae* were detected in any samples in this study. This is in contrast to recent studies that have detected low levels ($10^1 – 10^3$ copies/ml) of non-toxigenic *V. cholerae* in some of the Australian coastal environments examined here, including Darwin (Padovan et al., 2021) and Sydney Harbour (Siboni et al., 2016). Seasonal differences in the timing of sampling may explain these divergent observations.

V. parahaemolyticus can cause foodborne disease, and wound infections (Daniels et al., 2000). The highest levels of *V. parahaemolyticus* were detected in the tropical regions of the east Australian coast, where levels of this species were an order of magnitude higher than those observed in the temperate regions. The highest levels of *V. parahaemolyticus* were observed in Cooktown, where abundances reached levels similar to those recorded by Padovan et al. (2021), in the tropical waters around the Darwin area. However, it is notable that very high levels of *V. parahaemolyticus* were also observed in temperate samples, as far south as Jervis Bay (35° 00' 46.0" S, 150° 41' 38.5" E).

V. vulnificus causes foodborne disease, and severe wound infections, which can often result high rates of mortality (Baker-Austin et al., 2018). The abundance of *V. vulnificus* was not restricted to tropical waters, with levels 20 and 30 times higher in the subtropical sites compared to the tropical and temperate sites respectively. The highest levels of *V. vulnificus* were recorded at the Coffs Harbour beach (30° 18' 17.4" S, 153° 08' 34.9" E) and Gold Coast river (28° 10' 44.1" S, 153° 32' 30.1" E) sites. Notably, these levels were similar to levels previously recorded in tropical northern Australian waters (Padovan et al., 2021).

2.4.3 - Implications of high levels of Vibrio bacteria along Australia's east coast

This is the first study to examine the spatial dynamics of *Vibrio* abundance and diversity along Australia's eastern coast and has revealed levels of *Vibrio* to be higher in the tropical and subtropical sites compared to the temperate sites, with the highest levels in Darwin, the northern most site, which was characterised by the highest water temperature and lowest salinity. Models of future SST scenarios predict 38, 000 km of new coastal areas by 2100 being suitable for *Vibrio* growth as a result of climate change (Trinanes and Martinez-Urtaza, 2021), as well as an increase in *Vibrio* cases of 1.93 times for every 1 °C increase in SST (Baker-Austin et al., 2013). This is particularly concerning for Australia, whereby the SST is predicted to rise 1.5 °C – 3 °C by 2070, translating to a 2.9- to 5.8-times increase in the abundance of *Vibrio* spp in Australian waters.

Notably, *Vibrio* abundances were not always most strongly driven by temperature, which is contrast to numerous previous studies (Eiler et al., 2006; Froelich et al., 2013; Heidelberg et al., 2002; Nigro et al., 2011; Oberbeckmann et al., 2012; Turner et al., 2009; Vezzulli et al., 2009; Wetz et al., 2008). While the highest levels of total *Vibrio* were indeed detected in the very warm water tropical sites in Darwin, it is notable that I also observed high levels in higher latitude locations, including sub-tropical sites at Gold Coast and in Sydney. Notably these are two very densely populated coastal areas, where high levels of recreational use of waterways occurs, highlighting potential human health hazard through the exposure to these pathogens (Baker-Austin et al., 2018).

2.5 - Conclusions

The study of ecological patterns in the abundance and diversity of organisms is essential for developing an understanding of where and when they are abundant, and for predicting distributions in future scenarios. I observed significant differences in both the entire bacterial and *Vibrio* communities between the northern and southern sites. Across this transect, both pathogenic and non-pathogenic *Vibrio spp.* correlated positively with temperature and negatively with salinity. Interestingly, I also observed correlations between several pathogenic *Vibrio* species and specific phytoplankton species, highlighting ecological relationships with phytoplankton as a potentially important, but often over-looked, determinant of *Vibrio* spatial and temporal dynamics. During the summer period that this study was performed, I detected pathogenic *Vibrio* species not only in warm tropical waters, but southerly latitudes, including the highly urbanised environments, where opportunities for human exposure are significant. Given that ocean temperatures are rising (Doney et al., 2012), and severe rainfall events are increasing (Madakumbura et al., 2021) as a consequence of climate change, many coastal environments may become more ideal habitats for potentially pathogenic *Vibrio* species, indicating a potentially heightened human health risk.

Chapter 3 - Molecular microbiological approaches reduce ambiguity about the sources of faecal pollution and identify microbial hazards within an urbanised coastal environment

Author's state that author contributions are correct, and that the student has completed the work stated in the author contributions.

Author Signatures:

Author	Signature	Date
Nathan L.R. Williams	Production Note: Signature removed prior to publication.	11/08/2022
Nachshon Siboni	Production Note: Signature removed prior to publication.	11/08/2022
Jaimie Potts	Production Note: Signature removed prior to publication.	11/08/2022
Meredith Campey	Production Note: Signature removed prior to publication.	08/08/2022
Colin Johnson	Production Note: Signature removed prior to publication.	08/08/2022
Shivanesh Rao	Production Note: Signature removed prior to publication.	08/08/2022
Anna Bramucci	Production Note: Signature removed prior to publication.	08/08/2022
Peter Scanes	Production Note: Signature removed prior to publication.	1/09/2022
Justin R. Seymour	Production Note: Signature removed prior to publication.	11/08/2022

This work has been published: Williams, N.L.R., Siboni, N., Potts, J., Campey, M., Johnson, C., Rao, S., Bramucci, A., Scanes, P., Seymour, J.R., 2022. Molecular microbiological approaches reduce ambiguity about the sources of faecal pollution and identify microbial hazards within an urbanised coastal environment. Water Research. 218, 118534.

3.0 - Abstract

Urbanised beaches are regularly impacted by faecal pollution, but management actions to resolve the causes of contamination are often obfuscated by the inability of standard Faecal Indicator Bacteria (FIB) analyses to discriminate sources of faecal material or detect other microbial hazards, including antibiotic resistance genes (ARGs). I aimed to determine the causes, spatial extent, and point sources of faecal contamination within Rose Bay, a highly urbanised beach within Sydney, Australia's largest city, using molecular microbiological approaches. Sampling was performed across a network of transects originating at 9 stormwater drains located on Rose Bay beach over the course of a significant (67.5 mm) rainfall event, whereby samples were taken 6 days prior to any rain, on the day of initial rainfall (3.8mm), three days later after 43mm of rain and then four days after any rain. Quantitative PCR (qPCR) was used to target marker genes from bacteria (i.e., *Lachnospiraceae* and *Bacteroides*) that have been demonstrated to be specific to human faeces (sewage), along with gene sequences from *Heliobacter* and *Bacteriodes* that are specific to bird and dog faeces respectively, and ARGs (*sulI, tetA, qnrS, dfrA1 and vanB*). 16S rRNA gene amplicon sequencing was also used to discriminate microbial signatures of faecal contamination. Prior to the rain event, low FIB levels (mean: 2.4 CFU/100ml) were accompanied by generally low levels of the human and animal faecal markers, with the exception of one transect, potentially indicative of a dry weather sewage leak . Following 43 mm of rain, levels of both human faecal markers increased significantly in stormwater drain and seawater samples, with highest levels of these markers pinpointing several stormwater drains as sources of sewage contamination. During this time, sewage contamination was observed up to 1000 m from shore and was significantly and positively correlated with often highly elevated levels of the ARGs *dfrA1, qnrS, sulI* and *vanB*. Significantly elevated levels of the dog faecal marker in stormwater drains at this time also indicated that rainfall led to increased input of dog faecal material from the surrounding catchment. Using 16S rRNA gene amplicon sequencing, several indicator taxa for stormwater contamination such as *Arcobacter* spp. and *Comamonadaceae* spp. were identified and the Bayesian SourceTracker tool was used to model the relative impact of specific stormwater drains on the surrounding environment, revealing a heterogeneous contribution of discrete stormwater drains during different periods of the rainfall event, with the microbial signature of one particular drain contributing up to 50% of bacterial community in the seawater directly adjacent. By applying a suite of molecular microbiological approaches, I have precisely pinpointed the causes and point-sources of faecal contamination and other associated

microbiological hazards (e.g., ARGs) at an urbanised beach, which has helped to identify the most suitable locations for targeted management of water quality at the beach.

3.1 - Introduction

Beaches and estuaries used for recreational purposes deliver substantial societal and economic benefits (Bockstael et al., 1987; Lau et al., 2019). However, particularly when located within urbanised settings, these environments often experience reduced water quality, which can sometimes cause substantial public health risks (McLellan et al., 2015). Contamination of coastal waters can, often simultaneously, be derived from diverse sources, including urban and industrial runoff (Nevers et al., 2018), faeces from native (Nguyen et al., 2018) and domesticated animals (Green et al., 2014b), and sewage (McLellan et al., 2015). However, pinpointing the principal causes of contamination and subsequent degradation of water quality can often be challenging, impeding effective management.

Urban stormwater, which is washed into coastal environments in large volumes after rainfall events (Tsihrintzis and Hamid, 1997), can contain potential pathogens delivered into the environment from numerous sources, such as the surfaces of built infrastructure, soils and, animal faeces (McLellan et al., 2015). Stormwater pipes are also often contiguous to sewerage infrastructure and can experience sewage inputs during dry weather due to pipe blockages and leaks, and following rainfall during wet weather sewer over-flow events. As a result, untreated sewage can often be introduced to aquatic environments through stormwater infrastructure (Olds et al., 2018).

Contamination of urbanised beaches by sewage is a major public health concern (WHO, 2009) because sewage is enriched in pathogens, including viruses such as *Rotavirus*, *Norovirus* and *Adenovirus* (Strubbia et al., 2019) protistan parasites such as *Giardia duodenalis* and *Cryptosporidium* (Efstratiou et al., 2017), and bacteria such as *Escherichia coli* (Anastasi et al., 2012) and *Arcobacter* species (Fisher et al., 2014). The global economic impact of human illness linked to faecal contamination of coastal waters has been estimated to exceed $12 billion a year (Shuval, 2003).

In addition to pathogens, sewage and impacted water infrastructure also contains other microbiological hazards, including high levels of antibiotic resistant microbes (Karkman et al., 2019). Widespread use of antibiotics in medicine and agricultural settings (Kunin et al., 1973) results in large quantities of these chemicals in wastewater, which are difficult to remove during wastewater treatment (Ahmed et al., 2015). As a result, microbial assemblages inhabiting human waste-streams are exposed to consistently high levels of antibiotics (Michael et al., 2013), resulting in selection for antibiotic resistance (Bougnom et al., 2019). In addition,

antimicrobial resistance can also accumulate in the guts of medicated patients, who then shed resistant bacteria into sewage (Steinbakk et al., 1992). These antibiotic resistant bacteria can be introduced into coastal environments during stormwater and sewage over-flows (Carney et al., 2019), where they can pose a public health risk (Leonard et al., 2018).

Faecal contamination of aquatic habitats can also originate from agricultural (Dwight et al., 2005), domestic (Ervin et al., 2014) and native animals (Araujo et al., 2014), and can enter the environment in urban and agricultural (Lewis et al., 2019) runoff or via animals excreting their faeces directly into the environment (Araújo et al., 2014; Lewis et al., 2019). While often not given the same attention as sewage contamination, high levels of contamination by animal faeces can also potentially pose a human health hazard because animal faeces also harbour both pathogens (Sobsey et al., 2011) and antibiotic resistance bacteria (Ortega-Paredes et al., 2019).

Most coastal water quality monitoring programs quantify the presence of faecal contamination in the environment using standardised approaches to enumerate specific microbes, referred to as faecal indicator bacteria (FIB). FIB include bacterial species (e.g., *Escherichia coli*, *Clostridium perfringens* and enterococci (WHO, 2021) that reside in the faeces of warm-blooded animals (Layton et al., 2010), but rarely exist in significant numbers within uncontaminated waters, meaning they can be used as indicators of faecal contamination (Byappanahalli et al., 2012). FIB-based assessments of coastal water quality, however, have two significant limitations. Firstly, most FIB are not restricted to human faeces (sewage) but are present in the faeces of many other warm-blooded animals (Byappanahalli et al., 2012), which can create ambiguity around the true source of faecal contamination (i.e., human vs animal) within an environment. The second limitation of FIB methods is that they are insensitive to other microbial hazards in the environment, including endemic aquatic pathogens (Fisher et al., 2014), antibiotic resistance genes (ARGs) (Carney et al., 2019) and other emerging pathogens present in wastewater infrastructure (McLellan and Roguet, 2019). These limitations can both obfuscate the source of contamination and overlook potential health hazards.

To overcome the shortcomings of FIB analyses, Microbial Source Tracking (MST) approaches have been increasingly adopted to deliver more precise information on the sources of faecal contamination in natural environments (Ahmed et al., 2020a). MST typically employs molecular microbiological methods, such as quantitative PCR (qPCR) (Feng et al., 2018; Green et al., 2014a, 2014b, 2012; Templar et al., 2016), and more recently DNA sequencing

approaches (Brumfield et al., 2021; Newton et al., 2013), to quantify specific microbial marker genes. Whilst one potential caveat of DNA-based approaches is that they may sometimes detect a signal from unviable cells, potentially leading to over-estimates of impact, they have continuously been able to unambiguously identify sources of faecal contamination within an environment (Ahmed et al., 2019; Ahmed et al., 2020a; Alm et al., 2018; Green et al., 2019a; Li et al., 2021; Shrestha et al., 2018).

Urbanised coastal ecosystems are regularly negatively impacted by a wide variety of contamination sources, which can enter the environment from multiple potential origins, and it is often very difficult for managers to pinpoint both the cause and point sources of contamination. At Rose Bay, the location of this study, it was known that there was a high level of faecal contamination, however it was not clear if this faecal contamination was animal or human. It was also not know where in the catchment this faecal contamination was originating, with multiple drains having suspected sewage leaks within them. Finally, with drains as the suspect contamination source, it was unknown how strongly each of these drains impacted the water quality of Rose Bay. Therefore, our principal goals were to determine the source and location of input of fecal contamination, and to do this, I used a combination of FIB and MST qPCR techniques, in addition to detailing the spatial and temporal distribution of contamination using 16S rRNA amplicon sequencing, which together form the scientific basis for protecting public health with informed management decisions. In this study, Rose Bay has been utilised as a model environment to demonstrate the utility of microbial source tracking and DNA sequencing approaches to elucidate the source (i.e., animal faeces vs sewage) and location of faecal contamination.

3.2 - Methods

3.2.1 - Sampling Sites

Rose Bay is an urban beach located in the Sydney Harbour estuary and near to the centre of Sydney, which is Australia's largest city, with a population of over 5 million people. This site was targeted based on consistently poor water quality ratings, according to regularly high FIB levels, within the regional water quality monitoring program *Beachwatch* (OEH, 2018). The beach receives stormwater runoff from nine drain networks, which feed directly onto the beach and is also a popular dog-walking beach.

Water samples were collected from a network of 10 transects, comprising a total of 41 sampling locations (Figure 1), which were chosen according to proximity to potential points of contamination. These included sampling points within the outlets of 9 stormwater drains, which are mainly conduits for urban stormwater, but in some instances may be impacted by wet weather sewer overflow events. Water samples were collected from points located along transects originating at points adjacent to each of these drains, to examine the extent of dispersal of contamination from drains into Rose Bay. Surface seawater samples were collected along the transect from immediately adjacent to drains at the shoreline in water of 50cm depth [x.1], 250m offshore [x.2] and 500m offshore [x.3]. Samples were also collected from a suite of reference points, including the 'Beachwatch' routine monitoring site located at the western end of Rose Bay, and a deep-water transect across the entrance to Rose Bay (x.4), located 1000m offshore and used here to determine the broader spatial extent of faecal pollution from Rose Bay and the background contamination in Sydney Harbour. Finally, samples were also collected from a 'Control' site, within Nielsen Park (Sydney Harbour National Park), which is located 2km from Rose Bay, has no urban stormwater infrastructure and dogs are prohibited on the beach.

Sampling was conducted over the course a significant rainfall event, which involved a total of 69.8 mm of rain falling over a period of five days, including 43 mm within one 24-hour period. Samples were collected from the locations described above on four occasions, corresponding to six days before rain (21/8/19), a light rainfall event (3.8 mm) (27/8/19), the peak rainfall event (43 mm) (30/8/19), and four days after rain (3/9/19). Of note, drains 2, 7, 9 and 10 did not have sufficient flow to be sampled on the 21/8/19, nor did drain 7 on the 27/8/19 or drains 2, 5, 7, 9 and 10 on the 3/8/19.

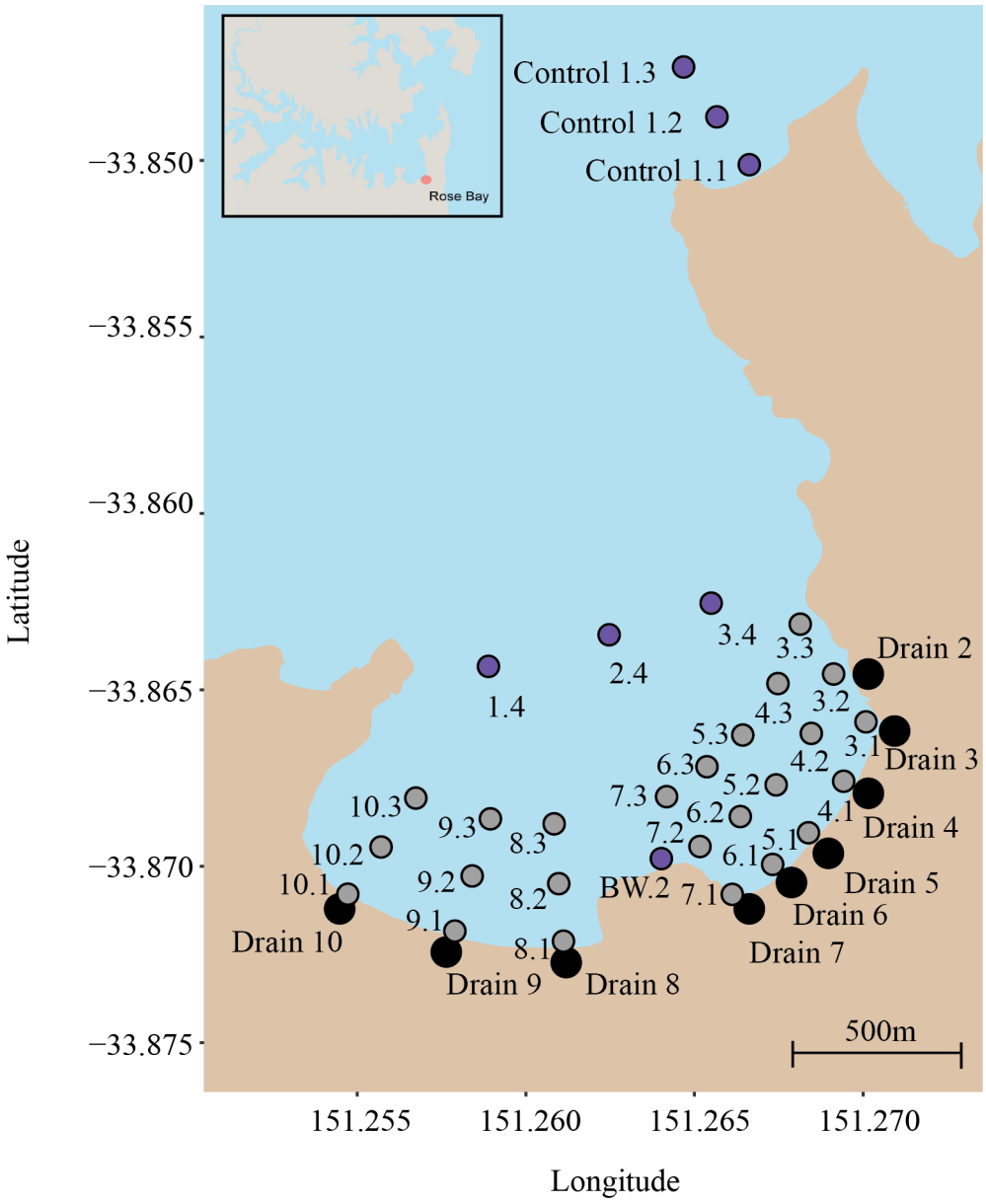

Figure 1. Map of Rose Bay sampling points. Black circles are drain samples, while grey circles refer to seawater transect samples collected from surface seawater from the shoreline (x.1), and 250m (x.2) and 500m (x.3) offshore. Purple circles refer to reference samples which were collected from Nielsen Park (1.1, 2.1 and 3.1), which has no storm water drains running into it, a deep-water transect across the entrance to Rose Bay (1.4, 2.4 and 3,4), approximately 1000m offshore and the regularly monitored Beachwatch site (BW.2).

3.2.2 - Sample Processing and Analyses

Water samples were collected using 10L pre-sterilised plastic containers and filtered through 47mm, 0.22 µm pore-size membrane filters (Millipore, DURAPORE PVDF .22UM WH PL) using a peristaltic pump (100rpm), within 2hrs of sample collection. Before each sample was filtered 250ml 10% bleach was run through the pump, followed by 500ml MiliQ water, and then sample. Volume filtered of each sample (between 500 ml and 2000 ml) was recorded to allow for normalisation of gene copy numbers. Filters were stored at -80°C, until DNA was extracted using the PowerWater DNA isolation Kit (QIAGEN). DNA extractions were performed in batches of either 48 or 96, with every batch including 3 kit blanks, which were subsequently included in in all qPCR analyses. Physiochemical parameters including temperature, dissolved oxygen, salinity, and pH were measured in situ using a WTW multiprobe meter (Multi3430, Germany). Salinity ratio was calculated as per methods described by (Ho et al., 2021) (Appendix 2 Section 1.2).

To quantify Chl-a concentrations, a 110ml water sample was taken at each site and filtered through a 0.45 µm glass fibre filter. The filter was immediately frozen and returned to the laboratory for analysis of Chl-a concentration using a modified APHA Method 10200-H (Eaton and Franson, 2005).

At all sites, three water samples were collected for nutrient analysis. One unfiltered sample was collected using a disposable syringe and transferred directly into a 30ml sterile vial for total nutrient analysis. Two additional samples were collected and passed through a 0.45mm cellulose acetate syringe filter into two additional tubes for dissolved total and inorganic nutrient analysis. All nutrient samples were immediately frozen prior to analysis using standard methods; Nitrate and Nitrite (APHA 4500-NO3-I -Cadmium reduction method), Ammonium N (APHA 4500-NH3-H: Phenate method), filterable reactive phosphorus (FRP) (APHA 4500-P-E-Ascobic acid method), Total Nitrogen (TN), Total Phosphate (TP), Total Dissolved Nitrogen (TDN), Total Dissolved Phosphate (TDP) (APHA 4500-P-J: Persulfate digestion method) (Eaton and Franson, 2005).

3.2.3 - Enterococci analysis

Levels of the FIB enterococci were measured using standard membrane filtration techniques at a commercial diagnostic laboratory following the Australian standard (AS/NZS 4276.9:2007), as per the sampling technique performed regularly by the local government.

3.2.4 - Quantitative PCR (qPCR) analysis of MST markers

Quantitative PCR (qPCR) targeting the bacterial 16S rRNA gene, using the BACT1369F and PROK1492R primer pair and the TM1389F probe was used to provide a measure of bacterial abundance within each sample (Suzuki et al., 2000). To detect the presence of human faeces, I employed two qPCR analyses, including the HF183 assay (Templar et al., 2016), which targets human gut microbiome-associated HF183 *Bacteroidales* cluster and the Lachno3 assay (Feng et al., 2018), which targets human gut microbiome-associated *Lachnospiraceae*. To detect faeces from dogs, I used the DG3 assay (Green et al., 2014b), which targets dog-specific *Bacteroidales,* and to detect faeces from birds I used the GFD assay (Green et al., 2012), which targets bird-specific *Heliobacter* (Table 1, Appendix 2).

QPCR was also used to quantify a suite of antibiotic resistance genes (ARGs) that have previously been detected in high abundances at two Sydney beaches exposed to wet weather associated sewage incursions (Carney et al., 2019), including the genes *sulI* which confers resistance to sulfonamide antibiotics in gram-negative bacteria (Huovinen et al., 1995), *tetA* which encodes an inner membrane protein antiporter (Allard and Bertrand, 1992) which aids resistance to tetracycline, *qnrS* encodes a pentapeptide protein that defends DNA gyrase and topoisomerase IV from inhibition by quinolone (Berglund et al., 2014), *dfrA1* which encodes a dihydrofolate reductase that confers resistance to the antibiotic trimethoprim (Lombardo et al., 2016) and *vanB* which encodes resistance to vancomycin (Berglund et al., 2014), which is a last line of defence antibiotic (Berglund et al., 2014). Each qPCR assay was performed using a BIO-RAD CFX384 Touch™ Real-Time PCR Detection System™. (For QPCR assay details see Table 1, Appendix 2).

In each case, gene copies were calculated for each target, using a (6-7 point) standard curve using BIO-RAD's CFX MAESTROTM software version 1.1. Standard curves were generated from known concentrations of a synthesised DNA fragment of each targeted gene, with a standard curve run with each plate. Samples outside of the calibration curve were considered below the limit of detection and included in the analysis as 0. Each DNA fragment for the standard curve was checked using MEGA7 to ensure they matched both primers, the probe (if applicable) and target gene and blasted in the NCBI database to ensure it was from the correct target gene. Along with standard curves, a no template control (NTC) was added to each qPCR run. For further details on qPCR analysis, see Appendix 2 section 1.1.

3.2.5 - 16S sequencing and analysis

To characterise bacterial community composition in seawater and stormwater drain samples, the V3–V4 region of the bacterial 16S rRNA gene was amplified using the 341f/805r primer set (Suzuki et al., 2000), with the following cycling conditions: 95°C for 3 minutes followed by 25 cycles of: 95°C for 30 seconds, 55°C for 30 seconds, 72°C for 30 seconds, and then 72°C for 5 minutes with a final hold at 4°C (Pichler et al., 2018). Amplicons were subsequently sequenced using the Illumina MiSeq platform (300 bp paired-end analysis at the Ramaciotti Institute of Genomics, University of New South Wales). For sequencing analysis details, refer to Appendix 2. Raw sequences were uploaded to NCBI, BioProject ID PRJNA766238.

Paired R1 and R2 reads were subsequently processed using the DADA2 pipeline (Callahan et al., 2016). Reads with any 'N' bases were removed and bacterial V3-V4 primers were truncated using cutadapt (Martin, 2011). Reads were trimmed to remove low quality terminal ends (trunc (R1= 280; R2= 250)). To produce the highest number of merged reads after learning error rate and removing chimeric sequences, I used the dada2 removeBimeraDenovo program at the default threshold stringent minFoldParentOverAbundance=1. ASVs were annotated against the SILVA v138 database with a 50% probability cut-off. The ASV table was subsequently filtered to remove ASVs not assigned as kingdom Bacteria, as well as any ASVs classified as chloroplast or mitochondria. Finally, the dataset was rarefied to 30,000 reads using vegan (Dixon, 2003).

3.2.6 - Statistical Analysis

To test for differences in abiotic variables, enterococci counts and qPCR copies/100 ml, the nonparametric Kruskal-Wallis test was used, followed by Mann-Whitney pairwise comparisons with Bonferroni corrected p-values. Correlations between enterococci counts, and data derived from qPCR assays were determined using Spearman's RS, with Bonferroni corrected p values. These statistics were performed in Past Version 4 (Hammer et al., 2001).

To test for differences in microbial community composition and alpha diversity (16S rRNA data) between samples I used the Adonis function from *Vegan* (Dixon, 2003) and the pairwise.adonis function from the *PairwiseAdonis* (Martinez Arbizu, 2020) R package. To determine which ASVs were responsible for the dissimilarity between dry weather (before and after rain event) and wet weather (both days of rain), performed a SIMPER analysis on square

root transformed data. To determine which ASVs represented 'indicator taxa' for drain communities, the multipatt function within the *indicspecies* package (de Caceres and Jansen, 2018) was implemented using the drain and seawater communities. Identified ASVs with an average relative abundance <0.01% were filtered from the resulting dataset. Finally, I used the 16S rRNA bacterial community profiles as a tracer of contamination from each stormwater drain experienced at the Beachwatch reference site by applying the predict function within the R package *SourceTracker* (Knights et al., 2011). This was performed by measuring the extent of microbial signature from source samples, which included each of the stormwater drains as well as a seawater community "control" (Rose Bay Entrance 1km offshore) within a sink sample (the 'Beachwatch' site). I also used the output of *SourceTracker* to calculate and display the spatial extent of impact from specific stormwater drains across Rose Bay. In this case, the source samples were again, drains, and the sink samples were the Rose Bay seawater samples. Given that each drain had a significantly different bacterial community, I were able to analyse what percentage of each drains unique "source" bacterial community contributed to each seawater "sink" bacterial community, allowing for an assessment of the impact of each drain on the Bay. I analysed the contribution of Drain 5 during dry weather, Drain 5 after 3.8mm of rain, Drain 3 after 43mm of rain and Drain 6 post rain event, as on each given day, these drains had the highest levels of the Lachno3 qPCR marker for sewage. For each analysis I created a grid with a high resolution of co-ordinates (53578 points) and used the R package "Raster" (R. Hijmans et al., 2010) to predict the data at these 53578 points which were then plotted onto the map of Rose Bay. For further details on indicator species and *SourceTracker* analysis see R scripts on GitHub (https://github.com/Nwilliams96/Rose-Bay-Wet-Weather-2019). To test for differences between the contribution of individual drains on the 'Beachwatch' site and then differences between the contribution of single drains at the Rose Bay seawater sites, I used the nonparametric Kruskal-Wallis test followed by Dunn's Post Hoc pairwise comparisons with Bonferroni corrected p-values (Hammer et al., 2001). Drain 3 (21/8/19, 27/8/19), Drain 9 (27/8/19) and Drain 10 (27/8/19) had evidence of seawater washing into them and were removed from this specific analysis.

3.3 - Results

3.3.1 - Environmental Conditions

Six days before the rain event (21/8/19), mean seawater temperature, salinity and turbidity levels at Rose Bay were 15.5°C ± 0.3 [n = 31], 35ppt ± 0.5 [n = 31] and 0.70 NTU ± 0.56 [n = 31] respectively. Notably, on this day, freshwater from the drains [mean salinity: 0.25 ± 0.06 ppt, n = 4] impacted salinity levels nearshore, which were significantly lower [$p < 0.01$] when compared to samples that were taken 500m offshore. On the 27/8/19 (second day of sampling), a total of 3.8mm of rainfall was recorded and on the 30/8/19 (third day of sampling) 43mm of rain was recorded. Following this rain, inputs of significantly [$p < 0.01$] more turbid [mean: 18.3 NTU, ± 9.04, n = 8] and fresh [mean: 3 ppt, ± 0.05, n = 8] stormwater led to significant drops [$p < 0.01$] in both salinity and optical density. Of note, after 43mm of rain, the samples nearshore were most impacted by stormwater, with the salinity at these sites being significantly lower [$p < 0.01$] than sites 250m and 500m offshore, with a mixing ratio of 1:34 (one part freshwater to 34 parts seawater). Three days after the rain event (3/9/19), with 4/9 stormwater drains still running, the salinity nearshore was again significantly lower nearshore [$p < 0.01$] compared to sites 250m and 500m offshore.

Inputs of stormwater also led to a significant rise [$p < 0.01$] in chlorophyll, filterable reactive phosphorus, and total dissolved phosphate levels. In contrast to the patterns observed within Rose Bay, the rainfall event did not lead to a significant change within any of the tested environmental variables at the control site at Nielsen Park. Three days after the rain event, levels of total phosphate in Rose Bay decreased significantly [$p < 0.01$] relative to during the rainfall event. Levels of nitrate-nitrite, total dissolved nitrogen and total nitrogen did not change significantly when comparing samples taken before the rain event (21/8/19) to samples taken during rainfall (27/8/19 and 30/8/19) but were significantly elevated [$p < 0.01$] after three days of no rain (Appendix 2 Table 4 and 5).

3.3.2 - Bacterial Abundance

Prior to the rainfall event levels of the 16S rRNA gene, used here as a proxy for bacterial abundance, were significantly lower within the drain samples [$p < 0.01$] compared to the Rose Bay seawater. After 3.8mm of rain the levels of the 16S gene (mean: 7.64×10^{10} copies/100ml ± 3.87×10^{10}, n = 79) increased by 95% within the Rose Bay seawater samples (mean: 3.91×10^{10} copies/100ml ± 3.74×10^{10}, n = 86), and increased significantly [$p < 0.01$] within the drain

water, where levels were an order of magnitude higher than those observed in the seawater. After 43mm of rain, mean levels of the 16S rRNA gene decreased by 37% within Rose Bay seawater samples, but in contrast increased significantly [$p < 0.01$] within the drain samples relative to the preceding sampling date, where again, levels of the 16S gene were an order of magnitude higher than those observed in the seawater. Three days after the rain event (3/9/19), 16S rRNA gene concentrations with the drains were not statistically distinguishable to those observed during the rainfall event but were significantly elevated within the seawater [$p<0.01$] relative to the other sampling time-points.

3.3.3 - Faecal Indicator Bacteria

Significant changes in enterococci levels were observed between sites and over time (Figure 2, A). Throughout the dataset enterococci levels were negatively correlated with salinity [$p < 0.05$, $r_s = -0.60$], but positively correlated with pH, turbidity, FRP, NH_4, NO_x, TDN, TDP and TN [$p < 0.05$, $r_s > 0.46$]. Prior to rainfall, enterococci levels were low (mean: 2.4 ± 31.7 CFU/100ml, n = 30) within all seawater samples, with the exception of the sample located immediately adjacent to Drain 5 (site 5.1), which reached 180 CFU/100ml. Enterococci levels were elevated within all sampled stormwater drains (mean: 154 ± 183.2 CFU/100 ml, n = 5), with the highest levels observed in Drain 3 (470 CFU/100ml). Following a light rainfall (3.8mm, 27/8/19) event, enterococci levels within all drains increased by an order of magnitude, with levels reaching [mean: 1,072 ± 1113.7 CFU/100ml, n = 8]. However, marked spatial variability in enterococci counts occurred between drains (Figure 2, A), with highest levels observed in Drains 3, 4 and 5. While notable increases in enterococci levels were observed in several drains, levels generally remained very low (mean: 8.6 ± 14.4 CFU/100ml, n = 31) within the seawater samples collected from Rose Bay, indicating minimal impact from the drains during this low rainfall event.

Following 43mm of rain (30/8/19), enterococci levels within all samples were elevated relative to samples taken after 3.8mm of rain and before the rain event (21/8/19). Within stormwater drains, enterococci levels became extremely high (mean: 95,250 ± 67711.0 CFU/100ml, n = 8), with highest levels observed in Drains 10 (190,000 CFU/100ml) and 3 (170,000 CFU/100ml). During this period, enterococci levels also increased significantly [$p<0.01$] within Rose Bay seawater samples relative to seawater samples taken before the rain event (21/8/19), with levels reaching (mean: 18, 268 ± 60468.7 CFU/100ml, n = 31).

enterococci levels within the seawater samples were also significantly greater [$p < 0.01$] than those observed at the control site at Nielsen Park (mean: 20.7 CFU/100ml, SD ± 2.9, n = 3). However, there was substantial spatial variability in the extent of impact within Rose Bay, with Enterococci levels significantly higher near to stormwater drains, relative to the offshore points in transects (Figure 2, A). Specifically, while enterococci levels within the most offshore samples only reached 26 CFU/100ml, enterococci levels reached (mean: 21,590 CFU/100ml ± 40382.9 CFU/100ml, n = 8) at the sampling points closest to the shore and drain outlet points. Highest enterococci levels were observed in samples collected between Drains 2 and 3 (320,000 CFU/100ml; sample 3.2) and adjacent to Drain 10 (120,000 CFU/100ml). Following a period of 72 hours without further rainfall, enterococci levels within Rose Bay seawater samples dropped by two orders of magnitude (mean: 30 ± 107.8 CFU/100ml, n=31). Among drains that could be sampled at this time, enterococci levels also dropped (mean: 269 ± 254.1 CFU/100ml, n=4), but remained high in Drains 3 (480 CFU/100ml) and 5 (600 CFU CFU/100ml).

3.3.4 - Microbial Source Tracking

3.3.4.1 - Human faecal markers

Within Rose Bay seawater samples, the two human faecal marker genes employed here, Lachno3 and HF183, indicative of human gut microbiome associated *Lachnospiraceae* and *Bacteriodes* bacteria (Feng et al., 2018;Templar et al., 2016), were detected in 79% (n=95/120) and 61% (n=74/120) of samples respectively. Across the data set, both Lachno3 and HF183 levels were negatively correlated with salinity [$p < 0.05$, $r_s = -0.53$] and positively correlated with turbidity, FRP, NH_4, NO_x, TDN and TDP [$p < 0.05$, $r_s > 0.23$]. Levels of both markers across the entire dataset (HF183 – mean: 33.35 $x10^4$ ± 1.35 x 10^5 copies/100ml, n = 284. Lachno3 – mean: 1.71 x 10^5 ± 1.28 x 10^5 copies/100ml, n = 271) were significantly [$p < 0.01$] higher within Rose Bay than within the control site at Nielsen Park (HF183 – mean: 2.39 x 10^4 ± 4.90 x 10^4 copies/100ml, n = 29. Lachno3 – mean: 1.62 x 10^4 ± 3.15 x 10^4 copies/100ml, n = 30). Both markers displayed moderate, but statistically significant correlations to total enterococci counts (Lachno3: $r_s = 0.363$, $p = 0.012$; HF183: $r_s = 0.365$, $p = 0.0163$).

Before the rain event (21/8/19), the Lachno3 and HF183 human faecal marker genes were detected in 90% (n = 27/30) and 50% (15/30) of Rose Bay seawater samples respectively, but detectable concentrations were only 2.1 and 0.7 times higher, and not statistically

distinguishable from those observed within the Nielsen Bay control site. Except for HF183 in the Drain 9 transect, highest seawater concentrations of these human faecal markers were always observed in samples immediately adjacent to drains (Figure 2 B, C). This pattern was in-line with the significantly higher [$p < 0.01$] concentrations of both human faecal marker genes (HF183 – mean: $6.09 \times 10^4 \pm 1.12 \times 10^5$ copies/100ml, n = 12, Lachno3 – mean: $9.86 \times 10^4 \pm 31.57 \times 10^5$ copies/100ml, n = 15) within the drain samples, which were 24 and 23 times greater than in the seawater samples (HF183 – mean: $1.02 \times 10^3 \pm 2.07 \times 10^3$ copies/100ml, n = 82. Lachno3 – mean: $4.79 \times 10^3 \pm 9.40 \times 10^3$ copies/100ml, n = 77), with highest levels of both markers observed in Drain 5.

Following a light rainfall (3.8mm, 27/8/19) event, concentrations of the Lachno3 and HF183 human faecal markers in drain samples increased by 2.6 and 22 times respectively, with highest concentrations again observed in Drain 5. Among Rose Bay seawater samples, Lachno3 levels (mean: 1.15×10^4 copies/100ml $\pm 4.80 \times 10^4$, n =77) increased by 17-fold relative to seawater samples taken before the rain event (21/8/19), with highest concentrations observed in samples adjacent to Drain 5. Consistent with patterns observed in the enterococci counts, concentrations of both markers were generally very low beyond the immediate shoreline (i.e., >250m offshore).

Further significant [$p < 0.01$] increases of both human faecal markers occurred within drains and adjacent seawater samples following a larger (43mm, 30/8/19) rainfall event. Across all drain samples, concentrations of Lachno3 and HF183 increased significantly [$p < 0.01$] by 109 and 76 times relative to conditions before the rain event on the 21/8/19, with highest concentrations of both markers observed within Drain 3 (Figure 2 B, C). The high concentrations of human faecal markers in Drain 3, were reflected within the Rose Bay seawater samples, with highest concentrations of both markers observed in Rose Bay transect samples adjacent to Drain 3 (Figure 2 B, C), where the highest seawater concentrations of human faecal markers recorded during this study period were observed. While clear gradients in both Lachno3 and HF183 were observed across the transect adjacent to Drain 3, in most other transects there was an immediate decay in human faecal marker levels beyond the sample collected from immediately proximate to the drain, which was consistent with the patterns observed in the enterococci analysis.

Following a period of 72 hours without further rainfall on the 3/9/19, concentrations of HF183 and Lachno3 (HF183 – mean: $6.4 \times 10^4 \pm 7.27 \times 10^4$ copies/100ml, n=74. Lachno3 – mean: $3.07 \times 10^4 \pm 7.94 \times 10^4$ copies/100ml, n = 74) dropped by over 11- and 60-times

respectively (Figure 2 B, C). However, this pattern was highly variable among sampling locations and the two assays, with Lachno3 and HF183 (detected in 100% (n= 34/34) and 82% (n = 28/34) of samples) levels being significantly lower within Rose Bay seawater [$p < 0.01$] in comparison to the preceding time point. Highest levels of the human faecal markers persisted in Drain 3, 4 and 6 and water samples immediately adjacent to Drains 7 and 10. It is noteworthy, that levels of the Lachno3 and HF183 markers remained elevated in several seawater samples for 4 days after rainfall, and after enterococci levels had decreased.

3.3.4.2 - Dog Faecal Marker

Across the entire dataset, the dog faeces marker, DG3 was detected in only 40% (n = 60/148) of samples but was significantly correlated to enterococci levels [$r_s = 0.47$, $p < 0.05$]. DG3 levels were also positively correlated with turbidity, FRP, NH_4, NO_x, TDN, TDP and TN [$p<0.05$, $r_s > 0.32$] and negatively correlated with salinity [$p < 0.05$, $rs = -0.51$]. Prior to the rainfall event on the 21/8/19, DG3 was detected in only 22% (n= 8/36) of samples, with all detections in nearshore samples (except BW.2 and 3.2) (Figure 2, D). This dog faeces specific marker was not detected in any of the tested drain samples during this time.

After 3.8mm rain (27/8/19), detection levels of the dog faeces marker remained low [20% (n = 8/39)], yet concentrations of the marker (mean: $1.76 \times 10^3 \pm 7.04 \times 10^3$ copies/100ml, n = 81)increased significantly [$p < 0.01$] by 6-fold. Notably, there was also a clear shift in the location of DG3 detections (Figure 2, D), with half (50%, n = 4/8) of detections observed in drain samples (highest concentrations observed in Drains 8 and 6) rather than seawater samples.

Following 43mm of rain (30/8/19), DG3 levels (mean: 8.91×10^5, $\pm 1.08 \times 10^6$ copies/100ml, n = 24) were significantly elevated [$p<0.01$] within the drains (highest in Drains 3, 5 and 8) compared to conditions before the rain event (21/8/19). Within nearshore seawater samples, DG3 levels (mean: $5.25 \times 10^4 \pm 5.44 \times 10^4$ copies/100ml, n = 21) were statistically indistinguishable compared to levels recorded prior to rainfall (mean: $1.59 \times 10^4 \pm 2.40 \times 10^4$ copies/100ml, n = 23), but in offshore samples were significantly elevated [$p<0.01$] relative to conditions before the rain event and highest along transects 3, 5 and 8 (Figure 2, D).

Following the rainfall event (3/9/19), the DG3 marker was only detectable in one drain (Drain 3), at significantly lower levels [$p < 0.01$] than during the rainfall event (both 27/8/19 and 30/8/19), but was detected in all nearshore seawater samples (except 9.1) and in 37 % (n =

6/13) of offshore samples (Figure 2, D), although concentrations of this marker were significantly lower [$p < 0.01$] than during rainfall periods.

3.3.4.3 - Bird Faecal Marker

The GFD avian faecal marker was detected in 88 % (n = 130/148) of samples, but levels of this marker were not significantly correlated [$r_s = 0.1$, $p > 0.05$] with enterococci counts and were statistically indistinguishable between Rose Bay and the control site, during both dry (before rain on the 21/8/19 and after rain on the 3/9/19) and wet weather conditions (3.8 mm rain on the 27/8/19 and 43 mm on the 30/8/19). No trend of increasing levels of GFD following rainfall was observed, in either drains or seawater samples, with concentrations of this marker often in fact decreasing following rainfall (Figure 2, E).

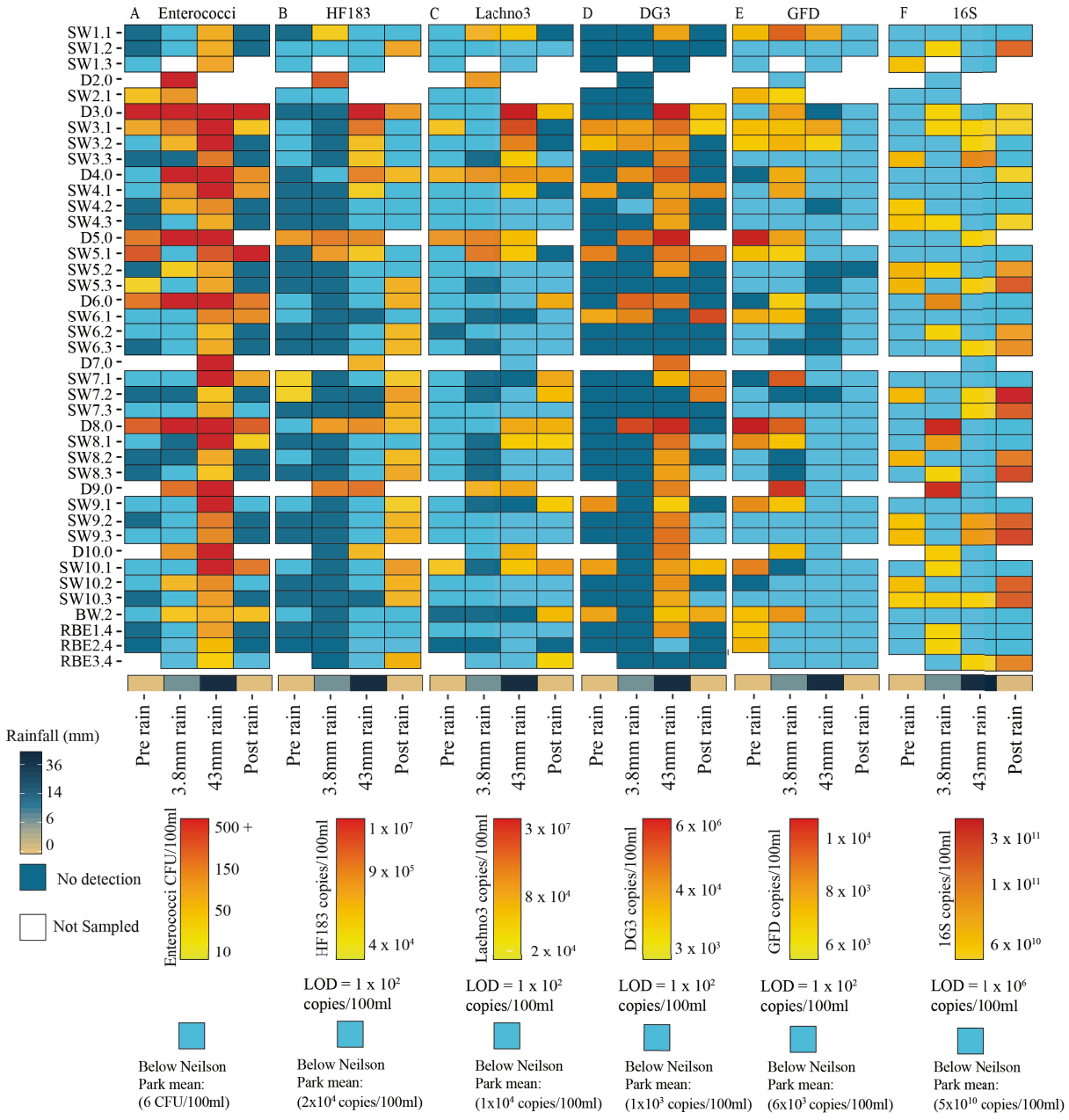

Figure 2. Source tracking qPCRs and FIB CFU before and following rain events. Heatmaps of the enterococci Counts using standard membrane filtration techniques (AS/NZS 4276.9:2007) and the 4 source tracking qPCRs. (A) enterococci (B) HF183, (C) Lachno3, (D) DG3 and (E) GFD, (F) 16S across sampling locations (Y axis) and days (x axis). Colour scale corresponds to CFU or copy number per 100mL, with the lower scale (Aqua) representing the average of that marker detected at the reference Nielsen Park transects, over the course of the study. Blank cells represent samples not collected either due to lack of water flow in drains or due to safety concerns during the rainfall event. Dark blue cells correspond to no detection. Below each qPCR heatmap is a small heatmap displaying daily rainfall (mm) at the time sampling. Limit of detection (LOD) is in copies/100ml.

3.3.5 - *Genes conferring Antibiotic Resistance*

Throughout the sampling period, levels of the antibiotic resistance genes *dfrA1, qnrS, sulI* and *vanB* were correlated with the human faecal marker HF183 [$r_s > 0.25$, $p < 0.01$]. Before the rain event *sulI* was detected in 19% (n = 6/30) of seawater samples. However, *sulI* levels were an order of magnitude lower within the seawater samples (mean: $7.96 \times 10^1 \pm 2.16 \times 10^2$ copies/100ml, n = 29) than within the drain samples (mean: $2.07 \times 10^4 \pm 3.19 \times 10^4$ copies/100ml, n = 15). *qnrS* was detected in 43% (n = 13/30) of seawater samples. However, levels of this gene within the drains (mean: $9.77 \times 10^2 \pm 2.52 \times 10^3$ copies/100ml, n = 14) and seawater samples (mean: $1.38 \times 10^3 \pm 3.23 \times 10^3$ copies/100ml, n = 67) could not be statistically distinguished. *tetA* was detected within 100% (n = 30/30) of seawater samples. The levels of this gene displayed another discrete, but notable, pattern, whereby significantly higher [$p<0.01$] levels occurred within the samples 250m, 500m and 1000m offshore (mean: $2.87 \times 10^5 \pm 2.50 \times 10^5$ copies/100ml, n =57) relative to both drain (mean: $9.56 \times 10^3 \pm 7.95 \times 10^3$ copies/100ml, n = 15) and nearshore (mean: $9.98 \times 10^3 \pm 3.03 \times 10^3$, n = 30) samples. *dfrA1* was only present in one drain sample (drain 5), and *vanB* was not detected either before or after the rain event.

Following 3.8mm of rain, levels of *tetA* (mean: $2.32 \times 10^5 \pm 3.61 \times 10^5$ copies/100ml, n = 30), *qnrS* (mean: $7.26 \times 10^3 \pm 9.34 \times 10^3$ copies/100ml, n = 23) and *sulI* (mean: $7.62 \times 10^3 \pm 1.16 \times 10^4$ copies/100ml, n = 28) all increased significantly [$p < 0.01$] in nearshore samples. Similarly, levels of these ABR genes also increased significantly [$p < 0.01$] within the stormwater drain samples, with highest levels observed within drains 6 and 8 (Figure 3 A, B, C). There was, however, no statistically distinguishable impact of rain on ABR gene levels either 250m, 500m or 1000m offshore on this day. However, the number of samples that ABR were detected within increased. *sul1* was detected in 46% (n = 14/30) of samples, *qnrS* was detected in 70% (n = 21/30) of samples and *tetA* again was detected in 100% (n = 30/30) of samples (Figure 3 A, B and D). Rainfall also did not impact *dfrA1* levels within the drains. Rainfall did however impact the spatial dynamics of *dfrA1* in Rose Bay seawater samples, with the proportion of samples this gene was detected in increasing from 1% (n = 1/30) to 16% (n = 5/30) of samples (Figure 3 E). Notably, following this rainfall event *vanB* was detected in Drain 9.

Following 43mm of rain, levels of all ABRs within the drains increased by an order of magnitude. Within Rose Bay seawater samples, however, the ABRs followed one of two trends: (i) increasing by an order of magnitude (*qnrS* and *vanB*) or (ii) remaining statistically indistinguishable from the preceding measurements (*tetA* and *sulI*) (Figure 3 A-E). The only

ABR gene that did not follow one of these trends was *dfrA1*, with levels decreasing by two orders of magnitude after heavy rain. Spatially, patterns varied between genes, with *sulI* detected in 48% (n=14/30) of samples and *tetA* detected in one less sample relative to the preceding sampling day. In contrast, *qnrS*, *dfrA1* and *vanB* were all detected in a higher proportion (83% (n = 25/30), 20% (n = 6/30) and 6% (n = 2/30) respectively) of seawater samples compared to the preceding sampling day. The highest levels of all antibiotic resistance genes (except *tetA*) were observed within drain 3 and along the seawater sample transect adjacent to it, where, for example *vanB* was observed up to 500m offshore (Figure 3 C).

Three days after the rain event, levels of most of the ABR genes (except *tetA* and *dfrA1*) dropped significantly within the drains [$p < 0.01$], but remained high in the nearshore seawater samples, as well as in samples collected 250m and 500m offshore, with levels statistically indistinguishable from those recorded during the rainfall event. In contrast to the other ABR genes*, tetA* levels displayed a similar spatial pattern to those observed during heavy rainfall, whereby levels of this gene within the drain and nearshore samples were significantly higher [$p<0.01$] than those within in the samples taken 250 m, 500 m, and 1,000 m offshore.

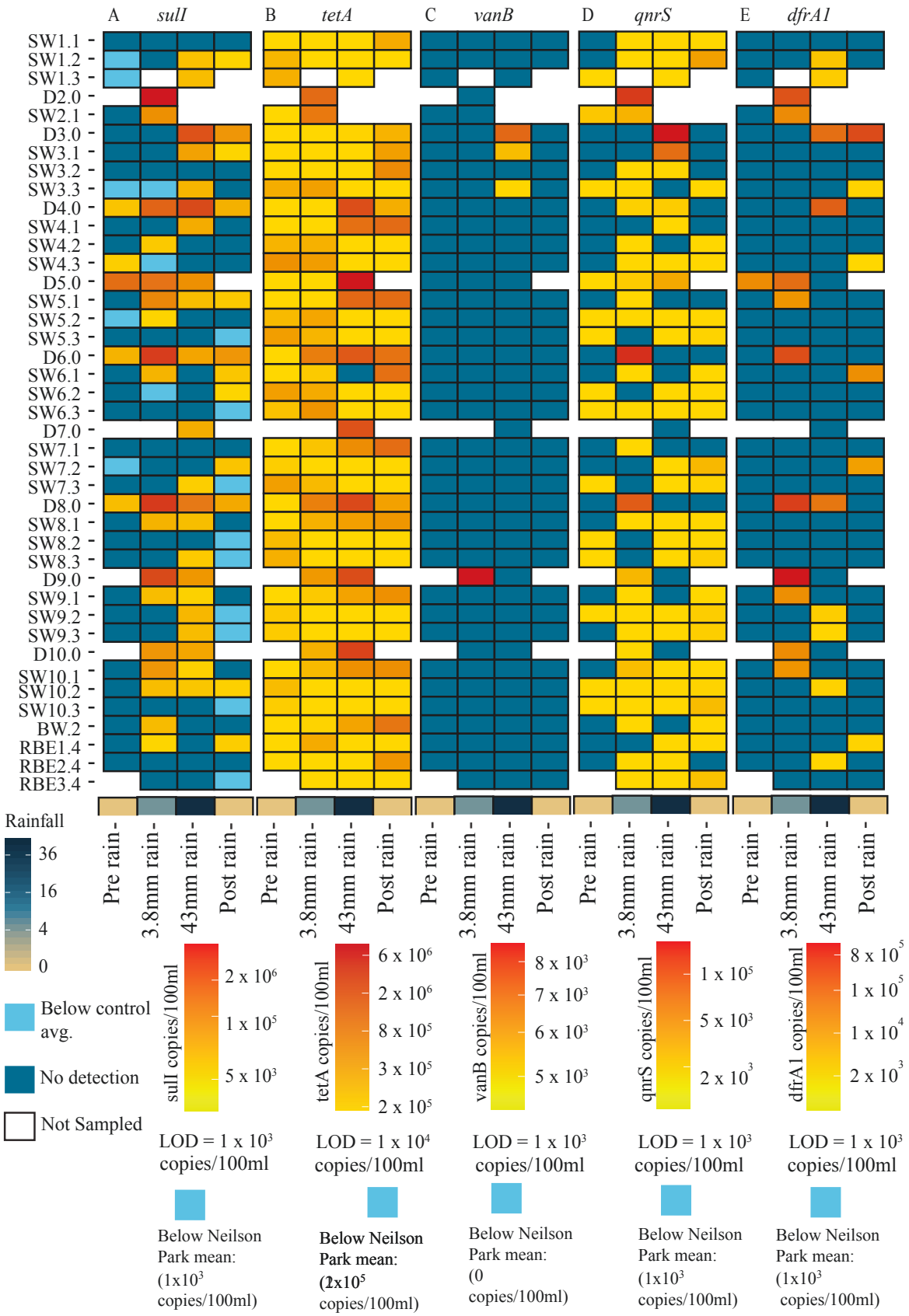

Figure 3. Antibiotic resistance gene markers. Heatmaps of the five antibiotic resistance gene qPCRs, (A) *sulI,* (B) *tetA,* (C) *vanB,* (D) *qnrS* and (E) *dfrA1* across sampling locations (Y axis)

and days (x axis). Colour scale corresponds of copy number per 100mL defined using qPCR, with the lower scale representing the average of that marker detected at the reference Nielsen Park transects, over the course of the study. Blank cells represent samples not collected either due to lack of water flow in drains or due to safety concerns during the rainfall event. Dark blue cells correspond to no detection. Below each qPCR heatmap is a small heatmap displaying daily rainfall (mm) at the time of sampling. Limit of detection (LOD) is in copies/100ml.

3.3.6 - 16S Sequencing community data

3.3.6.1 - Bacterial diversity

The total number of ASVs detected in the entire data set was 17, 158. There were 13, 574 ASVs detected within drain samples and 13, 565 ASVs detected within the seawater samples. Within Rose bay seawater samples, bacterial community diversity (Shannon diversity [$F = 44.4$, $p < 0.01$]) and composition [$F = 19.7$, $p < 0.01$] differed significantly between dry (before the rain event) and wet weather conditions (43 mm on the 30/8/19) (Figure 4A). The most abundant ASVs in seawater samples were members of *SAR11 Clade I*, the *SAR86 clade* and an *Actinomarinales*. The dissimilarity in seawater bacterial communities observed between dry (before the rain event) and wet weather conditions (3.8 mm rain on the 27/8/19 and 43 mm on the 30/8/19) was primarily driven by a significant [$F = 22.5$, $p < 0.01$] decrease in the relative abundance of *SAR11 Clade I* following rain and a concomitant increase in an ASV classified as Pseudarcobacter defluvii.

Significant differences in the composition of bacterial communities inhabiting the stormwater drains relative to the seawater samples [$F = 14.5$, $p < 0.01$] were also apparent (Figure 4B). Within stormwater drains, the most abundant ASVs included the same *Pseudarcobacter defluvii* ASV noted above, a member of the *Spirosomaceae* family and *Flavobacterium succinicans*. The dissimilarity in bacterial communities within the drains and seawater communities was largely driven by the same *Pseudarcobacter defluvii* ASV mentioned above and a member of the *Spirosomaceae* family, which were both over-represented within the drain samples, and a *SAR 11 Clade I* ASV that was over-represented in the seawater samples. Additionally, the bacterial community also differed significantly between each individual drain [$F = 5.5$, $p < 0.01$].

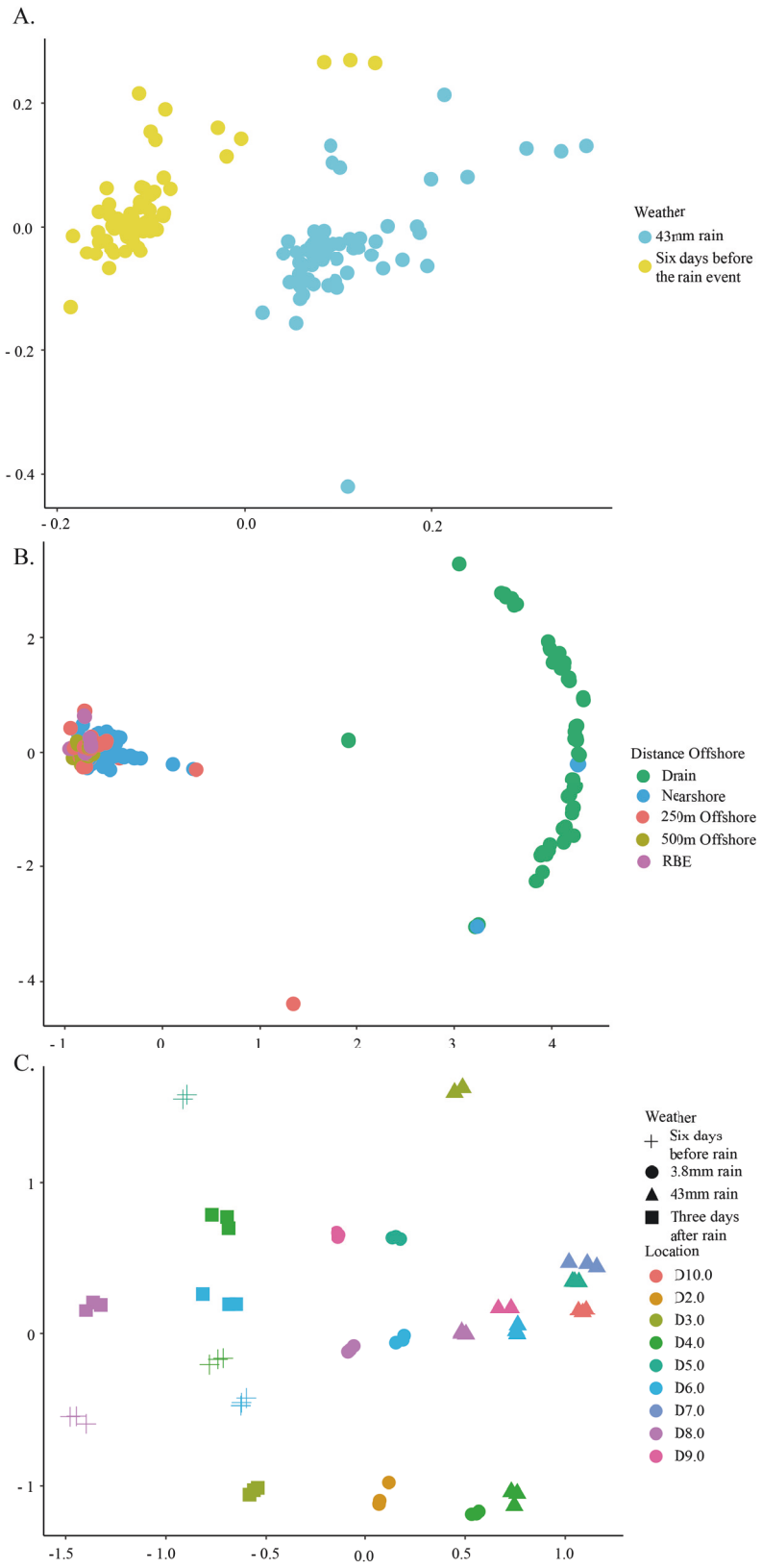

Figure 4. Bacterial communities in drain and seawater. (A) NMDS (stress < 0.2) showing the Bray-Curtis distances between dry (0mm rain) and wet (43mm rain) seawater samples. (B) NMDS (stress < 0.2) showing the Bray-Curtis distances between all samples, coloured by

distance offshore. (C) NMDS (stress < 0.2) showing the Bray-Curtis distances between drain samples. Weather conditions are represented by shapes and the drains are represented by colours.

3.3.6.2 - Indicator species within the drains

A total of 6,651 ASVs were identified as 'bacterial indicators' of the stormwater drain microbial communities. After removing ASVs present in an average relative abundance of less than 0.1% within the drain samples, 6 ASVs remained, including the same *Pseudarcobacter* and *Spirosomaceae* ASVs that were most responsible for the significant differences between drain and seawater bacterial communities, as well as 4 *Comamonadaceae* ASVs.

During dry weather prior to the rainfall event, these drain indicator ASVs were detected in only 23% (n = 7/30) of Rose Bay seawater samples, where their cumulative relative abundance was a mean of 0.05% ± 0.08 (n = 14). Most of these detections (85% n = 6/7) were in the nearshore samples (Figure 5 A), with highest relative abundances observed in 5.1 (0.19 %). Drain indicator ASVs were detected at one other site, 10.3, 500m offshore. No drain indicator ASVs were detected within samples 250 m or 1000 m offshore, nor were they detected at the control site.

Following 3.8 mm of rain, the occurrence of drain indicator ASVs in seawater samples increased significantly, with these ASVs now detectable in 60 % (n = 18/30) of Rose Bay seawater samples. Again, the prevalence of drain indicator ASVs was highest in the nearshore samples, where they were detected within all samples except 7.1 (mean cumulative relative abundance: 0.09% ± 0.02, n = 37). The highest levels of drain indicator ASVs were recorded at site 5.1, where the cumulative relative abundance of 1.2% was two orders of magnitude higher than the mean of all other nearshore samples (mean: 0.09% ± 0.14, n = 7). During this time, drain indicator ASVs were also detected at 11 of the sites located 250m and 500m offshore. No drain indicator ASVs were detected at the control site.

After 43mm of rain, the occurrence of drain indicator ASVs increased further, with these indicator organisms now detected in 66 % (n = 20/30)of seawater samples. These indicator organisms were most prevalent in the nearshore samples 3.1 and 4.1, where their cumulative relative abundance was 0.1 % and 0.7 % respectively, with highest levels again observed in the near shore samples. The drain indicator ASVs were mainly restricted to transects 3, 4, 5, 8 and 9, extending from nearshore to 500 m offshore (Appendix 2 Figure 3,

C). Of note, the drain indicator taxa were detected in one site 1000 m offshore and up to 500 m offshore at the control site.

Three days after the rainfall event, the occurrence of drain indicator ASVs remained high within Rose Bay seawater samples, where they were detected in 87 % (n = 25/29) of samples. These ASVs were detected in all nearshore samples, and up to 500 m offshore along transects 3, 5 and 10.

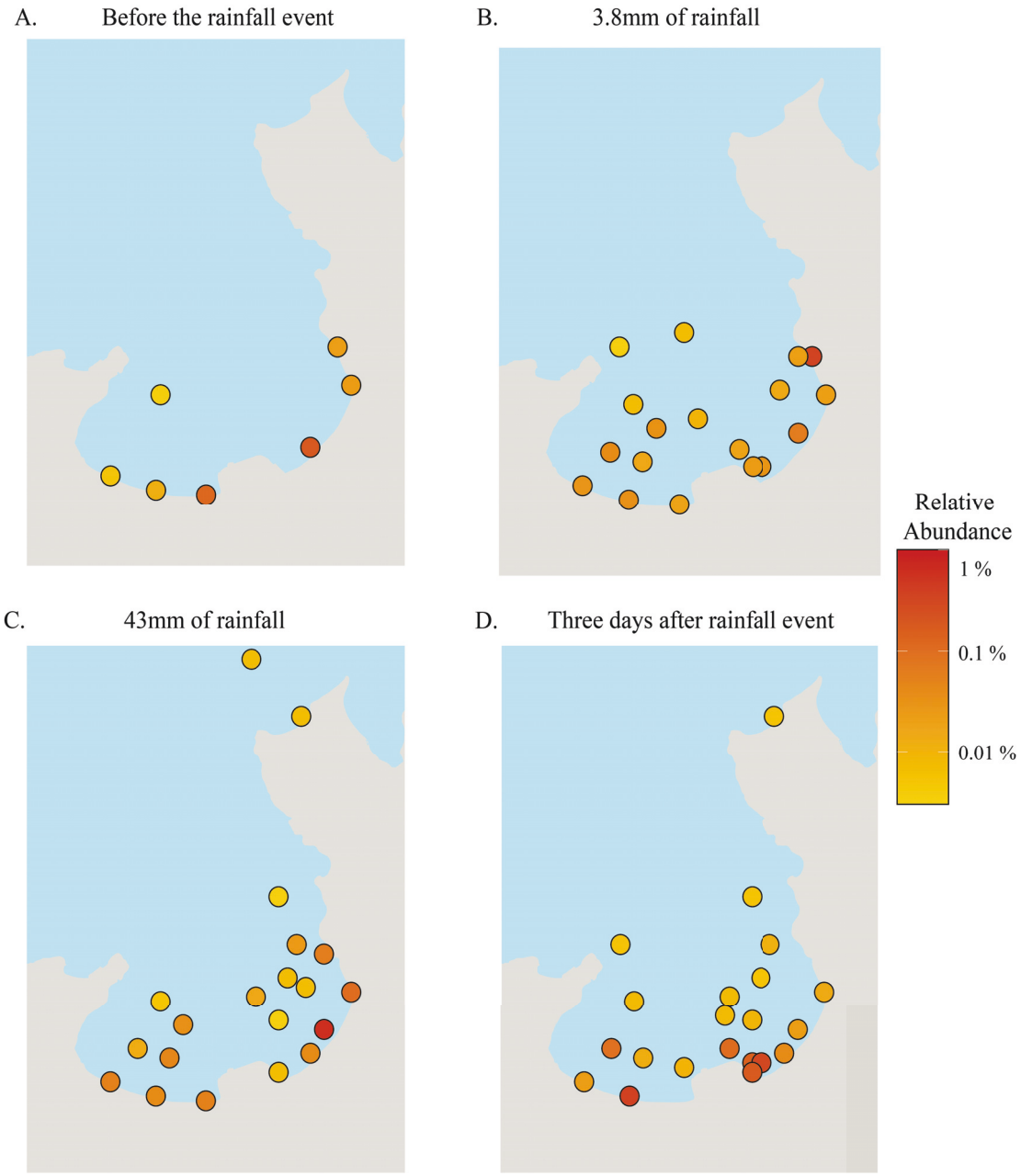

Figure 5. Sewage Indicator Taxa within Rose-Bay seawater. Sewage indicator taxa within seawater samples as a bubble plot within Rose Bay. The bubble colour scale represent the % of the Relative Abundance that the indicator taxa (a *Pseudarcobacter, Spirosomaceae* ASV

and 4 *Comamonadaceae* ASVs) ASVs add up to per sample. (A) Shows distribution pre-rain, (B) shows distribution during 3.8mm of rain, (C) shows distribution during 43mm of rain and (D) shows distribution post-rain.

3.3.6.3 - Impact of microbial signature from drain communities on Rose Bay

To estimate the influence of each storm water drain on water quality at the Beachwatch reference site (BW.2) (Appendix 2 Figure 3), I used *SourceTracker* (Knights et al., 2011) to examine the relative contribution of the microbial signature from each drain within at this reference sampling point used by local monitoring programs. The relative contribution of the microbial signature from each drain on BW.2 mostly consisted of the Rose Bay Entrance microbial community (99 %), which in this test was our control. However, our main focus was the change in impact from the drains, which differed significantly over the time-course of this study [$F = 37.69$, $p < 0.01$].

Before the rain event (21/8/19), the microbial signature from Drain 4 was 3 times higher than the cumulative contribution of the other running drains (Appendix 2 Figure 3 A). After 3.8 mm of rain, the impact of all stormwater drains on the BW.2 bacterial community (mean: 0.001 ± 0.0015 %, $n = 12$) was significantly higher [$p < 0.01$] relative to dry weather conditions before the rain event (mean: 0.005 ± 0.003 %, $n = 12$). The relative impact of the drains also shifted, with Drain 5 now contributing between 1-4 times more than any of the other drains (Appendix 2 Figure 3 B). After the more significant rainfall event, when 43 mm of rain fell, the microbial signature of Drains 3, 5 and 9 had the largest impact on the BW.2 bacterial assemblage (Appendix 2 Figure 3 C). The over-all level of impact from the drains on BW.2 did not change significantly 3 days after the rainfall event. The impact source however, shifted from Drain 3, Drain 5 and Drain 9, to Drains 4 and 6, which now had the largest level of impact on BW.2 (Appendix 2 Figure 3 D).

To investigate the spatial impact of specific stormwater drains on Rose Bay over the course of the rainfall event, I again, used *SourceTracker* (Knights et al., 2011) to investigate the contribution of the microbial assemblages within specific drains (used here as a source) on the microbial community within each sample within Rose Bay (sink). For each day of the study, the specific drain chosen was the drain that had the highest levels of the Lachno3 marker, which equated to Drain 5 before the rain event (21/8/19) and after 3.8mm of rain, Drain 3 after 43mm of rain and Drain 6 after the rainfall event.

Six days before the rain event (21/8/19), the microbial signature of Drain 5 impacted all nearshore samples and samples located 250m offshore, but only impacted 50 % (n = 4/8) of samples located 500m offshore (Figure 6 A). After 3.8mm of rain, the extent of impact from Drain 5 increased to 93 % (n = 28/30) of sites within Rose Bay, impacting all but one site 500 m offshore and reaching two sites 1000m offshore. Whilst the impact of this drain increased spatially (mean: 0.002 ± 0.002, n = 80) the contribution was significantly lower [$p<0.01$] relative to dry weather conditions before the rain event (mean: 0.001 ± 0.0007, n = 92) (Figure 6 B). After 43mm of rain, the impact of the microbial signature from Drain 3 reached 1000m offshore (Figure 6, C) and was significantly greater [$p < 0.01$] than the microbial impact from Drain 5 relative to conditions before the rain event (21/8/19) and after 3.8mm of rain (27/8/19). Indeed, using this approach, it was apparent that the impact of Drain 3 at this time was the greatest of any drain throughout the entire study period. Four days following the rainfall event, the spatial impact of Drain 6 on Rose Bay extended 500m offshore (Figure 6 D) but had a significantly lower [$p<0.01$] level of impact than Drain 3 during heavy rain.

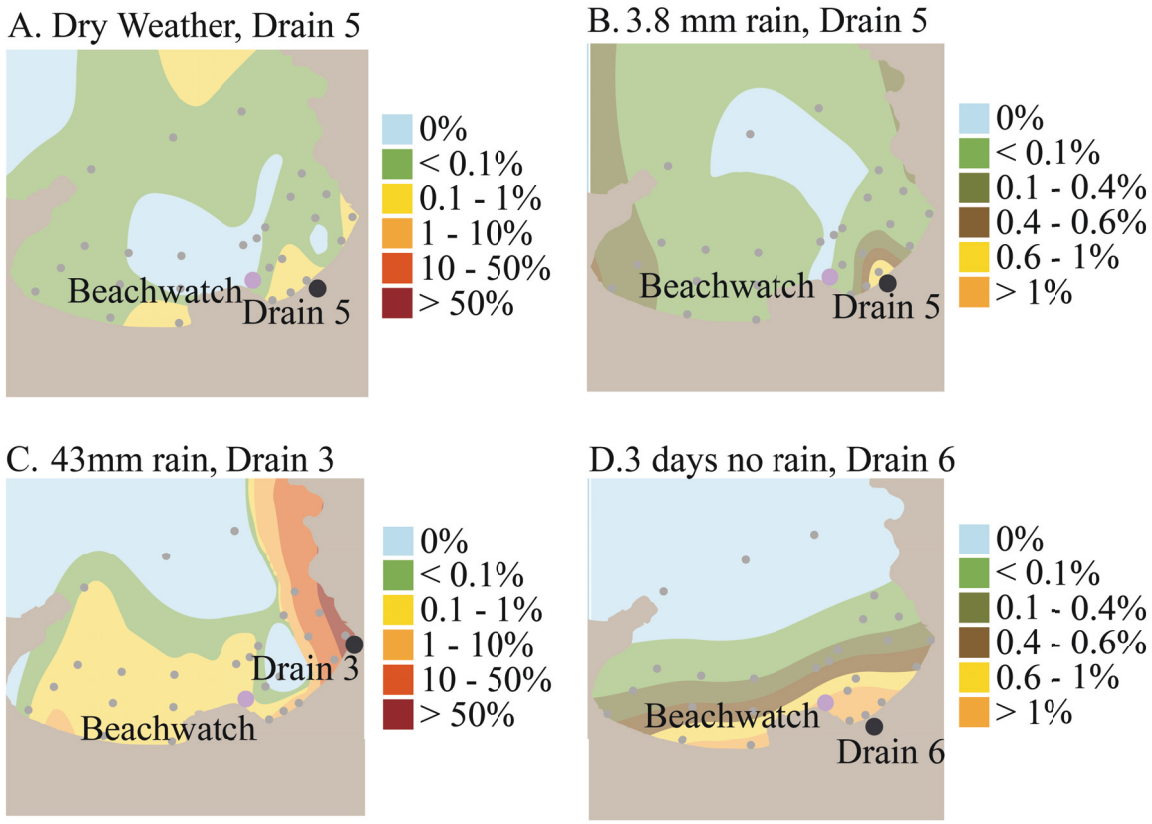

Figure 6. Sewage pollution and distribution within Rose Bay before and after rain events. Interpolated contribution percentages of microbial communities from the most impactful drains

to at each sampled seawater site (grey dots) and the Beachwatch reference site (purple dot) on a geographical map of Rose Bay. (A) Shows the contribution of Drain 5 during dry weather, (B) Shows the contribution of Drain 5 after 3.8mm of rain, (C) Shows the contribution of Drain 3 after 43mm of rain and (D) Shows the contribution of Drain 6 post rain event. Colour scale on each map refers to the contribution percentage of the drain on Rose Bay on each day.

3.4 - Discussion

3.4.1 - What is the principal cause of faecal contamination at Rose Bay?

Urban beaches are often characterised by poor water quality, which has implications for human and ecosystem health (McLellan et al., 2015). Routine FIB monitoring has indicated that water quality at Rose Bay has been regularly impacted by faecal contamination for at least the last 7 years (OEH, 2013; DPIE, 2020), yet the causes and point-sources of this contamination have not been identified. By applying a suite of molecular microbiological approaches, I have revealed significant levels of markers for human faeces, indicative of sewage contamination during both dry weather periods (before and after rainfall events), which increased further during rain (3.8 mm rain on the 27/8/19 and 43 mm on the 30/8/19), to levels that are comparable to, and sometimes higher than, other aquatic environments known to be impacted by raw sewage (Liang et al., 2021). This was paired with intermittent impacts from dog faeces in dry weather (pre- and post-rain event) detected only in nearshore, and not drain, samples, indicating that it was sourced from dog faeces on the beach rather than the catchment serviced by the stormwater drains, and most likely from runoff in the catchment during wet weather (3.8 mm rain on the 27/8/19 and 43 mm on the 30/8/19) due to the large amount of DG3 present within the drains.

Before the rainfall event (21/8/19), enterococci levels within the seawater samples were generally low, indicating good water quality, but these levels became substantially elevated following rainfall. The single exception to this pattern was the sample collected adjacent to Drain 5 (5.1), where enterococci levels were 180 CFU/100ml. Notably, these levels were higher than those recorded in the adjacent drain. During this time, both human markers were highly elevated (relative to all other samples) within Drain 5. However, the dog faecal marker was also elevated at site 5.1 but absent with the Drain 5 sample. These patterns imply one of two explanations for the moderate enterococci levels observed in this nearshore site: (1) A combination of sewage and dog faecal material sourced from Drain 5 has impacted this location; (2) Dog faecal material sourced from the beach has contributed to the moderately high enterococci levels measured at this location. Given that comparable levels of DG3 were recorded at other near-shore sites (3.1, 4.1, 5.1, 6.1, 9.1, 10.1) that did not exhibit elevated enterococci levels at this time, I propose that the elevated enterococci levels within this sample were the result of a combinatory effect of human (sewage from Drain 5) and dog faecal material. This potential dry weather sewage overflow resulted in levels of HF183 within the seawater that were in some cases higher than those that have elsewhere been estimated to

indicate a significant health risk from sewage-borne pathogens (Boehm and Soller, 2020). The *SourceTracker* analysis (Figure 6. A) showed that the microbial signature from Drain 5 was the strongest around transects 3, 5, 6, 7, and offshore towards Neilson park. This aligns with locations that also had a higher level of HF183, therefore, a sewage leak within Drain 5 is a possible explanation for high background levels of HF183 before the rain event.

Following a 43mm rain on the 30/8/19, mean bacterial abundances within drains (as estimated by 16S rRNA qPCR) increased by an order of magnitude, and were over an order of magnitude higher than seawater bacterial abundances preceding the rainfall event. When this stormwater entered Rose Bay in a mixing ratio of 1:34, levels of bacteria increased by 95% and 23% within Rose Bay seawater. This pattern was confirmed by our SourceTracker analysis, which revealed that the bacterial assemblages within seawater samples surrounding drain 3 were comprised of between 10-50% bacteria from Drain 3. Enterococci levels also increased significantly within both stormwater drain samples and seawater samples immediately adjacent to some drains. Within the drain and seawater samples where the highest enterococci levels occurred (i.e., Drain 3 and adjacent seawater samples, Drains 4, 8 and 10), increases in both human faecal markers and the dog faecal marker were observed. In Drain 3, a substantial peak in both human faecal markers was observed, with the elevated seawater enterococci levels spanning the Drain 3 transect into Rose Bay also mirrored by increases in the human faecal markers. I conclude that Drain 3 and the surrounding waters within Rose Bay experience the most pronounced influence of sewage during rainfall events, where levels of HF183 sometimes reached four orders of magnitude higher than those predicted to indicate a human health risk from sewage (Boehm and Soller, 2020). However, in this drain, as well as several of the other drains experiencing high enterococci levels during the rainfall event (specifically Drains 4, 5, 6 and 8), significant peaks in the dog faeces marker co-occurred with peaks in the human faecal markers. This indicates that both sewage and dog faeces potentially contribute to the high enterococci levels observed in stormwater drains during rainfall at Rose Bay, which is a pattern consistent with reports from other coastal environments (Ahmed et al., 2020). I posit that this pattern of concentration in, and near to, the stormwater drains is likely indicative of dog faeces being washed into the stormwater system from the surrounding catchment, rather than significant levels of dog faeces being washed from the beach into the seawater at Rose Bay.

Using 16S rRNA gene amplicon sequencing data I revealed the occurrence of a set of "indicator bacteria", which were present at a high relative abundance (relative to seawater) within stormwater samples but became detectable within seawater samples after rainfall.

Notably, these indicator bacteria, including *Pseudarcobacter* are known to be members of the bacterial communities inhabiting sewage (McLellan et al., 2015), providing further evidence for the impact of sewage within Rose Bay. Some of these taxa were intermittently detected within nearshore seawater samples before the rain event (21/8/19), but following the major rainfall event examined here were observed up to 1000m offshore, providing evidence for a spatially pronounced influence of sewage contamination across Rose Bay after rain.

While coastal environments can also be subject to faecal contamination from native animals, in particular water birds (Jarma et al., 2021), the marker for avian faeces did not display a statistically significant correlation to total enterococci counts, nor an increase associated with either rainfall or proximity to drains. Furthermore, given that (i) the levels of this bird faecal marker were not higher in Rose Bay than the control site and (ii) bird faecal marker levels in the seawater were always within the range of those observed in other coastal habitats pre-rainfall (Ahmed et al., 2020), I conclude that bird faeces played a minimal role in driving the elevated total enterococci levels observed during rainfall. This, however, does not negate the possible health risks associated with a high level of bird faeces. It has been demonstrated that the guts of birds can be colonised by antimicrobial resistant bacteria (ARB) when birds ingest food from polluted water sources containing antimicrobial bacteria (Franklin et al., 2020). This can then make them environmental reservoirs and vectors for ARB and ARGs (Ahlstrom et al., 2018; Bonnedahl and Jarhult, 2014) and vectors for dissemination of ARGs in the environment. Furthermore it has been shown that bird faeces can contain human bacterial pathogens (Benskin et al., 2009).

Cumulatively, our results indicate that sewage input and input of dog faeces into Rose Bay contribute to high enterococci counts during periods of significant rainfall. The main points of input of both forms of faecal material are stormwater drains, which appear to experience contamination from sewage and, in some cases, dog faecal material from the catchment.

3.4.2 - What are the primary points of contamination within Rose Bay?

Prior research has concluded that stormwater drains are responsible for input of sewage into recreationally used coastal environments during both dry and wet weather (Converse et al., 2011; Parker et al., 2010; Parker and Shaw, 2011; Sauer et al., 2011; Sercu et al., 2011; Sercu et al., 2009). Given the elevated levels of both FIB and the human faecal MST markers

within stormwater drains, during both dry (before and after rainfall) and wet weather (3.8 mm rain on the 27/8/19 and 43 mm on the 30/8/19), it is clear that the network of stormwater drains at Rose Bay are the key source of seawater contamination, rather than the surrounding beach environment. However, some drains had a greater influence than others, with the level of impact also varying according to whether sampling was conducted during dry (before and after the rain event) or wet weather (3.8 mm rain on the 27/8/19 and 43 mm on the 30/8/19) periods.

Before the rain event on the 21/8/19, Drain 5 exhibited elevated levels of both of the human faecal markers, with these levels increasing further and extending into the adjacent seawater sample after the first moderate (3.8 mm) rainfall event. I suggest that these patterns are potentially indicative of a dry weather sewage leak into Drain 5, which may have contributed to the slightly elevated enterococci levels within the 5.1 seawater sample before the rain event. Indeed, at site SW5.1 levels of the Lachno3 marker were 1.1 x 10^5 copies/100ml prior to the rainfall event and the Lachno3 and HF183 markers reached 1.98 x 10^7 copies/100ml and 2.45 x 10^6 copies/100ml respectively after 3.8mm of rain. While these levels are an order of magnitude lower observed in raw sewage (Sauer et al., 2011; D. Li et al., 2021), they are high relative to concentrations observed in other coastal environments (Liang et al., 2021; Rothenheber and Jones, 2018). It is not uncommon for dry weather sewage leaks to occur within stormwater drains (Sercu et al., 2009), and, notably, Drain 5 is adjacent to a sewage pumping station behind Rose Bay beach, which may contribute to high background levels of both sewage markers at Neilson park and is potentially worthy of further examination. These patterns are supported by our analysis of the 16S rRNA gene amplicon sequencing data using *SourceTracker*, which highlighted Drain 5 as the greatest point of impact on the Beachwatch reference sample after 3.8mm of rain. This impact was not only high at the Beachwatch site, but extended 1000m offshore both before the rain event and after 3.8mm of rain. Additionally, the 16S rRNA gene amplicon sequencing data also revealed the highest levels of sewage associated indicator species at site 5.1, both before the rain event and after 3.8mm of rain.

Following the major rainfall event, highly elevated enterococci levels occurred in all drains, with highest levels within Drains 3, 4, 8 and 10. Notably, the Rose Bay seawater samples adjacent to several of these drains also showed highly elevated enterococci levels, indicating a substantial impact on seawater quality in Rose Bay. Both human faecal markers were highly elevated within each of these drains, and adjacent seawater samples, with Drains 3 and 10 clearly hotspots of sewage contamination, in Drain 3, HF183 reaching levels an order of magnitude lower than what has been previously detected in raw sewage HF183 (Sauer et al.,

2011; D. Li et al., 2021). A similar pattern was observed upon inspection of the 16S rRNA gene amplicon sequencing data, whereby the *SourceTracker* data revealed drains 3 and 9 as the input points that had the highest impact on the Beachwatch reference sample on this day. This data also revealed that Drain 3 had the highest impact on seawater samples across the entirety of Rose Bay.

Given that concentrations of the human faecal markers became significantly elevated within these drains following the major rainfall event, I suggest that drains 3 and 9 potentially represent sites most influenced by wet weather sewage overflows. This is supported by the *SourceTracker* data whereby I observed these two drains as having the highest impact on the Beachwatch site during the heavy rain event (Appendix 2 Figure 3 C).

3.4.3 - Spatiotemporal dynamics of contamination

The sampling design employed during this study permitted a detailed investigation of the spatial and temporal patterns of multiple markers for faecal contamination over the course a rainfall event. This analysis revealed that FIB levels within Rose Bay increase significantly following rainfall and with proximity to stormwater drains, with this pattern largely driven by sewage contamination of the drains, with a further contribution from dog faecal material likely sourced from the catchment serviced by these drains. While previous studies have shown increases of faecal contamination from either sewage or animal sources during rainfall events (Ahmed et al., 2020; Shrestha et al., 2020), only few studies (Newton et al., 2013) have assessed the spatial extent of impact.

For the most part, high levels of the human and dog faecal markers were restricted to near-shore samples. Drain 3 displayed highly elevated levels of the human faecal markers across several samples extending away from the shoreline, and when used as a "source" when 16S rRNA bacterial community data was employed as a tracer, contributed to up to 50% of the bacterial communities within "sink" samples up to 500m offshore along transects 3 and 4. This is indicative of a substantial influence of Drain 3 on water quality within Rose Bay following rainfall.

Four days after the major rainfall event, slightly elevated levels of both human faecal markers persisted within the environment. There are two potential explanations for this pattern: (i) The *Lachnospiraceae* and *Bacteriodes* targeted by their respective assays can persist for longer periods than FIB in the environment as shown by (Ahmed et al., 2020b), or (ii) The

DNA- based, rather than culture-dependent, approach used to quantify these markers detect unviable bacteria that would not grow via a culture-based approach.

3.4.4 - Other microbiological hazards in Rose Bay

Our results indicate that Rose Bay is extensively impacted by sewage contamination likely linked to sewage overflows into stormwater drains, which may consequently create several hazardous microbiological implications. Over the course of the experiment, I observed evidence for increased levels of ARGs in the environment following rainfall, which is consistent with recent studies in other urbanised beaches that are impacted by sewage contamination (Carney et al., 2019). The putative links between elevated ARG occurrence and sewage contamination (Akiyama and Savin, 2010; Auguet et al., 2017; Gaviria-Figueroa et al., 2019) was confirmed here by significant correlations between the HF183 human faecal marker and ARGs; *dfrA1, qnrS, sulI* and *vanB*. Notably, I observed levels of *qnrS* that were over two orders of magnitude higher than those previously reported within wastewater (Paulus et al., 2019) and levels of *vanB* that were over 3 times higher than those observed at other highly contaminated beaches in Sydney (Carney et al., 2019). This emerging occurrence of high levels of ARGs at Rose Bay represents a largely uncharacterised, but potentially significant (Leonard et al., 2018) health risk for swimmers.

3.4.5 - Bacterial community analysis provides another powerful tool to analyse coastal water quality

I coupled 16S rRNA gene amplicon sequencing with the Bayesian *SourceTracker* package (Knights et al., 2011), which uses Bayesian statistics to predict the percentage of 'source' microbial communities within selected 'sink' samples. *SourceTracker* has previously been used to track the occurrence of sewage bacterial communities in the environment (Newton et al., 2013), and discern the relative contribution of faecal contamination from different sources, including sewage plants and animals (Ahmed et al., 2015b; Brown et al., 2017). Similarly, to our study, (Neave et al., 2014) used *SourceTracker* to analyse the microbial signature from different inputs, including a sewage outfall and a number of lakes (sources), at different beach sites (sinks). However, to the best of our knowledge, ours is the first study to use this approach to (i) track the spatiotemporal dynamics of specific bacterial signatures for

individual stormwater drains and (ii) use this data to quantify the relative strength of the microbial signature from different stormwater drains.

Additionally, I coupled 16S rRNA gene amplicon sequencing with the *indicspecies* r package (de Caceres and Jansen, 2018), to identify specific microbial indicators of the water within stormwater drains and Rose Bay seawater samples. This analysis revealed that several of the bacteria that could be characterised as indicators for stormwater drains were often aligned with organisms previously identified as indicators of sewage (e.g., *Arcobacter* (McLellan et al., 2015)). One of the most prevalent indicator taxa was *Pseudarcobacter defluvii*, which was formerly known as *Arcobacter defluvii* (Perez-Cataluna et al., 2018). *Pseudarcobacter defluvii* has been isolated from sewage (Collado et al., 2011), with strains of this organism isolated from sewage shown to be potential human pathogens (Levican et al., 2013). Furthermore, our microbial indicator analysis also revealed other, previously unrecognised, putative markers for contamination of urbanised coastal habitats. These included four *Comamonadaceae* ASVs and a *Spirosomaceae* ASV. *Comamonadaceae* are a family of bacteria which have also been reported as a core member of sewage sludge (Xu et al., 2017), where they can make up to 10% of the cumulative relative abundance of effluent (Yasir, 2020), while *Spirosomaceae* has also been isolated from sewage sludge in Korea (Lu et al., 2007), implying that these ASVs are likely sewage markers.

I acknowledge that this was indeed a single rain event with only four time points and that while our results are reflective of what happened at this time, they may not be generalisable to Rose Bay at all times and in all rain events. However, in light of the outcomes of our analysis of 16S rRNA community profiles, I argue that DNA sequencing data provides a powerful and largely untapped means to trace the extent and impact of water contamination in aquatic ecosystems. This has the potential to augment other FIB and MST approaches.

3.5 - Conclusions

Many urban beaches are characterised by poor water quality because of often undefined sources of faecal contamination. By employing molecular microbiological tools including MST assays and DNA sequencing I have delivered a precise assessment of the causes and sources of contamination at an intermittently contaminated beach within Sydney Harbour, Australia. Whilst traditional FIB methods indicated high levels of faecal contamination, I used MST approaches to precisely identify the likely source of this contamination (i.e., sewage vs animal). Our analysis demonstrated that Rose Bay is moderately impacted by dog and human faeces during dry weather (both before and after the rainfall event), but heavily impacted by human faeces (sewage) during wet weather (after 3.8mm and 43mm rain). Additionally, I identified the relative impact of individual stormwater drains on seawater quality by combining MST assays with DNA sequencing techniques to trace the spatial and temporal dynamics of contamination. This confirms that in cases where consistently high levels of FIB are recorded by regular monitoring practises, but the source of contamination remains ambiguous, MST tools like those used here provide a powerful means for informing subsequent remediation and management efforts. Finally, I identified the spatial and temporal dynamics of microbiological hazards associated with contamination, including an increased occurrence of antibiotic resistance. These more nuanced insights into the contributing factors to poor water quality at this highly urbanised coastal environment will inform efforts to resolve the causes of contamination and subsequently help to safeguard public health.

Chapter 4 - Rainfall leads to elevated levels of antibiotic resistance genes within seawater at an Australian beach

Author's state that author contributions are correct, and that the student has completed the work stated in the author contributions.

Author Signatures:

Author	Signature	Date
Nathan L.R. Williams	Production Note: Signature removed prior to publication.	11/08/2022
Nachshon Siboni	Production Note: Signature removed prior to publication.	09/08/2022
Sandra L. McLellan	Production Note: Signature removed prior to publication.	08/08/2022
Jaimie Potts	Production Note: Signature removed prior to publication.	09/08/2022
Peter Scanes	Production Note: Signature removed prior to publication.	1/09/22
Colin Johnson	Production Note: Signature removed prior to publication.	08/08/2022
Melanie James	Production Note: Signature removed prior to publication.	9/8/2022
Vanessa McCann	Production Note: Signature removed prior to publication.	09/08/2022
Justin R. Seymour	Production Note: Signature removed prior to publication.	11/08/2022

This work has been published: Williams, N.L.R., Siboni, N., McLellan, S., Potts, J., Scanes, P., Johnson, C., James, M., McCann, V., Seymour, J.R., Rainfall leads to elevated levels of antibiotic resistance genes within seawater at an Australian beach, Environmental Pollution (2022). https://doi.org/10.1016/j.envpol.2022.119456.

4.0 - Abstract

Anthropogenic waste streams can be major sources of antibiotic resistant microbes within the environment, creating a potential risk to public health. I examined patterns in the occurrence of a suite of antibiotic resistance genes (ARGs) and their links to enteric bacteria at a popular swimming beach in Australia that experiences intermittent contamination by sewage, with potential points of input including stormwater drains and a coastal lagoon. Samples were collected throughout a significant rainfall event (40.8mm over 3 days) and analysed using both qPCR and 16S rRNA amplicon sequencing. Before the rainfall event, low levels of faecal indicator bacteria and a microbial source tracking human faeces (sewage) marker (Lachno3) were observed. These levels increased over 10x following rainfall. Within lagoon, drain and seawater samples, levels of the ARGs *sulI*, *dfrA1* and *qnrS* increased by between 1-2 orders of magnitude after 20.4mm of rain, while levels of *tetA* increased by an order of magnitude after a total of 40.8mm. After 40.8mm of rain *sulI*, *tetA* and *qnrS* could be detected 300m offshore with levels remaining high five days after the rain event. Highest levels of sewage markers and ARGs were observed adjacent to the lagoon (when opened) and in-front of the stormwater drains, pinpointing these as the points of ARG input. Significant positive correlations were observed between all ARGs, and a suite of Amplicon Sequence Variants that were identified as stormwater drain indicator taxa using 16S rRNA amplicon sequencing data. Of note, some stormwater drain indicator taxa, which exhibited correlations to ARG abundance, included the human pathogens *Arcobacter butzleri* and *Bacteroides fragilis*. Given that previous research has linked high levels of ARGs in recreationally used environments to antimicrobial resistant pathogen infections, the observed patterns indicate a potentially elevated human health risk at a popular swimming beach following significant rainfall events.

4.1 - Introduction

The increasing occurrence of antibiotic resistance (AbR) is of large concern globally (Klein et al., 2021). While the majority of focus on the impacts of AbR has been placed on clinical settings (Paulus et al., 2019), the spread and environmental reservoirs of AbR within natural ecosystems are of increasing interest (Berendonk et al., 2015). While AbR occurs naturally within environmental microbiomes (Allen et al., 2010), high levels of antibiotic use and subsequent contamination related to the agricultural industry (Foley and Lynne, 2008; Sarmah et al., 2006), and inadequate management of human wastewater streams (Baquero et al., 2008) are contributing to concerningly high levels of AbR in aquatic environments (Auguet et al., 2017). This concern is in part due to the fact that environmental AbR presents a largely undefined health risk, particularly to community groups that are consistent users of aquatic environments, including swimmers (Leonard et al., 2015) and surfers (Leonard et al., 2018).

The spread of AbR into coastal environments via anthropogenic wastewater streams occurs because of excretion of large quantities of antibiotics from human populations into sewage (Steinbakk et al., 1992). Antibiotics are difficult to remove during wastewater treatment and therefore occur in both sewage influent and effluent waste streams, where they have the potential to select for AbR within resident bacterial communities (Baquero et al., 2008; Chow et al., 2015). Stormwater infrastructure is often contiguous to sewage infrastructure, where both pipe blockages during dry weather and wet weather sewer over-flow events during rainfall can lead to sewage leaks into the stormwater infrastructure, and as a result, can further lead to untreated sewage entering aquatic environments (Olds et al., 2018).

Recently, it has been shown that antibiotic resistance gene (ARG) levels linked to stormwater within the environment vary depending on the presence of sewage contamination within the stormwater (Carney et al., 2019; Karkman et al., 2019), however our knowledge on the spatial and temporal dynamics of ARGs at beaches where there are multiple potential input points is limited. Moreover, sewage can also harbour microbial pathogens, however, while recent work has illustrated correlations between pathogens and ARGs in urbanised coastal settings (Carney et al., 2020), there is little research linking these ARGs and pathogens to a particular source i.e., sewage leaks within stormwater drains. Therefore, our aim was to determine the extent of ARG pollution within a coastal environment and if this pollution is linked to sewage contamination. Furthermore, I aimed to determine whether sewage contamination has the potential to transmit AbR pathogens into the environment.

Here I examined the potential links between sewage contamination and the occurrence of ARGs within a popular swimming beach Australia's East Coast. This site is characterised by a network of potential contamination sites, incorporating a coastal lagoon that is intermittently open to the ocean and the outputs from three stormwater drains. I performed sampling during a heavy rainfall event, with the central goal of defining the extent, spatiotemporal dynamics, and points of input of ARGs into a coastal environment used widely for human recreation.

4.2 - Methods

4.2.1 - Sampling sites

Terrigal Beach is located on the east coast of Australia (3.4462° S, 151.4447° E), and is a popular site for recreational use by surfers and ocean swimmers. However, this beach regularly experiences poor water quality linked to faecal contamination, particularly after significant rainfall events (OEH, 2018). However, the exact sources and impacts of this contamination are complex and unclear, with a broad network of potential input sources including three storm water drain outlets, as well as an intermittently closed and open saline coastal lagoon, Terrigal Lagoon, that is intermittently open to the ocean, particularly after intense rain events.

Table 1. Sampling dates, locations, and information.

Sampling Date	Sampling Time (AM/PM)	Rainfall information
20/5/19	AM	6mm of the 19/5/19
31/5/19	AM	2mm rain on the 28/5/2019
4/6/19	AM	20.4mm rain in preceding 3 days, with 12mm in the preceding 24hrs
6/6/19	AM & PM	40.8mm in preceding 48hrs, 3.6mm on that day. Afternoon sample taken as mouth of lagoon was manually opened.
11/6/19	AM	Five days of no rain.

Water samples were collected from a suite of potential points of contamination (Figure 1), including the outlets of three stormwater drains (Drains 1, 2 and 4), and from five locations within Terrigal Lagoon. This lagoon receives water from 34 stormwater outlets, has a surface area of 30 ha, a mean depth of 50 cm and is mostly closed, but after intense rain events is manually or naturally opened resulting in drainage into the ocean. Surface seawater samples were also collected from 27 locations along Terrigal Beach, spanning 9 on-shore to off-shore transects. Each transect comprised of nearshore sampling points (1 metre from shore), sites where the water depth reached 5m (~150m offshore) and sites where the water depth reached 10m (~300m offshore). Three of these transects were located within Terrigal Haven, which is a 200m long beach, protected by 20m high Broken Head (Figure 1). These three transects

originated immediately adjacent to three stormwater drains (Drain 1, 2 and 4, SW1.X, SW2.X and SW4.X). Drains 1 and 2 are separated by approximately 20m while Drain 4 is approximately 400m north of Drain 2 (Figure 1). A reference transect corresponding to the sampling point for the regional water monitoring program, Beachwatch (DPIE, 2020), was located approximately 200m north of Drain 4 and 350m south of the mouth of Terrigal Lagoon (SW5.X, Figure 1). To examine the spatial impacts of faecal contamination and related microbial hazards from Terrigal Lagoon, a transect was also established from the mouth of Terrigal Lagoon (SW6.X). Four additional reference transects were added in locations without nearby stormwater drains. The first was at Wamberal beach 1.5km north of Terrigal Beach, the second in front of Wamberal Lagoon 2km north of Terrigal beach, the third at Forresters Beach 4 km north of Terrigal Beach (SW7.X, SW8.X and SW9.X) and the fourth at nearby Avoca Beach (SW0.X, Figure 1), which is approximately 3km south of Terrigal Haven. The regional water quality monitoring program, Beachwatch, (DPIE, 2020) indicates Forrester's beach as generally characterised by low Faecal Indicator Bacteria (FIB) levels, and samples collected from this point were used as a reference for comparisons to more highly contaminated samples from Terrigal Haven.

Sampling was conducted at each location on six occasions, which spanned the period before, during and after a significant rainfall event that resulted in 40.8mm of rain (Table 1). Due to large ocean swell conditions, it was not possible to safely sample SW9.2 on the 31/5/19, all sites 100m and 300m offshore on the 4/6/19, and SW0.2, SW8.2 and SW9.2 on the 6/6/19. Additionally, the stormwater drains were only sampled when running - Drain 1 was only running on the 4/6/19, Drain 2 on the 4/6/19 and 6/6/19, and Drain 4 on the 4/6/19, 6/6/19 and 11/6/19.

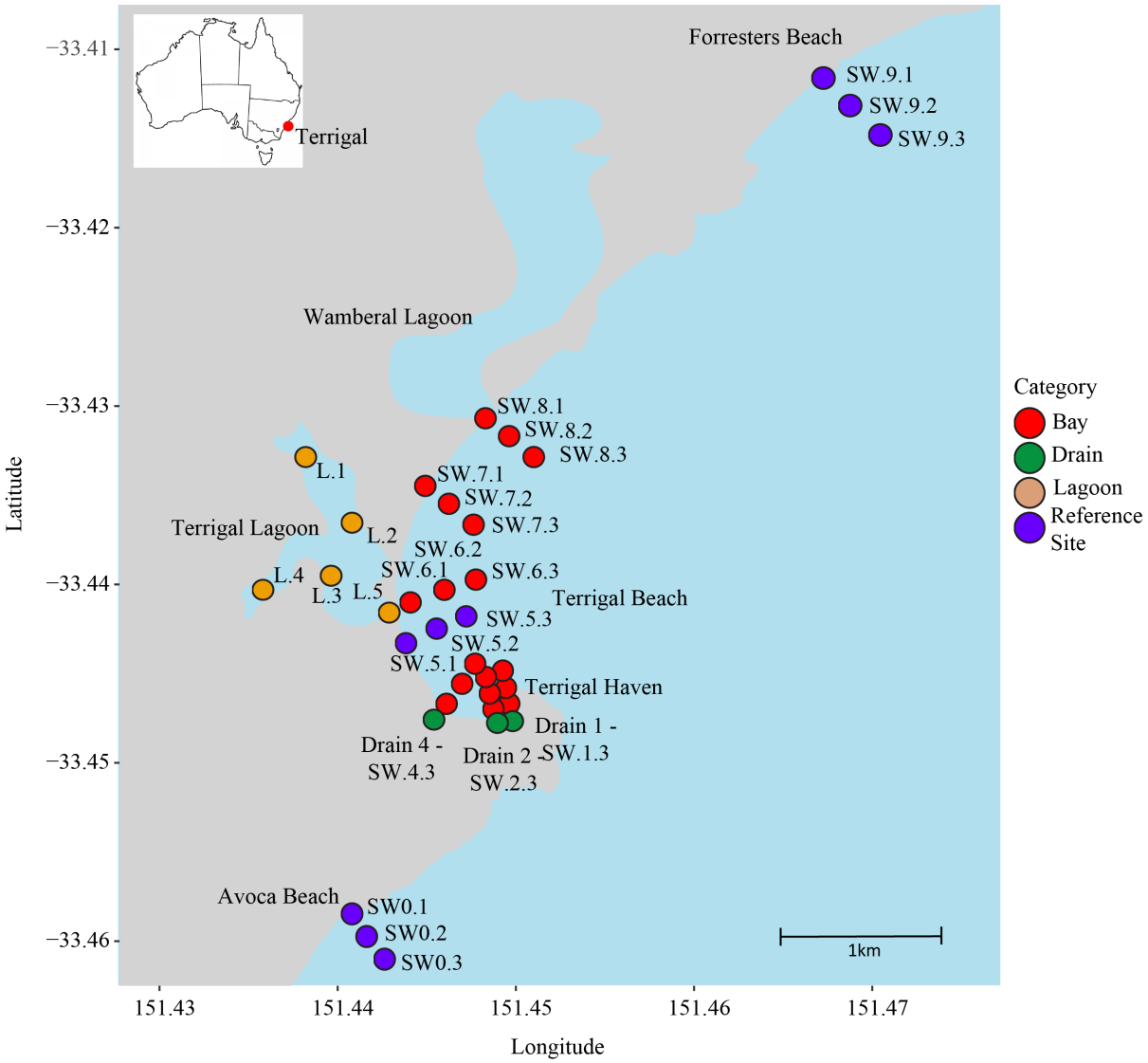

Figure 1. Map of sampling sites within Terrigal. Purple circles refer to reference transects, SW0.1, SW0.2 and SW0.3 represent the Avoca reference transect, a beach 2km south of Terrigal Haven, SW5.1, SW5.2 and SW5.3 represent the Beachwatch reference site transect, with SW5.1 being regularly sampled by the central coast Beachwatch program and SW9.1, SW9.2 and SW9.3 represent the Forrester's beach reference transect, a beach 9km north of Terrigal Haven. Yellow circles represent sites within Terrigal Lagoon, green samples represent sites where samples were taken from within a drain and red circles represent sea water samples, taken from either a beach transect (SW7), drain transect (SW1, SW2 and SW4) or lagoon transect (SW6 and SW8).

4.2.2 - Water sampling, processing, and analysis

On each sampling occasion, physiochemical parameters including temperature, dissolved oxygen, salinity, and pH were measured in situ at each site using a WTW multiprobe meter (Multi3430, Germany). Samples were also taken for chlorophyll, nutrient, and enterococci analysis (Appendix 3 material section 1.1-1.3). Water samples were collected using 10L pre-washed plastic containers that were soaked in 10% bleach for 24 hours, thoroughly rinsed with miliQ, and washed three times with water from the collection point prior to sampling. Water samples were transported to a field laboratory (< 2hrs) and filtered through 47mm diameter, 0.22µm pore-size membrane filters (Millipore, DURAPORE PVDF .22UM WH PL) using a peristaltic pump (100rpm). Between each sample, 500ml of 10% bleach was run through the pumping system, followed by 500ml of MilliQ water and then 1 L of sample. Following this, the filter was aseptically placed into the pumping system, and the volume of sample water filtered was recorded (between 500 ml and 2000 ml) for later normalisation of gene copy. Filters were immediately frozen and stored in liquid nitrogen prior to being stored at -80°C. Within a week of sample collection, DNA was extracted from filters using the PowerWater DNA Isolation Kit (QIAGEN) according to the manufacturer's instructions, in batches of 45 samples, including 3 kit blanks per batch. DNA was stored at -80ºC prior to downstream analysis.

4.2.3 – Quantitative PCR (qPCR) analysis

To determine the presence of human faeces, indicative of sewage contamination, I used quantitative PCR (qPCR) to measure levels of the Lachno3 assay (Feng et al., 2018), which targets human gut microbiome associated *Lachnospiraceae* and has been demonstrated to be an excellent marker of human sewage within the environment. I also quantified levels of *Arcobacter,* which is a genus of bacteria that is regularly associated with stormwater, sewage infrastructure (McLellan and Roguet, 2019) and sewage sludge (Collado et al., 2011). The *Arcobacter* genus includes species that are associated with human illness (Ferreira et al., 2016), and recently was shown to be correlated with some ARG in marine environments (Carney et al. 2019). *Arcobacter* were quantified using the ARCO assay, which targets the 23S rRNA gene (Bastyns et al., 1995). Furthermore, I characterised patterns in the class 1 integron-integrase gene (*intI1*), which facilitates the mobility of integron related ARG cassettes, is present within diverse pathogenic bacteria, and has been proposed as an excellent indicator of

anthropogenic pollution within natural environments (Gillings et al., 2015). To quantify *intI1* gene abundances, I used the *intI1* primer set (Mazel et al., 2000) (Table 1, Appendix 3).

Growing evidence suggests the birds are environmental reservoirs of ARB and ARGs (Bonnedahl and Järhult, 2014; Ahlstrom et al., 2018) and vectors for dissemination of ARGs in the environment (Jarma et al. 2021). In addition to sewage markers, I also used qPCR to determine levels of the GFD assay (Green et al., 2012) which is an indicator of bird feaces (Table 1, Appendix 3).

Quantitive PCR was also used to quantify a suite of ARGs that have previously been detected in high abundances at two Sydney beaches exposed to wet weather associated sewage incursions (Carney et al., 2019), including the *sulI, tetA, qnrS, dfrA1* and *vanB* genes. *sulI* encodes resistance to sulphonamide, an antibiotic used widely in clinical settings (Pei et al., 2006); *tetA* encodes resistance to tetracyclines, which are a group of antibiotics widely used to treat bacterial infections in both human and animals (Borjesson et al., 2009); *qnrS* confers resistance to quinolones, a group of antibiotics mostly used in clinical settings (Berglund et al., 2014); *dfrA1* confers resistance to trimethoprims (Grape et al., 2007), a group of antibiotics used widely to treat urinary tract infections; *vanB* encodes resistance to vancomycin (Berglund et al., 2014), which is a last line of defence antibiotic (Berglund et al., 2014). Details on all qPCR assays are provided in table 1, Appendix 3 and details on qPCR methods are provided in Appendix 3 section 1.4.

4.2.4 – 16S rRNA amplicon sequencing and analysis

To characterise bacterial community composition in all seawater and stormwater drain samples, the V3–V4 region of the bacterial 16S rRNA gene was amplified using the 341f/805r primer set (Suzuki et al., 2000), with the following cycling conditions: 95°C for 3 minutes followed by 25 cycles of: 95°C for 30 seconds, 55°C for 30 seconds, 72°C for 30 seconds, and then 72°C for 5 minutes with a final hold at 4°C (Pichler et al., 2018). Amplicons were subsequently sequenced using the Illumina MiSeq platform (300 bp paired-end analysis at the Ramaciotti Institute of Genomics, University of New South Wales). For a detailed description of 16S rRNA amplicon sequencing data processing details refer to Appendix 3 section 1.5.

4.2.5 – Statistical analysis

To test for differences in abiotic variables, and spatiotemporal differences in the levels of enterococci and qPCR markers, data was first transformed using ln(x+1) and tested for normality. Normally distributed data was compared using the parametric ANOVA test, paired with Tukey pairwise comparisons, while non-normal data was compared using the nonparametric Kruskal-Wallis test, followed by Mann-Whitney pairwise comparisons with Bonferroni corrected p-values. To test for correlations between enterococci plate counts (single replicate) and the qPCR samples (three biological replicates), average values from the qPCR data were used. Correlations between enterococci counts, and data derived from qPCR assays were determined using Spearman's R_S, with Bonferroni corrected p values.

To test for differences in microbial community composition (16S rRNA data) and alpha diversity between samples I used the Adonis function from Vegan (Dixon, 2003) and the pairwise.adonis function from the PairwiseAdonis (Martinez Arbizu, 2020) R package. Three separate tests were undertaken using the multipatt function within the indicspecies package (De Caceres and Jansen, 2018) to identify ASVs that represented 'indicator taxa' for: a) stormwater drain, b) lagoon and c) seawater communities. Three separate Mictools (Albanese et al., 2018) analysis were also run with the aim of determining the Spearman's RS correlations between the suite of ARGs detected via qPCR and a) drain indicator ASVs, b) lagoon indicator ASVs and c) seawater indicator ASVs. For complete R scripts used in statistical analysis of 16S data see (https://github.com/Nwilliams96/Terrigal_Wet_Weather_2019).

4.3 – Results

4.3.1 – Environmental data and FIB (enterococci) analysis

Substantial changes in abiotic parameters occurred over the course of the rainfall event. Following 20mm of rainfall (on 4/6/19), there was a significant decrease in both temperature [$p = 0.0006$] and salinity [$p = 0.0026$] from the preceding two sampling points taken before the rain event. This initial rainfall event also led to significant increases in levels of total dissolved phosphate (TDP) [$p = 1.36 \times 10^{-5}$], total phosphate (TP) [$p = 8.10 \times 10^{-9}$], total dissolved nitrogen (TDN) [$p = 1.19 \times 10^{-8}$], filterable reactive phosphorus (FRP) [$p = 0.0178$], and ammonia [$p = 0.0002$], relative to the two sampling points that were taken before the rain event. After the opening of the entrance to Terrigal Lagoon (6/6/19), input of lagoon water into Terrigal Beach resulted in significant increases [$p = 0.001$] in levels of TP, FRP, TDN, ammonia and dissolved oxygen (DO %) in the Terrigal seawater samples, relative to samples taken on before the lagoon opening on the 6/6/19. Five days after the end of the rainfall event, levels of all measured abiotic parameters returned to levels that were statistically indistinguishable from what was observed before the rain event.

During dry weather, enterococci levels were below limit of detection (10 MPN/100ml) within all seawater samples on the 20/5/19 and 29/31 (94 %) of samples on the 31/5/19 (Figure 2A). Following 20.4 mm of rain (4/6/19), enterococci levels reached the maximum limit for detection (24,196 MPN/100 ml) within all three drains (Figure 2A). Within the nearshore water samples, enterococci levels increased by over 450-times relative to samples taken before the rain event. On the 6/6/19, after a further 20.4 mm of rain, average enterococci levels within seawater samples decreased three orders of magnitude. Enterococci levels were notably high within Drain 2 and the adjacent seawater sample (SW2.1) and at one Terrigal Lagoon site (TL2) which exceeded 10,000 MPN/100ml. After the entrance to Terrigal Lagoon was mechanically opened to the ocean, enterococci levels were elevated along transect 6 (immediately adjacent to the mouth of the lagoon Figure 2A). Five days after the rainfall event (11/6/19), enterococci levels within all Terrigal Beach seawater samples had decreased to the lower limit of detection (10 MPN/100ml).

4.3.2 – Sewage signals – qPCR markers Lachno3, Arcobacter and intI1

Throughout the study, there was both a statistically significant correlation between Lachno3, *intI1* and *Arcobacter* [Lachno3: $r_s > 0.59$; $p < 0.01$] as well as between each of these

markers and enterococci [*Arcobacter:* $r_s = 0.33$; $p < 0.01$; Lachno3: $r_s = 0.67$, $p < 0.001$; *intI1*:$r_s = 0.28$; $p < 0.001$]. Before the rain event concentrations of Lachno3 were detected within only 9/53 (17 %) of samples taken from seawater on the 20/5/19 and 31/5/19, however *Arcobacter* and *intI* were detected in substantially more samples 50/53 (95 %) and 52/53 (98 %) of samples respectively, but concentrations of both were statistically indistinguishable between either Terrigal Beach or Lagoon samples with the 'pristine' reference site at Forrester's Beach.

Following 20.4mm of rain (4/6/19), within the nearshore seawater samples, Lachno3 was recorded at concentrations two orders of magnitude higher [mean = 50979 ± 130926 copies/100ml] than were observed before the rain event [mean = 820 ± 2693 copies/100ml], with highest levels within samples immediately adjacent to stormwater drains (Figure 2B). At these sites *Arcobacter* levels also increased substantially by between 16- to over 1000-fold and *intI1* levels increased over 100-fold. The maximum concentrations of Lachno3, *Arcobacter* and *intI1* all occurred in Drain 4. In accordance with this pattern, the highest levels of Lachno3 present in Terrigal Beach seawater samples occurred in the sample immediately adjacent to Drain 4 (Figures 2B, C and D). Unfortunately, due to rough ocean conditions, it was not possible to acquire offshore transect samples on this date, precluding an assessment of the seaward spatial extent of contamination from stormwater drains. During this period, concentrations of Lachno3 [mean = 51860 ± 433 copies/100ml] and *intI1* [mean = 7005 ± 9147 copies/100ml] also increased by three orders of magnitude and by 13-times respectively within all Terrigal Lagoon samples (Figure 2B and D) in comparison to what was observed during dry weather [Lachno3 mean = 81 ± 433 copies/100ml, *intI1* mean = 501 ± 488 copies/100ml].

On 6/6/19, after 40.8mm of rain in the preceding 48 hours, levels of Lachno3 decreased significantly [$p = 0.0377$] within the drains and adjacent seawater samples, while *Arcobacter* and *intI1* levels remained at statistically indistinguishable compared to levels detected two days prior. Lachno3 and *intI* levels remained elevated at other points along Terrigal Beach, in particular within samples adjacent to Drains 1 and 2. Although, significant concentrations of these markers did not extend beyond the shore-line samples in any of the off-shore transects (Figures 2B and D). Levels of Lachno3 [mean = $7.8 \times 10^4 \pm 4.1 \times 10^4$ copies/100ml] and *Arcobacter* [mean = $1.47 \times 10^7 \pm 6.03 \times 10^6$ copies/100ml] increased significantly [$p = 0.02$, 0.0006 respectively] within Terrigal Lagoon compared to the 4/6/19 [Lachno3, mean = 51860 ± 433 copies/100ml, *Arcobacter*, mean = $1.69 \times 10^6 \pm 1.99 \times 10^6$], (Figure 2C).

Following the opening of the lagoon entrance on the afternoon of 6/6/19, a significant increase in the concentrations of Lachno3 [$p = 1.25 \times 10^{-5}$], *intI1* [$p = 0.0019$] and *Arcobacter*

[p = 0.003] compared to the morning, was observed at, and surrounding, the lagoon entrance (i.e., transects 4, 5 and 6). Of note, increased levels of Lachno3 were observed up to 300 m offshore in transects 5 and 6.

Following 5 days without rain (11/6/19) concentrations of Lachno3 and *Arcobacter* decreased significantly [p = 0.0239 and 3.46 x 10^{-6} respectively] from those observed during the peak rainfall events but remained significantly [p = 2.69 x 10^{-4} and 2.81 x 10^{-9}, 3.32 x 10^{-21} and 2.81 x 10^{-15} respectively] elevated relative to the samples taken during before any rain (i.e., 20/5/19 and 31/5/19). Most notably, high levels of Lachno3, *intI1* and *Arcobacter* occurred within Drain 4, where concentrations were higher than those observed during the rainfall event. Concomitantly high levels of Lachno3 and *Arcobacter* were observed in the adjacent seawater sample (SW4.1), indicating an impact of this drain on the surrounding environment.

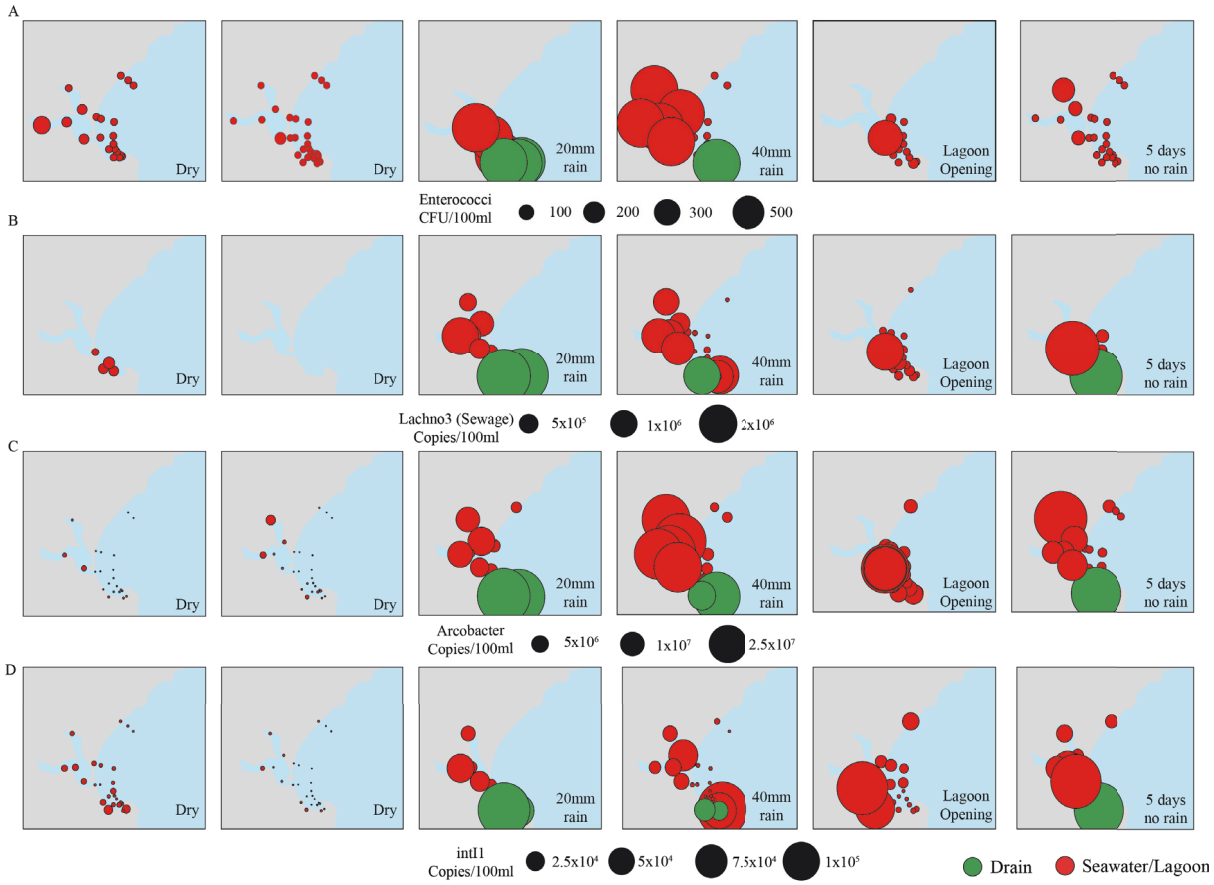

Figure 2. Bubble plots on map of Terrigal showing sewage signals. A) colony forming units per 100ml of enterococci, b) copy number per 100ml of the *Lachno3* qPCR assay, c) copy number per 100ml of the *Arco* qPCR assay and d) copy number per 100ml of the *intI1* qPCR assay. For each of A, B, C and D, each map tile represents a sampling day, left to right as follows 20/5/19 (Dry), 31/5/19 (Dry), 4/6/19 (20.4mm rain), 6/6/19 (further 20.4mm rain or cumulative 40.8mm rain), 6/6/19 (after lagoon opening), and 11/6/19 (five days post rain).

4.3.3 – Bird faeces signal

Levels of the GFD Avian faecal marker were not significantly elevated in Terrigal seawater samples relative to the relatively pristine control site at Forrester's Beach, during either dry (pre- or post-rain) or wet conditions (both days of rainfall). Within Terrigal Lagoon, rainfall led a significant [$p = 0.0016$] increase in concentrations of this marker. Five days after rainfall, concentrations of the GFD marker were comparable to those observed during the rainfall event.

4.3.4 – ARG dynamics

Throughout the study period, levels the *sulI* gene were significantly correlated with levels of Lachno3, *Arcobacter* and *intI1* [Lachno3 $r_s > 0.31$, *Arcobacter* $r_s > 0.32$, *intI1* $r_s > 0.41$; $p < 0.05$]. Levels of the *qnrS* gene were significantly positively correlated with *Arcobacter* [$r_s = 0.28$; $p < 0.05$], but not enterococci or Lachno3, nor any other ARGs, while levels of the *dfrA1* gene were positively correlated with levels of enterococci and *sulI* [enterococci $r_s = 0.36$, *sulI* $r_s = 0.23$; $p < 0.05$]. *vanB* was not detected in any samples.

Before the rain event (20/5/19 and the 31/5/19), *sulI* and *dfrA1* were present in 13/53 (24%) and 12/53 (22%) of samples respectively, with detected levels of both genes an order of magnitude higher in the nearshore samples than the samples taken approximately 100 m and 300m offshore. The ARGs *tetA* and *qnrS* displayed substantially different patterns, whereby these genes were detected in 49/53 (92%) and 43/53 (81%) of samples before the rainfall event (20/5/19 and 31/5/19) (Figure 3 C and D), however there was no statistically distinguishable differences between levels of either gene in the Terrigal Beach seawater samples compared to the samples taken at the relatively clean reference site, Forrester's Beach.

After 20.4mm of rain (4/6/19), *sulI* and *qnrS* levels increased significantly [$p = 8 \times 10^{-10}$], with levels of *sulI* increasing by almost three orders of magnitude within the nearshore samples. In contrast, *dfrA1* was only detected within a single seawater sample (SW4.1), but levels within this sample were two orders of magnitude higher than the nearshore levels observed before the rain event. Interestingly, highest levels of *sulI* were observed in sample SW4.1 (directly adjacent to Drain 4), where levels of this gene were an order of magnitude higher than those observed in other nearshore samples. This was consistent with the patterns observed within Drain 4, which had significantly higher [$p = 6.66 \times 10^{6}$] levels of *sulI* and *dfrA1* than any other drain. Levels of both *dfrA1* and *sulI* increased significantly [$p = 0.0002$]

in Terrigal Lagoon relative to conditions before the rain event. The ARG *tetA*, again, displayed substantially differing patterns to the other ARGs, whereby in the nearshore seawater sample levels were not statistically different to levels observed before the rain event. During this time, the highest levels of *tetA* were recorded within Drains 1 and 2 but decreased significantly [$p = 0.0001$] within the lagoon samples (Figure 3C) compared to samples taken before the rain event.

On the morning of the 6/6/19 after a further 20.4mm of rain, levels of *sulI* and *qnrS* in nearshore samples were statistically indistinguishable from the preceding sampling point, and an order of magnitude lower within the drain samples relative to 4/6/19. However, in samples taken 100m and 300m offshore, concentrations of both genes were an order of magnitude higher than conditions before the rain event. At this time the *dfrA1* gene was not detected within any of the Terrigal Beach seawater samples, while within the stormwater drains concentrations of this gene dropped by two orders of magnitude relative to the 4/6/19. In contrast, levels of *tetA* within Terrigal Beach seawater samples were significantly higher [$p < 0.01$] than those observed before the rain event. Within the lagoon samples, *sulI* and *dfrA1* levels remained high, but were statistically indistinguishable from those observed on the 4/6/19, while *tetA* levels increased significantly [$p = 0.0008$]. At this time, *qnrS* was only detectable in 1/5 lagoon samples (Figure 3D). Consistent with this pattern, the opening of the mouth of Terrigal Lagoon on the afternoon of 6/6/19 did not lead to an increase in *qnrS* levels in Terrigal Beach seawater samples. Conversely, the opening of the lagoon led to a 5 order of magnitude increase in levels of *sulI* at the site adjacent to the mouth of the lagoon (SW6.1) (Figure 3B, Appendix 3 Figure 1), while levels of *tetA* doubled in the seawater samples near to the mouth of the lagoon (SW5.X, 6.X and 7.X) (Figure 3C) and *dfrA1* was detected in the nearshore sites SW5.1 and SW6.1, where, notably, it had been undetected on the same morning

Five days after the rain event (11/6/19), *dfrA1* was not detected, and *sulI* and *qnrS* levels dropped significantly [$p = 3.57 \times 10^{-12}$, $p = 3.77 \times 10^{-11}$] within both nearshore and offshore samples. Opposing this trend, levels of *tetA* were statistically indistinguishable from those recorded during the rainfall event (4/6/19 and the 6/6/19). At this time, levels of all ARGs remained high within Drain 4 and were statistically indistinguishable from those observed during the rainfall event. However, within Terrigal lagoon samples each ARG displayed a different pattern. Levels of *tetA* and *sulI* remained high and were statistically indistinguishable from those observed on the 4/6/19, while *qnrS* levels increased significantly [$p=0.003$]. The

dfrA1 gene was detected within a single lagoon sample (L5), but levels were 26-fold lower than those observed on the 6/6/19.

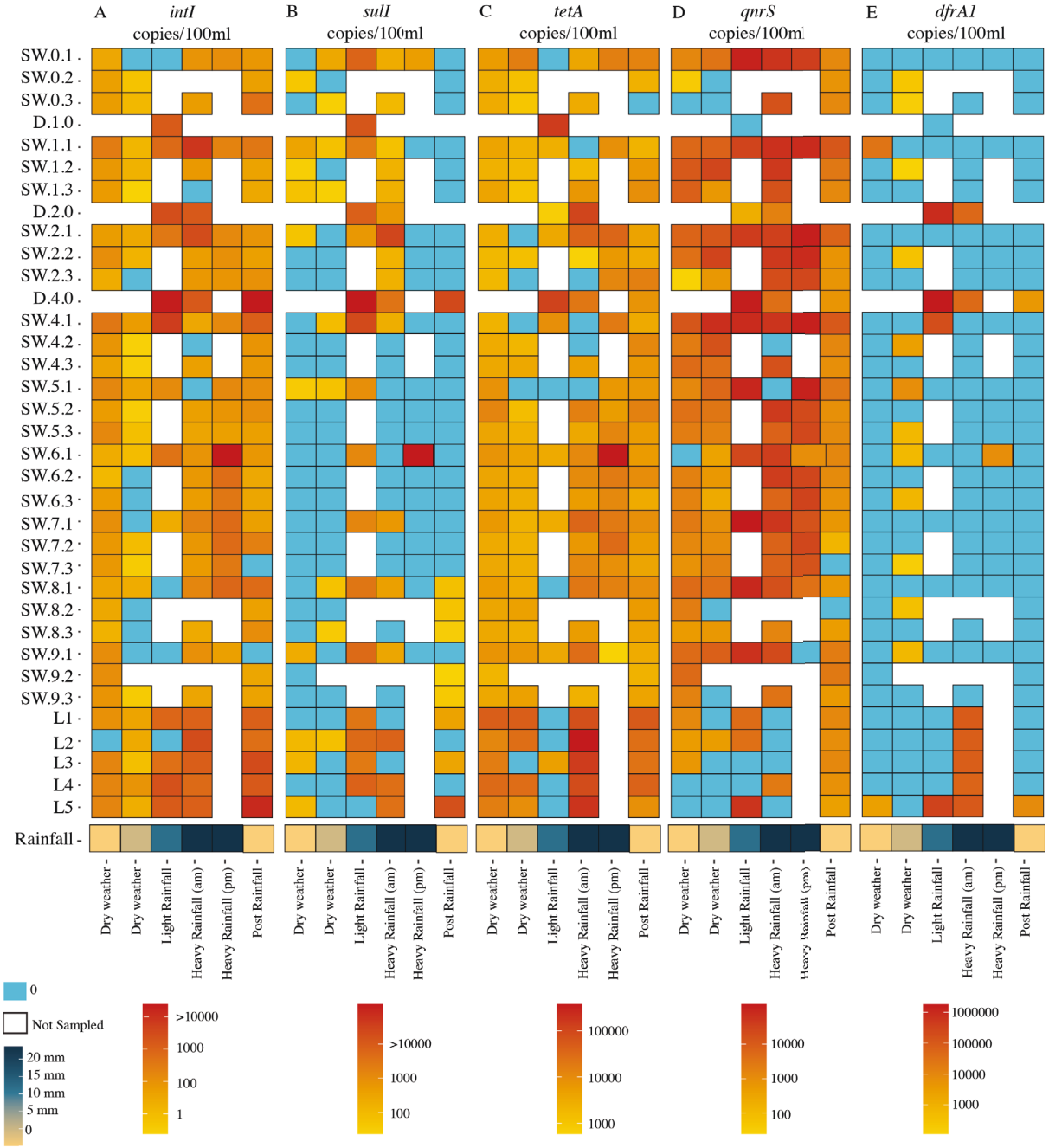

Figure 3. Heatmaps of antibiotic resistant gene qPCRs (*intI, sulI, tetA, dfrA1, qnrS*) across sampling locations (Y axis) and days (x axis). Colour scale (yellow to red) corresponds of copy numbers defined using qPCR over the course of the study. Below each heatmap is a small heatmap (yellow to blue) displaying rainfall (mm). Blank cells represent samples not collected either due to lack of water flow in drains or low safety levels during the rainfall event and blue cells no detection. Note maximum/minimum values on colour scales vary among presented ARGs, to allow for spatial and temporal patterns of each ARG to be clearly represented

4.3.5 – Bacterial Community Analysis

4.3.5.1 – Patterns in bacterial community diversity and composition

Throughout the study period, bacterial diversity (Shannon) was significantly lower within the Drain 1 [$F = 45.15$, $p < 0.001$], Drain 2 [$F = 127.3$, $p < 0.001$] and Drain 4 [$F = 309.9$, $p < 0.001$] samples relative to Terrigal Beach seawater samples. Bacterial community composition also differed significantly between Drain 1 [$F = 37.5$, $p < 0.001$], Drain 2 [$F = 78.4$, $p < 0.001$] and Drain 4 [$F = 101.5$, $p < 0.001$] samples and seawater samples. Stormwater drain bacterial communities were also significantly less diverse [$F = 123$, $p < 0.001$], and dissimilar in community composition to Terrigal Lagoon samples [$F = 46.2$, $p = 0.001$]. In contrast, bacterial communities within Terrigal lagoon were significantly [$F = 46.2$, $p = 0.001$] more diverse and significantly different in community composition [$F = 101.5$, $p = 0.001$] to the nearshore Terrigal Beach seawater samples. Bacterial composition was also significantly different between drains [$F = 5.04$, $p = 0.001$].

4.3.5.2 – Associations between indicator taxa and AbR genes

To determine whether specific amplicon sequence variants (ASVs) resolved in the 16S rRNA amplicon sequencing data were indicative of stormwater, lagoons, or seawater samples, I identified 'indicator taxa' using the indicspecies package (De Caceres and Jansen, 2018). Network analysis was then used to identify putative links between these indicator taxa and the measured ARGs.

Within seawater samples, there were 507 indicator ASVs identified. Of these, none displayed a statistically significant correlation in their relative abundance to any of the measured ARGs. In contrast, 10,283 indicator ASVs were identified from stormwater drain samples, and from among these 5493 correlations occurred between the relative abundance of stormwater indicator ASVs and ARGs. The highest number of significant correlations with stormwater drain indicator ASVs occurred with *intI1* (Figure 4) (1,940/10283; 19 %), followed by *sulI* (1,838/10283; 18 %), *tetA* (1,167/10283; 11 %), *dfrA1* (1,122/10283; 11 %) and lastly *qnrS* (1,037/10283; 10 %). Among stormwater sample indicator taxa, a number of positive correlations to ARGs occurred among members of the *Comamonadaceae* family, including 317 positive correlations with *intI1*. I also observed 319 *Comamonadaceae* ASVs displaying

positive correlations with *sulI*, along with 150 with *dfrA1*, 149 with *tetA* and 71 with *qnrS*. Within the *Comamonadaceae* family, discrete ASVs identified as *C. testosteroni,* displayed four positive relationships with *intI1* [$p < 0.05$, $r_s = 0.77, 0.44, 0.40, 0.33$], five with *sulI* [$p < 0.05$, $r_s = 0.78, 0.66, 0.36, 0.09, 0.07$], three with *dfrA1* [$p < 0.05$, $r_s = 0.56, 0.50, 0.36$] and three with *qnrS* [$p < 0.05$, $r_s = 0.25, 0.18, 0.05$]. Stormwater drain indicator taxa, identified as *Bacteroides* ASVs also displayed many statistically significant correlations with levels of the ARGs measured here. *Bacteroides* ASVs in fact had the most (40) positive correlations with *intI1*, followed by 38 correlations with *sulI*, 8 with *dfrA1*, 8 with *tetA* and 6 with *qnrS*. Of note, *B. fragilis*, correlated with *intI1* and *sulI* [$p < 0.05$, $r_s = 0.76, 0.08$]. *intI1* levels were also correlated with 12 *Arcobacter* ASVs, the strongest being with *A. butzleri* (B1000019013) [$p < 0.05$, $r_s = 0.82$]. Levels of the ARGs *sulI*, *dfrA1* and *qnrS* were also positively correlated with *A. butzleri* (B1000019013) [$p < 0.05$, $r_s = 0.46, 0.36, 0.10$].

A further 1,160 ASVs were identified as indicators of lagoon samples. Of note, 1.5 % of these taxa were identified as members of the *Arcobacteraceae* family, 3.6 % were members of the *Comamonadaceae* family and 1 % were members of the *Vibrionaceae* family. Interestingly, levels of the *qnrS* gene were positively correlated with 98 % (n = 1,141) of these lagoon indicator ASVs, which was more than those observed with drain indicator ASVs. Positive correlations were also observed between lagoon indicator taxa and *tetA* (1080) *intI1* (967), *sulI* (707), and *dfrA1* (471). Similar to the patterns observed with stormwater drain indicator ASVs, significant positive correlations were observed between all five measured ARGs and indicator ASVs identified as *Comamonadaceae* and *Arcobacter/Pseudarcobacter*.

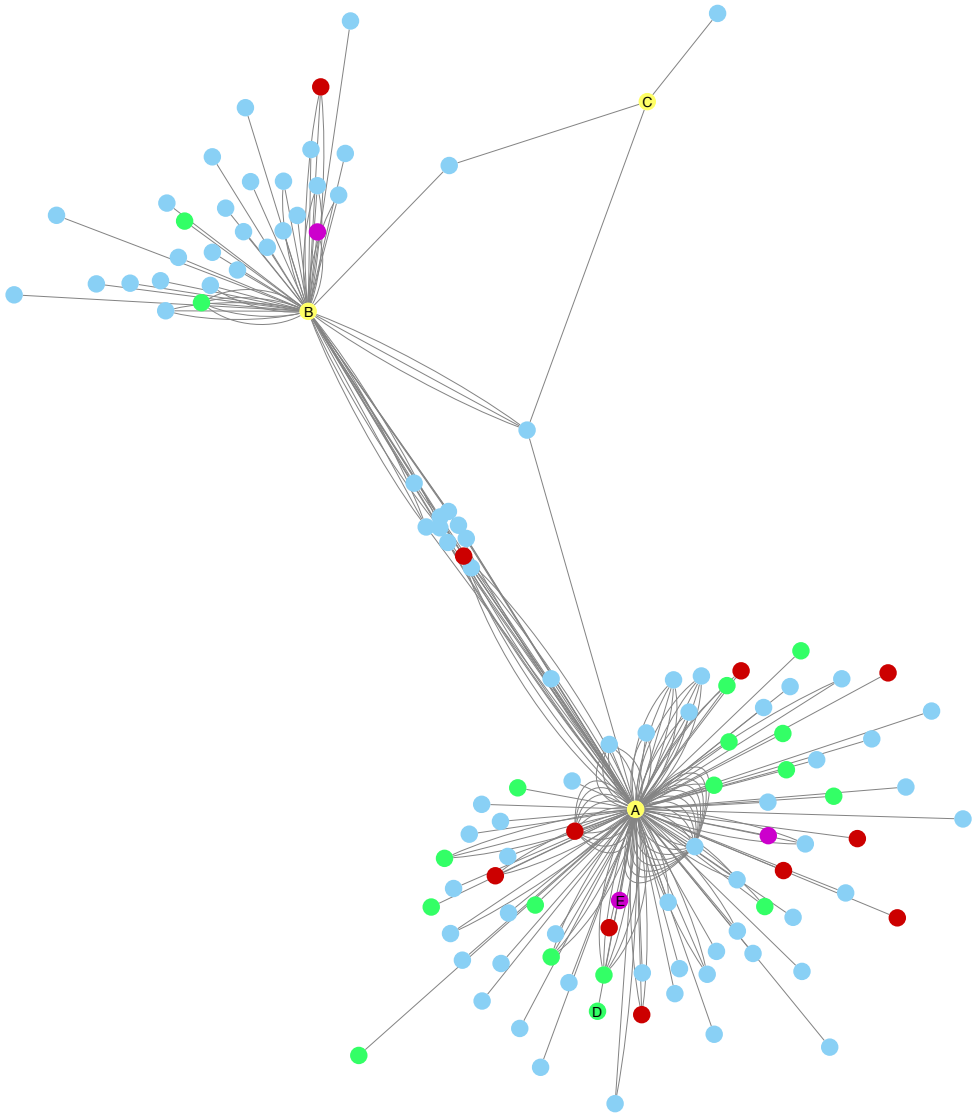

Figure 4. Correlations between drain indicator ASVs and antibiotic resistance genes. Correlations with a Pearson's R > 0.70 between drain indicator ASVs and antibiotic resistance genes detected via qPCR. Distance between circles indicates power of R. Yellow circles are ARGs with (a) representing *intI1*, (b) representing *sulI*, and (c) representing *dfrA1*. Green circles *Bacteroides* with (D) representing *B. fragilis* represent, while purple circles are *Arcobacter*/*Pseudarcobacter* with (E) representing *A. butzleri,* red circles represent *Comamonadaceae,* and blue circles represent all other correlations.

4.4 – Discussion

ARG contamination within coastal environments poses a potential health risk to people who use coastal environments recreationally (Leonard et al., 2018), but the extent of this issue and the underlying dynamics and mechanisms are not well resolved. The central goal of our study was to determine to what extent sewage contamination leads to an increased presence of ARGs in coastal environments. I focussed on a popular swimming beach in eastern Australia, which has regularly poor water quality ratings due to faecal contamination (DPIE, 2020). Terrigal Beach has multiple potential input points for faecal contamination, including a network of stormwater drains and an adjacent coastal lagoon, Terrigal Lagoon, which is periodically opened to the ocean during heavy rain events. I hypothesised that these features may act as conduits for ARG contamination at Terrigal Beach.

4.4.1 – Sewage contamination of a beach leads to elevated ARGs

To determine if sewage contamination was linked to ARG abundance at Terrigal Beach, I first quantified two indicators of human faeces, enterococci and the Lachno3 qPCR marker (Feng et al., 2018) as well as the *intI1* gene which has been identified as an excellent microbial measure of anthropogenic contamination in aquatic habitats (Gillings et al., 2015), and *Arcobacter*, a genus of bacteria linked to human sewage, urban stormwater, and sewage pipe infrastructure (McLellan and Roguet, 2019). All markers displayed a significant increase from low levels observed before the rain event, to high levels following 20.4 mm of rain. Levels within all stormwater drains increased significantly relative to what was observed before rainfall, becoming highly elevated within nearshore seawater and Terrigal Lagoon samples. It is notable however, that in nearshore seawater samples that were not located immediately adjacent to stormwater drains, concentrations of Lachno3 remained low or often undetectable. This was particularly true for transects outside of the Terrigal Haven region (i.e., at North Avoca, SW0.1, Wamberal Beach SW8.1 and Forresters beach SW9.1 Figure 2B). The highest levels of all markers were detected adjacent to Drain 4, indicating it as a major source of sewage contamination. Notably, adjacent to Drain 4, levels of enterococci were 49-times higher than the WHO safe swimming guidelines category D, which indicates a high level of potential illness transmission (WHO, 2021) and levels of Lachno3 were only an order of magnitude lower than levels that have been detected within human faeces (Ahmed et al., 2019), a strong indication that raw sewage was entering the environment from this drain.

When Terrigal Lagoon was opened to the ocean, it had a pronounced impact on water quality at Terrigal Beach, particularly at sites immediately adjacent to the entrance of the lagoon. Near to the opening of Terrigal Lagoon, Lachno3, *intI1* and *Arcobacter* levels increased significantly at the surrounding sites, demonstrating widespread sewage contamination following the opening of the lagoon entrance indicating that opening Terrigal Lagoon had an impact on the surrounding coastal environment that extended up to a few hundred metres to the east and south of the lagoon entrance. Taken together, these patterns confirm that both Terrigal Lagoon and the network of stormwater drains (particularly Drain 4) are sources of sewage contamination at Terrigal Beach, presenting a human health risk given that sewage has been previously linked to microbial pathogens (Collado 2011), and ARGs (Steinbakk et al., 1992).

Of note, concentrations of *intI1* and all ARGs investigated in this study (except *qnrS*), correlated positively with concentrations of either enterococci or Lachno3. While the causes of elevated ARG levels within the environment are potentially multifaceted, the clear correlations between our MST markers for sewage and targeted ARGs indicate that sewage contamination following rainfall contributes to increased ARG levels at Terrigal Beach supporting our proposition that sewage contaminated water is the major conduit for ARG contamination at this site. While there was no statistically significant spatiotemporal links between *qnrS* and the human faecal marker, it should be noted that the samples with the highest levels of *qnrS* coincided with very high levels of Lachno3, particularly Drain 4 and the seawater sample directly adjacent to it, SW4.1. The strong evidence for sewage contamination through the stormwater drains and the lagoon being linked to a high load of ARG and *intI1* input into Terrigal Beach is in-line with other research in China, Europe, and the USA (Karkman et al., 2019).

After confirming the presence of sewage contamination at Terrigal Beach, and that levels of sewage markers correlated with 75% of detected ARGs, I next investigated the principal input points of these ARGs into the environment. Concentrations of all ARGs, as well as the *intI1* gene, displayed a dramatic increase during and after rainfall. After a total of 40.8 mm of rainfall, levels of all four detected ARGs and *intI1* were highest within Drain 4, and among the seawater samples collected at Terrigal Beach, highest levels were observed in the samples adjacent to Drain 4 (SW4.1). Indeed, levels of *dfrA1* and *sulI* at this site were an order of magnitude higher and levels of *tetA* were two orders of magnitude higher, than levels of these genes previously observed in a highly contaminated urbanised beach in Sydney, which

has previously been demonstrated to have high levels of sewage and ARG contamination (Carney et al., 2019). While Drain 4 certainly appears to be a significant source of ARG contamination at Terrigal Beach, our analysis also revealed that Terrigal Lagoon also contained high levels of all four targeted ARGs following rainfall, and that the opening of the lagoon's entrance led to dramatic, and spatially extensive, increases in ARG levels at Terrigal Beach.

While the levels of 75% of the targeted ARGs were significantly correlated with either enterococci or Lachno3 levels, not all the ARGs displayed the same spatial or temporal dynamics. Indeed, the only ARGs which correlated significantly with each other were *dfrA1* and *sulI*. In general, detectable, and sometimes relatively high levels of *tetA* and *qnrS* occurred during dry weather both before and after the rain event, whereas *dfrA1* and *sulI* were largely undetectable at this time. This may be indicative of background levels of these genes in the environment, as both genes have been detected in remote areas that are subject to little or no anthropogenic pollution (Scott et al., 2021; Tan et al., 2018). Both tetracycline and quinolone resistance has been detected in avian faeces (Skarzynska et al., 2021) which could explain them being widespread before the rain event, however no correlation was observed between either *tetA* or *qnrS* and the GFD qPCR marker (Green et al., 2012) for avian faeces (Appendix 3 section 2.1).

Throughout the rain event on both the 4/6/19 and 6/6/19, both Drain 4 and Terrigal Lagoon displayed high levels of all 4 ARGs, however within Drains 1 and 2 the different ARGs displayed different patterns. On the 4/6/19, high levels of both *sulI* and *tetA* were detected within Drain 1, but *qnrS* and *dfrA1* were undetectable, and from the 4/6/19 – 6/6/19 *sulI* and *dfrA1* levels decreased substantially within Drain 2, while *qnrS* and *tetA* levels increased substantially. Differing abundance patterns of ARGs has previously been linked to shifting bacterial communities (Zhu et al., 2017). Our analysis revealed different bacterial communities between the drains, presenting a possible explanation for these differing abundances of ARGs.

After determining links between human faecal markers and ARGs, I wanted to explore the possible vehicles for ARGs entering the environment. To do this, I employed the *indicspecies* package (De Caceres and Jansen, 2018), which enabled us to identify ASVs that are indicative of storm water infrastructure from the 16S rRNA sequencing dataset and coupled this with network analysis to determine correlations between these ASVs, and levels of ARGs identified via qPCR. I identified three groups of indicator taxa, that were representative of the stormwater drains, Terrigal Lagoon, and seawater at Terrigal Beach. All targeted ARGs displayed over 1000 correlations to bacterial indicators of the stormwater drains, which

included a large proportion of *Comamonadaceae*, *Arcobacter* and *Bacteroides*. Notably, members of each of these groups are regularly associated with sewage (Fisher et al., 2014; Shanks et al., 2013). Similarly, the bacterial indicators for Terrigal Lagoon that showed the highest levels of correlations to ARGs included *Comamonadaceae* and *Arcobacter/Pseudarcobacter*. Of note, none of the bacterial indicators for seawater at Terrigal Beach displayed significant correlations to ARGs, further confirming that ARG levels at this swimming beach are linked to input of water from stormwater drains and Terrigal Lagoon, which is linked to sewage contamination of these samples. Differences in the putative vehicles for ARG input into Terrigal Beach may also account for the spatial differences in *tetA* compared to *sulI* and *dfrA1*, as discussed above.

Considering that many *Arcobacter* ASVs were correlated to levels of *tetA*, I examined levels of *Arcobacter* determined via qpCR, finding strong correlations between *tetA* and the qPCR results. One example of this was in Drain 2 on the 6/6/19: after a total of 40.8mm of rain in the preceding 3 days, I found both *tetA* and *Arcobacter* to be at levels more than double than Drain 4 which had the highest levels of both markers for faecal contamination. An explanation for this is that *Arcobacter* may have been a vehicle for *tetA* entering the environment; indeed, of all the ARGs, *tetA* shared the strongest positive correlation (r_s=0.45) with *Arcobacter* detected via qPCR. This pattern is in line with previous research identifying *tetA* resistant *A. butzleri* (Jasim et al., 2021), however it should be noted that other bacteria may harbour *tetA* but weren't detected in this analysis.

In this study, I have shown a significant relationship between sewage markers and ARGs in the environment. I have also shown that both sewage and ARG contamination enter from two major sources, Drain 4 and Terrigal Lagoon, and I suggest these locations as the most relevant sites for pollution remediation strategies. Considering recent research has determined consistent surfing and swimming are activities that can lead to exposure to AbR bacteria (Leonard et al., 2018), high levels of ARGs in Terrigal represent a previously over-looked but potentially noteworthy indicator of a health risk to recreational beach users.

Not only does sewage harbour ARGs, but it can also harbour numerous enteric pathogens (Garcia-Aljaro et al., 2019) such as bacteria from the genus *Arcobacter* (Collado et al., 2011; Fisher et al., 2014; Millar and Raghavan, 2017). Amongst the *Arcobacter* ASVs detected via 16S sequencing I detected *A. butzleri*, which is a known human enteric pathogen (Levican et al., 2013). Relative abundances of this bacteria were correlated with the ARGs *sulI*, *dfrA1* and *qnrS*. ASVs identified as *Comamonadaceae testosteroni*, and *Bacteroides fragilis*,

which are other known enteric pathogens (Tiwari and Nanda, 2019; Wexler, 2007) also displayed correlations to all targeted ARGs. While it should be noted that the resolution of 16S rRNA sequencing is insufficient to provide unequivocal species or strain-level identification, and our correlative analysis does not prove that these bacteria host the measured ARGs, our results provide evidence that the potential human health impacts of coastal ARG contamination potentially require further attention. Further research could include culturing of pathogenic bacteria from untreated raw sewage at local sewage treatment plants, stormwater drains and the environment. These isolates could then be screened for ARGS, providing a more definitive conclusion.

4.5 – Conclusions

The increase of AbR within natural environments is a point of rising global concern (Finley et al., 2013) and AbR within coastal environments represents a potential health threat to recreational users of these environments (Leonard et al., 2018). This study has shown a direct link between sewage contamination and an increase in ARGs at a popular coastal beach, and in doing so was also able to discriminate the point sources of ARGs, which were identified as stormwater drains and a nearby coastal lagoon that also receives sewage contaminated stormwater. Finally, I demonstrated that not all ARGs display the same spatial and temporal dynamics in coastal environments. This study serves as a warning of the potential health risk associated with recreational use of sewage contaminated beaches and highlights the links between contaminated stormwater and ARGs in the environment, elevating the necessity for remediation of beaches impacted by faecal contamination.

Chapter 5 – Defining the importance of natural environmental variability and anthropogenic impacts on bacterial assemblages within intermittently opened and closed lagoons

Author's state that author contributions are correct, and that the student has completed the work stated in the author contributions.

Author Signatures:

Author	Signature	Date
Nathan L.R. Williams	Production Note: Signature removed prior to publication.	24/10/2022
Nachshon Siboni	Production Note: Signature removed prior to publication.	24/10/2022
William L. King	Production Note: Signature removed prior to publication.	24/10/2022
Nine Le Reun	Production Note: Signature removed prior to publication.	24/10/2022
Jaimie Potts	Production Note: Signature removed prior to publication.	24/10/2022
Peter Scanes	Production Note: Signature removed prior to publication.	24/10/2022
Colin Johnson	Production Note: Signature removed prior to publication.	24/10/2022
Melanie James	Production Note: Signature removed prior to publication.	24/10/2022
Vanessa McCann	Production Note: Signature removed prior to publication.	24/10/2022
Justin R. Seymour	Production Note: Signature removed prior to publication.	24/10/2022

This work has been submitted for publication: Williams, N.L.R., Siboni, N., Potts, J., Scanes, P., Johnson, C., James, M., McCann, Le Reun, N., King, W.L., V., Seymour, J.R., Defining the importance of natural environmental variability and anthropogenic impacts on bacterial assemblages within intermittently opened and closed lagoons, Water Research (submitted).

5.0 – Abstract

Intermittently closed/opened lakes and lagoons (ICOLLs) provide important ecosystem services, including food provision and nutrient cycling. These ecosystems generally experience low watershed outflow, resulting in substantial fluctuations in environmental parameters that are often compounded by anthropogenic contamination. I aimed to determine how seasonal environmental heterogeneity, as well as anthropogenic impacts including sewage inputs, alter the dynamics of microbial communities inhabiting ICOLLs on the eastern Australian coast. I sampled four ICOLLs on a monthly basis for one year, using 16S rRNA gene amplicon sequencing to monitor patterns in bacterial diversity as well as qPCR-based microbial source tracking (MST) approaches to measure faecal contamination from humans (sewage), dogs, and birds as well as a suite of antibiotic resistance genes (ARGs) including *sulI*, *tetA*, *qnrS*, *dfrA1*, and *vanB*. Diversity and abundance of bacterial assemblages changed significantly between seasons, and during periods of dry and wet weather. Differences in community composition were often associated with temporal shifts in salinity, temperature, pH, DO, and fDOM, but following periods of high rainfall, bacterial assemblages in two of four ICOLLs changed in direct response to sewage inputs. Within these ICOLLs, indicator taxa for stormwater identified using the 16S rRNA amplicon sequencing data, as well as MST markers for sewage and dog faeces, and levels of the antibiotic resistance genes (ARGs) *sulI*, *tetA*, and *dfrA1* were significantly more abundant after rainfall. Notably many of the stormwater indicator taxa included potential human pathogens including *Arcobacter* and *Aeromonas hydrophilia*, which also displayed correlations with levels of the ARGs *sulI*, *tetA*, and *dfrA1*. I conclude that, following rainfall events, sewage was a principal driver of shifts in the microbiology of ICOLLs exposed to stormwater, while natural seasonal shifts in the physio-chemical parameters controlled microbial communities at other times. Increased occurrence of intense precipitation events is predicted as a ramification of climate change, which will lead to increased impacts of stormwater and in sewage contamination on important ICOLL ecosystems in the future.

5.1 – Introduction

The microbial assemblages inhabiting coastal and estuarine environments play important roles in regulating ecosystem productivity (Kirchman and Gasol, 2018) and biogeochemistry (Curtis et al., 2002; Flemming and Wuertz, 2019). The diversity and spatiotemporal dynamics of these microbial communities are shaped by a suite of natural environmental factors, including seasonal and shorter-term shifts in temperature, salinity, pH, dissolved oxygen, nutrients, organic matter availability (Gilbert et al. 2012; Fuhrman et al., 2006; Hu et al., 2014; Staley et al., 2015) and interactions with other organisms (Steele et al., 2011). However, due to their proximity to urbanised areas, coastal and estuarine ecosystems are often subject to anthropogenic contamination, including inputs of sewage, which can also shape microbial community composition (Pascual-Benito et al., 2020). This can result in the introduction of pathogens (McLellan et al., 2015) and increases in antibiotic resistant (AbR) microbes (Williams et al., 2022a), which can pose potential human health threats (Fewtrell and Kay, 2015; Leonard et al., 2015).

Intermittently closed and open lakes and lagoons (ICOLLs) are a form of lagoonal estuary that is episodically open to the ocean. ICOLLs are relatively common, making up between 8 – 13 % of the of the total global coastline (McSweeney et al., 2017). These environments provide a suite of important ecosystem service s (Basset et al., 2013) and are also often used for recreation by human populations. ICOLLs are characterised by low watershed outflow which, when paired with ocean wave energy and sediment deposition, leads to the formation of a sand bar large enough to periodically separate the ocean and estuary. High outflow events or significant wave action can, however, breach the sandbar, allowing for periodic exchange between the ocean and estuary (Rich and Keller, 2013). Often, ICOLLs are opened mechanically, with the main goals of flood prevention and flushing poor water quality (Schallenberg et al., 2010). This variable connection to the ocean, which often occurs in parallel with significant variability in temperature, salinity, and other seasonal factors such as rainfall, results in substantial fluctuations in habitat state and ecology of ICOLLs (Cousins et al., 2010). Additionally, periodic separation from the ocean means that ICOLLs can become accumulation basins, whereby they are not regularly drained of contaminants, and are therefore extremely sensitive to anthropogenic disturbances (Haines et al., 2006; Sadat-Noori et al., 2016; Schallenberg et al., 2010). Given the known impact of environmental perturbations on coastal microbial assemblages (Jeffries et al., 2016; Laas et al., 2022; Zhang et al., 2014), defining how the intrinsic

environmental heterogeneity of ICOLLs governs the microbiology of these systems is an important requirement to understand their health and function.

In addition to natural environmental perturbations, many ICOLLs occur within highly urbanised coastal environments and are therefore often subject to anthropogenic pollution, including faecal contamination (Williams et al., 2022a). Sewage contamination of ICOLLs, estuaries, and other coastal environments can often occur due to poor or failing wastewater infrastructure, and during wet weather sewage overflow events (McLellan et al., 2015; Newton et al., 2015; Olds et al., 2018; Williams et al., 2022b), while faeces from both domesticated and wild animals can also enter the environment from the surrounding catchment (McLellan et al., 2015; Williams et al., 2022a, 2022b). This faecal contamination has the potential to lead to significant shifts in the composition and function of endemic estuarine microbial assemblages (Pearman et al., 2018), as well as the allochthonous input of bacteria associated with human and animal faeces, which often includes human pathogens (Carney et al., 2020; Gholami-Ahangaran et al., 2022; Houf et al., 2008), sometimes with heightened levels of antibiotic resistance (Carney et al., 2019; Derakhshandeh et al., 2018; Gholami-Ahangaran et al., 2022; Vredenburg et al., 2014).

While the relative influence of natural environmental variability and anthropogenic impacts on the microbiology of other aquatic ecosystems has been widely studied (Danovaro and Pusceddu, 2007; Savio et al., 2015; Staley et al., 2015), examinations of these impacts on the ecology of important ICOLL ecosystems have been largely restricted to sediment communities (Filippini et al., 2019), and chlorophyll or zooplankton levels (Everett et al., 2007; Gamito et al., 2019). As a consequence, the key factors shaping the bacterial communities within ICOLL environments are not well defined. Here I examined the relative influence of natural environmental determinants and faecal contamination, from both sewage and animals, in shaping bacterial composition within four ICOLLs and aimed to determine to what extent any changes pose a public health threat. To achieve this, I sampled four ICOLLs on the east coast of Australia, on a monthly basis over a period of one year, and linked changes in bacterial composition to environmental determinants, including faecal contamination, using a combination of DNA sequencing and microbial source tracking (MST) techniques.

5.2 – Methods

5.2.1 – Sampling design

Water samples were collected from four ICOLLs, situated on the New South Wales Central Coast, which is located on the eastern coastline of Australia. These included Wamberal, Terrigal, Avoca, and Cockrone Lagoons (Figure 1). For detailed information on the characteristics of each ICOLL, please see Table 1.

Table 1. Information on the features of each ICOLL.

	Wamberal	Terrigal	Avoca	Cockrone
Latitude	33° 25’ 48” S	33° 26’ 24” S	33° 27’ 36” S	33° 29’ 24” S
Longitude	151° 27’ 0” E	151° 26’ 24” E	151° 26’ 24” E	151° 25’ 48” E
Catchment Area	5.8 km^2	8.9 km^2	10.8 km^2	6.9 km^2
Estuary Area	0.5 km^2	0.3 km^2	0.7 km^2	0.3 km^2
Volume	880.2 ML	151.2 ML	293.2 ML	187.4 ML
Average depth	1.7 m	0.5 m	0.4 m	0.6 m
Open to ocean at:	2.4 m	1.23 m	2.4 m	2.53 m
Catchment Description	Proximate surrounds include a nature reserve, but 90% of catchment is urban.	Majorly surrounded by urban development and 10% of the catchment is forest.	Forest makes up 50% of the Avoca catchment, with the other 50% being collectively urban and rural-residential development, horticulture, and grazing.	Mostly surrounded by a conservation bushland area, with urban and rural-residential development making up 1/3 of the catchment.

To measure temporal changes in bacterial composition related to seasonal variability and more acute perturbations in environmental conditions, water samples were collected monthly from August 2019 until July 2020 (with the exception of March and April 2019 due to COVID19 field work restrictions). Over the course of the sampling regime, three significant wet-weather events were captured, during October 2019, February 2020, and July 2020, when 40 mm, 65 mm, and 8.6 mm of rainfall occurred in the 5 days preceding sample collection, respectively. To gain a high-resolution spatial assessment of the bacterial community structure within each ICOLL, discrete water samples were collected in triplicate from 5 locations in each lagoon (7 in Avoca; Figure 1). Samples were also collected from two stormwater drains that flow into Terrigal Lagoon (DT1 and DT2) and two drains that flow into Avoca Lagoon (DA1 and DA2) during the rainfall event in February.

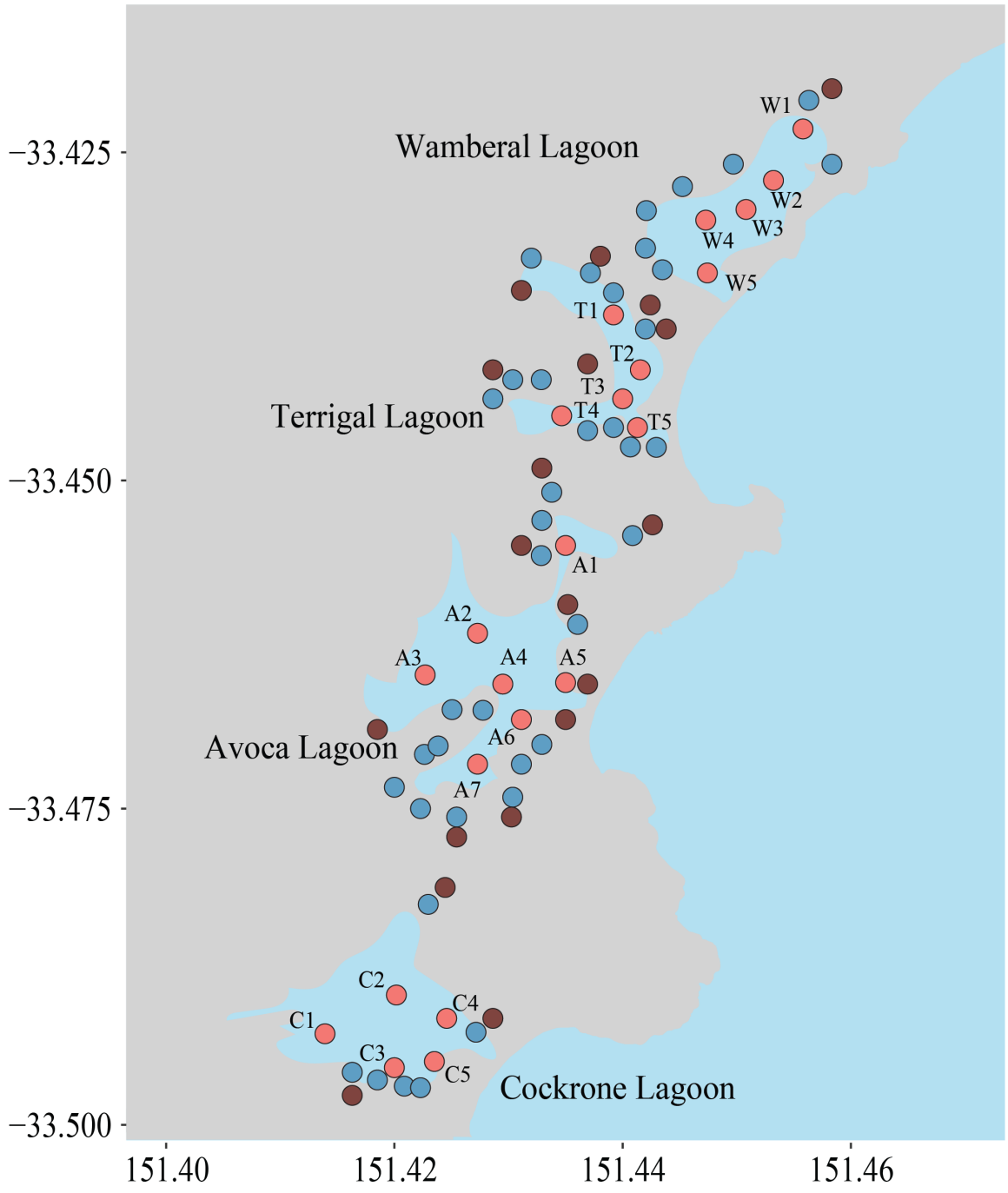

Figure 1. Map of sampling sites. Blue circles are storm water drains, brown circles are sewage pumping stations, and red circles are sampling sites.

5.2.2 – Sample processing and analyses

At each sampling location, triplicate 2 L water samples were collected using an integrated pole sampler that collected surface water to 1 m depth. Within 2 hours, samples were transported to a portable laboratory and filtered through 0.22 μm pore-size membrane filters (Merk-Millipore) using a peristaltic pump (100 rpm). Volume of each sample was recorded (between 500 ml and 2000 ml) to allow for normalisation of gene copy numbers. Filtered samples were frozen on site and then transported to the lab on dry ice, prior to being stored at -80 °C until DNA extraction.

During each sampling event, physio-chemical parameters were measured using a Xylem EXO-2 multiparameter water quality sonde. Data was recorded at approximately 0.5 m depth at one second intervals for a total of 3 minutes at each site. Triplicate samples were taken for chlorophyll a. Chlorophyll-a samples were filtered through a 0.45 μm glass fibre filters under vacuum, with the filter subsequently frozen until analysis. Concentrations were determined by fluorometry following extraction with 90 % acetone solution, in accordance with standard methods (APHA 10200H) (APHA, 2012).

A water sample was also collected from each sampling location at each time for nutrient analysis. The sample was split among three disposable syringes. One syringe was transferred directly into a clean 30 ml vial for total nitrogen and phosphorus (TN and TP) analysis, while the other two samples were passed through a 0.45 mm cellulose acetate syringe filter (Sartorius Minisart) into two additional tubes for total dissolved nitrogen and phosphorus (TDN and TDP) and inorganic nutrient (NH_4^+, NO_x and SRP) analysis. All nutrient samples were kept on ice, frozen within 2 hours and analysed using standard methods (Eaton and Franson, 2005). Water samples were also collected to determine enterococci levels, which were derived using Enterolert (ASTM, 2019). For more details, please see Section 1.1 in the Supplementary Material.

5.2.3 - 16S rRNA gene amplicon sequencing

To characterise bacterial composition in all seawater and stormwater drain samples 16S rRNA gene amplicon sequencing was used. The V3–V4 region of the bacterial 16S rRNA gene was amplified using the 341f/805r primer set (Herlemann et al., 2011), with the following cycling conditions: 95°C for 3 minutes followed by 25 cycles of: 95°C for 30 seconds, 55°C for 30 seconds, 72°C for 30 seconds, and then 72°C for 5 minutes with

a final hold at 4°C (Pichler et al., 2018). Amplicons were subsequently sequenced using the Illumina MiSeq platform (300 bp paired-end analysis at the Ramaciotti Institute of Genomics, University of New South Wales). For a detailed description of 16S rRNA amplicon sequencing data processing details, refer to Supplementary Material Section 1.4. Raw sequences were uploaded to NCBI, BioProject PRJNA884124. R scripts have been uploaded to (https://github.com/Nwilliams96/ Central_Coast_Lagoons_2021).

5.2.4 - Microbial Source Tracking and ARG qPCR Assays

To determine the presence of human faeces, indicative of sewage contamination, as well as animal faeces, I used quantitative PCR (qPCR) to measure levels of four MST assays. These included the Lachno3 (Feng et al., 2018) assay which targets human gut specific *Lachnospiraceae* and is a marker for human faeces, as well as the DG3 (Green et al., 2014) assay which targets a dog gut specific *Bacteriodales* and is a marker for dog faeces in the environment, and the GFD assay (Green et al., 2012), which targets bird gut *Heliobacteria* and is a marker for bird faeces in the environment. Quantitive PCR was also used to quantify a suite of ARGs that have previously been detected in high abundances in eastern Australian coastal environments (Carney et al. 2019; Williams et al., 2022a), including the *sulI, tetA, qnrS, dfrA1* and *vanB* genes (Borjesson et al., 2009; Huovinen et al., 1995). These genes confer resistance to sulfonamide, tetracycline, quinolone, trimethoprim, and vancomycin, respectively. For assay details see Table 1 Supplementary Material, for descriptions of genes targeted see Section 1.2 Supplementary Material, and for qPCR technical details see Section 1.3 Supplementary Material.

5.2.5 - Statistical analysis

I tested for differences in abiotic variables, levels of enterococci, MST markers, and ARGs, between ICOLL, season, and weather conditions using the pairwise.adonis function from the PairwiseAdonis (Martinez Arbizu, 2020) R package, with Bonferroni corrected p-values. For pairwise.adonis tests between weather conditions, samples were grouped into wet weather samples, defined by a total of more than 5 mm of rain in the previous five days, and dry weather, defined by a total of less than 5 mm of rain in the previous five days. To test for correlations between enterococci plate counts (single replicate), abiotic data (single replicate), and qPCR samples (three biological replicates),

average values from the qPCR data were used and correlations were determined using Spearman's R_S, with Bonferroni corrected p-values.

To test for differences in microbial community composition (16S rRNA data) and alpha diversity between samples, I used the Adonis function from Vegan (Dixon, 2003) and the pairwise.adonis function from the PairwiseAdonis (Martinez Arbizu, 2020) R package. To determine the environmental drivers of the microbial community at each site, I used the CCA function within the Vegan package (Dixon, 2003), utilising the ANOVA function within this package to determine the significance of the impact that each environmental determinant was having on the difference in community composition. To identify the bacterial families that were responsible for dissimilarity between bacterial communities within each sample, I used SIMPER analysis with 999 permutations within the vegan package (Dixon, 2003).

During the rainfall event in February 2020, I sampled from five drains, two of which deposit stormwater into Avoca Lagoon and three of which deposit stormwater into Terrigal Lagoon. Given that rainfall was proposed to be a major driver of changes in bacterial diversity and community composition, I wished to identify bacteria amplicon sequence variants (ASVs) that were representative of a stormwater bacterial community entering the ICOLL water. To do this I employed the indicspecies package (de Caceres and Jansen, 2018) as described in Williams et al. (2022a). A Mictools analysis (Albanese et al., 2018) was also run with the aim of determining the Spearman's R_S correlations between the suite of ARGs, faecal markers, and the drain indicator ASVs. For complete R scripts used in statistical analysis of 16S data see (https://github.com/Nwilliams96/Central_Coast_Lagoons_2021).

5.3 - Results

5.3.1 - Environmental conditions

During the year-long sampling period, water temperature displayed significant [$p < 0.05$] seasonal and inter-lagoon variability (Figure 2 A), ranging between 10.2°C during June in Wamberal Lagoon (W1) to 36.1°C during January in Terrigal Lagoon (T4). In general, during summer (December, January, and February), water temperatures were significantly higher [$p < 0.001$] compared to all other sampled months, within all sampled ICOLLs. Among the ICOLLs, Wamberal, Terrigal, and Avoca Lagoons generally had statistically indistinguishable temperatures at each time point, while Cockrone Lagoon was characterised by temperatures that were significantly lower [$p < 0.05$] than the other three ICOLLs.

Salinity also displayed significant [$p < 0.005$] variability within and between each ICOLL (Figure 2 B). Salinity was 38 % lower [$p < 0.05$] in all ICOLLs during the sampling months that coincided with rainfall [October (40 mm), February (65 mm), June (7 mm), and July (8.6 mm)], compared to samples taken throughout the remainder of the year. One exception to this pattern was Avoca Lagoon where, during the rainfall events in February, June, and July, the salinity remained stable. Of note, in all ICOLLs salinity was significantly lower [$p < 0.005$] in May compared to samples taken throughout the rest of the year, despite no rainfall in the five days preceding this sample date.

Over the course of the year, ICOLL depth also displayed significant variability [$p < 0.005$] between lagoon, and between month [$p < 0.005$] (Figure 2 E). Of note, ICOLL depth was significantly higher [$p < 0.05$] during periods of high rainfall [e.g., October (40 mm), February (65 mm), June (7 mm), and July (8.6 mm)]. On three occasions, the 1/9/19, 10/2/20, and 27/5/20, all four ICOLLs were mechanically emptied by government agencies, whereby their depth significant dropped [$p < 0.005$] (Figure 1 F), however these dates did not coincide with any sampling dates.

In Wamberal Lagoon, levels of total nitrogen (TN) and total phosphate (TP) displayed seasonal differences, whereby levels were significantly lower [$p < 0.05$] in August (winter), in comparison to levels during summer and spring. Interestingly, on average, levels of TN and TP were stable during the wet weather months, in contrast to levels of soluble reactive phosphorus (SRP) that were more than double [$p < 0.0001$] during the wet months in comparison to dry months. Similarly, levels of NO_x were more

than two-fold [$p < 0.05$] higher within Avoca Lagoon during the October rain event (40 mm), and within Terrigal Lagoon during the rainfall event in February (65 mm). Ammonia concentrations displayed a discrete temporal pattern, with no statistical variance between sampling months, other than a significant [$p < 0.0001$] spike in December (Austral summer).

Patterns in turbidity, *Cyanobacteria*, and chlorophyll a, were all significantly [$p < 0.05$] higher during summer than other periods. On average, during summer, chlorophyll *a* exceeded 40 ug/L, which was 4-times higher than the yearly average [8 ±SD 10 ug/L, n = 206], and turbidity exceeded 40 NTU, which was 8-times higher than the yearly average [5 ±SD 6 NTU, n = 206]. Levels of turbidity and chlorophyll *a* also varied significantly [$p < 0.0001$] between the ICOLLs, whereby levels of these parameters were 9.3 and 1.3 times lower [$p < 0.0001$] in Cockrone Lagoon compared to the other ICOLLs.

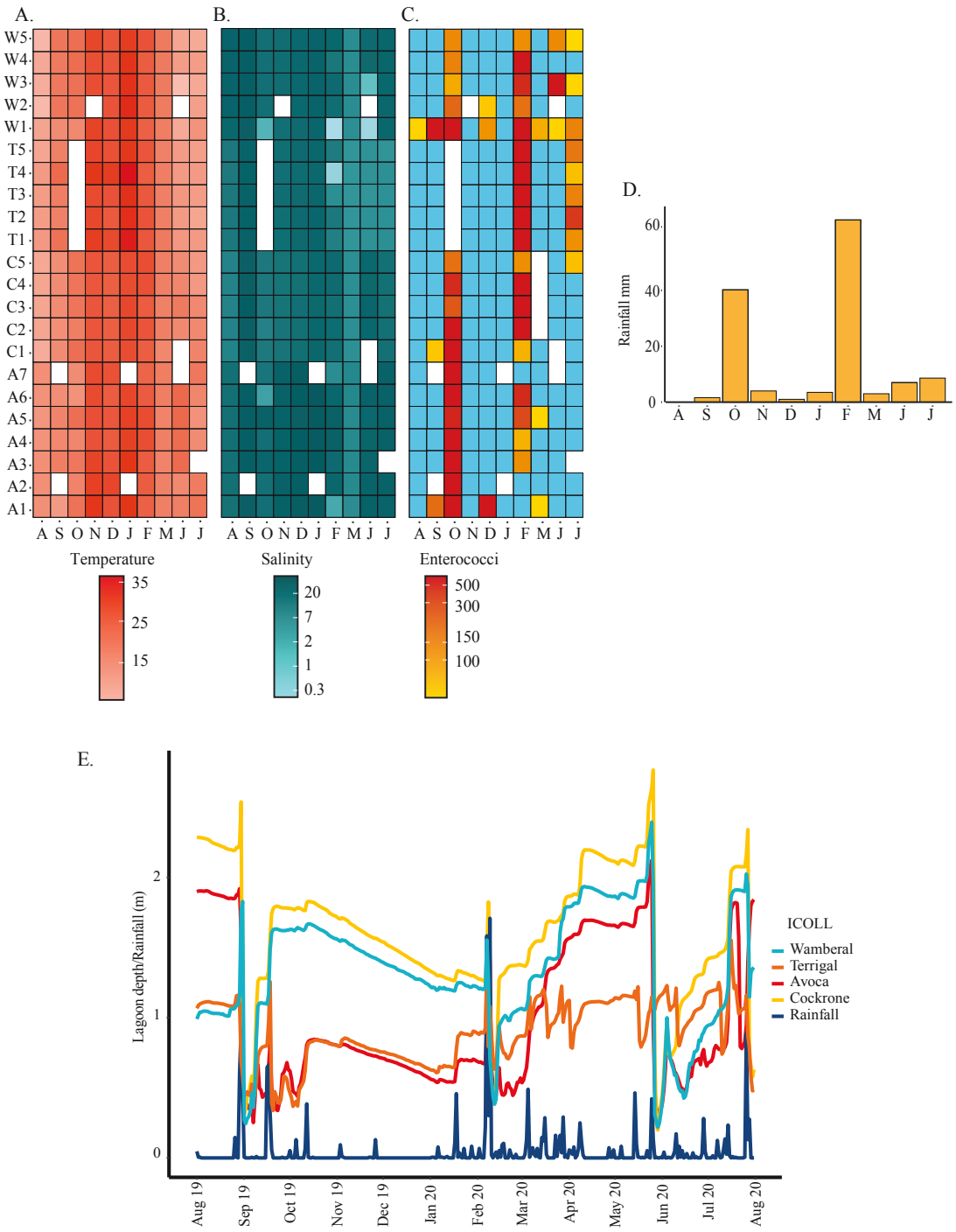

Figure 2. Abiotic Data. A-C, Heatmaps displaying **A)** Temperature in °C, **B)** Salinity ppt, and **C)** enterococci MPN/100ml, at sites A1-A7 in Avoca lagoon, C1 – C5 in Cockrone lagoon, T1 – T5 in Terrigal lagoon, and W1 – W5 in Wamberal lagoon. **D)** Displays the total rainfall (mm) in the five days leading up to sampling each month, and **E)** is a line graph of ICOLL depth and rainfall in metres.

5.3.2 - Faecal Indicator Bacteria - enterococci

Throughout the study period, enterococci levels were positively correlated [$p < 0.01$] with rainfall [$r_s = 0.51$], TN [$r_s = 0.28$], and TP [$r_s = 0.14$], and negatively correlated [$p < 0.01$] with salinity [$r_s = -0.20$]. During dry weather periods, the average enterococci levels were low [mean: 41 ±SD 147 MPN/100ml, n = 163], aside from spikes within Avoca Lagoon (A1) [487 MPN/100ml] in December, and Wamberal Lagoon (W1 and W3) intermittently throughout the year (Figure 1 C), when enterococci levels exceeded 100 MPN/100ml. During July, following 8.6 mm of rain in the preceding 5 days, enterococci levels within Terrigal Lagoon and at the W1 site within Wamberal Lagoon were over 4 times higher [$p < 0.001$] than in all other samples. In October, after 40 mm of rain in the 5 days prior to sampling, enterococci levels [mean: 9,382 ±SD 11500 MPN/100ml, n = 17] within all ICOLLs were 228 times higher [$p < 0.001$] than the levels recorded during dry weather. Meanwhile in February, after 65 mm of rain, enterococci levels within all ICOLLs [mean: 4236 ±SD 8957 MPN/100ml, n = 22] were 102 times higher [$p < 0.001$] compared to levels recorded during dry weather.

5.3.3 - Sewage marker

Across the dataset, the MST marker for human faeces (sewage), Lachno3, was detected in 37 % (n = 77/206) of samples (Figure 3 A). Lachno3 levels displayed positive, significant [$p < 0.001$] correlations with enterococci [$r_s = 0.32$], rainfall [$r_s = 0.26$], chlorophyll *a* [$r_s = 0.11$], and NO_x [$r_s = 0.26$], as well as a significant [$p < 0.001$] negative correlation with salinity [$r_s = 0.15$]. Sewage marker levels were significantly higher [$p < 0.001$] within the Terrigal and Avoca stormwater drain samples, than the other ICOLLs. Within Terrigal and Avoca Lagoons, the sewage marker was detected in 40 % (n = 17/46) and 56 % (n = 37/66) of samples respectively, and in both ICOLLs, levels were two orders of magnitude higher during wet weather in comparison to dry weather. During wet weather, the highest levels of the sewage marker in Terrigal Lagoon were detected at sites T3, T4, and T5, where levels were an order of magnitude higher than the average levels of these markers throughout the dataset. Within Wamberal Lagoon, Lachno3 was detected in only 21 % [n = 7/48] of samples, but similarly to Avoca and Terrigal Lagoons, levels were four orders of magnitude higher during wet weather compared to dry weather within Wamberal. The levels at site W1 within Wamberal Lagoon were an order of magnitude

higher than the mean levels throughout the dataset. Within Cockrone Lagoon, the Lachno3 sewage marker was detected in 31 % [n = 14/45] of samples, and levels were also significantly [$p < 0.001$] higher during wet weather months than dry weather periods.

5.3.4 - Animal faecal markers

Across the entire dataset, the MST marker for dog faeces, DG3, was detected in only 13 % [n = 33/206] of samples (Figure 3 B), but displayed significant [$p < 0.001$] positive correlations with enterococci levels [$r_s = 0.43$], rainfall [$r_s = 0.41$], as well as the sewage marker Lachno3 [$r_s = 0.41$], and a negative [$p < 0.001$] correlation with salinity [$r_s = -0.19$]. Highest [$p < 0.001$] levels were observed in the Avoca and Terrigal Lagoon stormwater drain samples [mean: 1.28×10^7 ±SD 7.23×10^5 copies/100ml, n = 3]. Within Terrigal and Avoca Lagoons, DG3 was detected in only 13 % [n = 6/46] and 12 % [n = 8/66] of samples, respectively, and was only detected during wet weather. Within Wamberal Lagoon, DG3 was detected in 23 % [n = 11/48] of samples, where levels were significantly [$p < 0.05$] higher during wet weather compared to during dry weather, and an order of magnitude higher at site W1 compared to other sites in the ICOLL. Within Cockrone Lagoon, the marker for dog faeces, DG3, was detected in 17 % of samples [n = 8/45] and again occurred at significantly [$p < 0.0001$] higher levels during wet weather periods.

The MST marker for bird faeces, GFD, was detected in 99% [n = 203/205] of samples across the entire dataset (Figure 3 C) and was significantly [$p < 0.001$] and positively correlated with enterococci levels [$r_s = 0.24$], turbidity [$r_s = 0.44$], chlorophyll a [$r_s = 0.39$], TFP [$r_s = 0.40$], TFN [$r_s = 0.27$], and rainfall [$r_s = 0.26$]. GFD was detected within 100% [n = 45/45] of samples within Cockrone Lagoon, where levels were significantly [$p < 0.001$] higher during wet weather in comparison to dry weather. Within Avoca Lagoon, GFD was detected in 99% [n = 65/66] of samples, and levels were also significantly [$p < 0.05$] higher during wet weather in comparison to dry weather. In contrast, within Terrigal Lagoon, levels of the bird faeces marker were significantly [$p < 0.001$] higher during dry weather compared to during wet weather. Within Wamberal Lagoon, GFD was detected in 100% [n = 47/47] of samples, and there was no statistical difference in levels between dry and wet weather.

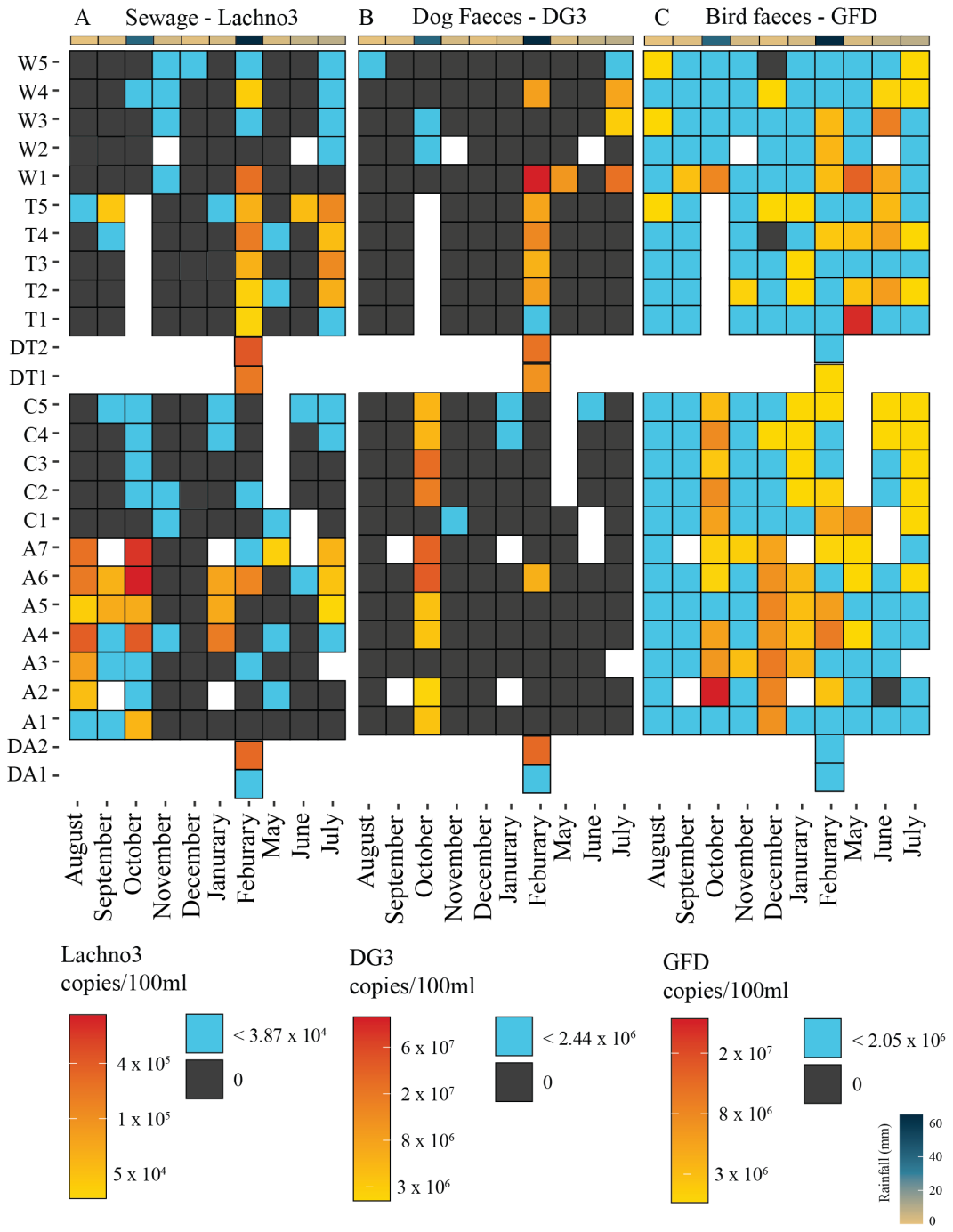

Figure 3. MST heatmaps. Heatmaps display the copy number/100 ml of each faecal marker with **A)** Lachno3 Sewage marker, **B)** DG3 Dog faeces marker, and **C)** GFD Bird faeces marker. Blue squares represent values below the average of all samples while black squares indicate no detection, and blank squares indicate samples that were not taken. The top bar indicates rainfall in mm.

5.3.5 - Antibiotic Resistance Genes

Throughout the study, levels of *sulI* and *dfrA1,* were significantly correlated with levels of the sewage marker, Lachno3 [*sulI*: $r_s = 0.26$, *dfrA1*: $r_s = 0.36$], the dog faecal marker, DG3 [*sulI*: $r_s = 0.37$, *dfrA1*: $r_s = 0.47$], and rainfall [*sulI*: $r_s = 0.38$, *dfrA1*: $r_s = 0.51$],while levels of *tetA*, were significantly correlated with dog faecal maker, DG3 [$r_s = 0.21$], GFD [$r_s = 0.46$], and rainfall [$r_s = 0.21$]. Concentrations of *qnrS* were significantly correlated with levels of the bird faecal marker, GFD [$r_s = 0.20$]. All detected ARGs displayed differing patterns between each ICOLL. While levels of *tetA* did not statistically differ between ICOLLs, levels of *dfrA1* were significantly [$p < 0.001$] higher in Wamberal Lagoon compared to the levels recorded in any other ICOLL. Concentrations of both *sulI* and *qnrS* were significantly higher [$p < 0.001$] within Terrigal Lagoon than those in both Avoca Lagoon and Cockrone Lagoon. Levels of *sulI, dfrA1*, and *qnrS* were all significantly [$p < 0.001$] lower in Cockrone, compared to levels recorded in any other ICOLL (Supplementary Figure 3). *vanB* was not detected in this study. The most distinct pattern that I observed, however, was that within all four ICOLLs concentrations of *tetA*, *sulI*, and *dfrA1* were all significantly [$p < 0.001$] elevated during wet weather in comparison to dry weather. In contrast, levels of *qnrS* were either statistically indistinguishable between dry and wet weather, or in some cases (e.g., Terrigal Lagoon), were significantly lower [$p < 0.001$] during wet weather compared to dry weather (Supplementary Figure 3).

5.3.6 - Inter-lagoon and temporal dynamics of ICOLL bacterial communities

Throughout the study period, bacterial diversity (Shannon) varied significantly [$p < 0.001$] between ICOLLs, with the exception of between Wamberal and Terrigal Lagoons. The bacterial communities within the ICOLL water samples from Terrigal and Avoca Lagoons were significantly less [$p < 0.001$] diverse than those observed in their relevant stormwater drains. Across the entire dataset, bacterial diversity was significantly correlated [$p < 0.001$] with enterococci levels [$r_s = 0.28$], sewage marker levels [Lachno3: $r_s = 0.26$], bird faecal marker levels [$r_s = 0.23$], chlorophyll *a* [$r_s = 0.48$], turbidity [$r_s = 0.47$], TP [$r_s = 0.29$] and rainfall [$r_s = 0.39$]. Across all samples, the most notable trend in bacterial diversity was a significantly [$p < 0.05$] higher diversity within Wamberal, Terrigal, and Avoca Lagoons during rainfall in comparison to during dry weather. Bacterial community composition also varied significantly [$p < 0.001$] between all of the

ICOLLs and was also significantly different [$p < 0.001$] between ICOLL and stormwater drain samples (Figure 4).

Within Wamberal Lagoon, *Cyanobiaceae* [mean relative abundance = 28.48 ±SD 2.12 %, n = 1264], *Microbacteriaceae* [mean relative abundance = 26.30 ± SD 1.59 %, n = 1888], and *Flavobacteriaceae* [mean relative abundance = 16.84 ± SD 9.40 %, n = 4005] were the most dominant bacterial families (Figure 4). Community composition was significantly different [$p < 0.001$] between all seasons, and between wet and dry weather. During the February rain event, community composition at sites W1 and W4 was associated with patterns in NO_x [$Chi^2 = 0.69$, $p = 0.0001$], which explained most of the variance between samples in this ICOLL (Figure 5 A). A lower abundance of *Sphingomonadaceae* and a higher abundance of *LWQ8* and *Chitinophagaceae* accounted for 5 % dissimilarity [$p < 0.05$] between these and the other Wamberal Lagoon samples. In contrast, from summer to early winter, community composition was significantly [$Chi^2 = 0.45, 0.36$, $p < 0.001$] influenced by fDOM and ICOLL depth, and to a lesser extent salinity and [$Chi^2 = 0.37, 0.36$, $p < 0.001$] during late winter (July-August) and early spring (September – October) (Figure 5 A). A lower abundance of *Flavobacteriaceae* and *Rhodobacteraceae* and a higher abundance of *Vibrionaceae* was associated with salinity, which accounted for 10 % [$p < 0.05$] dissimilarity between these samples.

Within Terrigal Lagoon, the most dominant families of bacteria were *Marinifilaceae* [mean relative abundance = 39.86 ± SD 18.41 %, n = 901], *SAR11 Clade I* [mean relative abundance = 23.66 ± SD 17.27 %, n = 901], and *Microbacteriaceae* [mean relative abundance = 20.96 ± SD 10.95 %, n = 2183] (Figure 4). Here, the community composition was significantly different [$p < 0.001$] between all seasons, as well as between wet and dry weather months. The strongest determinant of separation in the community in Terrigal was salinity [$Chi^2 = 0.41$, $p = 0.001$], which distinguished the community composition in spring (September – November) and summer (December – February), however during the February rainfall event, the community at three sites, T3 and T4, was significantly influenced by sewage and ICOLL depth [$Chi^2 = 0.31, 0.30$, $p = 0.001$] (Figure 5 B). A total of 6 % [$p < 0.05$] of the dissimilarity between the community composition at these sites was accounted for by a greater relative abundance of *Comamonadaceae*, *Sphingomonadaceae*, and *Lachnospiraceae* and a lower relative abundance of *SAR11 Clade I* in the sewage associated communities compared to the other communities.

Within Avoca Lagoon, the most dominant families of bacteria were *Cyanobiaceae* [mean relative abundance = 27.58 ± SD 19.52 %, n = 1567], *Rhodobacteraceae* [mean relative abundance = 16.07 ± SD 10.72 %, n = 4337], and *Microbacteriaceae* [mean relative abundance = 13.53 ± SD 9.85 %, n = 2158]. Within Avoca Lagoon, bacterial community composition was significantly different [$p < 0.001$] between seasons, as well as between wet and dry weather. The strongest determinant of bacterial community composition in Avoca Lagoon was pH [$Chi^2 = 0.57$, $p = 0.001$], which had the most influence on samples taken in spring (September) and winter (June-July) (Figure 5 C). Temperature and ICOLL depth also had a significant impact on community composition [$Chi^2 = 0.16$, $p = 0.0027$], where it had the greatest impact on samples taken during late spring into summer (November-February) (Figure 5 C). NO_x [$Chi^2 = 0.29$, $p = 0.0001$] and sewage [$Chi^2 = 0.20$, $p = 0.024$] had a significant impact on community composition during the October rainfall event. At this time there was a higher relative abundance of *Lachnospiraceae* and *Comamonadaceae*.

The most dominant families of bacteria within Cockrone Lagoon were *Microbacteriaceae* [mean relative abundance = 40.58 ± SD 17.43 %, n = 1343], *Flavobacteriaceae* [mean relative abundance = 25.58 ± SD 15.26 %, n = 2862], and *Nitrincolaceae* [mean relative abundance = 22.34 ±SD 23.63 %, n = 440]. Within Cockrone Lagoon, the bacterial community was significantly different [$p < 0.001$] between seasons, with the exception of autumn relative to spring and winter. The bacterial community composition also differed significantly [$p < 0.001$] between dry and wet months. In Cockrone Lagoon, the strongest determinant of bacterial community composition was salinity [$Chi^2 = 0.52$, $p = 0.001$], which strongly influenced community composition in September and June, while all other samples were most significantly influenced by temperature [$Chi^2 = 0.47$, $p = 0.001$]. Of note, the bacterial community at two sites, C2 and C3, were strongly influenced by the presence of dog faeces [$Chi^2 = 0.36$, $p = 0.001$] and NO_x [$Chi^2 = 0.42$, $p = 0.001$] during the October rainfall event (Figure 5 D), with decreases in the relative abundance of *Cryomorphaceae* and *Oxalobacteraceae* accounting for a total of 5 % of the dissimilarity [$p < 0.005$] at this time.

Figure 4. Bacterial diversity at the family level. Stacked bar graphs show seasonal shifts in relative abundance of the 10 most abundant bacteria at the family level within each ICOLL. Top bar above each stacked bar graph indicates rainfall in mm.

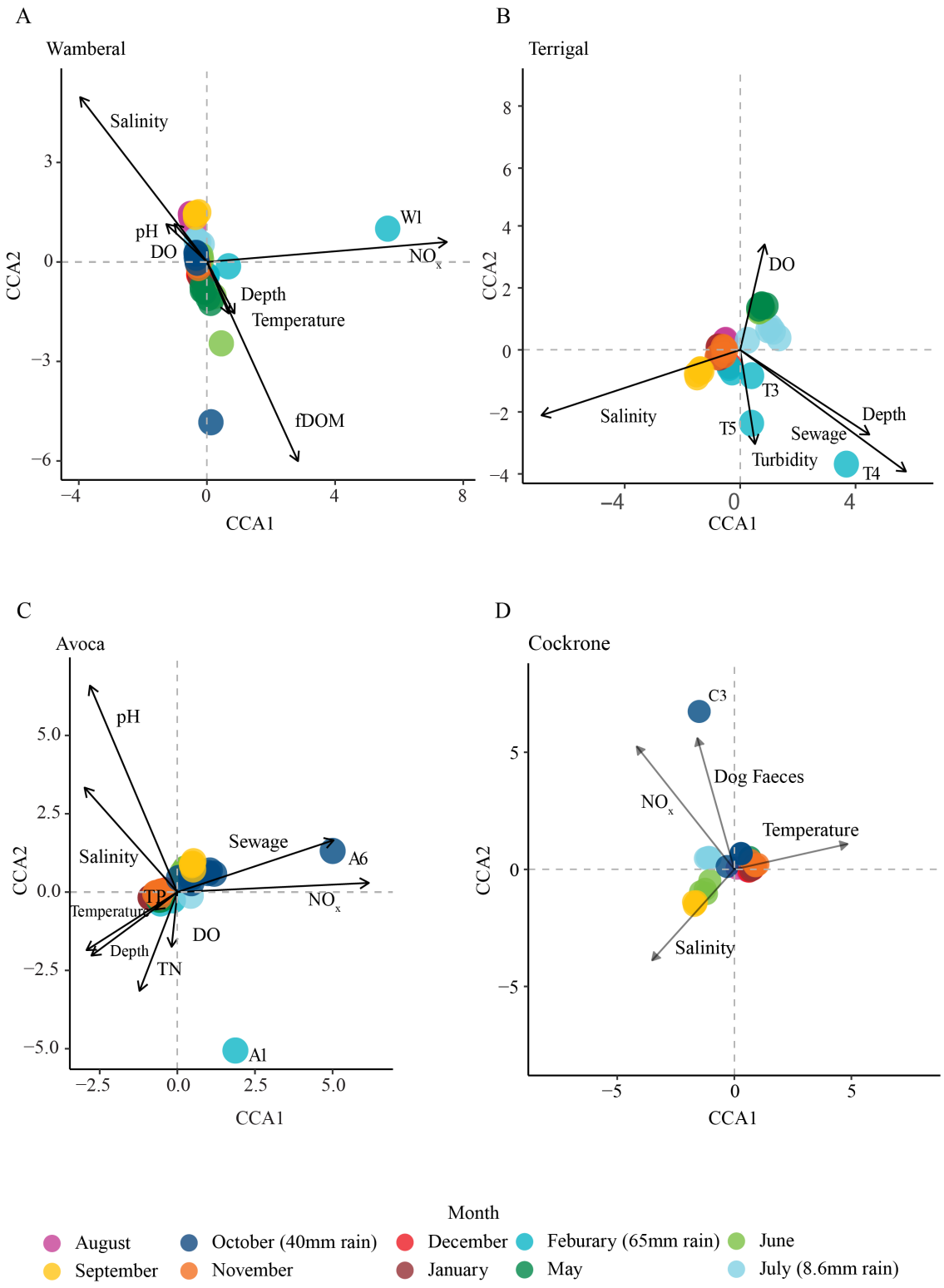

Figure 5. Bacterial community distribution and drivers. The points on each CCA plot represent the spatial difference in bacterial community composition with **A)** Wamberal, **B)** Terrigal, **C)** Avoca, and **D)** Cockrone ICOLLs. The vectors on each graph represent the strength [$p < 0.05$] that each environmental variable had on community composition.

5.3.7 - Indicator species analysis

During the rainfall event in February 2020, water samples were collected from five stormwater drains, two of which deposit stormwater into Avoca Lagoon and three of which deposit stormwater into Terrigal Lagoon. The bacterial ASVs that were representative of stormwater bacterial communities entering the ICOLLs were determined using the indicspecies package (de Caceres and Jansen, 2018), which compared stormwater and ICOLL water communities as described in Williams et al. (2022a). A total of 2,164 bacterial ASVs were identified as stormwater drain indicator bacteria that could be detected within the ICOLL water. Of these indicator taxa, the largest proportion [9.4 %, n = 204/2164] were ASVs belonging to the *Comamonadaceae* family.

A correlation analysis revealed 2,015 significant correlations between stormwater indicator taxa and the sewage marker Lachno3, and 2,055 with the dog faecal marker, DG3 (Figure 6). Most of these correlations involved ASVs from the *Comamonadaceae*, *Bacteroidaceae*, and *Enterobacteriaceae* families, as well as with ASVs assigned to the species *Bacteroides thetaiotaomicron*, and *Bacteroides vulgatus*, *Arcobacter butzleri*, and *Aeromonas* hydrophila. For r_s values see Table 2.

Table 2. Average r_s values between indicator ASVs and the human faecal marker Lachno3, as well as the dog faecal marker DG3, and the bird faecal marker GFD.

	Sewage marker Lachno3	Dog faeces marker DG3	Bird faeces marker GFD
Indicator	Average r_s	Average r_s	Average r_s
Comamonadaceae	0.22 ± 0.08, n = 187	0.24 ± 0.10, n = 192	0.10 ± 0.04, n = 27
Bacteroidaceae	0.15 ± 0.02, n = 9	0.21 ± 0.04, n = 9	
Enterobacteriaceae	0.22 ± 0.08, n = 40	0.31 ± 0.12, n = 0.12	0.14 ± 0.1, n = 4
Pseudomonas	0.21 ± 0.08, n = 51	0.30 ± 0.11, n = 51	0.18 ± 0.07, n = 8
Klebsiella	0.26 ± 0.08, n = 20	0.36 ± 0.11, n = 20	0.14, n = 6
Escherichia-Shigella	0.25 ± 0.12, n = 2	0.32 ± 0.18, n = 2	0.15, n = 1
Salmonella	0.24, n = 1	0.24, n = 1	
Arcobacter	0.26 ± 0.14, n = 3	0.30 ± 0.11, n = 3	
Bacteriodes		0.21 ± 0.04, n = 9	
Enterococcus	0.18 ± 0.05, n = 5	0.24 ± 0.08, n = 5	
A. hydrophila	0.43, n = 1	0.43, n = 1	0.16, n = 1

The stormwater indicator organisms also exhibited 2,085, 1,325, and 2,069 significant correlations with the ARGs *sulI*, *tetA*, and *dfrA1* respectively (Figure 6), while only 2 indicator taxa were correlated with *qnrS*. Similar to the human faecal markers, and the dog faecal marker, *sul1*, *tetA*, and *dfrA1* were significantly correlated with ASVs from the *Enterobacteriaceae*, *Comamonadaceae*, and *Bacteroidaceae* families, as well as ASVs from the *Aeromonas*, *Escherichia-Shigella*, *Klebsiella*, *Salmonella*, *Pseudomonas*, *Enterococcus*, *Arcobacter*, and *Bacteroides* genera. Meanwhile, *qnrS* displayed significant

correlations with an ASV from the *Occallatibacter*, and the *Rurimicrobium* genera. For r_s values see Table 3.

Table 3. Average r_s values between indicator ASVs and the ARGs; *sulI, tetA, dfrA1,* and *qnrS.*

	sulI	*tetA*	*dfrA1*	*qnrS*
Indicator	**Average r_s**	**Average r_s**	**Average r_s**	**Average r_s**
Comamonadaceae	0.19 ± 0.07, n = 216	0.15 ± 0.05, n = 126	0.18 ± 0.07, n = 192	-
Bacteroidaceae	0.13 ± 0.02, n = 9	0.12 ± 0.03, n = 2	0.17 ± 0.03, n = 9	-
Enterobacteriaceae	0.21 ± 0.07, n = 41	0.14 ± 0.04, n = 22	0.23 ± 0.08, n = 40	-
Pseudomonas	0.21 ± 0.07, n = 53	0.16 ± 0.05, n = 30	0.23 ± 0.09, n = 52	-
Klebsiella	0.24 ± 0.06, n = 20	0.16 ± 0.03, n = 12	0.26 ± 0.07, n = 20	-
Escherichia-Shigella	0.26 ± 0.08	0.19, n = 1	0.24 ± 0.16, n = 2	-
Salmonella	0.22, n = 1	0.13, n = 1	0.21, n =1	-
Arcobacter	0.16 ± 0.04, n = 3	0.14, n = 1	0.22 ± 0.07, n = 3	-
Bacteriodes	0.13 ± 0.02	0.12 ± 0.03, n = 2	0.17 ± 0.03, n = 9	-
Enterococcus	0.19 ± 0.07, n = 5	0.19 ± 0.06, n = 5	0.30, n = 1	-
A. hydrophila	0.39, n = 1	0.26, n = 1		-
Occallatibacter	-	-	-	0.12, n = 1
Rurimicrobium	-	-	-	0.01, n = 1

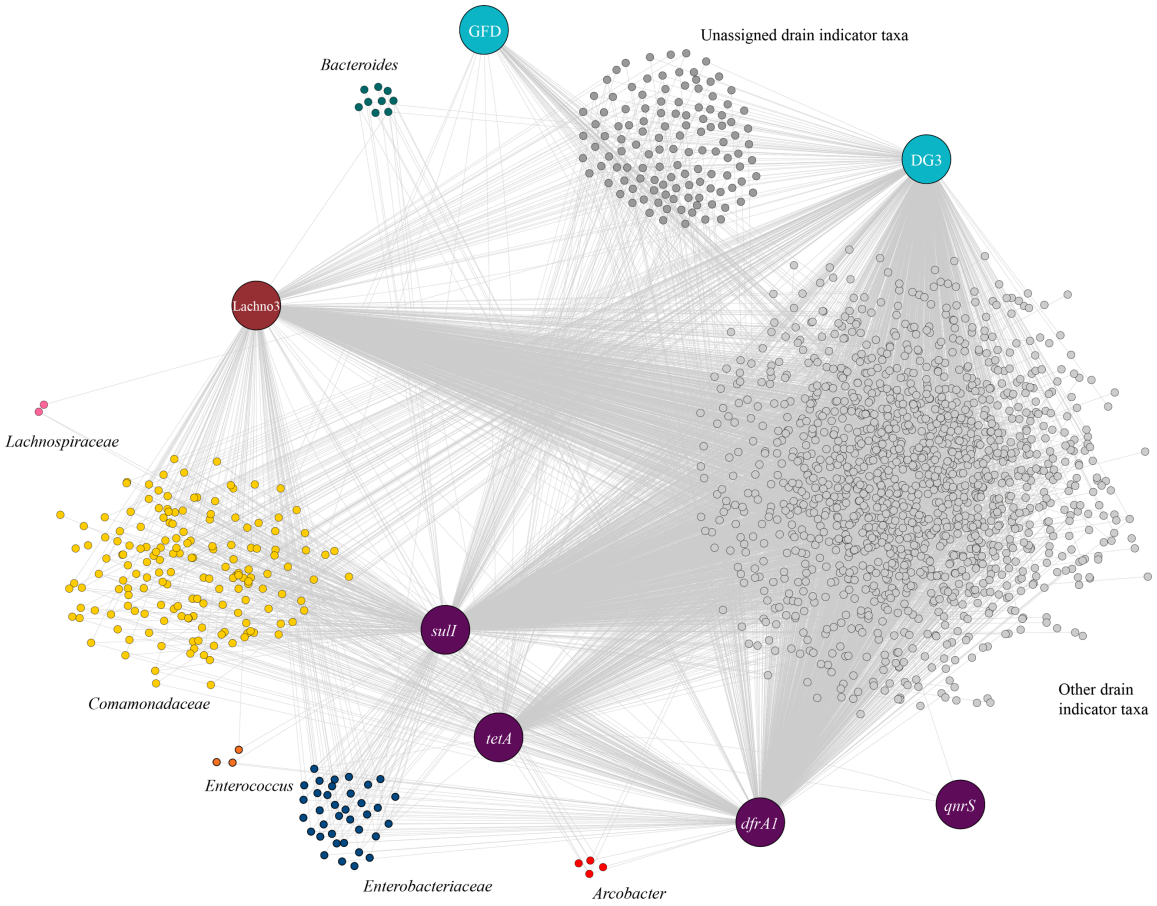

Figure 6. Network showing correlations between indicator taxa, faecal markers, and antibiotic resistance genes. Note that lines indicate a statistically significant relationship, but line length does not represent strength of relationship.

5.4 - Discussion

5.4.1 - ICOLL environments are dynamic

The principal aim of this study was to determine the relative importance of natural seasonal environmental variability and anthropogenic contamination in defining the microbial communities inhabiting four ICOLLs on Australia's south-eastern coast. Understanding the characteristics of the microbial communities inhabiting ICOLLs, and the environmental processes shaping them, is important because ICOLLs provide a range of critical environmental services and are used widely for recreation (Barbier et al., 2011; Basset et al., 2013; Newton et al., 2018). ICOLLs are characterised by shallow waters and are isolated from the ocean, which accentuates their vulnerability to environmental perturbations (Haines et al., 2006), and makes them potential reservoirs for anthropogenic contamination (Haines et al., 2006; Schallenberg et al., 2010).

Throughout the year-long time-series, the physiochemical properties of each ICOLL varied significantly, with substantially warmer temperatures in summer, and considerably lower salinity during rainfall. Across all four ICOLLs, the overall temperature (10 °C - 36.1°C) and salinity range (0.27 ppt – 39.22 ppt) was large, which is typical of these environments and has been observed within multiple ICOLLs (Crawshaw et al., 2018; Scanes et al., 2020a; Scanes et al., 2020b).

Despite the relatively close proximity of the four ICOLLs studied here (9 km), there were often significant differences in the physiochemical properties between ICOLLs at a given time. For example, water temperature was substantially lower at multiple time points within Cockrone Lagoon compared to the other ICOLLs. Notably, Cockrone Lagoon does not have a larger volume or depth than the other ICOLLs. The turbidity at Cockrone Lagoon, however, was also significantly lower compared to the other ICOLLs, which can cause light rays to be scattered and absorbed, rather than transmitted through water, and this has been reported to increase surface temperature in estuarine environments (Paaijmans et al., 2008).

Another example of physio-chemical variability between ICOLLs, involved levels of NO_x, which were particularly high within Avoca Lagoon during the October rain event and within Terrigal Lagoon during the February rain event. Overall, both of these ICOLLs also had the highest levels of the sewage marker detected, and indeed, levels of the NO_x correlated significantly with levels of the sewage marker. Given the high levels of NO_x

usually present in untreated sewage (Ge et al., 2015), inputs of raw sewage are a proposed source of these high NO_x levels.

5.4.2 - Environmental determinants of microbial communities within ICOLLs

The bacterial structure of each ICOLL was significantly different. While *Microbacteriaceae* was a dominant taxa within all ICOLLs, *Cyanobiaceae* were dominant within Wamberal and Avoca, while *Flavobacteriaceae* were dominant within Wamberal and Cockrone (Figure 3). These families of bacteria are commonly reported in estuaries and other marine environments, and their levels generally fluctuate according to patterns in different environmental variables (Gomez-Pereira et al., 2010; Jeffries et al., 2016; Needham et al., 2017). However, our study revealed that the environmental determinants of bacterial community structure differed between ICOLLs, and over time within each individual ICOLL.

Marine bacterial diversity and composition have been widely observed to be shaped by multiple environmental determinants including temperature, salinity, and nutrients (Fortunato et al., 2013; Gilbert et al., 2012). Across all ICOLLs salinity was a key determinant of the bacterial community, and in most cases, salinity governed the relative abundance of bacteria from the families *Flavobacteriaceae* and *Microbacteriaceae*. Salinity has previously been observed to govern levels of these groups in the Coorong estuary, Australia (Newton et al., 2018), as well as levels of *Microbacteriaceae* in several lakes across the United States (Aanderud et al., 2016). Other key determinants of the bacterial community structure across the ICOLLs were temperature, fDOM, pH, and DO, which have been previously shown to govern microbial communities in the Sydney Harbour estuary (Jeffries et al., 2016), as well as other marine environments (Gilbert et al., 2012). Given the significant fluctuations in water depth, I expected this to have a significant impact on the bacterial community. In Wamberal, Terrigal, and Avoca Lagoon, water depth impacted the microbiology of each ICOLL. Within Wamberal Lagoon during November this was related to water temperature, whereby at this time water depth was low and water temperature was high, while in Terrigal Lagoon this was related to sewage contamination. In both cases this highlights the impact of the extreme environmental variability linked to water depth and open-closed nature of ICOLLs, a defining feature of these environments. Whilst these drivers were the

most commonly observed natural determinates of the bacterial community across all four ICOLLs, within Wamberal, Terrigal and Avoca Lagoon, NO_x was a key determinant of the bacterial community composition, as was sewage within Terrigal and Avoca Lagoon.

5.4.3 - Sewage contamination determines structure of microbial communities within ICOLLs

The levels of the sewage marker Lachno3 were significantly elevated during the rainfall event in the October rainfall event in Avoca Lagoon (NB. samples were not taken from Terrigal Lagoon in October), and during February were significantly elevated in both Terrigal and Avoca Lagoon. During the October rainfall event, the highest levels of the sewage marker were detected in Avoca Lagoon at sites A1 and A4 - A7, and during the February rain event at sites W1 (Wamberal), A6 (Avoca), and T3 - T5 (Terrigal). Site A1 in Avoca is contiguous to four stormwater drains, and three of these are located next to sewage pumping stations and site A7 receives input from seven stormwater drains, two of which are located next to sewage pumping stations (Figure 1), while sites A4-6 are subject to the input of three stormwater drains, none of these are close by to sewage pumping stations (Figure 1). Likewise, site W1 receives input from one stormwater drain, which is located next to a sewage pumping station and sites T3 – T5 in Terrigal Lagoon receive input from seven stormwater drains, four of which are located next to sewage pumping stations (Figure 1). The concentrations of the sewage marker observed here were comparable to levels detected during heavy rainfall and contamination in other beach (Williams et al., 2022a), and estuarine environments (Williams et al., 2022b) in this region of Australia's east coast. During these rainfall events, the significant sewage contamination indicated by high levels of Lachno3, was a strong determinant of bacterial community composition in both Avoca and Terrigal Lagoons.

During the rain event in October, both sewage and NO_x were the strongest drivers of bacterial community composition within several sites in Avoca Lagoon including A1 and A4 - A7. The dissimilarity between the bacterial communities in these sewage driven samples compared to other samples was primarily contributed to by differences in the relative abundance of bacteria from the *Comamonadaceae* and *Lachnospiraceae* families. Similarly, sewage was also the strongest determinant of the bacterial community composition within Terrigal Lagoon (specifically sites T3 – T5) during the February

rainfall event, and the dissimilarity between the community at these sites and the other Terrigal Lagoon sites was largely driven by an increase in levels of bacteria from the families *Comamonadaceae*, *Sphingomonadaceae*, and *Lachnospiraceae*. Notably, both *Comamonadaceae* and *Lachnospiraceae* are known to be highly abundant in sewage (Cheng et al., 2021; Feng et al., 2018; Gonzalez-Martinez et al., 2016; McLellan et al., 2013; Zhang et al., 2018; Zhang et al., 2009). *Lachnospiraceae* is also used as a marker for sewage in the environment (Feng et al., 2018), and *Comamonadaceae* has been linked to indicator taxa of stormwater impact on the environment in previous studies (Williams et al., 2022b, 2022a). Increases in these bacteria provides further confirmation that sewage was a strong driver of the microbiology of these sites during heavy rainfall.

5.4.4 - Sewage contamination is linked to microbiological hazards within ICOLLs

Over 95 % of stormwater indicator taxa were correlated with the Lachno3 sewage marker, implying both that these bacteria were present within sewage and that the sewage content in stormwater at these sites is significant. Notably many of these indicator taxa were significant human pathogens including *E. coli* (Anastasi et al., 2012), *Salmonella* (Foley and Lynne, 2008), *Arcobacter butzleri* (Ferreira et al., 2016), and *Aeromonas hydrophila* (Janda and Abbott, 2010). Additionally, the antibiotic resistance genes *sulI*, *tetA*, *dfrA1*, and *qnrS*, which confer to sulfonamide, tetracycline, trimethoprim, and quinolone resistance, respectively (Berglund et al., 2014; Borjesson et al., 2009; Grape et al., 2007; Pei et al., 2006), often displayed significant correlations with the storm water indicator taxa, as well as with the sewage marker Lachno3. This provides evidence that sewage within the storm water infrastructure acted as a vehicle for antibiotic resistant bacteria to enter the environment. These ARGs have previously been detected in stormwater (Williams et al., 2022b, 2022a), in polluted urban waters (Carney et al., 2019), and in sewage (Chen and Zhang, 2013; Mokracka et al., 2012; Zhang et al., 2009), further supporting the proposition that sewage within the stormwater infrastructure was the vector for antimicrobial resistant (AMR) bacteria entering the environment.

Notably, levels of *tetA*, *sulI*, and *dfrA1* also exhibited significant positive correlations with levels of the dog faeces marker, DG3. Tetracyclines (White et al., 1992), sulfonamides (Bloom, 2014), and trimethoprims (Blondeau and Fitch, 2021) are all used in veterinary hospitals to treat various canine diseases, and *tetA*, *dfrA1*, and *sulI* have all

been previously detected in either dog guts or faeces (Bryan et al., 2004; Derakhshandeh et al., 2018; Shaheen et al., 2010). Furthermore, the bird faecal marker displayed significant, positive correlations to levels of *qnrS*, which is also consistent with previous observations of this gene being detected in bird faeces (Vredenburg et al., 2014). There is evidence that when birds feed from polluted water sources, they can be colonised by ARB (Franklin et al., 2020), making them environmental reservoirs and vectors for dissemination of ARB in the environment (Bonnedahl and Järhult, 2014; Ahlstrom et al., 2018). Together, our results indicate that levels of ARGs within coastal waterways can be impacted by inputs of both sewage and animal faeces.

Many of the indicator taxa that correlated with ARGs were also human pathogens. I observed strong correlations between *sulI*, *tetA*, and *dfrA1* and stormwater indicator taxa including *Escherichia-Shigella, Salmonella, Arcobacter, Bacteriodes, Enterococcus,* and *A. hydrophila* all of which include species/strains that are human pathogens (Bonetta et al., 2016; Bonnedahl and Jarhult, 2014; Dessie et al., 2013; Ferreira et al., 2016; Mobaraki et al., 2018; Rasmussen-Ivey et al., 2016; Tiwari and Nanda, 2019; Wexler, 2007) and have in some cases been reported to harbour ARGs in clinical settings (Dessie et al., 2013; Jacobs and Chenia, 2007; Jasim et al., 2021; Jindal et al., 2021; Lombardo et al., 2016). This highlights the potential for human pathogens associated with urban wastewater to be resistant to antibiotics, and that these organisms can be introduced to natural aquatic environments, particularly after rainfall.

5.4.5 - Implications of heavy rain events on ICOLL microbiology

During this study I determined that natural fluctuations in environmental factors such as temperature, salinity, pH, DO, and fDOM significantly influence the microbiology of ICOLLs throughout much of the year, but during and after rainfall, inputs of sewage and animal faecal material can significantly shape bacterial community composition. This was particularly true for Avoca and Terrigal Lagoons, where bacteria identified as indicators for stormwater, that included taxa known to occur in high levels in sewage, such as *Comamonadaceae* and *Lachnospiraceae,* were most responsible for discriminating samples from these environments. This finding corresponds with previous waterway health reports done by the Central Coast Council where these two ICOLLs have been highlighted as contaminated environments (DPIE, 2020). Notably, this pattern was often

underpinned by increases in the relative abundance of ASVs identified as significant human pathogens such as *E. coli* (Anastasi et al., 2012), *Salmonella* (Foley and Lynne, 2008), *A. butzleri* (Ferreira et al., 2016), and *A. hydrophila* (Janda and Abbott, 2010), which often were correlated with antibiotic resistance gene abundance. Gastrointestinal illness (GI) caused from recreational use of marine environments results in economic costs exceeding $30 million per year in the USA alone, where over 350,000 gastrointestinal illnesses linked to recreational use of waterways occur annually (Ralston et al., 2011). Previous reports have also linked recreational use of coastal environments such as surfing and bathing as a risk of contracting AMR microbes (Leonard et al., 2018, 2015). Clearly, the input of sewage enriched in both human pathogens and AMR bacteria into ICOLLs following rainfall poses a potential human health.

5.5 - Conclusions

In this study I have demonstrated that while variations in natural environmental parameters are key determinants of the microbiology of ICOLLs, heavy rain events can lead to sewage contamination that can dramatically alter the composition of bacterial communities. I have also shown that these more acute shifts in the microbiology of ICOLLs associated with rain events can include substantial increases in the relative abundance of putative human pathogens and antibiotic resistant bacteria, and potentially AbR pathogens. These important implications of rainfall events are notable, given that climate change is leading to increases in the occurrence of heavy rainfall events in coastal regions (Madakumbura et al., 2021), which in many cases will subsequently cause increased occurrence of sewage contamination events of coastal ecosystems including ICOLLs.

Chapter 6 – General Discussion and Synthesis of Results

6.1 - Summary

The goal of this thesis was identify the occurrence of potential microbial hazards within eastern Australian coastal environments and to define the key environmental determinants behind these hazards. Coastal environments are key to the processes that happen within many coastal ecosystems such as nutrient cycling (Testa et al., 2013), and conservation of biodiversity (Danovaro and Pusceddu, 2007), whilst also been used widely for recreational activities. Microbial communities within coastal environments underpin many of these services (Coelho et al., 2013), but within these communities exist endemic pathogenic microbes, such as bacteria from the *Vibrio* genus (Baker-Austin et al., 2018) , as well as pathogens which are washed in through anthropogenic waste streams, such as bacteria from the *Arcobacter* genus (Carney et al., 2020). Often many of the bacteria which are washed in via anthropogenic waste streams are also resistant to antibiotics (Carney et al., 2019). Environmental perturbations such as heatwaves and heavy rainfall often underpin the dynamics of endemic microbial hazards, while heavy rainfall events often underpin the mechanisms of microbial hazards washed into the environment, such as their transportation into the environment (e.g., sewage overflow and animal faeces washing into the environment) (Agramont et al., 2020). These mechanisms, however, are not well defined, which often leaves remediation efforts obfuscated. Therefore, in this thesis, my main objectives were to define the environmental variables which drive the patterns of diversity and abundance of pathogenic *Vibrio* along the eastern coastline of Australia, to investigate molecular microbiological approaches that reduce ambiguity about the source of faecal pollution and identify microbial hazards in the environment, to investigate how rainfall leads to elevated levels of microbial hazards in coastal environments, and how natural perturbations in comparison to anthropogenic runoff alter the microbiology of estuarine like environments.

6.2 - Synthesis of results

6.2.1 - Defining the latitudinal dynamics of pathogenic Vibrio along the eastern coastline of Australia – endemic microbial hazards

Many of the microbial human pathogens within coastal environments are endemic. Microbes such as *Cyanobacteria* can form destructive blooms in aquatic environments (O'Neil et al., 2012), many of which can cause liver diseases and skin irritations (Chorus and Welker, 2021; Codd et al.; Codd et al., 2005; Humpage, 2008; Klisch and Häder, 2008; Li et al., 2001; Smith et al., 2011), while blooms of micro-algae such as *Karenia brevis* (Ryan and Campbell, 2016) can cause harmful algal blooms. Species from the genus of bacteria *Vibrio,* however, have a significant human health impact around the globe (Baker-Austin et al., 2018).

The most notable *Vibrio* species which are human pathogens are *V. cholerae*, *V. parahaemolyticus* and *V. vulnificus* (Baker-Austin et al., 2018). *V. cholerae* and *V. parahaemolyticus* cause gastrointestinal illnesses, while *V. vulnificus* causing necrotic skin lesions. The environmental drivers behind blooms and outbreaks of pathogenic *Vibrio* have been examined in a range of coastal environments (Amin et al., 2016; Froelich et al., 2019; Oberbeckmann et al., 2011; Takemura et al., 2014), but the role of large-scale spatial environmental variability on *Vibrio* abundance in Australian coastal ecosystems have not yet been defined. In Chapter 2, I detected several species of pathogenic *Vibrio* in coastal waters along the eastern coast of Australia and identified a suite of environmental determinants, primarily including temperature and salinity, as drivers of *Vibrio* abundance. These findings are consistent with patterns also reported in Chapter 5, as well as other studies (C. N. Johnson et al., 2010; Lipp et al., 2001; Oberbeckmann et al., 2012; Randa et al., 2004), which have determined these two environmental parameters as key drivers of bacterial community composition.

Of the significant *Vibrio* pathogens, I detected both *V. vulnificus* and *V. parahaemolyticus*. *V. parahaemolyticus* is a foodborne pathogen which infects people through contaminated seafood such as oysters (Daniels et al., 2000). *V. vulnificus* infections are contracted via direct contact from seawater, and can result in severe wound infections, which can sometimes be fatal (Baker-Austin et al., 2018). The abundance of *V. parahaemolyticus* was positively correlated with phytoplankton ASVs including a *Raphid-Pennate*, an *Arcocellulus*, two *Olisthodiscus*, a *Teleaulax*, and a *Marsupiomonas* ASV. To my knowledge this is the first evidence of links between these phytoplankton taxa and *V. parahaemolyticus*. *V. vulnificus*

relative abundances displayed a significant, albeit weak, correlation with temperature across the transect, but a much stronger negative correlation to salinity, which is consistent with previous observations (Blackwell & Oliver, 2008; Oberbeckmann et al., 2012).

The observed links between pathogenic *Vibrio* abundance in Australian waters and elevated temperatures and decreases salinity levels is significant because climate change is increasing sea surface temperature (Doney et al., 2012), as well as increasing the frequency of severe rainfall events (Madakumbura et al., 2021), which will lead to periodic reductions in coastal salinity. As a result, the environmental conditions within many coastal environments may become more ideal habitats for pathogenic *Vibrio* species, which could potentially pose a significant human health risk to people that use coastal environments for recreation and food production.

6.2.2 - Investigating molecular microbiological approaches to reduce ambiguity about the sources of faecal pollution and identify microbial hazards within an urbanised coastal environment

In contrast to endemic microbial hazards such as *Vibrio* bacteria, which often already exist in the environment, and can proliferate during environmental perturbations, urbanised coastal environments are also often contiguous to urban waste streams (McLellan et al., 2015), which can be a vehicle for microbial contamination. One major urban waste stream is raw sewage, which can enter the environment through inadequate stormwater infrastructure. Sewage entering the environment is a major public health concern (WHO, 2021), as it is enriched human pathogens (Efstratiou et al., 2017; Strubbia et al., 2019) and other microbial hazards such as AmR bacteria (Karkman et al., 2019). Current water quality monitoring programs use fecal indicator organism (FIO) enumeration techniques to detect sewage in recreationally used waterways, however this technique is unable to determine whether the FIO is sourced from sewage, or from animal faeces (e.g., dog, bird) and is also unable to detect significant human pathogens or other microbial hazards such as ARB. Therefore, a major goal of this thesis was to develop better methods to discriminate the animal/human source of faecal contamination using molecular microbial source tracking (MST) techniques (Feng et al., 2018; Green et al., 2012, 2014; Templar et al., 2016). It is important to discriminate between animal and human faecal contamination so that remediation efforts can be targeted, and because these two types of faecal contamination present substantially different health risks. Human faecal

contamination is a much greater health hazard than animal faecal contamination, as it contains many human pathogens including viruses such as human *Norovirus* (Strubbia et al., 2019), *Enterovirus* (Costán-Longares et al., 2008), and human *Adenovirus* (Yoshitomi et al., 2017), as well as bacterial pathogens such as species from the genus *Arcobacter* (Fisher et al., 2014) as well as pathogenic strains of *E. coli* (Anastasi et al., 2012). Within chapter 3, 4, and 5, the MST markers Lachno3 and HF183, which are markers for sewage (Feng et al., 2018; Templar et al., 2016), DG3 which is a marker for dog faeces (Green et al., 2014), and GFD which is a marker for bird faeces (Green et al., 2012) were used to elucidate the source of high levels of the FIO enterococci (indicative of faecal contamination) at three separate locations, during both periods of dry weather, and during rain events. Additionally, the source of faecal contamination (i.e., stormwater drain), and it's relative impact at contaminated sites is also often undefined, hindering remediation efforts. Therefore, another major goal of this study was to enhance molecular MST approaches by supplementing them with 16S rRNA gene amplicon sequencing to track stormwater impacts within the environment.

At the first location, Rose Bay (chapter 3), I determined sewage contamination as major source of high FIO, with an intermediate impact from dog faeces. Rose Bay is an urban city beach with a large surrounding population. This beach is conduit to 8 storm water drains, which have suspected sewage leaks, is a dog beach, and is inhabited by a range of avian species. Both the levels of the sewage markers, and the dog faecal marker were significantly and positively correlated with levels of FIO, indicating sewage and dog faeces to be major causes of high FIO levels at this location. Sewage markers were significantly higher in the drain water compared to the seawater, during both dry and wet weather, marking them as candidates for sewage leaks, while dog faeces was restricted to near-shore sites during dry weather, and was elevated within the drains when dog faeces as washed into the environment during rainfall. Within the stormwater drains, levels of HF183 and Lachno3 were similar to those detected within untreated sewage (Ahmed et al., 2022; Li et al., 2021; Sauer et al., 2011), and in some cases was less than an order of magnitude lower in the receiving waters. This indicates a high risk of contracting a GI illness, such as human *Adenovirus*, with this pathogen having displayed a strong association with both Lachno3 and HF183 in untreated wastewater (Ahmed et al., 2022). However, dog faeces also contributed to high levels of FIO. The abundance patterns of this marker were coherent with Rose Bay being a dog beach, with high levels nearshore during dry weather. In addition, I believe that the elevated concentrations of the dog marker, DG3, within the stormwater infrastructure and within the bay during heavy rain is a ramification of dog

faeces being washed from the catchment into the stormwater drains and then out into the bay. There was no correlation between the avian faeces marker and FIO, and the distribution of this indicator of bird faeces was largely homogenous across the measured environment. I therefore concluded that at Rose Bay, the major causes of high FIO were sewage and dog faeces.

In contrast to Rose Bay, which is located within Australia's largest city, the second location studied in this thesis, Terrigal Beach (Chapter 4), is located near a considerably smaller coastal town, approximately 60 km north of Sydney. At this location, the causes of high levels of FIO were also ambiguous, with suspected sewage leaks within several stormwater drains, a nearby dog park, and a large native bird population consisting of seagulls, pelicans, and other water birds. Similar to the observations in Rose Bay, levels of the Lachno3 sewage marker were elevated in all samples adjacent to stormwater infrastructure during heavy rainfall. This marker reached similar concentrations to those observed in Rose Bay (Chapter 3), and again, within seawater was often only one order of magnitude lower than concentrations previously described in raw sewage (Ahmed et al., 2022; Ahmed et al., 2019). However, in contrast to Rose Bay (Chapter 3) where sewage contamination could be detected up to 1 km offshore, at Terrigal Beach (Chapter 4) in seawater samples that were not located immediately adjacent to stormwater drains, concentrations of the Lachno3 sewage marker remained low or often undetectable. One possible explanation for this is that Rose Bay, is located within Sydney Harbour estuary where it is protected by multiple headlands from large swell, while Terrigal Beach faces the ocean where it is subject far more dynamic physical conditions in receiving waters. In conclusion, at Terrigal Beach, levels of sewage contamination were dramatically impacted by heavy rainfall induced sewage overflow, but this contamination was mostly restricted to the nearshore sites.

In chapter 5, the contrasting impact of natural environmental variables and faecal contamination on the microbiology of four coastal ICOLLs was studied, finding sewage contamination to alter the microbiology of two ICOLLs during heavy rainfall. ICOLL environments provide a suite of important ecosystem services (Basset et al., 2013) and are also often used for recreation by human populations but are often closed to the ocean via a sandbar, making them highly susceptible to environmental perturbations, as well as anthropogenic contamination. Two of the studied ICOLLs, Avoca, and Terrigal, were contiguous to multiple storm water drains, while one site (W1), within Wamberal Lagoon was situated close to a sewage pumping station, and the fourth ICOLL, Cockrone Lagoon, was surrounded primarily by parkland. The surrounding walking tracks of all four lagoons are used by dog walkers, and

all four lagoons were inhabited by multiple avian species such as seagulls and ducks. Similar to Rose Bay (chapter 3) the bird faecal marker GFD was largely homogenous between dry and wet weather. However, in contrast to Rose Bay (chapter 3), where the dog faecal marker, DG3, was detected nearshore during dry weather and in the bay during wet weather, in all four ICOLLs (chapter 5), detection of the dog faecal marker DG3 was typically restricted to wet weather samples. During rainfall, the highest concentrations of the Lachno3 sewage marker were detected in Avoca and Terrigal Lagoons, and these levels were only slightly lower than what has previously been detected in raw sewage (Ahmed et al., 2019). In conclusion, the major cause of high FIO within these lagoons was sewage contamination.

Within chapters 3, 4, and 5, MST qPCR techniques were supplemented with 16S rRNA gene amplicon sequencing to determine the bacteria community, and to incorporate the community data into statistical approaches to define the relative impact of stormwater drains on the environment, and to define a suite of stormwater indicator taxa. In chapter 3, I coupled the 16S rRNA gene amplicon sequencing data with the Bayesian SourceTracker package (Knights et al., 2011), which uses Bayesian statistics to predict the percentage of 'source' microbial communities within selected 'sink' samples. I utilised SourceTracker to both track the spatiotemporal dynamics of specific bacterial signatures for individual stormwater drains, and to quantify the relative strength of the microbial signature from different stormwater drains. While the molecular MST assays defined many of the stormwater drains in Rose Bay to be contiguous to sewage contamination, this analysis was able to depict the impact of specific drains on Rose Bay. While studies in the past have shown faecal contamination from either sewage or animal sources increasing during rainfall events (Ahmed et al., 2020; Shrestha et al., 2020), only a handful of studies (Newton et al., 2013) have assessed the spatial extent of faecal contamination, and, to my knowledge, no studies have assessed the spatial impact faecal contamination to the resolution performed in this study, allowing us to determine that in some cases, the microbial signatures of some sewage impacted drains reached up to 1 km offshore.

In chapters 3, 4, and 5 I coupled the 16S rRNA gene amplicon sequencing with the *indicspecies* package (de Caceres & Jansen, 2018). This technique compared the drain and seawater microbial communities, allowing for the identification of specific ASVs that were indicators of water from stormwater drains. *Arcobacter and Comamonadaceae* were consistently found to be indicator ASVs across all three chapters. Collectively, in Chapters 3, 4, and 5, detections of these indicator taxa were sporadic and at a low relative abundance, with levels dramatically increasing during and after significant rainfall, following similar trends to

the Lachno3 sewage marker. Indeed, in chapter 5, 93 % of the indicator taxa correlated significantly with the Lachno3 sewage marker. While these indicators taxa were robust markers for a stormwater signature in each study, of particular significance, many of these indicator taxa were both potential human pathogens, and many correlated with genes encoding antimicrobial resistance.

6.2.3 - Investigating how rainfall leads to elevated levels of AmR bacteria

Across all four chapters I observed through multiple lines of evidence that rainfall increases the abundance of microbial hazards within coastal environments. Among these was an increase in the presence of antibiotic resistance, which is notable because recent studies have shown an increase of AmR *E. coli* in the guts of people who recreationally used urban baths in the UK (Leonard et al., 2015; Leonard et al., 2018). In Chapters 2, 3, and 4, I analysed levels of five ARGs, *sulI*, *tetA*, *dfrA1*, *qnrS*, and *vanB* which are indicative of bacteria resistant to sulfonamide (Huovinen et al., 1995), tetracycline (Allard & Bertrand, 1992), trimethoprim (Lombardo et al., 2017), quinolone (Berglund et al., 2014), and vancomycin (Berglund et al., 2014) resistance respectively. Collectively, across Rose Bay (Chapter 3), Terrigal Beach (Chapter 4), and the Central Coast ICOLLs (Chapter 5), levels of *sulI*, *tetA*, and *dfrA1* all significantly increased during heavy rainfall. In each case, levels of these genes also correlated with sewage markers, indicating that AmR bacteria were entering the environment via raw sewage leaks within the storm water infrastructure. At all three study sites, levels of *sulI*, *tetA*, and *dfrA1* were either similar to concentrations than those previously detected at other severely contaminated beaches in Sydney (Carney et al., 2019). Of particular note, I detected *vanB* at Rose Bay (chapter 3) and not at any other sampling site. This is particularly concerning as *vanB* confers to vancomycin resistance, one of the last line of defence antibiotics (Berglund et al., 2014). This may have been due to the dense urban surroundings, and high population of Rose Bay, given that population density has elsewhere been linked to AMR bacteria abundance (Bruinsma et al., 2003). Indeed, *vanB* has previously been detected at another city beach in Sydney (Carney et al., 2019). While *vanB* was not detected at Terrigal Beach or within the Central Coast ICOLLs, many of the ARGs detected in these studies correlated to numerous stormwater indicator taxa, and many of these indicator taxa were species which have strains that are significant human pathogens. Across each of the study environments I observed strong correlations between the levels of antibiotic resistance genes and the relative abundance of

bacterial indicators for stormwater contamination, including several putatively pathogenic species.

6.3 - Implications of microbial hazards within coastal environments

Currently, health costs associated with marine water-borne pathogens are over US$12 billion per year globally (Shuval, 2003). Gastrointestinal illness (GI) caused from recreational use of marine environments costs the US government US $300 million per year, with over 350,000 gastrointestinal illnesses linked to recreation (Ralston et al., 2011). Of the most cases include Norwalk virus and *Campylobacter jejuni* infections, with costs of US$18 million and US $5 million respectively, however despite there being fewer cases reported, *Vibrio* bacteria are a particularly impactful water-borne marine pathogen which have health costs of over US $30 million per year (Ralston et al., 2011).

In Chapter 2, I demonstrated that several potentially pathogenic species of *Vibrio* occur along the eastern coastline of Australia. In 2020, it was estimated that there were half a million human infections by pathogenic *Vibrio* world-wide (Takemura et al., 2014), but this impact is predicted to increase as a consequence of climate change. Models of SST scenarios in the year 2100 predict that an additional 38,000 km of coastline will be suitable for *Vibrio* growth as a result of climate change (Trinanes and Martinez-Urtaza, 2021), with *Vibrio* infections predicted to increase by a factor of 1.93 times for every 1 °C increase in SST (Baker-Austin et al., 2013). This is particularly concerning in Australia, which is considered a global climate change hotspot, where SSTs are predicted to rise by 1.5 °C to 3 °C by 2070, which translates to a 2.9 – 5.8 times increase in the abundance of *Vibrio* spp in Australian waters (Trinanes and Martinez-Urtaza, 2021). This temperature induced increase in *Vibrios* will potentially impose a serious human health threat to recreational users of coastal environments.

In conjunction with temperature-driven increases in pathogenic *Vibrio* abundance, I also showed that decreased salinity is a significant determinant of many *Vibrio* species, including the significant human pathogen *V. vulnificus*. Severe rainfall events are predicted to increase with climate change (Madakumbura et al., 2021). These rainfall events lower the salinity of marine environments, and, paired with increasing SST create ideal conditions for the proliferation of dangerous *Vibrio* pathogens. Not only does this pose a significant human health threat but will also potentially be detrimental to the economy.

In addition to the endemic microbial hazards explored in Chapter 2, I also explored the microbial hazards that enter coastal environments via anthropogenic waste streams such as sewage contamination. In many cases, stormwater infrastructure is contiguous to sewage infrastructure. When sewage infrastructure becomes blocked or cracked, or there is a heavy rainfall event, sewage can enter into the stormwater infrastructure and then consequently drain untreated into the environment (Olds et al., 2018). This is particularly concerning for recreational users of the environment, as sewage is often enriched in pathogens such as protistan parasites such as *Giardia duodenalis* and *Cryptosporidium* (Efstratiou et al., 2017), bacteria such as *Escherichia coli* (Anastasi et al., 2012) and *Arcobacter* species, including *A. butzleri* and *A. defluvii* (Fisher et al., 2014), and viruses such as *Rotavirus*, *Norovirus* and *Adenovirus* (Strubbia et al., 2019). At Rose Bay, Terrigal Beach, and within the Central Coast Lagoons, in chapters 3, 4, and 5 I detected many indicators of stormwater to be notable human pathogens such as species from the *Arcobacter* genus.

There was an estimated with 1.27 million directly linked to AmR bacteria in 2019 (Murray et al., 2022). In chapters 3, 4, and 5 of this thesis, AmR bacteria were detected to increase during rainfall, and many of these were washed in through the stormwater drains, with levels within these drains being significantly higher within the drains in comparison to the seawater. Given that significant rainfall events are predicted to increase due to climate change (Madakumbura et al., 2021) the amount of AmR bacteria being washed into the environment via anthropogenic waste streams will be amplified. Furthermore, of the top six most impactful pathogens AmR, *E. coli* was found to be responsible for the most deaths (Murray et al., 2022) and recent research has shown that surfers and swimmers experienced heightened exposure to AmR *E.coli* (Leonard et al., 2015). In chapter 5 of this thesis, I identified *E. coli* to be an indicator of stormwater in the central coast ICOLLs, and this *E. coli* was found to significantly and positively correlate with the ARGs *sulI, tetA*, and *dfrA1*, highlighting a significant health threat at these locations.

6.4 - Relevance and impact of findings

Chapters 3, 4, and 5 of this thesis involved collaboration with the government organisations, the Department of Planning and Environment (DPE) and the NSW water quality monitoring agency Beachwatch. Beachwatch and DPE collaboratively produce a “state of the beaches” report on a yearly basis, and this report had consistently found high FIO levels at

Rose Bay, Terrigal Beach, and within the four studied central coast ICOLLs (DPIE, 2020). At all three locations, remediation efforts had been hindered as it was unknown if the source of high FIO was from a sewage leak within a stormwater drain, from dog faeces in the surrounding parkland and footpaths, or from avian faeces such as seagulls and ducks. It was also unknown how far the faecal contamination spread at each location. Once these questions were highlighted by DPE and Beachwatch, in collaboration, each location was investigated on site to identify key areas to target for sampling, and both Beachwatch and DPE took samples for enterococci enumeration, water filtration, and nutrients in the field, whilst I filtered the water for DNA extraction on site. As a result of this collaboration, the findings of this thesis have helped to develop three separate water quality reports provided to these agencies, focussed on Rose Bay (Chapter 3) (Seymour et al., 2020b), at Terrigal Beach (Chapter 4) (Seymour et al., 2020a), and within the Central Coast ICOLLs (Chapter 5) (Seymour et al., 2021). In addition to these audit reports, the findings of these chapters have directed remediation efforts at all three sites (Johnson, 2020; 2021). Furthermore, the methods applied within this thesis are now being applied to other investigations in collaboration with DPE and the Environmental Protection Agency (confidential reports). This represents a major real-world impact of the science presented in this thesis.

6.5 - Future directions

In all four chapters I used a combination of qPCR, as well as 16S rRNA gene amplicon sequencing, which enabled me to characterise bacterial community composition down to the ASV-level, whereby bacterial taxa can be discriminated down to one base pair difference in the 16S rRNA gene (Callahan et al., 2016). However, even with this high resolution, often, 16S rRNA gene amplicon sequencing cannot reliably differentiate between strains or in some cases, between species of bacteria. This limitation prevents discrimination between important bacteria, for example, *Vibrio cholera*, which has strains which are both pathogenic and non-pathogenic (Baker-Austin et al., 2017). Recently, an investigation of over 25,000 re-constructed genomes from more than 1000 seawater samples revealed novel information on phylogenomic and functionality of *Eudoremicrobiaceae* (Paoli et al., 2022). Whilst this study focused on *Eudoremicrobiaceae*, it highlighted the power of studying reconstructed genomes, and how this technique could be applied to other bacterial groups. Reconstructing *Vibrio* genomes from the sampling areas investigated in chapter 2 has the potential to reveal information on virulence genes that are harboured by specific *Vibrio* species. Recent laboratory

experiments investigating the metabolomics of *V. harveyi* have shown *V. harveyi* to express virulence genes as a response to increasing water temperature (Montánchez et al., 2019). Theses dynamics are not yet defined in the environment, or in other pathogenic species of *Vibrio*, which poses a key human health related question.

Within chapters 2, 3, and 4 I implemented molecular MST techniques to precisely determine the source of faecal contamination at multiple locations, however this technique has shortcomings. Recent work has shown that sediments can act as a reservoir for MST markers (Ahmed et al., 2020). This is important because the rate at which these markers decay is currently unknown, meaning that unviable organisms may be resuspended into the water during times of high ocean turbulence, obfuscating results. One solution for this problem would be to extract RNA from water samples to ensure detections of the MST markers were viable.

Another shortcoming of this technique is relating it back to a likelihood of contracting illness. Currently, the world health organisation has laid out standards for detections of the FIO enterococci which calculate back to a likelihood of contracting a gastrointestinal illness (WHO, 2021). Recently, a study by Warish A (2022) has detailed the ratios of human viruses which exist in sewage. Other studies have incorporated multiple faecal markers to define a risk-based water quality threshold for the sewage marker HF183 to range from 1 – 525 copies/100mL, resulting in 32 illnesses per 1000 swimmers (Boehm and Soller, 2020). However, this is yet to be standardised, and rigorous testing is still required to develop a standardised risk-based threshold that can be implemented world-wide, creating continuity in management and remediation decisions.

6.6 - Conclusions

The primary objective of this thesis was to define the extent of microbiological threats to human and ecosystem health and identify the environmental and anthropogenic factors causing them. Microbial hazards can be both endemic, (e.g., *Vibrio* bacteria), or introduced via anthropogenic waste streams such as sewage (e.g., *Arcobacter*). In chapter 2 of this thesis, I wished to determine the latitudinal dynamics *Vibrio* bacteria. I detected high *Vibrio* levels at both high and low latitudes, and, across this transect, both pathogenic and non-pathogenic *Vibrio* species correlating positively with temperature and negatively with salinity. Of note, I also observed significant positive correlations between pathogenic *Vibrio* species and specific phytoplankton species, highlighting their ecological relationships with phytoplankton. In

chapter 3, I aimed to improve molecular microbiological approaches to reduce ambiguity about the sources of faecal contamination and to additionally identify microbial hazards in coastal environments. In addition to defining the source of faecal contamination at this site to be predominantly sewage, I also defined the spatial dynamics of the contamination, showing that during heavy rainfall it impacted the environment up to 1 km offshore. I also determined that this contamination was linked to high levels of multiple ARGs in the environment. In chapter 4, my aim was to determine if rainfall led to elevated levels of antibiotic resistance genes within coastal environments, and if this was linked to rainfall induced sewage contamination. In this chapter I showed a direct link between sewage contamination and increased levels of ARGs, discriminating the point sources of these ARGs. Moreover, I was able to detect correlations between these ARGs and human pathogens that were identified as markers for stormwater in the environment. In my final data chapter, I wished to determine the importance of natural environmental variability and anthropogenic impacts on bacterial assemblages within ICOLLs. In this chapter I demonstrated that while natural environmental parameters were the major determinants of the microbial assemblages within ICOLLs, heavy rain events can lead to sewage contamination that can alter the microbial community, and introduce human pathogens, antibiotic resistant bacteria, and potentially AmR pathogens. In all four data chapters, I found rainfall to increase the potential for bacterial pathogens to proliferate in the environment, and with climate change induced rainfall events set to increase in frequency and severity (Madakumbura et al., 2021), I predict this situation to worsen. Overall, in this thesis, I have identified a number of microbiological hazards in changing coastal environments, which serves as a human health warning to recreational users of these environments, and, similar to within chapters 3-5, can help to guide the remediation efforts of government agencies.

Appendix 1 - Latitudinal dynamics of *Vibrio* along the Australian East Coast

Table 1. Primers used in study.

Host Organism	Target Gene	Primer Sequences	qPCR Conditions	Efficiency	Quantification limit	Ref
All Bacteria	16S rRNA	Forward: 5' CGGTGAATACGTTCYCGG 3' Reverse: 5' AAGGAGGTGATCCRGCCGCA 3' Probe: 5' CTTGTACACACCGCCCGTC 3'	95°C for 3 min; 40 cycles of: 95°C for 30 sec, 56°C for 1 min	99.4 %	10^2 copies/reaction	(Suzuki et al., 2000)
All *Vibrio*	16S rRNA	Forward: 5' GGCGTAAAGCGCATGCAGGT 3' Reverse: 5' GAAATTCTACCCCCCTCTACAG 3'	95°C for 3 min; 40 cycles of: 95°C for 15 sec, 60°C for 1 min	100.6%	10^1 copies/reaction	(Thompson et al., 2004)
Vibrio cholerae	ompW	Forward: 5' AACATCCGTGGATTTGGCATCTG 3' Reverse: 5' GCTGGTTCCTCAACGCTTCTG 3'	95°C for 3 min; 40 cycles of: 95°C for 15 sec, 60°C for 1 min	96.7%	10^1 copies/reaction	(Gubala and Proll, 2006)
Vibrio vulnificus	*vvhA*	Forward: 5' AACATCCGTGGATTTGGCATCTG 3' Reverse: 5' GCTGGTTCCTCAACGCTTCTG 3'	95°C for 3 min; 40 cycles of: 95°C for 15 sec, 56°C for 1 min	98.5%	10^1 copies/reaction	(Siboni et al., 2016)
Vibrio parahaemolyticus	*tdhS*	Forward: 5' GTAAAGGTCTCTGACTTTTGGAC 3' Reverse: 5' TGGAATATGAACCTTCATCTTCACC 3'	95°C for 3 min; 40 cycles of: 95°C for 15 sec, 50°C for 1 min	102%	10^2 copies/reaction	(Rizvi and Bej, 2010)

Table 2. List of locations sampled, detailing date, latitude, longitude, sample type and Koppen-Classification.

Location	Date	Latitude	Longitude	Type	Koppen-classification
Darwin B	17/1/18	12°22'42.8"S	130°50'30.8"E	Beach	Tropical
Darwin R	3/2/18	12°27'06.3"S	130°49'12.0"E	River	Tropical
Cooktown B	3/2/18	15°27'33.3"S	145°15'00.9"E	Beach	Tropical
Cooktown R	3/2/18	15°27'37.8"S	145°14'57.6"E	River	Tropical
Cairns B	15/1/18	16°55'03.9"S	145°46'50.2"E	Beach	Tropical
Cairns R	17/1/18	16°56'28.1"S	145°46'33.3"E	River	Tropical
Townsville B	18/1/18	19°14'39.5"S	146°48'39.6"E	Beach	Tropical
Townsville R	3/2/18	19°16'29.3"S	146°49'52.0"E	River	Tropical
Mackay B	16/2/18	21°06'37.6"S	149°13'33.4"E	Beach	Subtropical
Mackay R	16/2/18	21°08'29.3"S	149°11'53.4"E	River	Subtropical
Rockhampton B1	1/3/18	23°15'17.8"S	150°49'44.5"E	Beach	Subtropical
Rockhampton B2	11/1/18	23°16'01.7"S	150°49'42.2"E	Beach	Subtropical
Bundaberg R1	16/1/18	24°45'41.8"S	152°23'14.6"E	River	Subtropical
Bundaberg R2	16/1/18	24°51'53.9"S	152°20'37.1"E	River	Subtropical
Gold Coast B	1/3/18	28°09'45.0"S	153°31'09.5"E	Beach	Subtropical
Gold Coast R	26/12/17	28°10'44.1"S	153°32'30.1"E	River	Subtropical
Coffs Harbour R	1/2/18	30°17'46.9"S	153°08'12.7"E	River	Subtropical
Coffs Harbour B	1/2/18	30°18'17.4"S	153°08'34.9"E	Beach	Subtropical
Port Macquarie B	1/2/18	31°25'39.5"S	152°55'03.1"E	Beach	Subtropical
Port Macquarie R	18/1/18	31°25'40.3"S	152°54'28.6"E	River	Subtropical
Sydney R	1/2/18	33°83'97" S	151°25'24" E	River	Subtropical
Sydney B	18/1/18	33°91'00" S	151°25'91" E	Beach	Subtropical
Jervis Bay B	17/1/18	35°00'46.0"S	150°41'38.5"E	Beach	Temperate
Jervis Bay R	15/1/18	35°01'13.8"S	150°40'19.9"E	River	Temperate
Marimbula R	17/1/18	36°53'29.1"S	149°54'40.6"E	River	Temperate
Marimbula B	18/1/18	36°53'52.4"S	149°54'53.9"E	Beach	Temperate
Hobart B	1/2/18	42°51'05.7"S	147°31'16.2"E	Beach	Temperate
Hobart R	1/2/18	42°53'20.9"S	147°20'17.6"E	River	Temperate

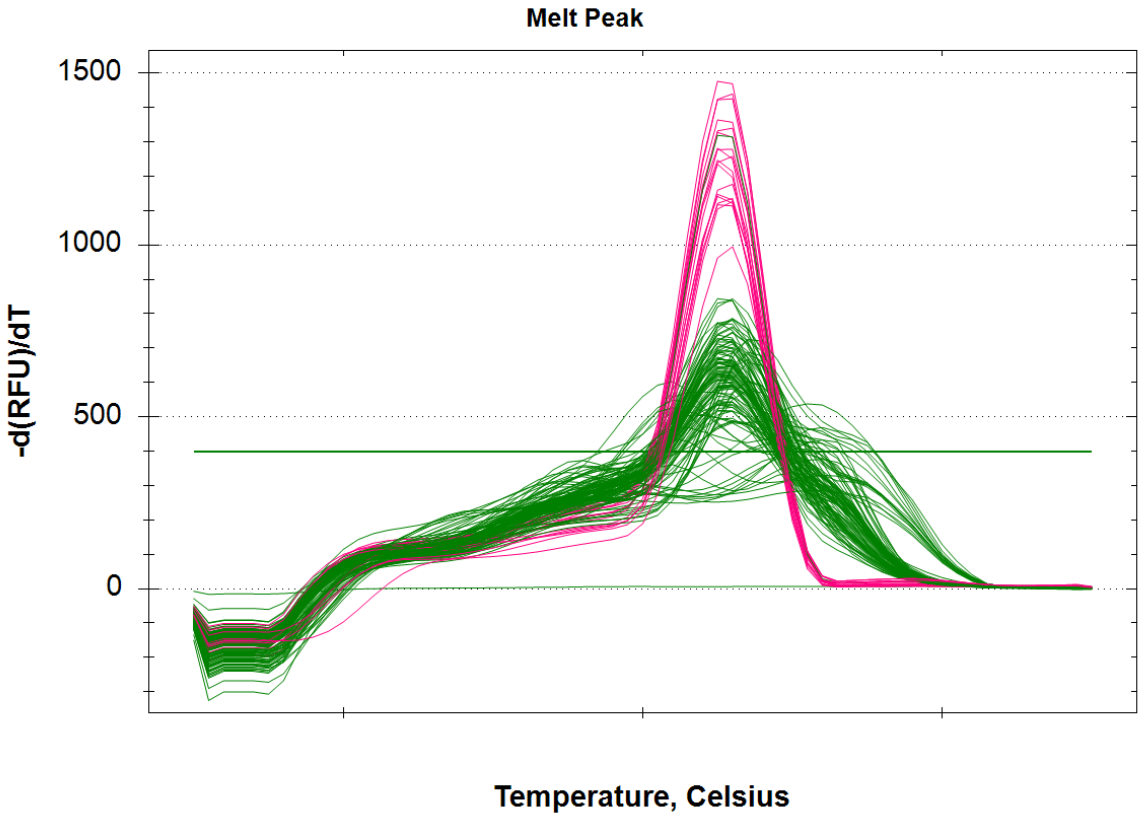

Figure 1. Total Vibrio qPCR melt curve. Pink indicates standard curve and green indicates samples.

Appendix 2 - Molecular microbiological approaches reduce ambiguity about the sources of faecal pollution and identify microbial hazards within an urbanised coastal environment

1.1 qPCR Methods

Prior to all qPCR analyses, I performed inhibition testing using the 16S qPCR assay. When performing the inhibition testing, I tested samples from Drains 3 and 5 along with immediately adjacent to these drains SW3.1 and SW5.1, as well as samples from the middle of Rose Bay (RBE.2) for all sampling days. These samples were chosen based on the enterococci data, which was employed as a proxy indicator for levels of contamination. The Drain 3 and 5 samples along with the SW3.1 and SW5.1 samples were chosen as representative 'contaminated samples' and the RBE.2 sample represented a relatively uncontaminated sample. I then performed a series dilution using these samples, incorporating dilution factors of 1:2, 1:5, 1:10, 1:20, 1:50 and 1:100, with 16S rRNA qPCR performed on all dilutions. I then calculated the copies of the 16S gene per 100 ml in each sample, which revealed identical copy numbers in the 1:10, 1:20, 1:50 and 1:100 dilutions for all sample types tested. Based on these results, I chose to dilute all samples to 1:20.

For SYBR Green based detection assays, reaction mixtures (5 µl) consisted of 2.5µl BIO-RAD iTaq UniveralSYBR® Green Supermix, 1.1 µl nuclease free water, 0.2 µl of each forward and reverse primer (10 mM) and 1 µl of diluted DNA template. The reaction mixes for analyses using probe assays (5 µl) consisted of 2.5 µl BIO-RAD iTaq UniversalProbes® Supermix, 1 µl nuclease free water, 0.2 µl of each forward and reverse primer (10 mM), 0.1 µl of probe (10 mM) and 1 µl of diluted (1:20) DNA. For all samples, plate preparation was performed using an epMotion® 5075 I Automated Liquid Handling System.

Quantitative PCR cycling conditions consisted of an initial denaturation step at 95°C for 3 minutes and then 45 cycles of: 95°C for 15 seconds and then variable annealing temperatures according to assay (see Table 2) for 1 minute, with the exception for intI1 and vanB which had annealing times of 1 minute. Melt curves were included in all SYBR Green based detection assays to confirm the amplification of a single, correctly sized product. To ensure the quality of CT values, I calculated the coefficient of variation % of each assay, removing samples with CV below 2.5%. Gene copy/100ml was then calculated via the following equation: $\mathrm{NSQ} = (\frac{Sq*Df*Ve}{Vf*Vq})$. NSQ was then multiplied by 100 to obtain copy/100ml.

NSQ = Normalized copy number.

Sq = Copy number (starting quantity, from the qPCR results file).

Df = Dilution factor (from sample preparation for qPCR).

Ve = Eluted volume (from DNA extraction [µl]).

Vf = Filtered volume (for DNA extraction [ml]).

Vq = Volume used for qPCR (per reaction [µl]).

1.2 Calculation of fresh to saline water ratio

To calculate the ratio of fresh to saline water, I used the equation as previously described by (Ho et al., 2021). In brief, the freshwater from the rainfall and drains was blended into the Rose Bay Seawater and I have attempted describe the impact of these drains on Rose Bay water chemistry by calculating this ratio.

Equation:

Concentrations:

$C_{w,drain}$: Mean salinity within the drains (Drain 2-Drain 10 after 43mm of rain) = (0.13 ± 0.05ppt, n=8).

$C_{w,300m}$: Mean salinity in the more saline samples 300m offshore (RBE) = (35.00 ± 0.11ppt, n=3).

$C_{w,Nearshore}$= Mean salinity of nearshore samples (i.e. SW2.1 – SW10.3) = (34.03 ± 0.24ppt, n=28)

Volumes:

$V_{w,drain}$= Volume of freshwater within the drains (Drain 2-Drain 10 after 43mm of rain).

$V_{w,300m}$= Volume of water within Rose Bay.

$V_{w,Nearshore}$= Volume of water within Rose Bay.

Ratio of $V_{w,drain}$: $V_{w,300m}$ from the concentration of conservative chemicals (i.e. salinity or conductivity as a proxy for salinity):

$$V_{w,drain}\ x\ C_{w,Nearshore} + V_{w,300m}\ x\ C_{w,Nearshore} = V_{w,drain}\ x\ C_{w,drain} + V_{w,300m}\ x\ C_{w,300m}$$

$$V_{w,drain}\ x\ C_{w,Nearshore} - V_{w,drain}\ x\ C_{w,drain} = V_{w,300m}\ x\ C_{w,300m} - V_{w,300m}\ x\ C_{w,Nearshore}$$

$$V_{w,drain}: V_{w,300m} = (C_{w,300m} - C_{w,Nearshore}): (C_{w,Nearshore} - C_{w,Drain})$$

Mixing ratio = (35.00 – 34.03)/(34.03-0.13)

Table 1. Primers used in study.

Target	qPCR Standard	Size (BP)	Primers	Primer Sequences	qPCR Conditions	Efficiency	Ref
16S	G-Block synthesised from NR_044853.1 by IDT	466	BACT1369F PROK1492R TM1389F	Forward: 5' CGG TGA ATA CGT TCY CGG 3' Reverse: 5' GGW TAC CTT GTT ACG ACT T 3' Probe: [FAM] 5' CTTGTACACACCGCCCGTC 3'	95°C for 3 min; 40 cycles of: 95°C for 30 sec, 56°C for 1 min	92% - 98.5%	(Suzuki et al., 2000)
Human *Bacteroidales*	G-Block synthesised from AY618282.1 by IDT	167	HF183 BFDRev BFDFAM	Forward: 5' ATCATGAGTTCACATGTCCG 3' Reverse: 5' CGTAGGAGTTTGGACCGTGT 3' Probe: [FAM] 5' CTGAGAGGAAGGTCCCCCACATTGGA 3'	95°C for 3 min; 45 cycles of: 95°C for 10 sec, 57°C for 1 min	99% - 104 %	(Templar et al., 2016)
Human *Lachnospiraceae*	G-Block synthesised from EF036467.1 by IDT	187	Lachno3F Lachno3R Lachno3P	Forward: 5' CAACGCGAAGAACCTTACCAAA 3' Reverse: 5' CCCAGAGTGCCCACCTTAAAT 3' Probe: [FAM] 5' CTCTGACCGGTCTTTAATCGGA 3' [MGB]	95°C for 3 min; 45 cycles of: 95°C for 10 sec, 64°C for 1 min	93% - 102.6%	(Feng et al., 2018)
Dog *Bacteroidales*	G-Block synthesised from DogGFE by IDT	185	DG3F DG3R DG3P	Forward: 5' TTTTCAGCCCCGTTGTTTCG 3' Reverse: 5' TGAGCGGGCATGGTCATATT 3' Probe: [FAM] 5' AGTCTACGCGGGCGTACT 3' [MGB]	95°C for 3 min; 45 cycles of: 95°C for 15 sec, 57°C for 30 sec	93% - 105%	(Green et al., 2014)
Bird *Heliobacter*	G-Block synthesised from JN084061.1 by IDT	163	GFDF GFDR	Forward: 5' TCGGCTGAGCACTCTAGGG 3' Reverse: 5' GCGTCTCTTTGTACATCCCA 3'	95°C for 3 min; 45 cycles of: 95°C for 15 sec, 57°C for 1 min	95.5% - 102.5%	(Green et al., 2012)
intI 1	Plasmid insert amplified from Sydney samples	484	int1.F int1.R	Forward: 5' GGGTCAAGGATCTGGATTTCG 3' Reverse: 5' ACATGCGTGTAAATCATCGTCG 3'	95°C for 3 min; 45 cycles of: 95°C for 15 sec 60°C for 30 sec	90% - 92%	(Mazel et al., 2000)
Sul1	Plasmid insert amplified from Sydney samples	163	sulI-FW sulI-RV	Forward: 5' CGCACCGGAAACATCGCTGCAC 3' Reverse: 5' TGAAGTTCCGCCGCAAGGCTCG 3'	95°C for 3 min; 45 cycles of: 95°C for 15 sec, 65°C for 30 sec	95.6% - 102.7%	(Pei et al., 2006)
tetA	Plasmid insert amplified from Sydney samples	96	tetA-F2-L tetA-R2	Forward: 5' CAG CCT CAA TTT CCT GAC GGG CTG A 3' Reverse: 5' GAA GCG AGC GGG TTG AGA G 3'	95°C for 3 min; 45 cycles of: 95°C for 15 sec, 58°C for 1 min	90% - 99.9%	(Borjesson et al., 2009)
VanB	Plasmid, bacteria w/plasmid pGEM-T with vanB cloned	3300	VB-F VB-R VB-P	Forward: 5' AAT CTT AAT TGA GCA AGC GAT TTC 3' Reverse: 5' CCT GAT GGA TGC GGA AGA TA 3' Probe: [FAM] 5' CCG GAT TTG ATC CAC TTC GCC GAC AAT CA 3'	95°C for 3 min; 45 cycles of: 95°C for 15 sec, 60°C for 30 sec	92.9% - 97.8%	(Berglund et al., 2014)
qnrS	Plasmid pGEM-T with qnrS cloned	3200	QnrS-F QnrS-R	Forward: 5' ATC AAG TGA GTA ATC GTA TGT ACT 3' Reverse: 5' CAC CTC GACTTAAGTCTGAC 3'	95°C for 3 min; 45 cycles of: 95°C for 15 sec, 72°C for 30 sec	92.9 % - 97.8%	(Berglund et al., 2014)
dfrA	Plasmid, bacteria w/plasmid	3500	dfr1s-f dfr1s-r	Forward: 5'ATG GAG TGC CAA AGG TGA AC 3' Reverse: 5' TAT CTC CCC ACC ACC TGA AA 3'	95°C for 3 min; 45 cycles of: 95°C for 15 sec, 62°C for 1 min	88% - 102.5%	(Grape et al., 2007)

Table 2. Indicator ASV sequences

Indicator ID		ASV
Comamonadaceae; unassigned	***genus***	TGGGGAATTTTGGACAATGGACGAAAGTCTGATCCAGCCATTCCGCGTGCAGGACGAAGGCCTTCGGGTTGTAAACTGCTTTTGTACAG AACGAAAAGGTCTCTATTAATACTAGGGGCTCATGACGGTACTGTAAGAATAAGCACCGGCTAACTACGTGCCAGCAGCCGCGGTAATA CGTAGGGTGCAAGCGTTAATCGGAATTACTGGGCGTAAAGCGTGCGCAGGCGGTTATATAAGACAGATGTGAAATCCCCGGGCTCAACC TGGGAACTGCATTTGTGACTGTATAGCTGGAGTACGGCAGAGGGGGATGGAATTCCGCGTGTAGCAGTGAAATGCGTAGATATGCGGAG GAACACCGATGGCGAAGGCAATCCCCTGGGCCTGTACTGACGCTCATGCACGAAAGCGTGGGGAGCAAACA
Comamonadaceae; unassigned	***genus***	TGGGGAATTTTGGACAATGGACGCAAGTCTGATCCAGCCATTCCGCGTGCAGGATGAAGGCCCTCGGGTTGTAAACTGCTTTTGTACAGA ACGAAAAGGCTCTTCCTAATACGGGGGGCTCATGACGGTACTGTAAGAATAAGCACCGGCTAACTACGTGCCAGCAGCCGCGGTAATAC GTAGGGTGCAAGCGTTAATCGGAATTACTGGGCGTAAAGCGTGCGCAGGCGGTTATATAAGACAGATGTGAAATCCCCGGGCTCAACCT GGGAACTGCATTTGTGACTGTATAGCTAGAGTACGGCAGAGGGGGATGGAATTCCGCGTGTAGCAGTGAAATGCGTAGATATGCGGAGG AACACCGATGGCGAAGGCAATCCCCTGGGCCTGTACTGACGCTCATGCACGAAAGCGTGGGGAGCAAACA
Spirosomaceae; unassigned	***genus***	TAGGGAATATTGGGCAATGGACGCAAGTCTGACCCAGCCATGCCGCGTGCAGGATGAAGGCGTTATGCGTTGTAAACTGCTTTTATACA GGAAGAAACGACTCTTGCGAGAGGCATTGACGGTACTGTATGAATAAGCACCGGCTAACTCCGTGCCAGCAGCCGCGGTAATACGGAG GGTGCAAGCGTTGTCCGGATTTATTGGGTTTAAAGGGTGCGCAGGTGGTTTATTAAGTCAGTGGTGAAAGACGGTCGCTCAACGATTGCA GTGCCATTGAAACTGGTAGACTTGAGTAAAGTAGAGGTGGGCGGAATTGATAGTGTAGCGGTGAAATGCATAGATATTATCAAGAACTC CAATTGCGTAGGCAGCTCACTTGGCTTTTACTGACACTCATGCACGAAAGTGTGGGTATCAAACA
Comamonadaceae; unassigned	***genus***	TGGGGAATTTTGGACAATGGGCGAAAGCCTGATCCAGCCATACCGCGTGCGGGAAGAAGGCCTTCGGGTTGTAAACCGCTTTTGTCAGG GAAGAAATCTTCTGGGTTAATACCTCGGGAGGATGACGGTACCTGAAGAATAAGCACCGGCTAACTACGTGCCAGCAGCCGCGGTAATA CGTAGGGTGCAAGCGTTAATCGGAATTACTGGGCGTAAAGCGTGCGCAGGCGGTTTTGTAAGACAGAGGTGAAATCCCCGGGCTCAACC TGGGAACTGCCTTTGTGACTGCAAGGCTTGAGTGCGGCAGAGGGGGATGGAATTCCGCGTGTAGCAGTGAAATGCGTAGATATGCGGAG GAACACCGATGGCGAAGGCAATCCCCTGGGCCTGCACTGACGCTCATGCACGAAAGCGTGGGGAGCAAACA
Comamonadaceae; unassigned	***genus***	TGGGGAATTTTGGACAATGGACGCAAGTCTGATCCAGCCATTCCGCGTGCAGGATGAAGGCCCTCGGGTTGTAAACTGCTTTTGTACGGA ACGAAAAGGTTTCCATTAATACTGGGAGCTCATGACGGTACCGTAAGAATAAGCACCGGCTAACTACGTGCCAGCAGCCGCGGTAATAC GTAGGGTGCGAGCGTTAATCGGAATTACTGGGCGTAAAGCGTGCGCAGGCGGTTATGTAAGACAGAGGTGAAATCCCCGGGCTCAACCT GGGAACGGCCTTTGTGACTGCATAGCTAGAGTACGGTAGAGGGGGATGGAATTCCGCGTGTAGCAGTGAAATGCGTAGATATGCGGAG GAACACCGATGGCGAAGGCAATCCCCTGGACCTGTACTGACGCTCATGCACGAAAGCGTGGGGAGCAAACA
Pseudarcobacter; cloacae/defluvii		TGGGGAATATTGCACAATGGACGAAAGTCTGATGCAGCAACGCCGCGTGGAGGATGACACATTTCGGTGCGTAAACTCCTTTTATATAG GAAGATAATGACGGTACTATATGAATAAGCACCGGCTAACTCCGTGCCAGCAGCCGCGGTAATACGGAGGGTGCAAGCGTTACTCGGAA TCACTGGGCGTAAAGAGCGTGTAGGCGGGTATATAAGTCAGAAGTGAAATCCAATAGCTTAACTATTGAACTGCTTTTGAAACTGTATA CCTAGAATGTGGGAGAGGTAGATGGAATTTCTGGTGTAGGGGTAAAATCCGTAGAGATCAGAAGGAATACCGATTGCGAAGGCGATCT ACTGGAACATTATTGACGCTGAGACGCGAAAGCGTGGGGAGCAAACA

Table 3. Limit of Detection/100ml for each assay as well as R^2 values for assay.

Assay	*LOD/100ml*	r^2
16S	1.00E+06	0.979
Lachno3	1.00E+02	0.997
HF183	1.00E+02	0.996
GFD	1.00E+02	0.994
DG3	1.00E+03	0.996
VanB	1.00E+03	0.996
sulI	1.00E+03	0.997
tetA	1.00E+04	0.993
qnrS	1.00E+03	0.996
dfrA1	1.00E+03	0.994
Arcobacter	1.00E+03	0.994

Table 4. Physiochemical Data

Location	Date	Temp °C	Sal ppt	OD%	pH	Turbidity NTU
SW10	21/8/19	15.41	35.24	100.64	8.02	0.87
SW10.2	21/8/19	15.43	35.24	95.34	7.93	0.28
SW10.3	21/8/19	15.51	35.27	96.79	7.94	0.38
SW2	21/8/19	14.47	34.97	98.89	7.94	1.24
SW3	21/8/19	15.04	33.66	110.73	8.07	2.97
SW3.2	21/8/19	15.87	35.16	103.80	7.95	0.48
SW3.3	21/8/19	15.50	35.25	97.30	7.94	0.28
SW4	21/8/19	15.26	34.07	104.42	8.07	1.15
SW4.2	21/8/19	15.78	35.12	97.53	7.93	0.35
SW4.3	21/8/19	15.51	35.26	97.32	7.94	0.35
SW5	21/8/19	15.69	32.93	107.91	8.08	1.71
SW5.2	21/8/19	15.75	35.26	97.93	7.93	0.19
SW5.3	21/8/19	15.52	35.26	97.53	7.94	0.36
SW6	21/8/19	15.40	35.26	100.96	8.05	0.60
SW6.2	21/8/19	15.51	35.27	96.81	7.94	0.38
SW6.3	21/8/19	15.53	35.26	97.63	7.94	0.50
SW7	21/8/19	15.40	35.18	102.05	8.09	0.74
SW7.2	21/8/19	15.61	35.23	98.07	7.94	0.27
SW7.3	21/8/19	15.54	35.22	97.65	7.94	0.44
SW8	21/8/19	15.27	34.11	95.58	7.98	1.41
SW8.2	21/8/19	15.55	35.17	98.06	7.94	0.58
SW8.3	21/8/19	15.50	35.23	97.77	7.94	0.55
SW9	21/8/19	15.17	35.14	99.06	8.05	0.72

SW9.2	21/8/19	15.56	35.26	97.28	7.94	0.36
SW9.3	21/8/19	15.51	35.26	97.96	7.94	0.30
RBE.1	21/8/19	15.42	35.25	96.68	7.94	0.43
RBE.2	21/8/19	15.44	35.25	97.10	7.94	0.42
RBE.3	21/8/19					
Beachwatch	21/8/19	15.88	35.11	102.64	7.96	0.69
Neilson Park.1	21/8/19	15.36	35.27	96.73	7.93	0.19
Neilson Park.2	21/8/19	16.10	35.43	95.23	7.96	0.35
Neilson Park.3	21/8/19	16.07	35.43	95.84	7.96	0.31
Drain 3	21/8/19					
Drain 4	21/8/19	19.80	0.20	96.14	7.73	0.61
Drain 5	21/8/19	16.70	0.35	67.88	7.94	3.81
Drain 6	21/8/19	15.30	0.25	86.59	8.14	2.52
Drain 8	21/8/19	13.99	0.24	108.27	8.49	1.63
SW10	27/8/19	16.39	35.11	105.40	8.13	5.13
SW10.2	27/8/19	15.72	35.19	94.34	8.08	0.50
SW10.3	27/8/19	15.70	35.24	95.47	8.08	0.32
SW2	27/8/19	17.05	34.92	120.41	8.19	NA
SW3	27/8/19	15.50	35.01	90.21	7.95	1.88
SW3.2	27/8/19	15.15	35.21	89.18	7.99	0.71
SW3.3	27/8/19	15.96	35.16	96.32	8.08	0.46
SW4	27/8/19	16.12	34.09	102.38	7.99	3.58
SW4.2	27/8/19	15.50	35.35	94.82	8.06	0.53
SW4.3	27/8/19	15.83	35.21	96.67	8.09	0.65
SW5	27/8/19	16.20	35.22	99.13	8.07	1.01
SW5.2	27/8/19	15.55	35.25	94.11	8.07	0.50
SW5.3	27/8/19	15.80	35.26	96.96	8.09	0.46*
SW6	27/8/19	15.70	35.20	95.01	8.06	0.75
SW6.2	27/8/19	15.50	35.37	94.80	8.07	1.10
SW6.3	27/8/19	15.79	35.28	97.29	8.09	0.46
SW7	27/8/19	16.51	34.93	122.39	8.20	2.63
SW7.2	27/8/19	15.66	35.26	95.15	8.08	0.30
SW7.3	27/8/19	15.78	35.15	97.24	8.09	0.50
SW8	27/8/19	16.05	35.22	98.14	8.07	0.79
SW8.2	27/8/19	15.62	35.18	95.28	8.08	0.72
SW8.3	27/8/19	15.58	35.19	96.40	8.09	0.46
SW9	27/8/19	16.20	35.15	97.74	8.10	1.98
SW9.2	27/8/19	15.67	35.19	95.14	8.08	0.57
SW9.3	27/8/19	15.77	35.09	96.86	8.08	0.54
RBE.1	27/8/19	15.71	35.28	97.19	8.09	0.40
RBE.2	27/8/19	15.76	35.28	97.50	8.09	0.26

RBE.3	27/8/19					
Beachwatch	27/8/19	15.85	35.14	94.45	8.08	1.14
Neilson Park.1	27/8/19	17.06	35.41	104.08	8.13	0.27
Neilson Park.2	27/8/19	16.42	35.42	98.52	8.11	0.25
Neilson Park.3	27/8/19	16.42	35.39	97.73	8.10	0.20
Drain 10	30/8/19	16.65	32.80	100.40	8.10	3.30
Drain 2	30/8/19					
Drain 3	30/8/19	15.14	0.20	103.39	8.07	0.53
Drain 4	30/8/19	19.08	0.19	94.10	8.80	1.85
Drain 5	30/8/19	18.20	0.27	66.75	8.30	4.15
Drain 6	30/8/19	16.22	0.34	92.62	8.51	3.38
Drain 8	30/8/19	18.30	0.18	113.40	8.23	5.03
Drain 9	30/8/19	16.09	33.39	95.78	8.09	1.43
SW10	30/8/19	15.72	34.46	88.32	8.00	0.87
SW10.2	30/8/19	15.71	34.68	94.74	8.04	0.42
SW10.3	30/8/19	15.71	34.78	95.06	8.03	0.44
SW3	30/8/19	15.60	33.25	91.15	8.08	1.91
SW3.2	30/8/19	15.62	34.39	93.00	8.02	0.87
SW3.3	30/8/19	15.84	34.85	95.31	8.04	0.59
SW4	30/8/19	15.70	33.71	92.84	8.04	47.85
SW4.2	30/8/19	15.82	34.93	94.64	8.03	0.43
SW4.3	30/8/19	15.90	35.11	95.36	8.04	0.56
SW5	30/8/19	15.80	32.83	94.88	8.09	1.93
SW5.2	30/8/19	15.88	35.01	94.88	8.03	0.53
SW5.3	30/8/19	15.92	35.14	95.29	8.04	0.49
SW6	30/8/19	15.88	34.08	95.16	8.10	1.37
SW6.2	30/8/19	15.92	35.12	94.78	8.03	0.51
SW6.3	30/8/19	15.88	35.08	95.60	8.04	0.55
SW7	30/8/19	16.00	34.58	94.52	8.08	1.76
SW7.2	30/8/19	15.89	35.00	95.23	8.04	0.66
SW7.3	30/8/19	15.85	35.09	95.60	8.04	0.38
SW8	30/8/19	15.87	33.44	96.54	8.01	1.21
SW8.2	30/8/19	15.87	34.99	95.33	8.04	0.49
SW8.3	30/8/19	15.80	35.09	95.56	8.04	0.75
SW9	30/8/19	15.86	34.74	90.92	8.02	0.86
SW9.2	30/8/19	15.85	34.53	94.68	8.03	0.44
SW9.3	30/8/19	15.85	34.66	94.98	8.03	0.67
RBE.1	30/8/19	15.61	34.78	95.10	8.01	0.75
RBE.2	30/8/19	15.93	35.00	95.71	8.02	0.54
RBE.3	30/8/19	15.85	34.83	94.68	8.02	0.67
Beachwatch	30/8/19	15.94	34.91	93.35	8.03	1.06

Neilson Park.1	30/8/19	16.32	35.18	94.70	7.88	0.33
Neilson Par.2	30/8/19	16.25	35.15	95.07	8.00	0.28
Neilson Park.3	30/8/19	16.43	35.22	95.33	8.03	0.32
Drain 10	30/8/19	13.90	0.07	98.67	8.82	10.75
Drain 3	30/8/19	13.85	0.11	99.95	8.67	29.32
Drain 4	30/8/19	16.16	0.17	96.97	7.50	4.75
Drain 5	30/8/19	13.30	0.10	97.40	8.25	25.50
Drain 6	30/8/19	13.50	0.14	98.10	9.02	28.90
Drain 7	30/8/19	13.60	0.09	88.01	8.49	20.04
Drain 8	30/8/19	13.80	0.20	97.74	7.56	12.98
Drain 9	30/8/19	13.80	0.21	97.01	7.98	14.40
SW10	3/9/19	16.33	34.58	95.82	7.76	1.45
SW10.2	3/9/19	16.64	34.72	97.02	7.87	0.63
SW10.3	3/9/19	16.63	34.83	99.12	7.89	0.34
SW3	3/9/19	16.60	34.65	102.80	8.02	3.80
SW3.2	3/9/19	16.28	34.86	97.08	7.88	0.96
SW3.3	3/9/19	16.27	34.88	97.09	7.88	0.48
SW4	3/9/19	15.93	33.83	98.88	7.97	2.41
SW4.2	3/9/19	16.20	34.86	96.80	7.88	0.49
SW4.3	3/9/19	16.24	34.90	97.26	7.89	0.41
SW5	3/9/19	16.00	33.58	100.84	8.06	29.21
SW5.2	3/9/19	16.27	34.84	96.65	7.88	0.40
SW5.3	3/9/19	16.30	34.88	97.40	7.88	0.31
SW6	3/9/19	16.10	33.95	95.56	8.03	5.21
SW6.2	3/9/19	16.26	34.84	97.01	7.88	0.49
SW6.3	3/9/19	16.42	34.86	97.60	7.88	0.43
SW7	3/9/19	16.10	33.87	97.13	8.06	1.90
SW7.2	3/9/19	16.63	34.32	97.70	7.87	0.62
SW7.3	3/9/19	16.51	34.84	97.68	7.88	0.36
SW8	3/9/19	16.00	34.65	93.88	8.01	0.93
SW8.2	3/9/19	16.26	34.88	97.34	7.88	0.37
SW8.3	3/9/19	16.30	34.87	97.60	7.88	0.51
SW9	3/9/19	15.91	33.30	92.20	7.77	0.87
SW9.2	3/9/19	16.70	34.91	97.20	7.88	0.41
SW9.3	3/9/19	16.59	34.85	97.90	7.88	0.37
RBE.1	3/9/19	15.93	34.87	96.19	7.88	0.36
RBE.2	3/9/19	15.99	34.91	96.10	7.88	0.39
RBE.3	3/9/19	16.12	34.88	96.22	7.88	0.45
Beachwatch	3/9/19	16.24	34.45	96.75	7.89	1.19
Neilson Park.1	3/9/19	16.15	34.95	95.27	7.87	0.42

Neilson Park.2	3/9/19	17.74	35.28	97.27	7.92	0.20
Neilson Park.3	3/9/19	17.60	35.24	97.46	7.93	0.09
Drain 3	3/9/19	15.56	0.26	95.38	8.72	1.33
Drain 4	3/9/19	19.60	0.21	95.55	8.10	1.58
Drain 6	3/9/19	17.03	0.86	88.55	8.08	2.79
Drain 8	3/9/19	15.82	0.23	89.11	7.45	1.99

Table 5. Nutrient Data (mg/L)

Site	Date	FRP	NH4-N	NOx-N	TDN	TDP	TN	TP
Beachwatch	21/8/19	0.006	0.008	0.006	0.08	0.005	0.1	0.009
Drain 4.0	21/8/19	0.001	0.01	4		0.004		0.004
Drain 5.0	21/8/19	0.036	0.26	3.1	3.8	0.033	4	0.047
Drain 6.0	21/8/19	0.026	0.017	2				
Drain 8.0	21/8/19	0.057	0.1	0.92	1.5	0.064	1.5	0.084
RBE1.4	21/8/19	0.005	0.006	0.003	0.08	0.005	0.08	0.008
RBE2.4	21/8/19	0.005	0.006	0.004	0.08	0.005	0.09	0.008
Neilson Park.1	21/8/19	0.004	0.005	0.004	0.07	0.005	0.08	0.007
Neilson Park.2	21/8/19	0.005	0.008	0.022	0.1	0.006	0.1	0.009
Neilson Park.3	21/8/19	0.005	0.006	0.013	0.08	0.005	0.1	0.008
SW10.1	21/8/19	0.006	0.014	0.027	0.11	0.006	0.12	0.011
SW10.2	21/8/19	0.005	0.007	0.007	0.08	0.005	0.08	0.009
SW10.3	21/8/19	0.006	0.007	0.005	0.08	0.005	0.08	0.008
SW2.1	21/8/19	0.008	0.017	0.026	0.15	0.01	0.17	0.013
SW3.1	21/8/19	0.005	0.013	0.11	0.23	0.006	0.26	0.015
SW3.2	21/8/19	0.004	0.007	0.007	0.09	0.006	0.08	0.009
SW3.3	21/8/19	0.005	0.005	0.003	0.07	0.005	0.1	0.008
SW4.1	21/8/19	0.004	0.006	0.13	0.22	0.004	0.21	0.009
SW4.2	21/8/19	0.005	0.009	0.006	0.1	0.009	0.08	0.007
SW4.3	21/8/19	0.005	0.005	0.003	0.08	0.006	0.07	0.008
SW5.1	21/8/19	0.004	0.008	0.28	0.37	0.005	0.37	0.009
SW5.2	21/8/19	0.005	0.008	0.005	0.09	0.007	0.09	0.008
SW5.3	21/8/19	0.005	0.006	0.003	0.08	0.005	0.08	0.007
SW6.1	21/8/19	0.005	0.007	0.007	0.08	0.005	0.09	0.008
SW6.2	21/8/19	0.005	0.008	0.004	0.08	0.005	0.08	0.007
SW6.3	21/8/19	0.005	0.006	0.003	0.08	0.005	0.08	0.007
SW7.1	21/8/19	0.005	0.01	0.01	0.09	0.005	0.11	0.01
SW7.2	21/8/19	0.004	0.007	0.003	0.08	0.005	0.09	0.008
SW7.3	21/8/19	0.005	0.006	0.003	0.08	0.005	0.08	0.007
SW8.1	21/8/19	0.008	0.015	0.038	0.15	0.007	0.16	0.014

SW8.2	21/8/19	0.005	0.007	0.003	0.08	0.004	0.09	0.008
SW8.3	21/8/19	0.005	0.006	0.002	0.07	0.006	0.09	0.008
SW9.1	21/8/19	0.005	0.009	0.011	0.11	0.005	0.1	0.009
SW9.2	21/8/19	0.005	0.006	0.003	0.08	0.005	0.09	0.009
SW9.3	21/8/19	0.005	0.006	0.003	0.08	0.006	0.07	0.007
Beachwatch	27/8/19	0.007	0.011	0.008	0.09	0.008	0.1	0.011
Drain 10.0	27/8/19	0.009	0.013	1.6	1.5	0.01	2.5	0.013
Drain 2.0	27/8/19	0.11	0.15	1.6	2.1	0.15	2.2	0.16
Drain 3.0	27/8/19	0.047	0.082	2.1	2.4	0.052	2.5	0.058
Drain 4.0	27/8/19	0.009	0.032	3.3	3.7	0.016	3.7	0.03
Drain 5.0	27/8/19	0.04	0.099	2.9	3.3	0.042	3.4	0.054
Drain 6.0	27/8/19	0.04	0.037	1.5	1.8	0.039	1.9	0.045
Drain 8.0	27/8/19	0.068	0.081	0.6	1.1	0.075	1.1	0.11
Drain 9.0	27/8/19	0.027	0.028	0.36	0.5	0.027	0.86	0.059
RBE1.4	27/8/19	0.006	0.006	0.005	0.08	0.007	0.08	0.008
RBE2.4	27/8/19	0.006	0.006	0.006	0.07	0.007	0.07	0.007
RBE3.4	27/8/19	0.006	0.008	0.01	0.08	0.007	0.08	0.007
Neilson Park.1	27/8/19	0.007	0.014	0.023	0.1	0.008	0.1	0.007
Neilson Park .2	27/8/19	0.007	0.013	0.017	0.09	0.007	0.1	0.008
SW10.1	27/8/19	0.007	0.009	0.017	0.1	0.006	0.11	0.014
SW10.2	27/8/19	0.007	0.007	0.008	0.08	0.006	0.08	0.008
SW10.3	27/8/19	0.006	0.007	0.005	0.08	0.008	0.08	0.009
SW2.1	27/8/19	0.009	0.012	0.045	0.14	0.01	0.41	0.075
SW3.1	27/8/19	0.006	0.009	0.02	0.1	0.007	0.11	0.01
SW3.2	27/8/19	0.006	0.01	0.024	0.1	0.007	0.11	0.009
SW3.3	27/8/19	0.005	0.009	0.01	0.08	0.006	0.09	0.009
SW4.1	27/8/19	0.005	0.01	0.096	0.18	0.007	0.2	0.015
SW4.2	27/8/19	0.006	0.009	0.013	0.09	0.007	0.1	0.01
SW4.3	27/8/19	0.006	0.007	0.006	0.08	0.007	0.08	0.008
SW5.1	27/8/19	0.006	0.008	0.008	0.09	0.008	0.1	0.011
SW5.2	27/8/19	0.006	0.009	0.01	0.1	0.007	0.09	0.008
SW5.3	27/8/19	0.005	0.008	0.006	0.08	0.007	0.07	0.007
SW6.1	27/8/19	0.006	0.011	0.011	0.09	0.007	0.09	0.005
SW6.2	27/8/19	0.006	0.009	0.007	0.09	0.006	0.09	0.009
SW6.3	27/8/19	0.005	0.007	0.006	0.08	0.006	0.08	0.01
SW7.1	27/8/19	0.007	0.008	0.005	0.08	0.008	0.11	0.012
SW7.2	27/8/19	0.006	0.01	0.008	0.09	0.006	0.09	0.008
SW7.3	27/8/19	0.006	0.006	0.005	0.08	0.007	0.09	0.01
SW8.1	27/8/19	0.006	0.009	0.006	0.08	0.008	0.13	0.017
SW8.2	27/8/19	0.006	0.007	0.006	0.09	0.006	0.08	0.007
SW8.3	27/8/19	0.006	0.006	0.005	0.08	0.007	0.08	0.008
SW9.1	27/8/19	0.007	0.01	0.01	0.09	0.009	0.12	0.015

SW9.2	27/8/19	0.006	0.007	0.006		0.007		0.008
SW9.3	27/8/19	0.005	0.008	0.006	0.07	0.006	0.09	0.007
Beachwatch	30/8/19	0.006	0.016	0.019	0.13	0.009	0.1	0.005
Drain 10.0	30/8/19	0.13	0.03	0.93	1.2	0.13	1.1	0.12
Drain 3.0	30/8/19	0.13	0.54	0.44	1.6	0.14	1.6	0.16
Drain 4.0	30/8/19	0.08	0.082	2.2	2.5	0.11	2.4	0.096
Drain 5.0	30/8/19	0.051	0.097	0.16	0.31	0.033	0.96	0.15
Drain 6.0	30/8/19	0.041	0.048	0.27	0.44	0.03	0.52	0.071
Drain 7.0	30/8/19	0.061	0.056	0.16	0.39	0.075	0.41	0.098
Drain 8.0	30/8/19	0.067	0.069	0.29	0.6	0.064	0.54	0.066
Drain 9.0	30/8/19	0.052	0.057	0.18	0.39	0.047	0.88	0.12
RBE1.4	30/8/19	0.007	0.012	0.013	0.11	0.008	0.09	0.006
RBE2.4	30/8/19	0.007	0.012	0.014	0.1	0.007	0.08	0.004
RBE3.4	30/8/19	0.007	0.015	0.016	0.1	0.007	0.09	0.004
Neilson Park.1	30/8/19	0.007	0.014	0.026		0.008		0.009
Neilson Park.2	30/8/19	0.007	0.015	0.024		0.008		0.01
Neilson Park.3	30/8/19	0.007	0.016	0.025	0.1	0.007	0.1	0.009
SW10.1	30/8/19	0.011	0.022	0.033	0.14	0.01	0.11	0.007
SW10.2	30/8/19	0.007	0.013	0.015	0.12	0.008	0.08	0.004
SW10.3	30/8/19	0.007	0.014	0.015	0.12	0.008	0.1	0.006
SW3.1	30/8/19	0.016	0.041	0.051	0.18	0.016	0.19	0.023
SW3.2	30/8/19	0.008	0.019	0.029	0.13	0.011	0.14	0.012
SW3.3	30/8/19	0.006	0.011	0.014	0.09	0.007	0.09	0.008
SW4.1	30/8/19	0.009	0.019	0.068	0.16	0.011	0.55	0.068
SW4.2	30/8/19	0.006	0.013	0.016	0.09	0.006	0.1	0.009
SW4.3	30/8/19	0.005	0.012	0.014	0.09	0.006	0.1	0.008
SW5.1	30/8/19	0.008	0.015	0.019	0.12	0.009	0.12	0.018
SW5.2	30/8/19	0.006	0.012	0.014	0.09	0.007	0.09	0.007
SW5.3	30/8/19	0.006	0.012	0.014	0.09	0.006	0.09	0.007
SW6.1	30/8/19	0.006	0.014	0.015	0.1	0.007	0.1	0.009
SW6.2	30/8/19	0.006	0.012	0.013	0.1	0.007	0.09	0.007
SW6.3	30/8/19	0.006	0.012	0.015	0.09	0.006	0.1	0.008
SW7.1	30/8/19	0.006	0.015	0.012	0.09	0.007	0.1	0.013
SW7.2	30/8/19	0.006	0.013	0.014	0.08	0.006	0.08	0.008
SW7.3	30/8/19	0.006	0.011	0.013	0.09	0.007	0.1	0.008
SW8.1	30/8/19	0.017	0.027	0.089		0.02		0.023
SW8.2	30/8/19	0.006	0.011	0.014	0.09	0.007	0.1	0.008
SW8.3	30/8/19	0.007	0.012	0.012	0.1	0.007	0.09	0.008
SW9.1	30/8/19	0.008	0.015	0.021	0.11	0.01	0.13	0.015
SW9.2	30/8/19	0.007	0.021	0.029	0.11	0.009	0.12	0.011
SW9.3	30/8/19	0.007	0.013	0.019	0.1	0.008	0.11	0.01
Beachwatch	3/9/19	0.008	0.021	0.27	0.41	0.009	0.42	0.013

Drain 3.0	3/9/19	0.042	0.19	2.8	3.6	0.074	3.6	0.068
Drain 4.0	3/9/19	0.004	0.023	3.7	4	0.004	4	0.011
Drain 6.0	3/9/19	0.056	0.069	2.1	2.5	0.058	2.5	0.067
Drain 8.0	3/9/19	0.08	0.11	1	1.7	0.071	1.7	0.12
RBE1.4	3/9/19	0.007	0.011	0.022	0.12	0.008	0.12	0.01
RBE2.4	3/9/19	0.006	0.01	0.022	0.11	0.008	0.12	0.01
RBE3.4	3/9/19	0.007	0.011	0.022	0.12	0.008	0.12	0.009
Neilson Park.1	3/9/19	0.006	0.012	0.023	0.13	0.009	0.09	0.004
Neilson Park.2	3/9/19	0.005	0.013	0.027	0.12	0.007	0.1	0.006
SW10.1	3/9/19	0.007	0.017	0.057	0.21	0.01	0.17	0.006
SW10.2	3/9/19	0.007	0.012	0.026	0.12	0.007	0.13	0.009
SW10.3	3/9/19	0.006	0.009	0.021	0.11	0.007	0.13	0.009
SW3.1	3/9/19	0.007	0.014	0.047	0.15	0.009	0.16	0.014
SW3.2	3/9/19	0.006	0.009	0.021	0.12	0.009	0.09	0.006
SW3.3	3/9/19	0.006	0.01	0.021	0.13	0.008	0.11	0.004
SW4.1	3/9/19	0.005	0.01	0.059	0.18	0.007	0.14	0.005
SW4.2	3/9/19	0.006	0.01	0.021	0.12	0.009	0.09	0.004
SW4.3	3/9/19	0.007	0.01	0.021	0.13	0.008	0.11	0.004
SW5.1	3/9/19	0.007	0.014	0.16	0.28	0.006	0.45	0.008
SW5.2	3/9/19	0.007	0.01	0.022	0.14	0.009	0.1	0.007
SW5.3	3/9/19	0.006	0.01	0.021	0.12	0.008	0.12	0.008
SW6.1	3/9/19	0.01	0.026	0.14	0.29	0.01	0.3	0.012
SW6.2	3/9/19	0.006	0.01	0.021	0.12	0.008	0.12	0.008
SW6.3	3/9/19	0.006	0.009	0.021	0.12	0.009	0.11	0.007
SW7.1	3/9/19	0.01	0.032	0.29	0.46	0.011	0.33	0.009
SW7.2	3/9/19	0.007	0.02	0.11	0.24	0.008	0.2	0.004
SW7.3	3/9/19	0.006	0.01	0.021	0.13	0.008	0.11	0.008
SW8.1	3/9/19	0.017	0.035	0.13	0.31	0.013	0.3	0.014
SW8.2	3/9/19	0.006	0.009	0.021	0.13	0.009	0.1	0.009
SW8.3	3/9/19	0.006	0.009	0.021	0.12	0.008	0.11	0.004
SW9.1	3/9/19	0.009	0.018	0.049	0.18	0.011	0.16	0.01
SW9.2	3/9/19	0.006	0.008	0.022	0.14	0.008	0.1	0.004
SW9.3	3/9/19	0.006	0.009	0.021	0.13	0.008	0.1	0.004

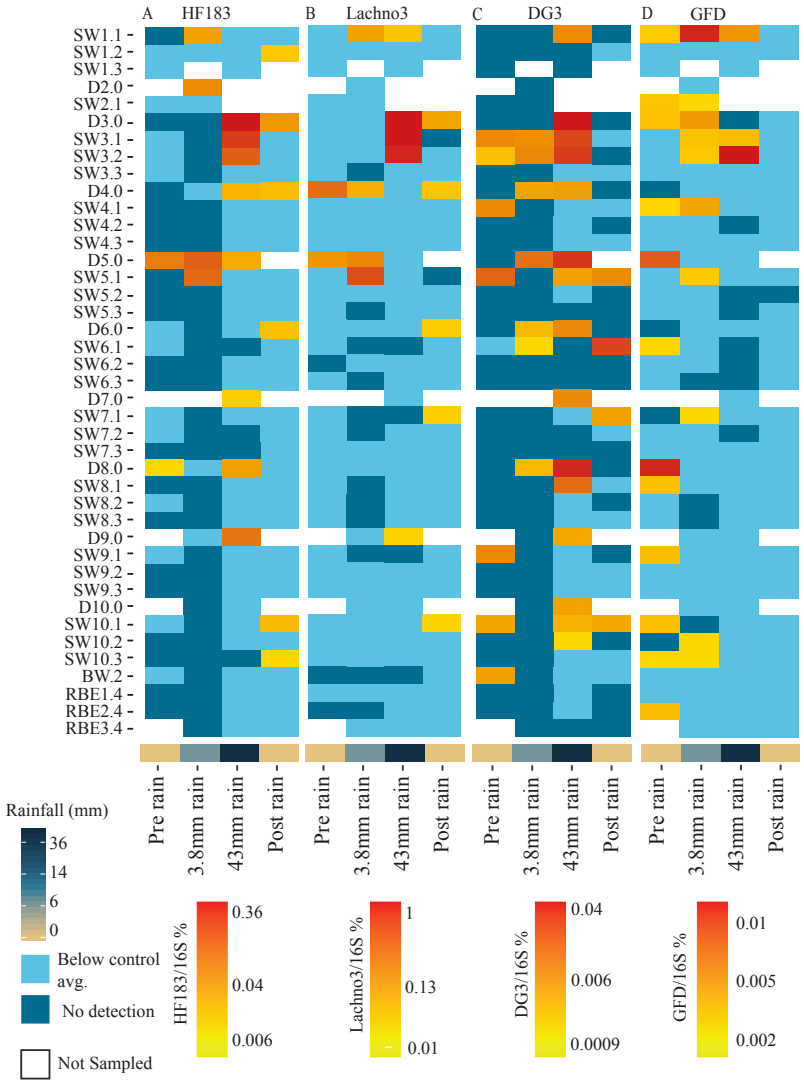

Figure 1. Source tracking qPCRs following rain events. Heatmaps of the 4 source tracking qPCRs. (A)HF183 (B) Lachno3, (C) DG3, and (D) GFD across sampling locations (Y axis) and days (x axis). Colour scale corresponds to the respective assay normalised to the 16S qPCR as a percentage, with the lower scale (Aqua) representing the average of that marker detected at the reference Nielsen Park transects, over the course of the study. Blank cells represent samples not collected either due to lack of water flow in drains or due to safety concerns during the rainfall event. Dark blue cells correspond to no detection. Below each qPCR heatmap is a small heatmap displaying daily rainfall (mm) at the time sampling.

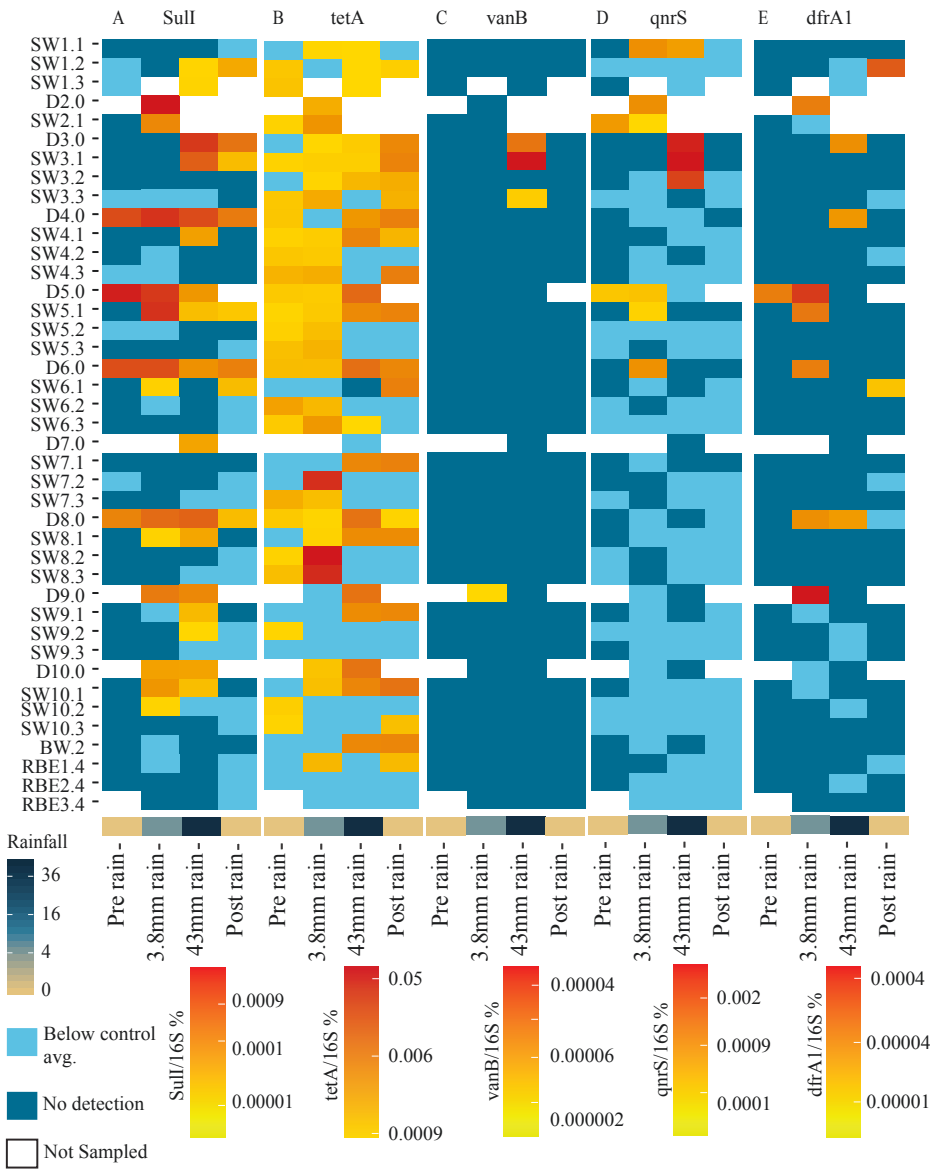

Figure 2. Antibiotic resistance gene markers. Heatmaps of the five antibiotic resistance gene qPCRs, (A) sulI, (B) tetA, (C) vanB, (D) qnrS and (E) dfrA1 across sampling locations (Y axis) and days (x axis). Colour scale corresponds to the respective assay normalised to the 16S qPCR as a percentage, with the lower scale representing the average of that marker detected at the reference Nielsen Park transects, over the course of the study. Blank cells represent samples not collected either due to lack of water flow in drains or due to safety concerns during the rainfall event. Dark blue cells correspond to no detection. Below each qPCR heatmap is a small heatmap displaying daily rainfall (mm) at the time of sampling.

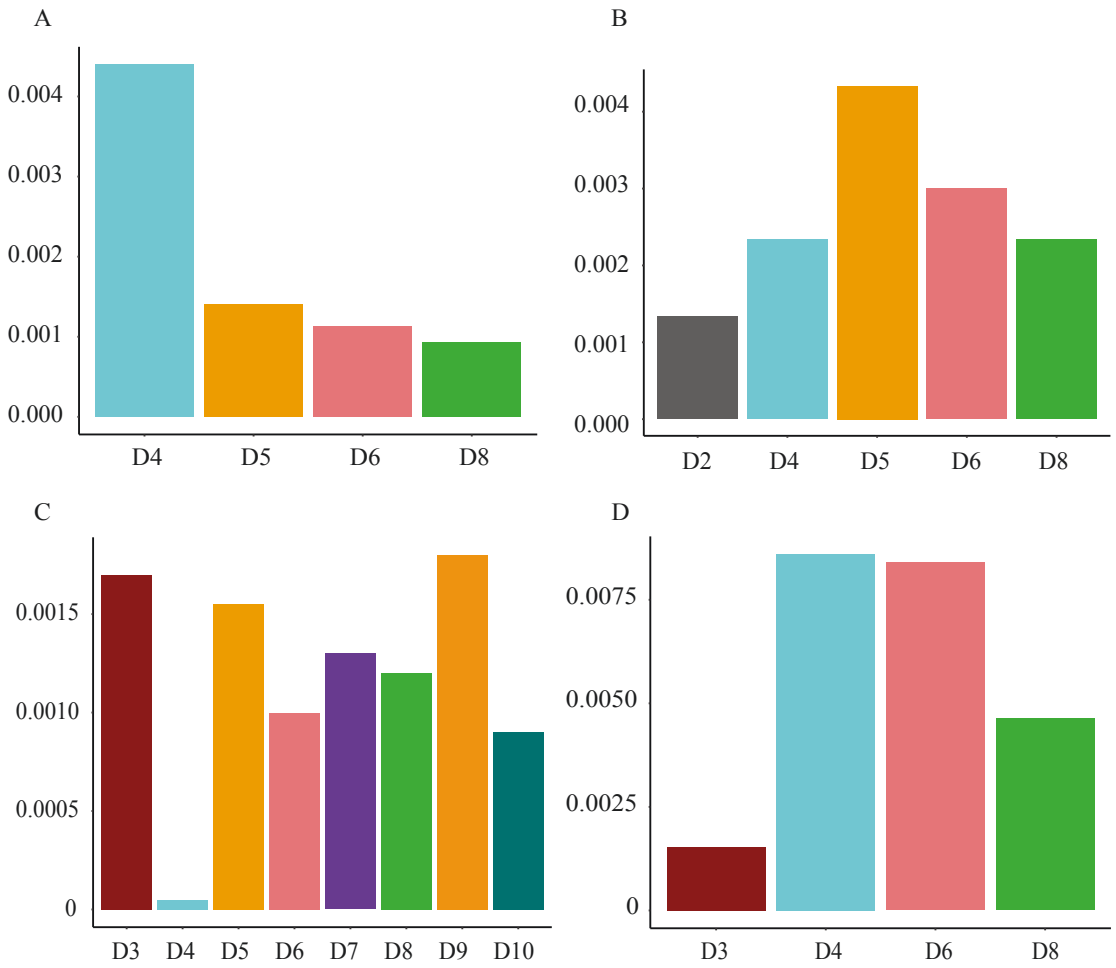

Figure 3. Drain system community signature contribute in Beachwatch reference before and after rain events. Column graphs of SourceTracker output as contribution percentage from each source drain at the Beachwatch reference site. Along the x axis is the drain number and along the y axis is the percentage that drains microbial community contributes to the microbial community at the Beachwatch site on that day. (A) Displays before the rain event, (B) Displays 3.8 mm of rainfall, (C) Displays 48mm of rainfall and (D) Displays after the rain event. Drains 2, 7, 9 and 10 did not have sufficient flow to be sampled on the 21/8/19 (pre-rain). Drain 3 (before the rain event (21/8/19) and after 3.8mm of rain (27/8/19)) and Drains 9 and 10 (after 3.8mm rain (27/9/19)) displayed evidence (visual observations of seawater entering drains along with high levels of ASVs indicative of marine bacteria [e.g., SAR11] in the 16S rRNA data) of seawater washing into them at high tide.

Appendix 3 - Rainfall leads to elevated levels of Antibiotic Resistance Genes within seawater at an Australian beach

1.0 Methods

1.1 – Chlorophyll

To quantify Chl-a concentrations, a 110ml water sample was taken at each sampling location and filtered in the field through a 0.45 µm glass fibre filter (Sartorius Glass microfibre discs FT-3-1103-047). The filter was immediately frozen and returned to the laboratory for analysis of Chl-a concentration using modified APHA Method 10200-H at the DPIE Water Studies laboratory (Eaton and Franson, 2005).

1.2 – Water nutrients

A water sample was collected from each sampling location at each time for nutrient analysis. The sample was split among three disposable syringes and one syringe was transferred directly into a clean 30ml vial for total nutrient analysis. The other two samples were passed through a 0.45mm cellulose acetate syringe filter into two additional tubes for total dissolved and inorganic nutrient analysis. All nutrient samples were kept on ice, frozen within 2 hours and analysed using standard methods; Nitrate and Nitrite (APHA 4500-NO3-I -Cadmium reduction method), Ammonium N (APHA 4500-NH3-H: Phenate method), FRP (Filterable Reactive Phosphorus) (APHA 4500-P-E-Ascobic acid method), TN (Total Nitrogen), TP (Total Phosphate), TDN (Total Dissolved Nitrogen), TDP (Total Dissolved Phosphate) (APHA 4500-P-J: Persulfate digestion method) (Eaton and Franson, 2005).

1.3 – Enterococci

Enterococci levels were quantified in all samples using Enterolert, a Defined Substrate Technology, used to test aquatic environments for faecal indicator organisms. For this analysis, 10ml water samples were diluted with 100ml of sterile deionized water (1:10 dilution) in a sterile polystyrene vessel, before powdered Enterolert reagent was added and mixed into the sample. The sample and reagents were then poured into a Quanti-Tray, a sterile panel with 51 wells containing the indicator substrate 4-methylumbelliferone-b-D-glucoside, which fluoresces when metabolized by enterococci. Quanti-Trays were then sealed and incubated for 24hrs at 41°C±0.5°C. The count of total fluorescent wells after 24hrs (using a 365-nmwavelength UV light with a 6-W bulb) was taken and then referred to a most probable number (MPN) table. The National Health and Medical Research Council Microbial

Assessment Categories (NHMRC Australia, 2008) were used to relate enterococci levels to degree of potential human health risk.

1.4 – qPCR Methods

Each qPCR assay was performed using a BIO-RAD CFX384 Touch™ Real-Time PCR Detection System™. In each case, gene copies were calculated for each target, using a (6-7 point) standard curve, along with a no template control (NTC), using BIO-RAD's CFX MAESTROTM software version 1.1. Standard curves were generated from known concentrations of a synthesised DNA fragment of each targeted gene and were included with every qPCR run. Each fragment was checked using MEGA7 to ensure they matched both primers, the probe (if applicable) and target gene and blasted in the NCBI database to ensure it was from the correct target gene and the correct length. Prior to all qPCR analyses, a dilution series using the DNA of representative drain and seawater samples was performed following by the *intI1* qPCR assay to test for the presence of PCR inhibitors, allowing for selection of the most suitable dilution factor (1:20) for all samples.

For SYBR Green based detection assays, reaction mixtures (5 µl) consisted of 2.5µl BIO-RAD iTaq UniveralSYBR® Green Supermix, 1.1 µl nuclease free water, 0.2 µl of each forward and reverse primer (10mm) and 1 µl of diluted (1:20) DNA template. The reaction mixes for probe assays consisted of 2.5 µl BIO-RAD iTaq UniversalProbes® Supermix, 1 µl nuclease free water, 0.2 µl of each forward and reverse primer (10mm), 0.1 µl of probe (10mm) and 1 µl of diluted (1:20) DNA template. For all samples, plate preparation was performed using an epMotion® 5075I Automated Liquid Handling System.

Quantitative PCR cycling conditions consisted of an initial denaturation step at 95°C for 3 minutes and then 45 cycles of: 95°C for 15 seconds and then variable annealing temperatures according to assay (Appendix 3 Table 1) for 1 minute, with the exception for intI1, sulI, qnrS and vanB which had annealing times of 30 seconds. Melt curves were included in all SYBR Green assays to confirm the amplification of a single, correctly sized product. To ensure the data quality, I calculated the coefficient of variation % of each assay, removing samples with CV below 2.5%. Limit of detection (Appendix 3 Table 1) was determined by only accepting samples from within the standard curve.

1.5 – 16S analysis

Paired R1 and R2 reads were subsequently processed using the DADA2 pipeline (Callahan et al., 2016). Reads with any 'N' bases were removed and bacterial V3-V4 primers were truncated using cutadapt (Martin, 2011). Reads were trimmed to remove low quality terminal ends (trunc (R1= 280; R2= 250)). To produce the highest number of merged reads after learning error rate and removing chimeric sequences, I used the dada2 removeBimeraDenovo program at the default threshold stringent minFoldParentOverAbundance=1. ASVs were annotated against the SILVA v138 database with a 50% probability cut-off. The ASV table was subsequently filtered to remove ASVs not assigned as kingdom Bacteria, as well as any ASVs classified as chloroplast or mitochondria. Finally, the dataset was rarefied to 30,000 reads using vegan (Dixon, 2003). Raw sequences were uploaded to NCBI, BioProject PRJNA779457. R scripts have been uploaded to (https://github.com/Nwilliams96/Terrigal_Wet_Weather_2019).

Table 1. Primers used in study.

Target	qPCR Standard	Size (BP)	Primers	Primer Sequences	qPCR Conditions	Efficiency	R^2	Quantification limit	Ref
Human *Lachnospiraceae*	G-Block synthesised from EF036467.1 by IDT	187	Lachno3F Lachno3R Lachno3P	Forward: 5' CAACGCGAAGAACCTTACCAAA 3' Reverse: 5' CCCAGAGTGCCCACCTTAAAT 3' Probe: [FAM] 5' CTCTGACCGGTCTTTAATCGGA 3' [MGB]	95°C for 3 min; 45 cycles of: 95°C for 10 sec, 64°C for 1 min	93% - 102.6%	0.997	1000 copies/100mL	(Feng et al., 2018)
Bird *Heliobacter*	G-Block synthesised from JN084061.1 by IDT	163	GFDF GFDR	Forward: 5' TCGGCTGAGCACTCTAGGG 3' Reverse: 5' GCGTCTCTTTGTACATCCCA 3'	95°C for 3 min; 45 cycles of: 95°C for 15 sec, 57°C for 1 min	95.5% - 102.5%	0.994	1000 copies/100mL	(Green et al., 2012)
Total *Arcobacter*	Plasmid insert amplified from Sydney samples	331	ARCO1 ARCO2	Forward: 5' GTCGTGCCAAGAAAAGCCA 3' Reverse: 5' TTCGCTTGCGCTGACAT 3'	95°C for 3 min; 45 cycles of: 95°C for 15 sec, 58°C for 1 min	90% - 95.9%	0.994	1000 copies/100mL	(Bastyns et al., 1995)
intI 1	Plasmid insert amplified from Sydney samples	484	int1.F int1.R	Forward: 5' GGGTCAAGGATCTGGATTTCG 3' Reverse: 5' ACATGCGTGTAAATCATCGTCG 3'	95°C for 3 min; 45 cycles of: 95°C for 15 sec 60°C for 30 sec	90% - 92%	0.995	100copies/100mL	(Mazel et al., 2000)
sul1	Plasmid insert amplified from Sydney samples	163	sulI-FW sulI-RV	Forward: 5' CGCACCGGAAACATCGCTGCAC 3' Reverse: 5' TGAAGTTCCGCCGCAAGGCTCG 3'	95°C for 3 min; 45 cycles of: 95°C for 15 sec, 65°C for 30 sec	95.6% - 102.7%	0.997	100 copies/100mL	(Pei et al., 2006)
tetA	Plasmid insert amplified from Sydney samples	96	tetA-F2-L tetA-R2	Forward: 5' CAG CCT CAA TTT CCT GAC GGG CTG A 3' Reverse: 5' GAA GCG AGC GGG TTG AGA G 3'	95°C for 3 min; 45 cycles of: 95°C for 15 sec, 58°C for 1 min	90% - 99.9%	0.993	100 copies/100mL	(Borjesson et al., 2009)
vanB	Plasmid, bacteria w/plasmid pGEM-T with vanB cloned	3300	VB-F VB-R VB-P	Forward: 5' AAT CTT AAT TGA GCA AGC GAT TTC 3' Reverse: 5' CCT GAT GGA TGC GGA AGA TA 3' Probe: [FAM] 5' CCG GAT TTG ATC CAC TTC GCC GAC AAT CA 3'	95°C for 3 min; 45 cycles of: 95°C for 15 sec, 60°C for 30 sec	92.9% - 97.8%	0.996	100 copies/100mL	(Berglund et al., 2014)
qnrS	Plasmid pGEM-T with qnrS cloned	3200	QnrS-F QnrS-R	Forward: 5' ATC AAG TGA GTA ATC GTA TGT ACT 3' Reverse: 5' CAC CTC GACTTAAGTCTGAC 3'	95°C for 3 min; 45 cycles of: 95°C for 15 sec, 72°C for 30 sec	92.9 % - 97.8%	0.996	100 copies/100mL	(Berglund et al., 2014)
dfrA	Plasmid, bacteria w/plasmid	3500	dfr1s-f dfr1s-r	Forward: 5'ATG GAG TGC CAA AGG TGA AC 3' Reverse: 5' TAT CTC CCC ACC ACC TGA AA 3'	95°C for 3 min; 45 cycles of: 95°C for 15 sec, 62°C for 1 min	88% - 102.5%	0.994	100 copies/100mL	(Grape et al., 2007)

Table 2. qPCR and *Enterococci* correlations over the course of the study period.

P-Value (Bonferroni Corrected, permutations) - Spearman's rs									
	Enterococci	Lachno3	IntI	Acro	Sul1	tetA	dfrA	VanB	qnrS
Enterococci		0.9108	0.0036	0.0036	1	0.0036	0.0036	1	1
Lachno3	0.9108		0.0036	0.0036	0.0036	0.0036	0.2304	1	1
IntI	0.0036	0.0036		0.0036	0.0036	0.0036	0.1656	1	1
Acro	0.0036	0.0036	0.0036		0.0036	0.0036	0.0756	1	0.0072
Sul1	1	0.0036	0.0036	0.0036		1	0.0324	1	1
tetA	0.0036	0.0036	0.0036	0.0036	1		1	1	1
dfrA	0.0036	0.2304	0.1656	0.0756	0.0324	1		1	1
VanB	1	1	1	1	1	1	1		1
qnrS	1	1	1	0.0072	1	1	1	1	
R value - Spearman's rs									
	Enterococci	Lachno3	IntI	Acro	Sul1	tetA	dfrA	VanB	qnrS
Enterococci		0.17723	0.28015	0.33253	0.14837	0.32089	0.36709	0	-0.0720
Lachno3	0.17723		0.61965	0.59417	0.3178	0.32788	0.21138	0	0.10545
IntI	0.28015	0.61965		0.66043	0.37286	0.48214	0.22143	0	0.10658
Acro	0.33253	0.59417	0.66043		0.41783	0.45004	0.23923	0	0.28113
Sul1	0.14837	0.3178	0.37286	0.41783		0.10598	0.26802	0	0.11845
tetA	0.32089	0.32788	0.48214	0.45004	0.10598		0.14352	0	-0.0846
dfrA	0.36709	0.21138	0.22143	0.23923	0.26802	0.14352		0	-0.1522
VanB	0	0	0	0	0	0	0		0
qnrS	-0.072089	0.10545	0.10658	0.28113	0.11845	-0.0846	-0.1522	0	

Table 3. Abiotic data taken over the course of the experiment. Blank spaces indicate data which either could not be taken due to technical issues, or which could not be taken due to weather conditions.

Site	Time	Date	Temp °C	SAL ppt	NH4-N (mg/L)	TDP (mg/L)	TDN (mg/L)	TN (mg/L)	TP (mg/L)	Chl a
SW0.1	am	20/5/19	14.10		0.01	0.00	0.11	0.12	0.01	1.01
SW0.2	am	20/5/19	21.28	33.66	0.01	0.01	0.12	0.13	0.01	0.95
SW0.3	am	20/5/19	21.24	35.61	0.01	0.00	0.09	0.09	0.01	1.22
SW1.1	am	20/5/19	20.30		0.02	0.01	0.13	0.14	0.01	3.14
SW1.2	am	20/5/19	21.08	37.51	0.02	0.01	0.13	0.13	0.01	0.81
SW1.3	am	20/5/19	21.17	35.36	0.01	0.00	0.10	0.11	0.01	1.47
SW2.1	am	20/5/19	20.65		0.02	0.00	0.13	0.14	0.01	0.71
SW2.2	am	20/5/19	20.95	36.94	0.01	0.01	0.11	0.12	0.01	0.96
SW2.3	am	20/5/19	21.00	35.08	0.01	0.00	0.10	0.12	0.02	1.03
SW4.1	am	20/5/19	20.60		0.01	0.00	0.11	0.12	0.00	0.66
SW4.2	am	20/5/19	20.85	35.80	0.01	0.01	0.10	0.18	0.06	1.01
SW4.3	am	20/5/19	21.09	34.45	0.01	0.00	0.10	0.10	0.00	0.94
SW5.1	am	20/5/19	20.30		0.02	0.00	0.12	0.12	0.00	1.31
SW5.2	am	20/5/19	21.14	35.15	0.01	0.00	0.09	0.10	0.01	1.11
SW5.3	am	20/5/19	21.22	35.54	0.01	0.00	0.10	0.11	0.01	1.25
SW6.1	am	20/5/19	20.70		0.01	0.00	0.12	0.11	0.00	0.79
SW6.2	am	20/5/19	21.33	34.64	0.01	0.00	0.09	0.10	0.01	0.88
SW6.3	am	20/5/19	21.27	35.26	0.01	0.00	0.09	0.11	0.01	0.83
SW7.1	am	20/5/19	21.25		0.01	0.00	0.08	0.10	0.01	1.11
SW7.2	am	20/5/19	21.31	34.26	0.01	0.01	0.11	0.11	0.01	1.45
SW7.3	am	20/5/19	21.30	35.15	0.01	0.00	0.09	0.10	0.01	1.47
SW8.1	am	20/5/19	21.30		0.01	0.00	0.10	0.12	0.01	1.30
SW8.2	am	20/5/19	21.35	33.48	0.01	0.00	0.09	0.10	0.01	1.21
SW8.3	am	20/5/19	21.30	34.74	0.01	0.00	0.09	0.11	0.01	1.69
SW9.1	am	20/5/19	21.10		0.01	0.01	0.14	0.14	0.01	0.72
SW9.2	am	20/5/19	21.19	34.65	0.01	0.01	0.10	0.11	0.01	0.67
SW9.3	am	20/5/19	21.22	35.34	0.01	0.00	0.11	0.12	0.01	2.56
TL1	am	20/5/19	20.49	23.34	0.03	0.00	0.33	0.42	0.02	3.38
TL2	am	20/5/19	20.09	22.89	0.02	0.00	0.29	0.45	0.02	3.03
TL3	am	20/5/19	19.90	23.09	0.03	0.00	0.29	0.35	0.01	2.95
TL4	am	20/5/19	21.23	21.83	0.03	0.01	0.32	0.52	0.04	5.07
TL5	am	20/5/19	19.56	23.07	0.02	0.01	0.27	0.32	0.01	2.19
SW0.1	am	31/5/19	17.66	33.74	0.01	0.01	0.13	0.14	0.01	2.43
SW0.2	am	31/5/19	19.40	35.69	0.01	0.01	0.12	0.15	0.01	1.69

SW0.3	am	31/5/19	19.46	35.54	0.01	0.01	0.12	0.13	0.01	1.49
SW1.1	am	31/5/19	18.21	33.88	0.04	0.03	0.27	1.43	0.16	2.41
SW1.2	am	31/5/19	19.07	35.64	0.01	0.01	0.15	0.16	0.01	1.05
SW1.3	am	31/5/19	19.05	35.69	0.01	0.01	0.12	0.13	0.01	1.54
SW2.1	am	31/5/19			0.01	0.01	0.17	0.18	0.01	0.81
SW2.2	am	31/5/19	19.26	35.77	0.01	0.01	0.13	0.13	0.01	1.00
SW2.3	am	31/5/19	19.00	35.45	0.01	0.01	0.12	0.14	0.01	1.59
SW4.1	am	31/5/19	18.25	35.14	0.01	0.01	0.12	0.13	0.01	0.76
SW4.2	am	31/5/19	19.23	35.61	0.01	0.01	0.12	0.13	0.01	
SW4.3	am	31/5/19	18.95	35.46	0.01	0.01	0.12	0.17	0.01	1.40
SW5.1	am	31/5/19	18.08	35.18	0.01	0.01	0.14	0.15	0.01	0.96
SW5.2	am	31/5/19	19.00	35.56	0.01	0.01	0.13	0.13	0.01	1.33
SW5.3	am	31/5/19	19.08	35.60	0.01	0.01	0.11	0.12	0.01	1.45
SW6.1	am	31/5/19	18.69	34.64	0.00	0.01	0.11	0.13	0.01	0.94
SW6.2	am	31/5/19	19.10	35.66	0.01	0.01	0.11	0.12	0.01	1.31
SW6.3	am	31/5/19	19.11	35.70	0.01	0.01	0.11	0.11	0.01	1.29
SW7.1	am	31/5/19	18.97	11.71	0.01	0.01	0.12	0.12	0.01	1.38
SW7.2	am	31/5/19	19.27	35.56	0.01	0.01	0.11	0.14	0.01	1.47
SW7.3	am	31/5/19	19.28	35.71	0.01	0.01	0.11	0.12	0.01	1.47
SW8.1	am	31/5/19	19.07	19.90	0.01	0.01	0.12	0.14	0.01	1.67
SW8.2	am	31/5/19	19.30	35.48	0.00	0.01	0.10	0.12	0.01	1.61
SW8.3	am	31/5/19	19.30	35.72	0.01	0.01	0.12	0.12	0.01	1.52
SW9.1	am	31/5/19	18.80	23.24	0.01	0.01	0.13	0.14	0.01	0.89
SW9.2	am	31/5/19								
SW9.3	am	31/5/19	19.36	35.86	0.00	0.01	0.12	0.17	0.01	1.01
TL1	am	31/5/19	11.18	23.49	0.02	0.01	0.39	0.38	0.01	1.51
TL2	am	31/5/19	13.53	23.40	0.02	0.01	0.30	0.31	0.01	2.03
TL3	am	31/5/19	13.41	23.08	0.02	0.02	0.29	0.30	0.01	1.64
TL4	am	31/5/19	12.91	20.31	0.01	0.01	0.31	0.35	0.01	3.68
TL5	am	31/5/19	12.53	22.76	0.02	0.00	0.29	0.31	0.01	1.14
SW0.1	am	4/6/19	19.38	33.38	0.02	0.02	0.16	0.31	0.03	4.61
SW0.2	am	4/6/19								
SW0.3	am	4/6/19								
SW1.1	am	4/6/19	18.00	32.57	0.03	0.01	0.16	0.48	0.04	6.00
SW1.2	am	4/6/19								
SW1.3	am	4/6/19								
SW2.1	am	4/6/19	19.01	33.68	0.01	0.01	0.10	0.11	0.01	1.03
SW2.2	am	4/6/19								
SW2.3	am	4/6/19								
SW4.1	am	4/6/19	15.74	16.78	0.03	0.03	0.27	0.28	0.03	0.94
SW4.2	am	4/6/19								

SW4.3	am	4/6/19								
SW5.1	am	4/6/19	19.76	34.74	0.01	0.01	0.16	0.16	0.01	1.24
SW5.2	am	4/6/19								
SW5.3	am	4/6/19								
SW6.1	am	4/6/19	17.69	35.62	0.01	0.01	0.11	0.14	0.01	0.91
SW6.2	am	4/6/19								
SW6.3	am	4/6/19								
SW7.1	am	4/6/19	19.72	35.07	0.01	0.01	0.10	0.14	0.01	2.94
SW7.2	am	4/6/19								
SW7.3	am	4/6/19								
SW8.1	am	4/6/19	19.26	34.76	0.01	0.01	0.14	0.14	0.01	1.69
SW8.2	am	4/6/19								
SW8.3	am	4/6/19								
SW9.1	am	4/6/19	19.15	34.54	0.01	0.01	0.17	0.25	0.03	3.71
SW9.2	am	4/6/19								
SW9.3	am	4/6/19								
TL1	am	4/6/19	11.21	16.97	0.04	0.01	0.27	0.38	0.02	2.51
TL2	am	4/6/19	11.83	16.99	0.03	0.01	0.31	0.43	0.03	5.95
TL3	am	4/6/19	12.36	20.01	0.02	0.00	0.25	0.29	0.01	4.47
TL4	am	4/6/19	11.12	11.68	0.03	0.02	0.30	0.38	0.04	3.00
TL5	am	4/6/19	11.84	19.33	0.02	0.01	0.27	0.31	0.02	3.04
SW0.1	am	6/6/19			0.01	0.01	0.10	0.12	0.01	0.52
SW0.2	am	6/6/19								
SW0.3	am	6/6/19	19.75	35.65	0.01	0.01	0.09	0.11	0.01	0.72
SW1.1	am	6/6/19	19.20		0.01	0.01	0.11	0.13	0.01	0.69
SW1.2	am	6/6/19	19.80	35.43	0.02	0.01	0.11	0.12	0.01	0.64
SW1.3	am	6/6/19	19.81	35.57	0.01	0.01	0.11	0.10	0.01	0.58
SW2.1	am	6/6/19	19.10		0.02	0.01	0.12	0.14	0.01	0.76
SW2.2	am	6/6/19	19.83	35.68	0.02	0.01	0.11	0.13	0.01	0.65
SW2.3	am	6/6/19	19.81	35.39	0.01	0.01	0.10	0.10	0.01	0.54
SW4.1	am	6/6/19	19.10		0.02	0.01	0.12	0.14	0.01	0.65
SW4.2	am	6/6/19	19.83	35.48	0.01	0.01	0.10	0.11	0.01	0.54
SW4.3	am	6/6/19	19.75	35.48	0.01	0.01	0.12	0.10	0.01	0.44
SW5.1	am	6/6/19	19.20		0.02	0.01	0.14	0.13	0.01	0.56
SW5.2	am	6/6/19	19.85	35.46	0.01	0.01	0.17	0.11	0.01	0.61
SW5.3	am	6/6/19	19.78	35.49	0.01	0.01	0.10	0.10	0.01	0.48
SW6.1	am	6/6/19	18.80		0.02	0.01	0.13	0.13	0.01	0.63
SW6.2	am	6/6/19	19.64	35.45	0.01	0.01	0.19	0.11	0.01	0.65
SW6.3	am	6/6/19	19.80	35.56	0.01	0.01	0.10	0.10	0.01	0.54
SW7.1	am	6/6/19	19.50		0.01	0.01	0.11	0.14	0.01	0.60
SW7.2	am	6/6/19	19.80	33.79	0.01	0.01	0.10	0.10	0.01	0.52

SW7.3	am	6/6/19	19.86	35.56	0.01	0.00	0.10	0.11	0.01	0.53
SW8.1	am	6/6/19	19.40		0.01	0.01	0.11	0.12	0.01	0.80
SW8.2	am	6/6/19								
SW8.3	am	6/6/19	20.19	35.58	0.01	0.01	0.15	0.08	0.01	0.51
SW9.1	am	6/6/19	18.80		0.01	0.01	0.13	0.12	0.01	0.40
SW9.2	am	6/6/19								
SW9.3	am	6/6/19	19.99	35.62	0.01	0.01	0.10	0.09	0.01	0.45
TL1	am	6/6/19	10.69	13.29	0.01	0.01	0.36	0.42	0.02	1.78
TL2	am	6/6/19	9.93	11.90	0.02	0.02	0.57	0.61	0.03	0.56
TL3	am	6/6/19	10.28	12.23	0.01	0.01	0.39	0.48	0.02	0.96
TL4	am	6/6/19	9.97	13.27	0.00	0.00	0.39	0.43	0.02	3.29
TL5	am	6/6/19	9.92	13.24	0.01	0.01	0.44	0.40	0.02	0.78
Drain 2	am	6/6/19	14.90							
Drain 4	am	6/6/19	13.80							
SW0.1	pm	6/6/19			0.01	0.01	0.11	0.18	0.01	
SW0.2	pm	6/6/19								
SW0.3	pm	6/6/19								
SW1.1	pm	6/6/19	19.75		0.02	0.01	0.12	0.25	0.02	
SW1.2	pm	6/6/19								
SW1.3	pm	6/6/19								
SW2.1	pm	6/6/19	19.80		0.03	0.01	0.20	0.14	0.01	
SW2.2	pm	6/6/19	19.95	35.74	0.02	0.01	0.11	0.11	0.01	0.58
SW2.3	pm	6/6/19	17.23	14.05	0.02	0.01	0.10	0.14	0.01	0.51
SW4.1	pm	6/6/19	19.67		0.02	0.01	0.11	0.15	0.01	
SW4.2	pm	6/6/19								
SW4.3	pm	6/6/19								
SW5.1	pm	6/6/19	19.90		0.02	0.01	0.20	0.44	0.02	
SW5.2	pm	6/6/19	19.91	35.77	0.02	0.01	0.11	0.11	0.01	0.52
SW5.3	pm	6/6/19	19.84	34.24	0.02	0.01	0.11	0.12	0.01	
SW6.1	pm	6/6/19			0.01	0.01	0.36	0.15	0.01	
SW6.2	pm	6/6/19	19.82	35.48	0.02	0.01	0.13	0.15	0.01	0.62
SW6.3	pm	6/6/19	19.84	34.28	0.03	0.01	0.11	0.13	0.01	0.54
SW7.1	pm	6/6/19	19.95		0.01	0.01	0.13	0.16	0.01	
SW7.2	pm	6/6/19	19.92	35.54	0.03	0.01	0.11	0.12	0.01	0.68
SW7.3	pm	6/6/19	19.97	35.73	0.04	0.01	0.11	0.11	0.01	0.60
SW8.1	pm	6/6/19	20.17		0.02	0.01	0.16	0.15	0.01	
SW8.2	pm	6/6/19								
SW8.3	pm	6/6/19								
SW9.1	pm	6/6/19	20.40		0.02	0.01	0.12	0.12	0.01	
SW9.2	pm	6/6/19								
SW9.3	pm	6/6/19								

TL1	pm	6/6/19								
TL2	pm	6/6/19								
TL3	pm	6/6/19								
TL4	pm	6/6/19								
TL5	pm	6/6/19								
SW0.1	am	11/6/19	20.39	34.66	0.12	0.04	0.39	0.39	0.03	0.89
SW0.2	am	11/6/19	20.29	35.51	0.01	0.01	0.13	0.10	0.01	1.01
SW0.3	am	11/6/19	20.32	35.52	0.01	0.01	0.11	0.12	0.01	0.71
SW1.1	am	11/6/19	19.20		0.04	0.01	0.17	0.96	0.07	5.16
SW1.2	am	11/6/19	20.27	35.52	0.01	0.01	0.10	0.11	0.01	0.87
SW1.3	am	11/6/19	20.28	35.71	0.01	0.00	0.10	0.11	0.01	0.79
SW2.1	am	11/6/19	19.30		0.03	0.01	0.15	0.25	0.02	0.96
SW2.2	am	11/6/19	20.26	35.64	0.01	0.01	0.13	0.10	0.01	0.88
SW2.3	am	11/6/19	20.11	35.56	0.01	0.01	0.13	0.13	0.01	0.86
SW4.1	am	11/6/19	18.73		0.02	0.01	0.22	0.19	0.01	0.43
SW4.2	am	11/6/19	19.95	35.52	0.01	0.01	0.14	0.14	0.01	0.82
SW4.3	am	11/6/19	20.15	35.76	0.01	0.01	0.17	0.13	0.01	0.75
SW5.1	am	11/6/19	19.63		0.01	0.01	0.33	0.29	0.01	0.75
SW5.2	am	11/6/19	20.16	35.60	0.01	0.01	0.11	0.14	0.01	0.86
SW5.3	am	11/6/19	20.17	35.60	0.01	0.00	0.13	0.13	0.01	0.93
SW6.1	am	11/6/19	20.27	35.16	0.01	0.01	0.14	0.14	0.01	0.80
SW6.2	am	11/6/19	20.14	35.61	0.01	0.01	0.12	0.11	0.01	0.89
SW6.3	am	11/6/19	20.15	35.71	0.01	0.01	0.14	0.11	0.01	0.71
SW7.1	am	11/6/19	21.28	35.24	0.01	0.01	0.15	0.13	0.01	0.59
SW7.2	am	11/6/19	20.24	35.57	0.01	0.01	0.10	0.12	0.01	1.00
SW7.3	am	11/6/19	20.26	35.81	0.01	0.01	0.11	0.11	0.01	0.94
SW8.1	am	11/6/19	20.49	34.51	0.01	0.01	0.12	0.17	0.01	1.04
SW8.2	am	11/6/19	20.18	35.66	0.01	0.01	0.10	0.10	0.01	0.98
SW8.3	am	11/6/19	20.23	35.75	0.01	0.01	0.11	0.10	0.01	0.87
SW9.1	am	11/6/19	19.75	34.82	0.01	0.01	0.16	0.16	0.01	0.43
SW9.2	am	11/6/19	20.10	35.63	0.01	0.01	0.13	0.14	0.01	0.41
SW9.3	am	11/6/19	20.29	34.85	0.01	0.01	0.11	0.13	0.01	0.82
TL1	am	11/6/19	19.50	28.32	0.09	0.00	0.33	0.40	0.01	1.24
TL2	am	11/6/19	17.98	32.08	0.10	0.01	0.29	0.33	0.01	2.30
TL3	am	11/6/19	19.80	33.17	0.07	0.01	0.22	0.28	0.02	0.90
TL4	am	11/6/19	19.64	33.62	0.08	0.01	0.25	0.29	0.02	3.74
TL5	am	11/6/19	18.48	33.48	0.06	0.01	0.24	0.27	0.01	1.02

Table 4. *Enterococci* data taken over the course of the experiment. Blank spaces indicate data which could not be taken due to weather conditions.

Site	20/5/19	31/5/19	4/6/19	06/06/19 AM	06/06/19 PM	11/06/19
SW0.1		<10		10	10	<10
SW0.2	<10	<10				<10
SW0.3	<10	<10		<10		<10
SW1.1		30.6		10	<10	10
SW1.2	<10	<10		<10		<10
SW1.3	<10	<10		10		<10
SW2.1		<10	9803.9	51.2	20.2	<10
SW2.2	<10	<10		10	10	<10
SW2.3	<10	<10		9.9	<10	10
SW4.1		<10	17328.9	<10	10	10
SW4.2	<10	10		<10		<10
SW4.3	<10	<10		10		
SW5.1		<10	1726	10	<10	<10
SW5.2	<10	<10		<10	<10	10
SW5.3	<10	<10		10	10	<10
SW6.1		<10	427.5	<10	262.1	<10
SW6.2	<10	<10		<10	41.3	<10
SW6.3	<10	<10		<10	10	<10
SW7.1	<10	<10		<10		<10
SW7.2	<10	<10		10	20.2	<10
SW7.3	<10	<10		10	10	<10
SW8.1	<10	<10		10		<10
SW8.2	<10	<10				<10
SW8.3	<10	<10		<10		<10
SW9.1		<10	1515.2	<10		10
SW9.2	<10					<10
SW9.3	<10	<10		<10		<10
Drain 1			>24196			
Drain 2			>24196	626.3	880.3	
Drain 4			>24196			
Lagoon 1	<10	<10		4611.1		119.9
Lagoon 2	20.1	<10		10462.4		40.9
Lagoon 3	20.1	<10		2841.4		<10

Lagoon 4	62.6	10		657.5		<10
Lagoon 5	20.2	30.4	2809.2	6488.2	669.5	41.3

Table 5. qPCR data in copies/100mL

Date	Site	Lachno3	*intI-1*	Acro	GFD	*sul1*	*tetA*	*dfrA*	*qnrS*
20/5/19	L.1.4	0.00E+00	4.70E+02	1.41E+05	42280	0.00E+00	5.10E+05	0.00E+00	8.26E+03
20/5/19	L.2.4	2.29E+03	0.00E+00	0.00E+00	69219	1.96E+03	1.52E+05	0.00E+00	3.67E+03
20/5/19	L.3.4	0.00E+00	1.10E+03	0.00E+00	16812	2.41E+03	2.09E+05	0.00E+00	4.71E+03
20/5/19	L.4.4	0.00E+00	1.06E+03	9.20E+05	69575	0.00E+00	3.75E+05	0.00E+00	0.00E+00
20/5/19	L.5.4	0.00E+00	1.11E+03	1.63E+06	146704	1.88E+03	1.99E+05	2.91E+04	0.00E+00
20/5/19	SW.0.1	0.00E+00	1.08E+02	1.77E+04	22457	0.00E+00	8.01E+04	0.00E+00	8.95E+03
20/5/19	SW.0.2	0.00E+00	1.75E+02	3.21E+04	31713	8.78E+02	4.43E+04	0.00E+00	3.98E+02
20/5/19	SW.0.3	0.00E+00	2.18E+02	2.51E+04	41512	0.00E+00	4.99E+04	0.00E+00	0.00E+00
20/5/19	SW.1.1	0.00E+00	1.97E+03	8.94E+04	21643	5.49E+03	6.39E+04	5.93E+05	3.08E+04
20/5/19	SW.1.1	0.00E+00	3.13E+02	9.56E+04	10793	6.22E+02	4.00E+04	0.00E+00	5.69E+04
20/5/19	SW.1.3	2.05E+03	2.49E+02	5.23E+04	70413	1.18E+03	6.33E+04	0.00E+00	4.12E+04
20/5/19	SW.2.1	0.00E+00	2.21E+02	1.24E+05	53237	1.02E+03	4.31E+04	0.00E+00	3.50E+04
20/5/19	SW.2.2	1.73E+03	5.90E+02	7.62E+04	78290	0.00E+00	3.13E+04	0.00E+00	2.28E+04
20/5/19	SW.2.3	0.00E+00	7.02E+01	3.26E+04	44301	0.00E+00	3.17E+04	0.00E+00	2.69E+02
20/5/19	SW.4.1	3.52E+03	2.63E+03	1.52E+05	21217	0.00E+00	3.66E+04	0.00E+00	6.07E+04
20/5/19	SW.4.2	7.18E+03	3.94E+02	6.51E+04	43358	0.00E+00	4.92E+04	0.00E+00	1.36E+04
20/5/19	SW.4.3	0.00E+00	1.51E+02	0.00E+00	17120	0.00E+00	5.48E+04	0.00E+00	2.62E+04
20/5/19	SW.5.1	7.80E+03	9.30E+02	2.87E+04	30847	7.60E+02	1.08E+05	0.00E+00	8.43E+03
20/5/19	SW.5.2	1.60E+04	2.31E+02	1.55E+04	19179	0.00E+00	1.62E+05	0.00E+00	2.16E+04
20/5/19	SW.5.3	0.00E+00	8.47E+02	0.00E+00	31974	0.00E+00	6.12E+04	0.00E+00	1.31E+04
20/5/19	SW.6.1	5.17E+03	7.60E+01	3.50E+04	82927	0.00E+00	1.05E+05	0.00E+00	0.00E+00
20/5/19	SW.6.2	0.00E+00	3.02E+01	2.11E+04	91650	0.00E+00	6.02E+04	0.00E+00	1.10E+04
20/5/19	SW.6.3	0.00E+00	2.38E+02	1.58E+04	40045	0.00E+00	6.37E+04	0.00E+00	1.02E+04
20/5/19	SW.7.1	0.00E+00	5.58E+02	1.55E+04	16626	0.00E+00	8.67E+04	0.00E+00	1.51E+04
20/5/19	SW.7.2	0.00E+00	2.98E+02	2.53E+04	33650	0.00E+00	5.15E+04	0.00E+00	8.41E+03
20/5/19	SW.7.3	0.00E+00	3.13E+02	2.36E+04	34388	0.00E+00	5.60E+04	0.00E+00	5.53E+03
20/5/19	SW.8.1	0.00E+00	1.38E+02	9.03E+03	52564	0.00E+00	8.20E+04	0.00E+00	2.65E+04
20/5/19	SW.8.2	0.00E+00	9.58E+01	1.64E+04	2445	0.00E+00	5.99E+04	0.00E+00	1.33E+04
20/5/19	SW.8.3	0.00E+00	4.74E+01	1.30E+04	6396	0.00E+00	5.32E+04	0.00E+00	3.83E+03
20/5/19	SW.9.1	0.00E+00	6.30E+02	1.58E+05	7351	3.77E+03	1.01E+05	0.00E+00	2.66E+04
20/5/19	SW.9.2	0.00E+00	6.29E+02	1.44E+05	0	0.00E+00	3.53E+04	0.00E+00	2.92E+04
20/5/19	SW.9.3	0.00E+00	3.82E+02	2.46E+04	1235	0.00E+00	5.28E+04	0.00E+00	1.06E+04
31/5/19	L.1.4	0.00E+00	1.42E+02	3.41E+05	47581	0.00E+00	4.98E+05	0.00E+00	0.00E+00
31/5/19	L.2.4	0.00E+00	8.90E+01	7.38E+05	4945	1.28E+03	3.12E+05	0.00E+00	3.64E+03
31/5/19	L.3.4	0.00E+00	1.56E+01	4.37E+05	1645	0.00E+00	0.00E+00	0.00E+00	0.00E+00
31/5/19	L.4.4	0.00E+00	4.18E+02	2.79E+05	3062	0.00E+00	3.27E+05	0.00E+00	0.00E+00
31/5/19	L.5.4	0.00E+00	6.33E+01	1.98E+05	10027	0.00E+00	1.25E+05	0.00E+00	0.00E+00
31/5/19	SW.0.1	0.00E+00	0.00E+00	6.07E+03	8810	4.15E+03	2.00E+05	0.00E+00	1.92E+04

31/5/19	SW.0.2	5.51E+01	1.08E+01	1.97E+04	4214	0.00E+00	2.18E+04	1.25E+03	0.00E+00
31/5/19	SW.0.3	1.73E+02	2.88E+01	2.34E+04	2166	6.16E+02	1.76E+04	6.99E+02	0.00E+00
31/5/19	SW.1.1	0.00E+00	3.30E+01	9.96E+03	2735	1.23E+03	3.82E+04	0.00E+00	3.93E+04
31/5/19	SW.1.1	0.00E+00	4.58E+01	2.42E+05	7577	0.00E+00	2.91E+04	4.71E+02	1.20E+05
31/5/19	SW.1.3	0.00E+00	3.57E+00	8.59E+03	5087	6.14E+02	1.91E+04	0.00E+00	4.46E+03
31/5/19	SW.2.1	4.76E+02	9.64E+01	7.32E+04	6120	0.00E+00		0.00E+00	5.91E+04
31/5/19	SW.2.2	5.87E+01	4.18E+01	2.54E+05	1600	0.00E+00	2.29E+04	1.85E+03	1.27E+05
31/5/19	SW.2.3	0.00E+00	0.00E+00	1.76E+04	4022	0.00E+00	0.00E+00	0.00E+00	4.42E+03
31/5/19	SW.4.1	6.75E+01	2.28E+02	7.52E+05	1666	1.72E+03	0.00E+00	0.00E+00	2.75E+05
31/5/19	SW.4.2	0.00E+00	4.29E+00	3.68E+04	438	0.00E+00	3.21E+04	2.79E+04	7.37E+04
31/5/19	SW.4.3	0.00E+00	4.90E+00	4.78E+04	2142	0.00E+00	5.37E+04	0.00E+00	2.36E+04
31/5/19	SW.5.1	0.00E+00	1.44E+02	7.90E+04	2381	1.20E+03	0.00E+00	1.03E+05	3.04E+04
31/5/19	SW.5.2	0.00E+00	4.87E+00	1.16E+05	1418	0.00E+00	2.54E+04	0.00E+00	1.84E+04
31/5/19	SW.5.3	0.00E+00	1.56E+01	1.16E+04	11522	0.00E+00	4.04E+04	4.29E+03	1.07E+04
31/5/19	SW.6.1	0.00E+00	2.30E+01	8.31E+03	6236	0.00E+00	6.61E+04	4.09E+03	2.88E+03
31/5/19	SW.6.2	0.00E+00	0.00E+00	3.98E+03	4714	0.00E+00	4.96E+04	0.00E+00	4.31E+03
31/5/19	SW.6.3	0.00E+00	0.00E+00	7.59E+03	1761	0.00E+00	4.40E+04	5.32E+03	2.05E+03
31/5/19	SW.7.1	0.00E+00		1.15E+04	2335	0.00E+00	3.74E+04	0.00E+00	6.26E+03
31/5/19	SW.7.2	0.00E+00	2.32E+01	3.16E+03	777	0.00E+00	3.80E+04	0.00E+00	7.11E+03
31/5/19	SW.7.3	0.00E+00	6.25E+00	1.82E+04	27052	0.00E+00	4.19E+04	7.17E+02	1.04E+04
31/5/19	SW.8.1	0.00E+00	7.59E+01	1.39E+04	31930	1.16E+03	4.89E+04	0.00E+00	2.27E+04
31/5/19	SW.8.2	0.00E+00	0.00E+00	1.10E+04	6887	0.00E+00	6.73E+04	2.15E+03	0.00E+00
31/5/19	SW.8.3	0.00E+00	0.00E+00	6.24E+03	3952	7.71E+02	4.28E+04	0.00E+00	4.53E+03
31/5/19	SW.9.1	0.00E+00	0.00E+00	3.52E+05	69992	0.00E+00	9.58E+04	4.87E+03	4.09E+04
31/5/19	SW.9.3	0.00E+00	6.02E+00	1.80E+04	6266	0.00E+00	6.79E+04	0.00E+00	0.00E+00
4/6/19	D.1.0	3.97E+05	1.46E+04	1.01E+06	9261	1.25E+05	1.36E+06	0.00E+00	0.00E+00
4/6/19	D.2.0	4.04E+04	3.10E+04	2.08E+07	0	1.42E+05	0.00E+00	2.31E+08	6.90E+03
4/6/19	D.4.0	5.15E+05	5.25E+05	1.90E+07	47929	1.09E+06	1.16E+06	1.49E+08	4.49E+05
4/6/19	L.1.4	2.34E+04	6.90E+03	4.76E+06	12964	3.74E+04		0.00E+00	2.52E+04
4/6/19	L.2.4	5.07E+04	0.00E+00	1.07E+05	0	5.89E+04	0.00E+00	0.00E+00	2.26E+04
4/6/19	L.3.4	2.34E+04	4.02E+03	1.90E+05	48751	3.05E+04	7.34E+04	0.00E+00	0.00E+00
4/6/19	L.4.4	1.17E+05	2.98E+04	3.01E+06	32295	7.87E+04	0.00E+00	0.00E+00	0.00E+00
4/6/19	L.5.4	3.47E+04	1.44E+04	1.40E+06	63525	0.00E+00	0.00E+00	1.55E+07	2.14E+05
4/6/19	SW.0.1	0.00E+00	0.00E+00	9.21E+05	1024021	7.20E+04	0.00E+00	0.00E+00	4.02E+05
4/6/19	SW.1.1	2.57E+04	6.06E+03	1.47E+06	18702	2.66E+04	4.16E+04	0.00E+00	1.27E+05
4/6/19	SW.2.1	5.08E+03	2.51E+03	6.00E+05	30689	8.79E+03	5.30E+04	0.00E+00	1.67E+05
4/6/19	SW.4.1	3.99E+05	9.79E+04	4.98E+06	10511	2.00E+05	1.23E+05	6.93E+06	3.06E+05
4/6/19	SW.5.1	0.00E+00	7.13E+02	7.68E+05	24645	1.29E+04	0.00E+00	0.00E+00	3.58E+05
4/6/19	SW.6.1	2.77E+04	3.35E+03	7.85E+05	19090	1.72E+04	5.20E+04	0.00E+00	1.10E+05
4/6/19	SW.7.1	0.00E+00	7.11E+01	5.78E+05	83520	1.91E+04	4.85E+04	0.00E+00	5.12E+05
4/6/19	SW.8.1	0.00E+00	0.00E+00	4.59E+05	91002	3.73E+04	0.00E+00	0.00E+00	3.33E+05

4/6/19	SW.9.1	0.00E+00	0.00E+00	1.35E+06	8226	5.94E+04	5.49E+04	0.00E+00	2.45E+05
6/6/19	D.2.0	9.62E+03	1.70E+04	9.82E+06	121838	8.63E+03	1.09E+06	1.28E+06	1.11E+04
6/6/19	D.4.0	1.36E+05	1.81E+04	3.31E+06	37562	3.85E+04	2.56E+05	1.20E+06	2.38E+04
6/6/19	L.1.4	5.43E+04	9.06E+03	1.03E+07	27951	0.00E+00	7.87E+05	2.91E+06	0.00E+00
6/6/19	L.2.4	4.65E+04	3.70E+04	2.08E+07	24108	7.83E+04	3.15E+06	2.45E+06	0.00E+00
6/6/19	L.3.4	6.92E+04	1.22E+04	1.59E+07	28328	0.00E+00	1.37E+06	2.50E+06	0.00E+00
6/6/19	L.4.4	9.83E+04	5.84E+03	1.02E+07	20131	4.78E+04	8.46E+05	1.56E+06	1.51E+04
6/6/19	L.5.4	1.23E+05	1.06E+04	1.01E+07	39408	4.30E+04	1.66E+06	3.36E+06	0.00E+00
6/6/19	SW.0.1	5.83E+03	4.28E+02	4.05E+05	28935	3.71E+03	5.85E+04	0.00E+00	2.13E+05
6/6/19	SW.0.3	8.90E+02	2.21E+02	4.06E+05	16595	1.93E+03	5.02E+04	0.00E+00	7.43E+04
6/6/19	SW.1.1	1.71E+03	2.78E+02	1.87E+06	0	2.75E+03	2.93E+04	0.00E+00	1.86E+05
6/6/19	SW.1.1	1.06E+05	1.37E+05	2.32E+06	44069	1.21E+03	0.00E+00	0.00E+00	2.53E+05
6/6/19	SW.1.3	7.75E+02	0.00E+00	2.35E+05	0	2.88E+03	9.49E+04	0.00E+00	7.49E+04
6/6/19	SW.2.1	5.69E+04	3.66E+04	2.47E+06	0	2.51E+05	4.26E+05	0.00E+00	1.44E+05
6/6/19	SW.2.2	1.67E+03	2.02E+02	4.32E+05	55092	2.49E+03	1.18E+04	0.00E+00	1.82E+05
6/6/19	SW.2.3	1.25E+03	2.97E+02	3.64E+05	21614	2.87E+03	0.00E+00	0.00E+00	8.72E+04
6/6/19	SW.4.1	0.00E+00	1.09E+02	4.06E+05	0	3.36E+03	0.00E+00	0.00E+00	2.13E+05
6/6/19	SW.4.2	0.00E+00	0.00E+00	0.00E+00	7304	0.00E+00	0.00E+00	0.00E+00	0.00E+00
6/6/19	SW.4.3	6.94E+02	1.71E+02	3.93E+05	46868	0.00E+00	7.15E+04	0.00E+00	7.69E+04
6/6/19	SW.5.1	0.00E+00	0.00E+00	0.00E+00	38834	0.00E+00	0.00E+00	0.00E+00	0.00E+00
6/6/19	SW.5.2	1.97E+02	1.80E+02	1.07E+06	17155	0.00E+00	1.87E+05	0.00E+00	1.77E+05
6/6/19	SW.5.3	2.66E+03	1.30E+02	4.21E+05	24829	0.00E+00	5.32E+04	0.00E+00	3.88E+04
6/6/19	SW.6.1	2.40E+03	4.36E+02	4.45E+05	11882	0.00E+00	1.44E+05	0.00E+00	1.56E+05
6/6/19	SW.6.2	3.29E+03	3.18E+02	6.44E+05	12609	0.00E+00	1.34E+05	0.00E+00	1.61E+05
6/6/19	SW.6.3	2.54E+03	2.12E+02	3.40E+05	25471	0.00E+00	7.66E+04	0.00E+00	3.15E+04
6/6/19	SW.7.1	4.78E+03	1.26E+03	1.26E+06	31977	8.70E+03	4.06E+05	0.00E+00	1.99E+05
6/6/19	SW.7.2	1.65E+03	3.36E+02	3.23E+05	13618	0.00E+00	9.04E+04	0.00E+00	3.78E+04
6/6/19	SW.7.3	9.92E+02	2.45E+02	3.97E+05	52047	0.00E+00	1.44E+05	0.00E+00	3.72E+04
6/6/19	SW.8.1	7.48E+02	1.01E+03	7.14E+05	45700	6.37E+03	2.51E+05	0.00E+00	7.97E+04
6/6/19	SW.8.3	1.09E+03	8.99E+01	2.62E+05	0	0.00E+00	7.78E+04	0.00E+00	9.89E+03
6/6/19	SW.9.1	0.00E+00	5.19E+02	6.15E+05	54597	4.84E+03	3.28E+05	0.00E+00	9.91E+04
6/6/19	SW.9.3	1.01E+03	1.25E+02	2.84E+05	48375	0.00E+00	4.09E+04	0.00E+00	2.04E+04
6/6/19 pm	SW.0.1	1.46E+04	6.00E+02	1.25E+06	46698	6.80E+03	1.95E+05	0.00E+00	1.55E+05
6/6/19 pm	SW.1.1	3.15E+03	1.13E+03	7.36E+05	77934	0.00E+00	1.17E+05	0.00E+00	2.95E+05
6/6/19 pm	SW.2.1	4.76E+03	7.85E+02	1.46E+06	193841	0.00E+00	4.06E+05	0.00E+00	4.28E+05
6/6/19 pm	SW.2.2	9.64E+03	5.23E+02	9.33E+05	22480	0.00E+00	8.67E+04	0.00E+00	2.98E+05
6/6/19 pm	SW.2.3	3.19E+03	3.71E+02	4.55E+05	79561	0.00E+00	1.52E+05	0.00E+00	1.15E+05
6/6/19 pm	SW.4.1	6.09E+03	8.02E+02	1.19E+06	16661	0.00E+00	2.30E+05	0.00E+00	4.20E+05
6/6/19 pm	SW.5.1	5.09E+03	8.20E+02	6.35E+05	7880	0.00E+00	9.02E+04	0.00E+00	3.97E+05
6/6/19 pm	SW.5.2	6.73E+03	3.52E+02	4.93E+05	32028	0.00E+00	7.88E+04	0.00E+00	1.00E+05
6/6/19 pm	SW.5.3	1.37E+03	1.78E+02	8.32E+05	36511	0.00E+00	1.58E+05	0.00E+00	1.06E+05

6/6/19 pm	SW.6.1.1	5.50E+04	1.15E+05	1.02E+07	49921	2.71E+04	8.99E+05	2.78E+05	2.07E+04
6/6/19 pm	SW.6.2	2.49E+03	4.76E+03	9.28E+05	45314	0.00E+00	2.22E+05	0.00E+00	1.17E+05
6/6/19 pm	SW.6.2.1	3.65E+04	3.28E+04	2.23E+06	32784	5.98E+04	6.90E+05		0.00E+00
6/6/19 pm	SW.6.3	3.40E+03	2.70E+03	9.39E+05	47247	0.00E+00	1.42E+05	0.00E+00	1.33E+05
6/6/19 pm	SW.6.3.1	5.01E+04	1.14E+05	8.52E+06	9185	7.48E+04	1.34E+06	3.39E+05	2.41E+04
6/6/19 pm	SW.6.4.1	6.90E+04	5.14E+04	7.82E+06	21098	5.16E+04	9.02E+05	8.15E+05	0.00E+00
6/6/19 pm	SW.7.1	2.85E+03	5.29E+03	8.11E+05	22854	0.00E+00	2.31E+05	0.00E+00	7.09E+04
6/6/19 pm	SW.7.2	1.73E+03	5.47E+03	8.36E+05	32986	0.00E+00	3.48E+05	0.00E+00	1.16E+05
6/6/19 pm	SW.7.3	1.90E+03	2.30E+03	5.74E+05	29114	0.00E+00	1.16E+05	0.00E+00	6.98E+04
6/6/19 pm	SW.8.1	6.81E+02	7.16E+03	7.12E+05	33189	0.00E+00	1.81E+05	0.00E+00	2.16E+04
6/6/19 pm	SW.9.1	0.00E+00	1.91E+02	4.34E+04	63172	0.00E+00	1.13E+04	0.00E+00	0.00E+00
11/6/19	D.4.0	2.46E+06	6.11E+05		53203	2.18E+05	1.06E+05	5.09E+04	5.00E+03
11/6/19	L.1.4	0.00E+00	1.08E+04	1.08E+07	59779	5.62E+03	5.63E+05	0.00E+00	8.33E+03
11/6/19	L.2.4	1.24E+03	4.44E+03	3.00E+06	0	0.00E+00	3.18E+05	0.00E+00	6.73E+03
11/6/19	L.3.4	0.00E+00	3.84E+04	1.68E+06	30413	5.13E+03	2.88E+05	0.00E+00	8.40E+03
11/6/19	L.4.4	0.00E+00	1.83E+04	1.97E+06	17290	0.00E+00	4.50E+05	0.00E+00	5.96E+03
11/6/19	L.5.4	1.40E+06	2.99E+05	3.90E+06	68150	1.62E+05	1.18E+05	1.22E+05	3.07E+03
11/6/19	SW.0.1	6.72E+03	3.38E+02	1.23E+07	35612	0.00E+00	1.69E+05	0.00E+00	7.99E+03
11/6/19	SW.0.2	3.20E+03	1.94E+02	4.26E+05	22286	0.00E+00	4.05E+04	0.00E+00	5.33E+03
11/6/19	SW.0.3	2.25E+03	4.26E+03	5.77E+05	37802	0.00E+00	0.00E+00	0.00E+00	8.16E+03
11/6/19	SW.1.1	2.23E+03	1.46E+02	2.80E+05	18392	0.00E+00	8.93E+04	0.00E+00	1.62E+04
11/6/19	SW.1.1	1.26E+04	2.76E+03	1.98E+05	53166	0.00E+00	3.68E+04	0.00E+00	5.81E+04
11/6/19	SW.1.3	2.99E+03	9.29E+01	2.71E+05	24125	0.00E+00	1.22E+05	0.00E+00	7.97E+03
11/6/19	SW.2.1	3.12E+03	4.22E+02	1.49E+05	42463	0.00E+00	6.58E+04	0.00E+00	3.37E+04
11/6/19	SW.2.2	5.85E+03	1.94E+02	2.09E+05	43522	0.00E+00	4.75E+04	0.00E+00	5.07E+03
11/6/19	SW.2.3	2.08E+03	4.83E+02	4.11E+05	21432	0.00E+00	1.88E+05	0.00E+00	5.15E+03
11/6/19	SW.4.1	8.72E+04	1.10E+04	3.82E+05	42216	0.00E+00	5.21E+04	0.00E+00	5.68E+04
11/6/19	SW.4.2	5.99E+03	3.79E+02	4.81E+05	39510	0.00E+00	1.51E+05	0.00E+00	8.86E+03
11/6/19	SW.4.3	4.49E+03	3.21E+02	3.01E+05	26058	0.00E+00	9.01E+04	0.00E+00	6.52E+03
11/6/19	SW.5.1	3.38E+03	5.91E+02	1.89E+05	21155	0.00E+00	9.23E+04	0.00E+00	1.64E+04
11/6/19	SW.5.2	1.84E+03	6.20E+02	6.09E+05	16302	0.00E+00	1.82E+05	0.00E+00	6.29E+03
11/6/19	SW.5.3	3.59E+03	1.82E+02	3.01E+05	8508	0.00E+00	8.16E+04	0.00E+00	7.57E+03
11/6/19	SW.6.1	1.65E+03	3.41E+02	2.65E+05	23409	0.00E+00	8.20E+04	0.00E+00	8.84E+03
11/6/19	SW.6.2	2.98E+03	1.06E+02	2.07E+05	22398	0.00E+00	1.30E+05	0.00E+00	7.52E+03
11/6/19	SW.6.3	5.71E+03	1.22E+02	2.74E+05	22527	0.00E+00	4.98E+04	0.00E+00	5.72E+03
11/6/19	SW.7.1	2.49E+03	1.86E+02	2.04E+05	34220	0.00E+00	1.21E+05	0.00E+00	4.80E+03
11/6/19	SW.7.2	1.60E+03	1.41E+03	2.53E+05	15160	0.00E+00	7.67E+04	0.00E+00	1.24E+03
11/6/19	SW.7.3	7.41E+03	0.00E+00	2.11E+05	11119	0.00E+00	6.16E+04	0.00E+00	0.00E+00

11/6/19	SW.8.1	2.93E+03	5.28E+03	4.00E+05	3713	1.31E+03	1.25E+05	0.00E+00	4.51E+03
11/6/19	SW.8.2	2.62E+03	1.65E+02	2.30E+05	12098	1.05E+03	8.35E+04	0.00E+00	0.00E+00
11/6/19	SW.8.3	3.85E+03	6.72E+02	1.88E+05	32210	6.93E+02	6.41E+04	0.00E+00	3.54E+03
11/6/19	SW.9.1	1.23E+03	0.00E+00	1.41E+06	67416	0.00E+00	4.88E+04	0.00E+00	1.39E+04
11/6/19	SW.9.2	3.53E+02	1.24E+02	2.12E+05	65984	5.21E+02	3.94E+04	0.00E+00	1.60E+04
11/6/19	SW.9.3	2.71E+03	1.46E+02	1.46E+05	50535	8.60E+02	6.25E+04	0.00E+00	4.19E+03

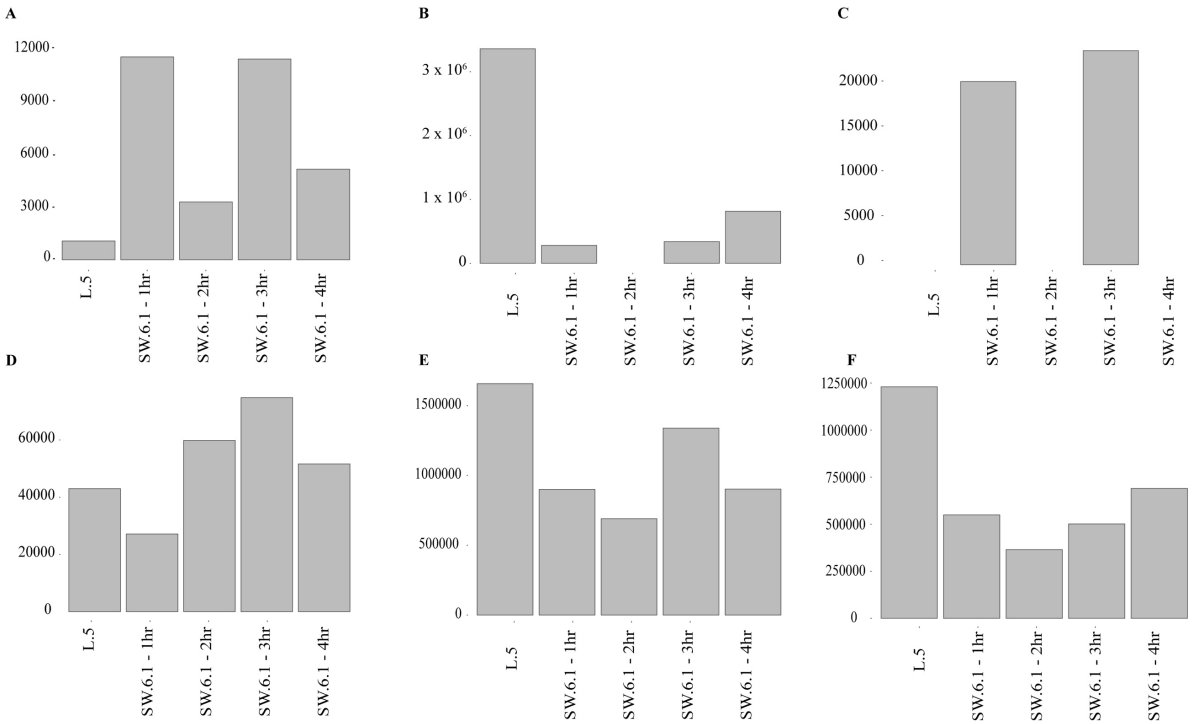

Figure 1. Impact of Lagoon opening over time. Each graph shows copies/100mL of a) intI1 b) dfrA1, c) qnrS, d) sulI, e) tetA and f) the Lachno3 human sewage marker after the lagoon was manually opened on the afternoon of the 6/6/21. A sample was taken at L5 just inside the lagoon mouth, and every hour at site SW6.1 (SW6.1 – 1hr, SW6.1 – 2hr, SW6.1 – 3hr, SW6.1 – 4hr) which is located in the ocean at the lagoon mouth.

Appendix 4 - Defining the importance of natural environmental variability and anthropogenic impacts on bacterial assemblages within intermittently opened and closed lagoons

Table 1. Site latitude and longitude

Site	Latitude (Decimal Degrees)	Longitude (Decimal Degrees)
W1	-33.4159	151.4558
W2	-33.41965	151.4529
W3	-33.42238	151.45013
W4	-33.42379	151.44539
W5	-33.42795	151.44742
T1	-33.43227	151.43855
T2	-33.43673	151.44174
T3	-33.439	151.43958
T4	-33.43935	151.43721
T5	-33.44188	151.4413
A1	-33.45603	151.43326
A2	-33.45853	151.42683
A3	-33.4613	151.42474
A4	-33.46228	151.43021
A5	-33.46298	151.43452
A6	-33.46539	151.42995
A7	-33.469	151.42747
C1	-33.48969	151.41748
C2	-33.48857	151.4212
C3	-33.4915	151.41997
C4	-33.4916	151.42542
C5	-33.4929	151.42697

1.1 Enterococci Analysis

As per the local governments methods, water samples (10 ml) were diluted with 100 ml of sterile deionized water (1:10 dilution) in a sterile polystyrene vessel and powdered Enterolert reagent mixed, and the sample-reagent combination added and mixed. The sample and reagents were then poured into a Quanti-Tray, a sterile panel with 51 wells containing indicator substrate, 4-methylumbelliferone-b-D-glucoside, that fluoresces when metabolized by Enterococci. Quanti-Trays were then sealed and incubated for 24 hrs at 41°C ± 0.5°C. The count of total fluorescent wells after 24 hrs (using a 365-nm-wavelength UV light with a 6-W bulb) was taken and then referred to a most probable number (MPN) table.

1.2 qPCR genes targeted

As described by Williams et al. (2022), these assays included Lachno3 assay (Feng et al., 2018), which targets human gut microbiome associated Lachnospiraceae, and the HF183 assay (Templar et al., 2016) which targets human gut microbiome associated Bacteroides. I also wished to determine levels of animal faeces which may be contributing to contamination within the Central Coast Lagoons. To determine the presences of dog faeces, I used the DG3 assay (Green et al., 2014), which targets dog-specific Bacteroidales, and to detect faeces from birds I used the GFD assay (Green et al., 2012), which targets bird-specific Heliobacter.

The gene *sulI* confers to sulphonamide resistance, a widely used clinical antibiotic (Pei et al., 2006); *tetA* encodes tetracycline resistance, an antibiotic which is used in both hospitals and vet clinics(Borjesson et al., 2009); *qnrS* confers to quinolone resistance, which are a group of antibiotics used in clinical settings (Berglund et al., 2014); *dfrA1* which encodes trimethoprims resistance (Grape et al., 2007), and these antibiotics are used to treat urinary tract infections; *vanB* which confers to vancomycin resistance (Berglund et al., 2014), vancomycin being a last line of defence antibiotic (Berglund et al., 2014).

Table 2. Primers used in study.

Target	qPCR Standard	Size (BP)	Primers	Primer Sequences	qPCR Conditions	Efficiency	Ref
16S	G-Block synthesised from NR_044853.1 by IDT	466	BACT1369F PROK1492R TM1389F	Forward: 5' CGG TGA ATA CGT TCY CGG 3' Reverse: 5' GGW TAC CTT GTT ACG ACT T 3' Probe: [FAM] 5' CTTGTACACACCGCCCGTC 3'	95°C for 3 min; 40 cycles of: 95°C for 30 sec, 56°C for 1 min	92% - 98.5%	(Suzuki et al., 2000)
Human *Bacteroidales*	G-Block synthesised from AY618282.1 by IDT	167	HF183 BFDRev BFDFAM	Forward: 5' ATCATGAGTTCACATGTCCG 3' Reverse: 5' CGTAGGAGTTTGGACCGTGT 3' Probe: [FAM] 5' CTGAGAGGAAGGTCCCCCACATTGGA 3'	95°C for 3 min; 45 cycles of: 95°C for 10 sec, 57°C for 1 min	99% - 104 %	(Templar et al., 2016)
Human *Lachnospiraceae*	G-Block synthesised from EF036467.1 by IDT	187	Lachno3F Lachno3R Lachno3P	Forward: 5' CAACGCGAAGAACCTTACCAAA 3' Reverse: 5' CCCAGAGTGCCCACCTTAAAT 3' Probe: [FAM] 5' CTCTGACCGGTCTTTAATCGGA 3' [MGB]	95°C for 3 min; 45 cycles of: 95°C for 10 sec, 64°C for 1 min	93% - 102.6%	(Feng et al., 2018)
Dog *Bacteroidales*	G-Block synthesised from DogGFE by IDT	185	DG3F DG3R DG3P	Forward: 5' TTTTCAGCCCCGTTGTTTCG 3' Reverse: 5' TGAGCGGGCATGGTCATATT 3' Probe: [FAM] 5' AGTCTACGCGGGCGTACT 3' [MGB]	95°C for 3 min; 45 cycles of: 95°C for 15 sec, 57°C for 30 sec	93% - 105%	(Green et al., 2014)
Bird *Heliobacter*	G-Block synthesised from JN084061.1 by IDT	163	GFDF GFDR	Forward: 5' TCGGCTGAGCACTCTAGGG 3' Reverse: 5' GCGTCTCTTTGTACATCCCA 3'	95°C for 3 min; 45 cycles of: 95°C for 15 sec, 57°C for 1 min	95.5% - 102.5%	(Green et al., 2012)
intI 1	Plasmid insert amplified from Sydney samples	484	int1.F int1.R	Forward: 5' GGGTCAAGGATCTGGATTTCG 3' Reverse: 5' ACATGCGTGTAAATCATCGTCG 3'	95°C for 3 min; 45 cycles of: 95°C for 15 sec 60°C for 30 sec	90% - 92%	(Mazel et al., 2000)
Sul1	Plasmid insert amplified from Sydney samples	163	sulI-FW sulI-RV	Forward: 5' CGCACCGGAAACATCGCTGCAC 3' Reverse: 5' TGAAGTTCCGCCGCAAGGCTCG 3'	95°C for 3 min; 45 cycles of: 95°C for 15 sec, 65°C for 30 sec	95.6% - 102.7%	(Pei et al., 2006)
tetA	Plasmid insert amplified from Sydney samples	96	tetA-F2-L tetA-R2	Forward: 5' CAG CCT CAA TTT CCT GAC GGG CTG A 3' Reverse: 5' GAA GCG AGC GGG TTG AGA G 3'	95°C for 3 min; 45 cycles of: 95°C for 15 sec, 58°C for 1 min	90% - 99.9%	(Borjesson et al., 2009)
VanB	Plasmid, bacteria w/plasmid pGEM-T with vanB cloned	3300	VB-F VB-R VB-P	Forward: 5' AAT CTT AAT TGA GCA AGC GAT TTC 3' Reverse: 5' CCT GAT GGA TGC GGA AGA TA 3' Probe: [FAM] 5' CCG GAT TTG ATC CAC TTC GCC GAC AAT CA 3'	95°C for 3 min; 45 cycles of: 95°C for 15 sec, 60°C for 30 sec	92.9% - 97.8%	(Berglund et al., 2014)
qnrS	Plasmid pGEM-T with qnrS cloned	3200	QnrS-F QnrS-R	Forward: 5' ATC AAG TGA GTA ATC GTA TGT ACT 3' Reverse: 5' CAC CTC GACTTAAGTCTGAC 3'	95°C for 3 min; 45 cycles of: 95°C for 15 sec, 72°C for 30 sec	92.9 % - 97.8%	(Berglund et al., 2014)
dfrA	Plasmid, bacteria w/plasmid	3500	dfr1s-f dfr1s-r	Forward: 5'ATG GAG TGC CAA AGG TGA AC 3' Reverse: 5' TAT CTC CCC ACC ACC TGA AA 3'	95°C for 3 min; 45 cycles of: 95°C for 15 sec, 62°C for 1 min	88% - 102.5%	(Grape et al., 2007)

1.3 qPCR technical methods.

Prior to all qPCR analyses, I performed inhibition testing using the 16S qPCR assay. When performing the inhibition testing, I tested samples from Drains 3 and 5 along with immediately adjacent to these drains SW3.1 and SW5.1, as well as samples from the middle of Rose Bay (RBE.2) for all sampling days. These samples were chosen based on the enterococci data, which was employed as a proxy indicator for levels of contamination. The Drain 3 and 5 samples along with the SW3.1 and SW5.1 samples were chosen as representative 'contaminated samples' and the RBE.2 sample represented a relatively uncontaminated sample. I then performed a series dilution using these samples, incorporating dilution factors of 1:2, 1:5, 1:10, 1:20, 1:50 and 1:100, with 16S rRNA qPCR performed on all dilutions. I then calculated the copies of the 16S gene per 100 ml in each sample, which revealed identical copy numbers in the 1:10, 1:20, 1:50 and 1:100 dilutions for all sample types tested. Based on these results, I chose to dilute all samples to 1:20.

For SYBR Green based detection assays, reaction mixtures (5 µl) consisted of 2.5µl BIO-RAD iTaq UniveralSYBR® Green Supermix, 1.1 µl nuclease free water, 0.2 µl of each forward and reverse primer (10 mM) and 1 µl of diluted DNA template. The reaction mixes for analyses using probe assays (5 µl) consisted of 2.5 µl BIO-RAD iTaq UniversalProbes® Supermix, 1 µl nuclease free water, 0.2 µl of each forward and reverse primer (10 mM), 0.1 µl of probe (10 mM) and 1 µl of diluted (1:20) DNA. For all samples, plate preparation was performed using an epMotion® 5075 I Automated Liquid Handling System.

Quantitative PCR cycling conditions consisted of an initial denaturation step at 95°C for 3 minutes and then 45 cycles of: 95°C for 15 seconds and then variable annealing temperatures according to assay (see Table 2) for 1 minute, with the exception for intI1 and vanB which had annealing times of 1 minute. Melt curves were included in all SYBR Green based detection assays to confirm the amplification of a single, correctly sized product. To ensure the quality of CT values, I calculated the coefficient of variation % of each assay, removing samples with CV below 2.5%.

In qPCR, gene copies were calculated for each target, using a (6-7 point) standard curve using BIO-RAD's CFX MAESTROTM software version 1.1. Standard curves were generated from known concentrations of a synthesised DNA fragment of each targeted gene, with a standard curve run with each plate. Samples outside of the calibration curve were considered below the limit of detection and included in the analysis as 0. Each DNA fragment for the

standard curve was checked using MEGA7 to ensure they matched both primers, the probe (if applicable) and target gene and blasted in the NCBI database to ensure it was from the correct target gene. Along with standard curves, a no template control (NTC) was added to each qPCR run.

1.4 16S rRNA gene amplicon sequencing pipeline

Paired R1 and R2 reads were subsequently processed using the DADA2 pipeline (Callahan et al., 2016). Reads with any 'N' bases were removed and bacterial V3-V4 primers were truncated using cutadapt (Martin, 2011). Reads were trimmed to remove low quality terminal ends (trunc (R1= 280; R2= 250)). To produce the highest number of merged reads after learning error rate and removing chimeric sequences, I used the dada2 removeBimeraDenovo program at the default threshold stringent minFoldParentOverAbundance=1. ASVs were annotated against the SILVA v138 database with a 50% probability cut-off. The ASV table was subsequently filtered to remove ASVs not assigned as kingdom Bacteria, as well as any ASVs classified as chloroplast or mitochondria. Finally, the dataset was rarefied to 20,000 reads using vegan (Dixon, 2003).

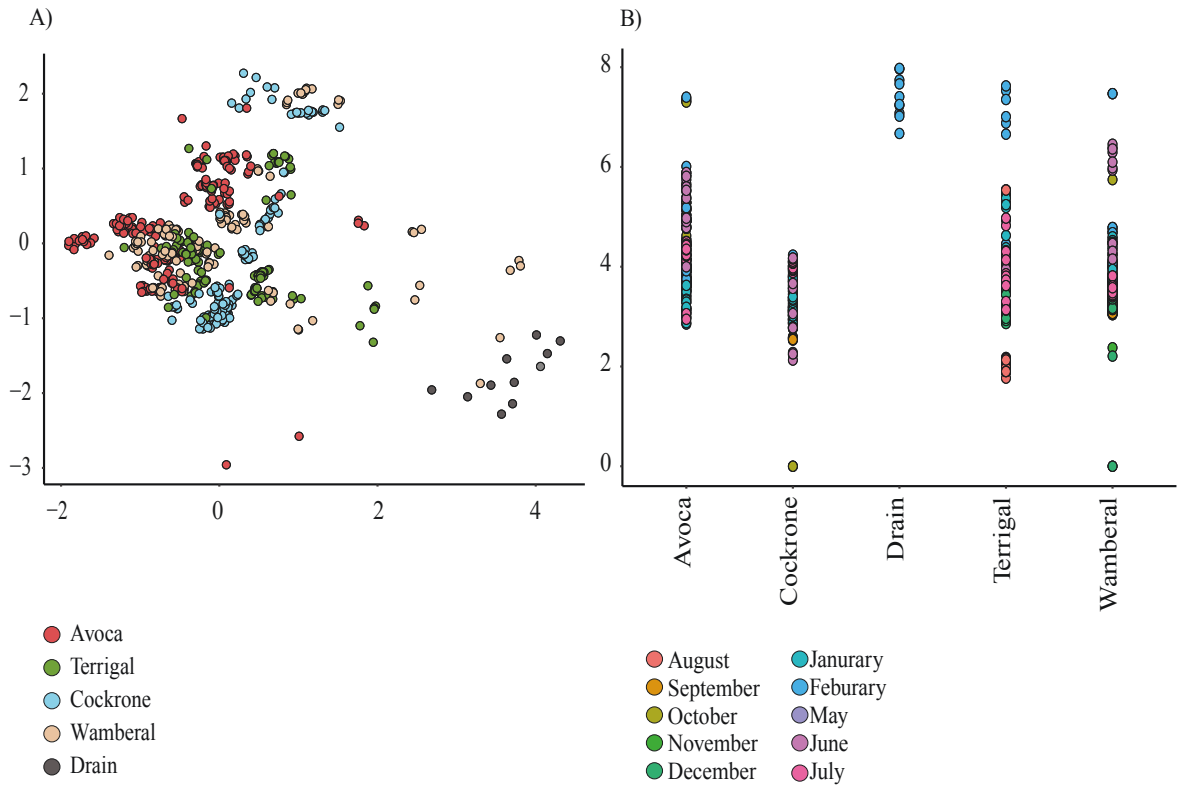

Figure 1. Alpha and Beta diversity of bacterial communities within each ICOLL. A) NMDS of 16SrRNA gene amplicon sequencing samples, B) Alpha diversity (Shannon's) of 16SrRNA gene amplicon sequencing samples.

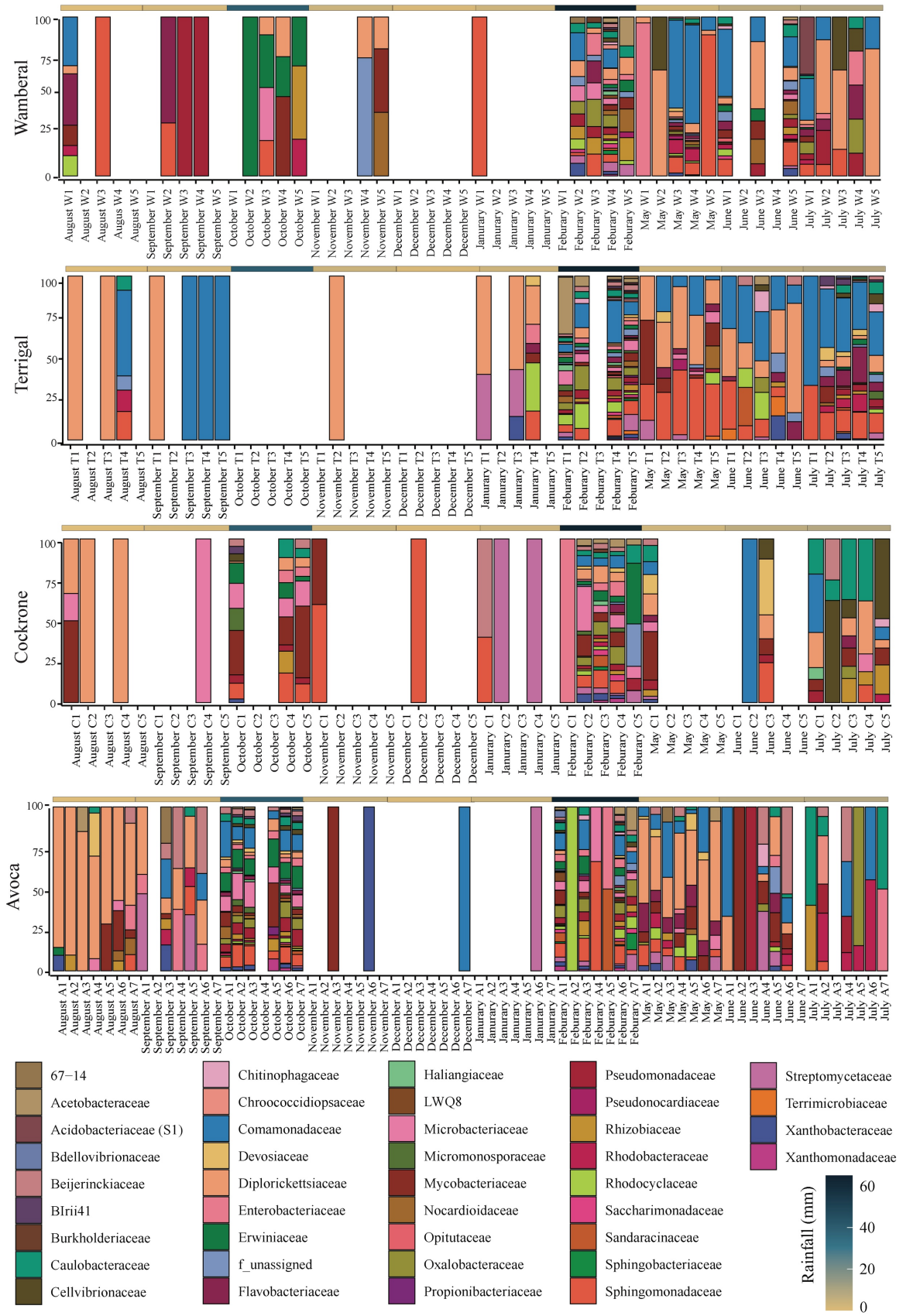

Figure 2. Stacked bar graph of the relative abundance of the top 20 indicator taxa at the family level. The top bar indicates rainfall in mm.

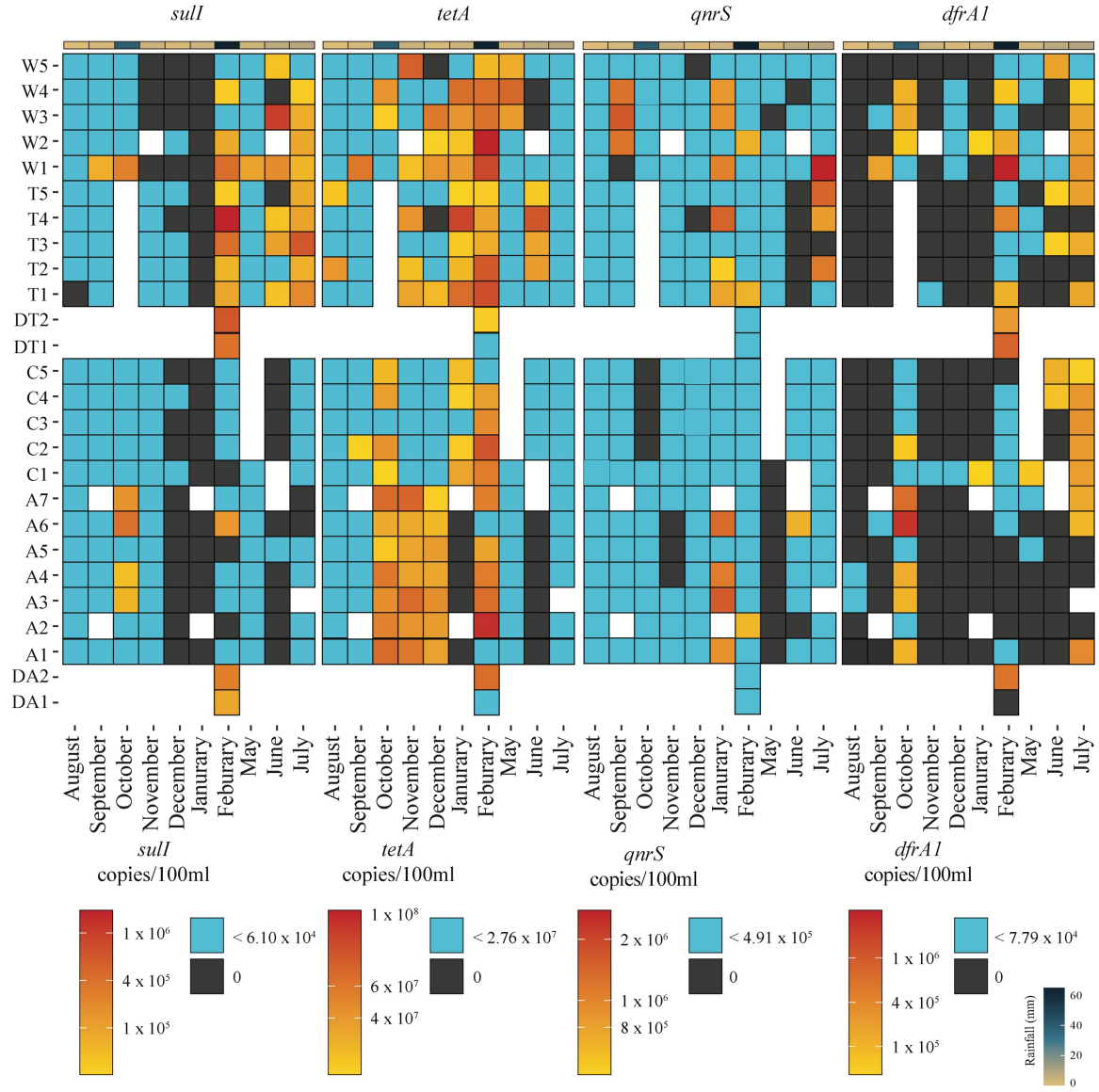

Figure 3. Heatmap showing the copy number per 100ml of each antibiotic resistance gene. Blue squares represent values below the average of all samples while black squares indicate no detection, and blank squares indicate samples that were not taken. The top bar indicates rainfall in mm.

References

Aanderud, Z.T., Vert, J.C., Lennon, J.T., Magnusson, T.W., Breakwell, D.P. and Harker, A.R. 2016. Bacterial Dormancy Is More Prevalent in Freshwater than Hypersaline Lakes. Front Microbiol 7, 853.

Agramont, J., Gutierrez-Cortez, S., Joffre, E., Sjoling, A. and Calderon Toledo, C. 2020. Fecal Pollution Drives Antibiotic Resistance and Class 1 Integron Abundance in Aquatic Environments of the Bolivian Andes Impacted by Mining and Wastewater. Microorganisms 8(8).

Ahlstrom, C.A., Bonnedahl, J., Woksepp, H., Hernandez, J., Olsen, B. and Ramey, A.M. 2018. Acquisition and dissemination of cephalosporin-resistant E. coli in migratory birds sampled at an Alaska landfill as inferred through genomic analysis. Sci Rep 8(1), 7361.

Ahmed, M.B., Zhou, J.L., Ngo, H.H. and Guo, W. 2015a. Adsorptive removal of antibiotics from water and wastewater: Progress and challenges. Sci Total Environ 532, 112-126.

Ahmed, W., Bivins, A., Payyappat, S., Cassidy, M., Harrison, N. and Besley, C. 2022. Distribution of human fecal marker genes and their association with pathogenic viruses in untreated wastewater determined using quantitative PCR. Water Research 226, 119093.

Ahmed, W., Hughes, B. and Harwood, V.J. 2016. Current status of marker genes of bacteroides and related taxa for identifying sewage pollution in environmental waters. Water (Basel) 8(6), 231.

Ahmed, W., Payyappat, S., Cassidy, M. and Besley, C. 2019. Enhanced insights from human and animal host-associated molecular marker genes in a freshwater lake receiving wet weather overflows. Sci Rep 9(1), 12503.

Ahmed, W., Payyappat, S., Cassidy, M., Harrison, N. and Besley, C. 2020a. Sewage-associated marker genes illustrate the impact of wet weather overflows and dry weather leakage in urban estuarine waters of Sydney, Australia. Sci Total Environ 705, 135390.

Ahmed, W., Payyappat, S., Cassidy, M., Harrison, N., Marinoni, O. and Besley, C. 2020b. Prevalence and abundance of traditional and host-associated fecal indicators in urban estuarine sediments: Potential implications for estuarine water quality monitoring. Water Res 184, 116109.

Ahmed, W., Staley, C., Sadowsky, M.J., Gyawali, P., Sidhu, J.P., Palmer, A., Beale, D.J. and Toze, S. 2015b. Toolbox Approaches Using Molecular Markers and 16S rRNA Gene Amplicon Data Sets for Identification of Fecal Pollution in Surface Water. Appl Environ Microbiol 81(20), 7067-7077.

Ahmed, W., Yusuf, R., Hasan, I., Goonetilleke, A. and Gardner, T. 2010. Quantitative PCR assay of sewage-associated Bacteroides markers to assess sewage pollution in an urban lake in Dhaka, Bangladesh. Canadian journal of microbiology 56(10), 838-845.

Akiyama, T. and Savin, M.C. 2010. Populations of antibiotic-resistant coliform bacteria change rapidly in a wastewater effluent dominated stream. Sci Total Environ 408(24), 6192-6201.

Albanese, D., Riccadonna, S., Donati, C. and Franceschi, P. 2018. A practical tool for maximal information coefficient analysis. Gigascience 7(4), 1-8.

Ali, M., Nelson, A.R., Lopez, A.L. and Sack, D.A. 2015. Updated global burden of cholera in endemic countries. PLoS Negl Trop Dis 9(6), e0003832.

Allard, J.D. and Bertrand, K.P. 1992. Membrane topology of the pBR322 tetracycline resistance protein. TetA-PhoA gene fusions and implications for the mechanism of TetA membrane insertion. Journal of Biological Chemistry 267(25), 17809-17819.

Allen, H.K., Donato, J., Wang, H.H., Cloud-Hansen, K.A., Davies, J. and Handelsman, J. 2010. Call of the wild: antibiotic resistance genes in natural environments. Nat Rev Microbiol 8(4), 251-259.

Alm, E.W., Daniels-Witt, Q.R., Learman, D.R., Ryu, H., Jordan, D.W., Gehring, T.M. and Santo Domingo, J. 2018. Potential for gulls to transport bacteria from human waste sites to beaches. The Science of the total environment 615, 123-130.

Alongi, D. (1998) Coastal Ecosystem Processes, Boca Raton, FL : CRC Press.

Alongi, D.M. and McKinnon, A.D. 2005. The cycling and fate of terrestrially-derived sediments and nutrients in the coastal zone of the Great Barrier Reef shelf. Mar. Pollut. Bull. 51(1-4), 239-252.

Anastasi, E.M., Matthews, B., Stratton, H.M. and Katouli, M. 2012. Pathogenic Escherichia coli found in sewage treatment plants and environmental waters. Appl Environ Microbiol 78(16), 5536-5541.

Anderson, D.M., Cembella, A.D. and Hallegraeff, G.M. (2012) Annual Review of Marine Science, Vol 4. Carlson, C.A. and Giovannoni, S.J. (eds), pp. 143-176, Annual Reviews, Palo Alto.

Anderson, T.R. and Ducklow, H.W. 2001. Microbial loop carbon cycling in ocean environments studied using a simple steady-state model. Aquat. Microb. Ecol. 26(1), 37-49.

Araujo, S., Henriques, I.S., Leandro, S.M., Alves, A., Pereira, A. and Correia, A. 2014. Gulls identified as major source of fecal pollution in coastal waters: a microbial source tracking study. Sci Total Environ 470-471, 84-91.

Arnosti, C. 2011. Microbial extracellular enzymes and the marine carbon cycle. Ann Rev Mar Sci 3, 401-425.

Asplund, M.E., Rehnstam-Holm, A.-S., Atnur, V., Raghunath, P., Saravanan, V., Härnström, K., Collin, B., Karunasagar, I. and Godhe, A. 2011. Water column dynamics of Vibrio in relation to phytoplankton community composition and environmental conditions in a tropical coastal area. Environmental microbiology 13(10), 2738-2751.

ASTM 2019 D6503 Standard Test Method for Enterococci in Water Using Enterolert.

Ateba, C.N. and Bezuidenhout, C.C. 2008. Characterisation of Escherichia coli O157 strains from humans, cattle and pigs in the North-West Province, South Africa. Int. J. Food Microbiol. 128(2), 181-188.

Auguet, O., Pijuan, M., Borrego, C.M., Rodriguez-Mozaz, S., Triado-Margarit, X., Giustina, S.V.D. and Gutierrez, O. 2017. Sewers as potential reservoirs of antibiotic resistance. Sci Total Environ 605-606, 1047-1054.

Azam, F. 1998. Microbial Control of Oceanic Carbon Flux: The Plot Thickens. Science 280(5364), 694-696.

Bahram, M., Hildebrand, F., Forslund, S.K., Anderson, J.L., Soudzilovskaia, N.A., Bodegom, P.M., Bengtsson-Palme, J., Anslan, S., Coelho, L.P., Harend, H., Huerta-Cepas, J., Medema, M.H., Maltz, M.R., Mundra, S., Olsson, P.A., Pent, M., Polme, S., Sunagawa, S., Ryberg, M., Tedersoo, L. and Bork, P. 2018. Structure and function of the global topsoil microbiome. Nature 560(7717), 233-237.

Baker-Austin, C., Oliver, J.D., Alam, M., Ali, A., Waldor, M.K., Qadri, F. and Martinez-Urtaza, J. 2018. Vibrio spp. infections. Nat Rev Dis Primers 4(1), 8.

Baker-Austin, C., Stockley, L., Rangdale, R. and Martinez-Urtaza, J. 2010. Environmental occurrence and clinical impact of Vibrio vulnificus and Vibrio parahaemolyticus: a European perspective. Environ Microbiol Rep 2(1), 7-18.

Baker-Austin, C., Trinanes, J., Gonzalez-Escalona, N. and Martinez-Urtaza, J. 2017. Non-Cholera Vibrios: The Microbial Barometer of Climate Change. Trends Microbiol 25(1), 76-84.

Baker-Austin, C., Trinanes, J.A., Taylor, N.G.H., Hartnell, R., Siitonen, A. and Martinez-Urtaza, J. 2012. Emerging Vibrio risk at high latitudes in response to ocean warming. Nature Climate Change 3(1), 73-77.

Baker-Austin, C., Trinanes, J.A., Taylor, N.G.H., Hartnell, R., Siitonen, A. and Martinez-Urtaza, J. 2013. Emerging Vibrio risk at high latitudes in response to ocean warming.

Balls, P.W., Macdonald, A., Pugh, K. and Edwards, A.C. 1995. LONG-TERM NUTRIENT ENRICHMENT OF AN ESTUARINE SYSTEM - YTHAN, SCOTLAND (1958-1993). Environ. Pollut. 90(3), 311-321.

Baquero, F., Martinez, J.L. and Canton, R. 2008. Antibiotics and antibiotic resistance in water environments. Curr Opin Biotechnol 19(3), 260-265.

Barbier, E.B., Hacker, S.D., Kennedy, C., Koch, E.W., Stier, A.C. and Silliman, B.R. 2011. The value of estuarine and coastal ecosystem services. Ecological monographs 81(2), 169-193.

Basset, A., Elliott, M., West, R.J. and Wilson, J.G. 2013. Estuarine and lagoon biodiversity and their natural goods and services. Estuarine, Coastal and Shelf Science 132, 1-4.

Bastyns, K., Cartuyvels, D., Chapelle, S., Vandamme, P., Goossens, H. and De Wachter, R. 1995. A Variable 23S rDNA Region is a Useful Discriminating Target for Genus-Specific and Species-Specific PCR Amplification in Arcobacter Species. Systematic and Applied Microbiology 18(3), 353-356.

Ben-Haim, Y. and Rosenberg, E. 2002. A novel Vibrio sp. pathogen of the coral Pocillopora damicornis. Marine Biology 141(1), 47-55.

Benskin, C.M., Wilson, K., Jones, K. and Hartley, I.R. 2009. Bacterial pathogens in wild birds: a review of the frequency and effects of infection. Biol Rev Camb Philos Soc 84(3), 349-373.

Berendonk, T.U., Manaia, C.M., Merlin, C., Fatta-Kassinos, D., Cytryn, E., Walsh, F., Burgmann, H., Sorum, H., Norstrom, M., Pons, M.N., Kreuzinger, N., Huovinen, P., Stefani, S., Schwartz, T., Kisand, V., Baquero, F. and Martinez, J.L. 2015. Tackling

antibiotic resistance: the environmental framework. Nat Rev Microbiol 13(5), 310-317.

Berglund, B., Khan, G.A., Weisner, S.E., Ehde, P.M., Fick, J. and Lindgren, P.E. 2014. Efficient removal of antibiotics in surface-flow constructed wetlands, with no observed impact on antibiotic resistance genes. Sci Total Environ 476-477, 29-37.

Betancourt, W.Q., Abd-Elmaksoud, S. and Gerba, C.P. 2018. Efficiency of Reovirus Concentration from Water with Positively Charged Filters. Food and environmental virology 10(2), 209-211.

Bibiloni-Isaksson, J., Seymour, J.R., Ingleton, T., van de Kamp, J., Bodrossy, L. and Brown, M.V. 2016. Spatial and temporal variability of aerobic anoxygenic photoheterotrophic bacteria along the east coast of Australia. Environ Microbiol 18(12), 4485-4500.

Blackstone, G.M., Nordstrom, J.L., Bowen, M.D., Meyer, R.F., Imbro, P. and DePaola, A. 2007. Use of a real time PCR assay for detection of the ctxA gene of Vibrio cholerae in an environmental survey of Mobile Bay. J Microbiol Methods 68(2), 254-259.

Blackwell, K.D. and Oliver, J.D. 2008. The ecology of Vibrio vulnificus, Vibrio cholerae, and Vibrio parahaemolyticus in North Carolina estuaries. J Microbiol 46(2), 146-153.

Blondeau, J.M. and Fitch, S.D. 2021. In vitro killing of canine urinary tract infection pathogens by ampicillin, cephalexin, marbofloxacin, pradofloxacin, and trimethoprim/sulfamethoxazole. Microorganisms (Basel) 9(11), 2279.

Bloom, P. 2014. Canine superficial bacterial folliculitis: current understanding of its etiology, diagnosis and treatment. Vet J 199(2), 217-222.

Blum, M.L. and Orbach, M.K. 2021. First Steps at First Point: Protecting California Surf Breaks and the Malibu Historic District. Coastal Management 49(2), 201-214.

Bockstael, N.E., Hanemann, W.M. and Kling, C.L. 1987. Estimating the value of water quality improvements in a recreational demand framework. Water resources research 23(5), 951-960.

Boehm, A.B. and Soller, J.A. 2020. Refined ambient water quality thresholds for human-associated fecal indicator HF183 for recreational waters with and without co-occurring gull fecal contamination. Microbial Risk Analysis 16.

Bonetta, S., Pignata, C., Lorenzi, E., De Ceglia, M., Meucci, L., Bonetta, S., Gilli, G. and Carraro, E. 2016. Detection of pathogenic Campylobacter, E. coli O157:H7 and Salmonella spp. in wastewater by PCR assay. Environ Sci Pollut Res Int 23(15), 15302-15309.

Bonnedahl, J. and Jarhult, J.D. 2014. Antibiotic resistance in wild birds. Ups J Med Sci 119(2), 113-116.

Borjesson, S., Dienues, O., Jarnheimer, P.A., Olsen, B., Matussek, A. and Lindgren, P.E. 2009. Quantification of genes encoding resistance to aminoglycosides, beta-lactams and tetracyclines in wastewater environments by real-time PCR. Int J Environ Health Res 19(3), 219-230.

Bougnom, B.P., McNally, A., Etoa, F.X. and Piddock, L.J. 2019. Antibiotic resistance genes are abundant and diverse in raw sewage used for urban agriculture in Africa and associated with urban population density. Environ Pollut 251, 146-154.

Brown, C.M., Staley, C., Wang, P., Dalzell, B., Chun, C.L. and Sadowsky, M.J. 2017. A High-Throughput DNA-Sequencing Approach for Determining Sources of Fecal Bacteria in a Lake Superior Estuary. Environ Sci Technol 51(15), 8263-8271.

Brown, M.V., Lauro, F.M., DeMaere, M.Z., Muir, L., Wilkins, D., Thomas, T., Riddle, M.J., Fuhrman, J.A., Andrews-Pfannkoch, C., Hoffman, J.M., McQuaid, J.B., Allen, A., Rintoul, S.R. and Cavicchioli, R. 2012. Global biogeography of SAR11 marine bacteria. Mol Syst Biol 8, 595.

Brumfield, K.D., Cotruvo, J.A., Shanks, O.C., Sivaganesan, M., Hey, J., Hasan, N.A., Huq, A., Colwell, R.R. and Leddy, M.B. 2021. Metagenomic Sequencing and Quantitative Real-Time PCR for Fecal Pollution Assessment in an Urban Watershed. Front Water 3, 626849.

Bruto, M., Labreuche, Y., James, A., Piel, D., Chenivesse, S., Petton, B., Polz, M.F. and Le Roux, F. 2018. Ancestral gene acquisition as the key to virulence potential in environmental Vibrio populations. ISME J 12(12), 2954-2966.

Bryan, A., Shapir, N. and Sadowsky, M.J. 2004. Frequency and distribution of tetracycline resistance genes in genetically diverse, nonselected, and nonclinical Escherichia coli strains isolated from diverse human and animal sources. Appl Environ Microbiol 70(4), 2503-2507.

Byappanahalli, M.N., Nevers, M.B., Korajkic, A., Staley, Z.R. and Harwood, V.J. 2012. Enterococci in the environment. Microbiol Mol Biol Rev 76(4), 685-706.

Callahan, B.J., McMurdie, P.J., Rosen, M.J., Han, A.W., Johnson, A.J. and Holmes, S.P. 2016. DADA2: High-resolution sample inference from Illumina amplicon data. Nat Methods 13(7), 581-583.

Caputi, N., Kangas, M., Denham, A., Feng, M., Pearce, A., Hetzel, Y. and Chandrapavan, A. 2016. Management adaptation of invertebrate fisheries to an extreme marine heat wave event at a global warming hot spot. Ecol Evol 6(11), 3583-3593.

Carney, R.L., Brown, M.V., Siboni, N., Raina, J.B., Kahlke, T., Mitrovic, S.M. and Seymour, J.R. 2020. Highly heterogeneous temporal dynamics in the abundance and diversity of the emerging pathogens Arcobacter at an urban beach. Water Res 171, 115405.

Carney, R.L., Labbate, M., Siboni, N., Tagg, K.A., Mitrovic, S.M. and Seymour, J.R. 2019. Urban beaches are environmental hotspots for antibiotic resistance following rainfall. Water Res 167, 115081.

Carugati, L., Gatto, B., Rastelli, E., Lo Martire, M., Coral, C., Greco, S. and Danovaro, R. 2018. Impact of mangrove forests degradation on biodiversity and ecosystem functioning. Sci Rep 8, 11.

Cavole, L., Demko, A., Diner, R., Giddings, A., Koester, I., Pagniello, C., Paulsen, M.-L., Ramirez-Valdez, A., Schwenck, S., Yen, N., Zill, M. and Franks, P. 2016. Biological Impacts of the 2013–2015 Warm-Water Anomaly in the Northeast Pacific: Winners, Losers, and the Future. Oceanography 29(2).

CDC 1998. From the Centers for Disease Control and Prevention. Outbreak of Vibrio parahaemolyticus infections associated with eating raw oysters--Pacific Northwest, 1997. JAMA : the journal of the American Medical Association 280(2), 126-127.

Celik, E. and Otlu, S. 2020. Isolation of Arcobacter spp. and identification of isolates by multiplex PCR from various domestic poultry and wild avian species. Ann. Microbiol. 70(1), 7.

Chapin Iii, F.S., Zavaleta, E.S., Eviner, V.T., Naylor, R.L., Vitousek, P.M., Reynolds, H.L., Hooper, D.U., Lavorel, S., Sala, O.E., Hobbie, S.E., Mack, M.C. and Díaz, S. 2000. Consequences of changing biodiversity. Nature (London) 405(6783), 234-242.

Chen, H. and Zhang, M. 2013. Occurrence and removal of antibiotic resistance genes in municipal wastewater and rural domestic sewage treatment systems in eastern China. Environ Int 55, 9-14.

Cheng, R., Zhu, H., Shutes, B. and Yan, B. 2021. Treatment of microcystin (MC-LR) and nutrients in eutrophic water by constructed wetlands: Performance and microbial community. Chemosphere 263, 128139.

Chimetto Tonon, L.A., Silva, B.S., Moreira, A.P., Valle, C., Alves, N., Jr., Cavalcanti, G., Garcia, G., Lopes, R.M., Francini-Filho, R.B., de Moura, R.L., Thompson, C.C. and Thompson, F.L. 2015. Diversity and ecological structure of vibrios in benthic and pelagic habitats along a latitudinal gradient in the Southwest Atlantic Ocean. PeerJ 3, e741.

Chorus, I. and Welker, M. (2021) Toxic Cyanobacteria in Water : A Guide to Their Public Health Consequences, Monitoring and Management (Edition 2), CRC Press.

Chow, L., Waldron, L. and Gillings, M.R. 2015. Potential impacts of aquatic pollutants: sub-clinical antibiotic concentrations induce genome changes and promote antibiotic resistance. Front Microbiol 6, 803.

Clark, G.F. and Johnston, E.L. 2017 Australia state of the environment 2016: coasts.

Codd, G.A., Lindsay, J., Young, F.M., Morrison, L.F. and Metcalf, J.S. (2022), pp. 1-23, Springer Netherlands, Dordrecht.

Codd, G.A., Morrison, L.F. and Metcalf, J.S. 2005. Cyanobacterial toxins: risk management for health protection. Toxicology and applied pharmacology 203(3), 264-272.

Codello, A., McLellan, S.L., Steinberg, P., Potts, J., Scanes, P., Ferguson, A., Hose, G.C., Griffith, M., Roguet, A., Lydon, K.A., Maher, W.A., Krikowa, F. and Chariton, A. 2021. A weight-of-evidence approach for identifying potential sources of untreated sewage inputs into a complex urbanized catchment. Environ Pollut 275, 116575.

Coelho, F., Santos, A.L., Coimbra, J., Almeida, A., Cunha, A., Cleary, D.F.R., Calado, R. and Gomes, N.C.M. 2013. Interactive effects of global climate change and pollution on marine microbes: the way ahead. Ecol. Evol. 3(6), 1808-1818.

Collado, L., Levican, A., Perez, J. and Figueras, M.J. 2011. Arcobacter defluvii sp. nov., isolated from sewage samples. Int J Syst Evol Microbiol 61(Pt 9), 2155-2161.

Converse, R.R., Piehler, M.F. and Noble, R.T. 2011. Contrasts in concentrations and loads of conventional and alternative indicators of fecal contamination in coastal stormwater. Water Res 45(16), 5229-5240.

Cooley, S., Schoeman, D., Bopp, L., Boyd, P., Donner, S., Ghebrehiwet, D.Y., Ito, S.-I., Kiessling, W., Martinetto, P., Ojea, E., Racault, M.-F., Rost, B. and Skern-Mauritzen, M. 2022 2022: Oceans and Coastal Ecosystems and Their Services. In: Climate Change 2022: Impacts, Adaptation and Vulnerability. Contribution of Working Group II to the Sixth Assessment Report of the Intergovernmental Panel on Climate Change.

H.-O. Pörtner, D.C.R., M. Tignor, E.S. Poloczanska, K. Mintenbeck, A. Alegría, M. Craig, S. Langsdorf, S. Löschke, V. Möller, A. Okem, B. Rama (ed), pp. 379-550, Cambridge University Press, Cambridge, UK and New York, NY, USA.

Costán-Longares, A., Mocé-Llivina, L., Avellón, A., Jofre, J. and Lucena, F. 2008. Occurrence and distribution of culturable enteroviruses in wastewater and surface waters of north-eastern Spain. Journal of applied microbiology 105(6), 1945-1955.

Cousins, M., Stacey, M.T. and Drake, J.L. 2010. Effects of Seasonal Stratification on Turbulent Mixing in a Hypereutrophic Coastal Lagoon. Limnology and oceanography 55(1), 172-186.

Craik, W. and Grafton, Q. 2018 The Marine Estate Management Strategy (2018-2028), NSW Marine Estate Management Authority.

Crawshaw, J.A., Schallenberg, M. and Savage, C. 2018. Physical and biological drivers of sediment oxygenation and denitrification in a New Zealand intermittently closed and open lake lagoon. New Zealand Journal of Marine and Freshwater Research 53(1), 33-59.

Curtis, T.P. and Sloan, W.T. 2004. Prokaryotic diversity and its limits: microbial community structure in nature and implications for microbial ecology. Curr. Opin. Microbiol. 7(3), 221-226.

Curtis, T.P., Sloan, W.T. and Scannell, J.W. 2002. Estimating prokaryotic diversity and its limits. Proc Natl Acad Sci U S A 99(16), 10494-10499.

Daniels, N.A., MacKinnon, L., Bishop, R., Altekruse, S., Ray, B., Hammond, R.M., Thompson, S., Wilson, S., Bean, N.H., Griffin, P.M. and Slutsker, L. 2000. Vibrio parahaemolyticus Infections in the United States, 1973–1998. The Journal of infectious diseases 181(5), 1661-1666.

Danovaro, R. and Pusceddu, A. 2007. Biodiversity and ecosystem functioning in coastal lagoons: Does microbial diversity play any role? Estuarine, Coastal and Shelf Science 75(1-2), 4-12.

De Caceres, M. and Jansen, F. 2018. Associations between species and groups of sites: indices and statistical inference. Ecology.

de Troch, M., Melgo-Ebarle, J.L., Angsinco-Jimenez, L., Gheerardyn, H. and Vincx, M. 2008. Diversity and habitat selectivity of harpacticoid copepods from sea grass beds in Pujada Bay, the Philippines. J. Mar. Biol. Assoc. U.K. 88(3), 515-526.

Dederen, L.H.T. 1990 MARINE EUTROPHICATION IN EUROPE - SIMILARITIES AND REGIONAL DIFFERENCES IN APPEARANCE, pp. 663-672, Elsevier Science Publ B V, Bologna, Italy.

Defoirdt, T. and Sorgeloos, P. 2012. Monitoring of Vibrio harveyi quorum sensing activity in real time during infection of brine shrimp larvae. ISME J 6(12), 2314-2319.

Deloitte 2016. Economic social value of improved water quality at sydneys coastal beaches.

Derakhshandeh, A., Eraghi, V., Boroojeni, A.M., Niaki, M.A., Zare, S. and Naziri, Z. 2018. Virulence factors, antibiotic resistance genes and genetic relatedness of commensal Escherichia coli isolates from dogs and their owners. Microb Pathog 116, 241-245.

Dessie, H.K., Bae, D.H. and Lee, Y.J. 2013. Characterization of integrons and their cassettes in Escherichia coli and Salmonella isolates from poultry in Korea. Poult Sci 92(11), 3036-3043.

Dick, L.K., Bernhard, A.E., Brodeur, T.J., Santo Domingo, J.W., Simpson, J.M., Walters, S.P. and Field, K.G. 2005. Host Distributions of Uncultivated Fecal Bacteroidales Bacteria Reveal Genetic Markers for Fecal Source Identification. Applied and Environmental Microbiology 71(6), 3184-3191.

Dixon, P. 2003. VEGAN, a package of R functions for community ecology. Journal of Vegetation Science 14(6), 927-930.

Doney, S.C., Ruckelshaus, M., Duffy, J.E., Barry, J.P., Chan, F., English, C.A., Galindo, H.M., Grebmeier, J.M., Hollowed, A.B., Knowlton, N., Polovina, J., Rabalais, N.N., Sydeman, W.J. and Talley, L.D. 2012. Climate change impacts on marine ecosystems. Ann Rev Mar Sci 4, 11-37.

DPIE 2020 State of the beaches 2019 - 2020, DPIE.

Dugan, J.E. and Hubbard, D.M. 2010. Loss of Coastal Strand Habitat in Southern California: The Role of Beach Grooming. Estuaries Coasts 33(1), 67-77.

Dwight, R.H., Fernandez, L.M., Baker, D.B., Semenza, J.C. and Olson, B.H. 2005. Estimating the economic burden from illnesses associated with recreational coastal water pollution--a case study in Orange County, California. J Environ Manage 76(2), 95-103.

Efstratiou, A., Ongerth, J.E. and Karanis, P. 2017. Waterborne transmission of protozoan parasites: Review of worldwide outbreaks - An update 2011-2016. Water Res 114, 14-22.

Eiler, A., Johansson, M. and Bertilsson, S. 2006. Environmental influences on Vibrio populations in northern temperate and boreal coastal waters (Baltic and Skagerrak Seas). Appl Environ Microbiol 72(9), 6004-6011.

Ervin, J.S., Van De Werfhorst, L.C., Murray, J.L. and Holden, P.A. 2014. Microbial source tracking in a coastal California watershed reveals canines as controllable sources of fecal contamination. Environ Sci Technol 48(16), 9043-9052.

Everett, J.D., Baird, M.E. and Suthers, I.M. 2007. Nutrient and plankton dynamics in an intermittently closed/open lagoon, Smiths Lake, south-eastern Australia: An ecological model. Estuarine, coastal and shelf science 72(4), 690-702.

Evers, C. 2009. 'The Point': surfing, geography and a sensual life of men and masculinity on the Gold Coast, Australia. Social & Cultural Geography 10(8), 893-908.

FAO 2018 STATE OF WORLD FISHERIES.

Feng, S. and McLellan, S.L. 2019. Highly Specific Sewage-Derived Bacteroides Quantitative PCR Assays Target Sewage-Polluted Waters. Appl Environ Microbiol 85(6).

Feng, S.C., Bootsma, M. and McLellan, S.L. 2018. Human-Associated Lachnospiraceae Genetic Markers Improve Detection of Fecal Pollution Sources in Urban Waters. Applied and Environmental Microbiology 84(14), 14.

Ferreira, S., Queiroz, J.A., Oleastro, M. and Domingues, F.C. 2016. Insights in the pathogenesis and resistance of Arcobacter: A review. Crit Rev Microbiol 42(3), 364-383.

Fewtrell, L. and Kay, D. 2015. Recreational Water and Infection: A Review of Recent Findings. Curr Environ Health Rep 2(1), 85-94.

Filippini, G., Bugnot, A.B., Johnston, E.L., Ruszczyk, J., Potts, J., Scanes, P., Ferguson, A., Ostrowski, M., Varkey, D. and Dafforn, K.A. 2019. Sediment bacterial communities associated with environmental factors in Intermittently Closed and Open Lakes and Lagoons (ICOLLs). Sci Total Environ 693, 133462.

Finley, R.L., Collignon, P., Larsson, D.G., McEwen, S.A., Li, X.Z., Gaze, W.H., Reid-Smith, R., Timinouni, M., Graham, D.W. and Topp, E. 2013. The scourge of antibiotic resistance: the important role of the environment. Clin Infect Dis 57(5), 704-710.

Fischer, A.G. 1960. Latitudinal Variations in Organic Diversity. Evolution 14(1), 64-81.

Fisher, J.C., Levican, A., Figueras, M.J. and McLellan, S.L. 2014. Population dynamics and ecology of Arcobacter in sewage. Front Microbiol 5, 525.

Flemming, H.C. and Wuertz, S. 2019. Bacteria and archaea on Earth and their abundance in biofilms. Nat Rev Microbiol 17(4), 247-260.

Flombaum, P., Gallegos, J.L., Gordillo, R.A., Rincon, J., Zabala, L.L., Jiao, N., Karl, D.M., Li, W.K., Lomas, M.W., Veneziano, D., Vera, C.S., Vrugt, J.A. and Martiny, A.C. 2013. Present and future global distributions of the marine Cyanobacteria Prochlorococcus and Synechococcus. Proc Natl Acad Sci U S A 110(24), 9824-9829.

Foley, S.L. and Lynne, A.M. 2008. Food animal-associated Salmonella challenges: pathogenicity and antimicrobial resistance. J Anim Sci 86(14 Suppl), E173-187.

Fortunato, C.S., Eiler, A., Herfort, L., Needoba, J.A., Peterson, T.D. and Crump, B.C. 2013. Determining indicator taxa across spatial and seasonal gradients in the Columbia River coastal margin. ISME J 7(10), 1899-1911.

Foster, G., Evans, J., Knight, H.I., Smith, A.W., Gunn, G.J., Allison, L.J., Synge, B.A. and Pennycott, T.W. 2006. Analysis of feces samples collected from a wild-bird garden feeding station in Scotland for the presence of verocytotoxin-producing Escherichia coli O157. Applied and Environmental Microbiology 72(3), 2265-2267.

Franklin, A.B., Ramey, A.M., Bentler, K.T., Barrett, N.L., McCurdy, L.M., Ahlstrom, C.A., Bonnedahl, J., Shriner, S.A. and Chandler, J.C. 2020. Gulls as Sources of Environmental Contamination by Colistin-resistant Bacteria. Sci Rep 10(1), 4408.

Froelich, B., Bowen, J., Gonzalez, R., Snedeker, A. and Noble, R. 2013. Mechanistic and statistical models of total Vibrio abundance in the Neuse River Estuary. Water Res 47(15), 5783-5793.

Frolicher, T.L., Fischer, E.M. and Gruber, N. 2018. Marine heatwaves under global warming. Nature 560(7718), 360-364.

Fuhrman, J.A., Hewson, I., Schwalbach, M.S., Steele, J.A., Brown, M.V. and Naeem, S. 2006. Annually reoccurring bacterial communities are predictable from ocean conditions. Proc Natl Acad Sci U S A 103(35), 13104-13109.

Fuhrman, J.A., Steele, J.A., Hewson, I., Schwalbach, M.S., Brown, M.V., Green, J.L. and Brown, J.H. 2008. A latitudinal diversity gradient in planktonic marine bacteria. Proc Natl Acad Sci U S A 105(22), 7774-7778.

Gamito, S., Coelho, S. and Pérez-Ruzafa, A. 2019. Phyto- and zooplankton dynamics in two ICOLLs from Southern Portugal. Estuarine, Coastal and Shelf Science 216, 110-117.

Garcia-Aljaro, C., Blanch, A.R., Campos, C., Jofre, J. and Lucena, F. 2019. Pathogens, faecal indicators and human-specific microbial source-tracking markers in sewage. J Appl Microbiol 126(3), 701-717.

Gaviria-Figueroa, A., Preisner, E.C., Hoque, S., Feigley, C.E. and Norman, R.S. 2019. Emission and dispersal of antibiotic resistance genes through bioaerosols generated during the treatment of municipal sewage. Sci Total Environ 686, 402-412.

Ge, S., Wang, S., Yang, X., Qiu, S., Li, B. and Peng, Y. 2015. Detection of nitrifiers and evaluation of partial nitrification for wastewater treatment: A review. Chemosphere (Oxford) 140, 85-98.

Gholami-Ahangaran, M., Haj-Salehi, M., Karimi-Dehkordi, M., Ansari, M.J., Mahdi, O.A. and Jawad, M.A. 2022. Tetracycline resistant genes in Escherichia coli isolated from enteric disease in companion birds. Vet Res Forum 13(2), 279-282.

Gilbert, J.A., Steele, J.A., Caporaso, J.G., Steinbruck, L., Reeder, J., Temperton, B., Huse, S., McHardy, A.C., Knight, R., Joint, I., Somerfield, P., Fuhrman, J.A. and Field, D. 2012. Defining seasonal marine microbial community dynamics. ISME J 6(2), 298-308.

Gillings, M.R., Gaze, W.H., Pruden, A., Smalla, K., Tiedje, J.M. and Zhu, Y.G. 2015. Using the class 1 integron-integrase gene as a proxy for anthropogenic pollution. ISME J 9(6), 1269-1279.

Gobler, C.J., Doherty, O.M., Hattenrath-Lehmann, T.K., Griffith, A.W., Kang, Y. and Litaker, R.W. 2017. Ocean warming since 1982 has expanded the niche of toxic algal blooms in the North Atlantic and North Pacific oceans. Proceedings of the National Academy of Sciences - PNAS 114(19), 4975-4980.

Gomez-Pereira, P.R., Fuchs, B.M., Alonso, C., Oliver, M.J., van Beusekom, J.E. and Amann, R. 2010. Distinct flavobacterial communities in contrasting water masses of the north Atlantic Ocean. ISME J 4(4), 472-487.

González-Escalona, N., Cachicas, V., Acevedo, C., Rioseco, M.L., Vergara, J.A., Cabello, F., Romero, J. and Espejo, R.T. 2005. Vibrio parahaemolyticus diarrhea, Chile, 1998 and 2004. Emerging infectious diseases 11(1), 129-131.

Gonzalez-Martinez, A., Rodriguez-Sanchez, A., Lotti, T., Garcia-Ruiz, M.J., Osorio, F., Gonzalez-Lopez, J. and van Loosdrecht, M.C. 2016. Comparison of bacterial communities of conventional and A-stage activated sludge systems. Sci Rep 6, 18786.

Grape, M., Motakefi, A., Pavuluri, S. and Kahlmeter, G. 2007. Standard and real-time multiplex PCR methods for detection of trimethoprim resistance dfr genes in large collections of bacteria. Clin Microbiol Infect 13(11), 1112-1118.

Green, H.C., Dick, L.K., Gilpin, B., Samadpour, M. and Field, K.G. 2012. Genetic markers for rapid PCR-based identification of gull, Canada goose, duck, and chicken fecal contamination in water. Appl Environ Microbiol 78(2), 503-510.

Green, H.C., Haugland, R.A., Varma, M., Millen, H.T., Borchardt, M.A., Field, K.G., Walters, W.A., Knight, R., Sivaganesan, M., Kelty, C.A. and Shanks, O.C. 2014a. Improved HF183 quantitative real-time PCR assay for characterization of human fecal pollution in ambient surface water samples. Applied and Environmental Microbiology 80(10), 3086-3094.

Green, H.C., Weller, D., Johnson, S. and Michalenko, E. 2019a. Microbial Source-Tracking Reveals Origins of Fecal Contamination in a Recovering Watershed. Water (Basel) 11(10).

Green, H.C., White, K.M., Kelty, C.A. and Shanks, O.C. 2014b. Development of rapid canine fecal source identification PCR-based assays. Environ Sci Technol 48(19), 11453-11461.

Green, T.J., Siboni, N., King, W.L., Labbate, M., Seymour, J.R. and Raftos, D. 2019b. Simulated Marine Heat Wave Alters Abundance and Structure of Vibrio Populations Associated with the Pacific Oyster Resulting in a Mass Mortality Event. Microb Ecol 77(3), 736-747.

Gubala, A.J. and Proll, D.F. 2006. Molecular-beacon multiplex real-time PCR assay for detection of Vibrio cholerae. Appl Environ Microbiol 72(9), 6424-6428.

Guillou, L., Bachar, D., Audic, S., Bass, D., Berney, C., Bittner, L., Boutte, C., Burgaud, G., de Vargas, C., Decelle, J., Del Campo, J., Dolan, J.R., Dunthorn, M., Edvardsen, B., Holzmann, M., Kooistra, W.H., Lara, E., Le Bescot, N., Logares, R., Mahe, F., Massana, R., Montresor, M., Morard, R., Not, F., Pawlowski, J., Probert, I., Sauvadet, A.L., Siano, R., Stoeck, T., Vaulot, D., Zimmermann, P. and Christen, R. 2013. The Protist Ribosomal Reference database (PR2): a catalog of unicellular eukaryote small sub-unit rRNA sequences with curated taxonomy. Nucleic Acids Res 41(Database issue), D597-604.

Haines, P.E., Tomlinson, R.B. and Thom, B.G. 2006. Morphometric assessment of intermittently open/closed coastal lagoons in New South Wales, Australia. Estuarine, coastal and shelf science 67(1-2), 321-332.

Halpern, B., Walbridge, S., Selkoe, K.A., Kappel, C.V., Micheli, F., D'Agrosa, C., Bruno, J.F., Casey, K.S., Ebert, C., Fox, H.E., Fujita, R., Heinemann, D., Lenihan, H.S., Madin, E.M.P., Perry, M.T., Selig, E.R., Spalding, M., Steneck, R. and Watson, R. 2008. Global Map of Human Impact on Marine Ecosystems. Science 319, 948-952.

Hammer, Ø., Harper, D.A.T. and Ryan, P.D. 2001. Past: Paleontological statistics software package for education and data analysis. Palaeontologia electronica 4(1), XIX-XX.

Hammerum, A.M. 2012. Enterococci of animal origin and their significance for public health. Clin Microbiol Infect 18(7), 619-625.

Hartwick, M.A., Berenson, A., Whistler, C.A., Naumova, E.N. and Jones, S.H. 2021. The seasonal microbial ecology of plankton and plankton-associated vibrio parahaemolyticus in the northeast united states. Applied and environmental microbiology 87(15), 1-15.

Haugland, R.A., Varma, M., Sivaganesan, M., Kelty, C., Peed, L. and Shanks, O.C. 2010. Evaluation of genetic markers from the 16S rRNA gene V2 region for use in quantitative detection of selected Bacteroidales species and human fecal waste by qPCR. Systematic and applied microbiology 33(6), 348-357.

Heidelberg, J.F., Heidelberg, K.B. and Colwell, R.R. 2002. Seasonality of Chesapeake Bay bacterioplankton species. Appl Environ Microbiol 68(11), 5488-5497.

Herve, V., Leroy, B., Pires, A.D. and Lopez, P.J. 2018. Aquatic urban ecology at the scale of a capital: community structure and interactions in street gutters. Isme J. 12(1), 253-266.

Hillebrand, H. 2004. Strength, slope and variability of marine latitudinal gradients. Marine ecology. Progress series (Halstenbek) 273, 251-268.

Hindson, C.M., Chevillet, J.R., Briggs, H.A., Gallichotte, E.N., Ruf, I.K., Hindson, B.J., Vessella, R.L. and Tewari, M. 2013. Absolute quantification by droplet digital PCR versus analog real-time PCR. Nat Methods 10(10), 1003-1005.

Hobday, A. and Lough, J.M. 2011. Projected climate change in Australian marine and freshwater environments: Climate Change and Australian Aquatic Environments, Fish and Fisheries. Marine and freshwater research 62(9), 1000-1014.

Hobday, A.J., Alexander, L.V., Perkins, S.E., Smale, D.A., Straub, S.C., Oliver, E.C.J., Benthuysen, J.A., Burrows, M.T., Donat, M.G., Feng, M., Holbrook, N.J., Moore, P.J., Scannell, H.A., Sen Gupta, A. and Wernberg, T. 2016. A hierarchical approach to defining marine heatwaves. Progress in Oceanography 141, 227-238.

Houf, K., De Smet, S., Bare, J. and Daminet, S. 2008. Dogs as carriers of the emerging pathogen Arcobacter. Vet Microbiol 130(1-2), 208-213.

Howardjones, N. 1984. MEDICAL HISTORY - KOCH,ROBERT AND THE CHOLERA VIBRIO - A CENTENARY. Br. Med. J. 288(6414), 379-381.

Hsieh, J.L., Fries, J.S. and Noble, R.T. 2008. Dynamics and predictive modelling of Vibrio spp. in the Neuse River Estuary, North Carolina, USA. Environ Microbiol 10(1), 57-64.

Hu, A., Yang, X., Chen, N., Hou, L., Ma, Y. and Yu, C.P. 2014. Response of bacterial communities to environmental changes in a mesoscale subtropical watershed, Southeast China. Sci Total Environ 472, 746-756.

Hughes, T.P., Kerry, J.T., Alvarez-Noriega, M., Alvarez-Romero, J.G., Anderson, K.D., Baird, A.H., Babcock, R.C., Beger, M., Bellwood, D.R., Berkelmans, R., Bridge, T.C., Butler, I.R., Byrne, M., Cantin, N.E., Comeau, S., Connolly, S.R., Cumming, G.S., Dalton, S.J., Diaz-Pulido, G., Eakin, C.M., Figueira, W.F., Gilmour, J.P., Harrison, H.B., Heron, S.F., Hoey, A.S., Hobbs, J.A., Hoogenboom, M.O., Kennedy, E.V., Kuo, C.Y., Lough, J.M., Lowe, R.J., Liu, G., McCulloch, M.T., Malcolm, H.A., McWilliam, M.J., Pandolfi, J.M., Pears, R.J., Pratchett, M.S., Schoepf, V., Simpson, T., Skirving, W.J., Sommer, B., Torda, G., Wachenfeld, D.R., Willis, B.L. and Wilson, S.K. 2017. Global warming and recurrent mass bleaching of corals. Nature 543(7645), 373-377.

Humpage, A. 2008. Toxin types, toxicokinetics and toxicodynamics. Advances in experimental medicine and biology 619, 383-415.

Huovinen, P., Sundstrom, L., Swedberg, G. and Skold, O. 1995. Trimethoprim and sulfonamide resistance. Antimicrobial agents and chemotherapy 39(2), 279-289.

Istiqomah, I., Sukardi, S., Murwantoko, M. and Isnansetyo, A. 2020. Review Vibriosis Management in Indonesian Marine Fish Farming. E3S Web of Conferences 147, 1001.

Jacobs, L. and Chenia, H.Y. 2007. Characterization of integrons and tetracycline resistance determinants in Aeromonas spp. isolated from South African aquaculture systems. Int J Food Microbiol 114(3), 295-306.

Janda, J.M. and Abbott, S.L. 2010. The genus Aeromonas: taxonomy, pathogenicity, and infection. Clin Microbiol Rev 23(1), 35-73.

Jarma, D., Sanchez, M.I., Green, A.J., Peralta-Sanchez, J.M., Hortas, F., Sanchez-Melsio, A. and Borrego, C.M. 2021. Faecal microbiota and antibiotic resistance genes in migratory waterbirds with contrasting habitat use. Sci Total Environ 783, 146872.

Jasim, S.A., Al-Abodi, H.R. and Ali, W.S. 2021. Resistance rate and novel virulence factor determinants of Arcobacter spp., from cattle fresh meat products from Iraq. Microb Pathog 152, 104649.

Jeffries, T.C., Schmitz Fontes, M.L., Harrison, D.P., Van-Dongen-Vogels, V., Eyre, B.D., Ralph, P.J. and Seymour, J.R. 2016. Bacterioplankton dynamics within a large anthropogenically impacted urban estuary. Frontiers in microbiology 6, 1438-1438.

Jindal, P., Bedi, J., Singh, R., Aulakh, R. and Gill, J. 2021. Phenotypic and genotypic antimicrobial resistance patterns of Escherichia coli and Klebsiella isolated from dairy farm milk, farm slurry and water in Punjab, India. Environ Sci Pollut Res Int 28(22), 28556-28570.

Johnson, C. 2020 Towards safer swimming – Rose Bay: Stormwater catchment audit. DPIE (ed).

Johnson, C. 2021 Towards safer swimming – Terrigal region: Terrigal Bay, Terrigal Lagoon and Avoca Lagoon stormwater catchment audit. DPIE (ed).

Johnson, C.N., Flowers, A.R., Noriea, N.F., 3rd, Zimmerman, A.M., Bowers, J.C., DePaola, A. and Grimes, D.J. 2010. Relationships between environmental factors and pathogenic Vibrios in the Northern Gulf of Mexico. Appl Environ Microbiol 76(21), 7076-7084.

Jones, H.F.E., Ozkundakci, D., McBride, C.G., Pilditch, C.A., Allan, M.G. and Hamilton, D.P. 2018. Modelling interactive effects of multiple disturbances on a coastal lake ecosystem: Implications for management. J. Environ. Manage. 207, 444-455.

Karkman, A., Parnanen, K. and Larsson, D.G.J. 2019. Fecal pollution can explain antibiotic resistance gene abundances in anthropogenically impacted environments. Nat Commun 10(1), 80.

Kennish, M.J. 2002. Environmental threats and environmental future of estuaries. Environmental Conservation 29(1), 78-107.

Kennish, M.J. (2017) Practical handbook of estuarine and marine pollution, CRC Press.

Kesy, K., Labrenz, M., Scales, B.S., Kreikemeyer, B. and Oberbeckmann, S. 2020. Vibrio Colonization Is Highly Dynamic in Early Microplastic-Associated Biofilms as Well as on Field-Collected Microplastics. Microorganisms 9(1).

King, W.L., Siboni, N., Kahlke, T., Green, T.J., Labbate, M. and Seymour, J.R. 2019. A New High Throughput Sequencing Assay for Characterizing the Diversity of Natural Vibrio Communities and Its Application to a Pacific Oyster Mortality Event. Frontiers in microbiology 10, 2907-2907.

Kirchman, D.L. and Gasol, J.M. (2018) Microbial Ecology of the Oceans, John Wiley & Sons, Incorporated, Newark.

Klein, E.Y., Milkowska-Shibata, M., Tseng, K.K., Sharland, M., Gandra, S., Pulcini, C. and Laxminarayan, R. 2021. Assessment of WHO antibiotic consumption and access targets in 76 countries, 2000–15: an analysis of pharmaceutical sales data. The Lancet Infectious Diseases 21(1), 107-115.

Klisch, M. and Häder, D.-P. 2008. Mycosporine-like amino acids and marine toxins--the common and the different. Marine drugs 6(2), 147-163.

Knights, D., Kuczynski, J., Charlson, E.S., Zaneveld, J., Mozer, M.C., Collman, R.G., Bushman, F.D., Knight, R. and Kelley, S.T. 2011. Bayesian community-wide culture-independent microbial source tracking. Nat Methods 8(9), 761-763.

Koskey, A.M., Fisher, J.C., Eren, A.M., Ponce-Terashima, R., Reis, M.G., Blanton, R.E. and McLellan, S.L. 2014. Blautia and Prevotella sequences distinguish human and animal fecal pollution in Brazil surface waters: Blautia and Prevotella distinguish human fecal pollution. Environmental microbiology reports 6(6), 696-704.

Kunin, C.M. 1993. RESISTANCE TO ANTIMICROBIAL DRUGS - A WORLDWIDE CALAMITY. Ann. Intern. Med. 118(7), 557-561.

Kushmaro, A., Banin, E., Loya, Y., Stackebrandt, E. and Rosenberg, E. 2001. Vibrio shiloi sp. nov., the causative agent of bleaching of the coral Oculina patagonica. Int J Syst Evol Microbiol 51(Pt 4), 1383-1388.

Laas, P., Ugarelli, K., Travieso, R., Stumpf, S., Gaiser, E.E., Kominoski, J.S. and Stingl, U. 2022. Water Column Microbial Communities Vary along Salinity Gradients in the Florida Coastal Everglades Wetlands. Microorganisms 10(2).

Lafferty, K.D., Harvell, C.D., Conrad, J.M., Friedman, C.S., Kent, M.L., Kuris, A.M., Powell, E.N., Rondeau, D. and Saksida, S.M. 2015. Infectious diseases affect marine fisheries and aquaculture economics. Ann Rev Mar Sci 7, 471-496.

Lau, J.D., Hicks, C.C., Gurney, G.G. and Cinner, J.E. 2019. What matters to whom and why? Understanding the importance of coastal ecosystem services in developing coastal communities. Ecosystem Services 35, 219-230.

Layton, B.A., Walters, S.P., Lam, L.H. and Boehm, A.B. 2010. Enterococcus species distribution among human and animal hosts using multiplex PCR. J Appl Microbiol 109(2), 539-547.

Lefeuvre, J.C., Laffaille, P., Feunteun, E., Bouchard, V. and Radureau, A. 2003. Biodiversity in salt marshes: from patrimonial value to ecosystem functioning. The case study of the Mont-Saint-Michel bay. C. R. Biol. 326, S125-S131.

Leonard, A.F., Zhang, L., Balfour, A.J., Garside, R. and Gaze, W.H. 2015. Human recreational exposure to antibiotic resistant bacteria in coastal bathing waters. Environ Int 82, 92-100.

Leonard, A.F.C., Zhang, L., Balfour, A.J., Garside, R., Hawkey, P.M., Murray, A.K., Ukoumunne, O.C. and Gaze, W.H. 2018. Exposure to and colonisation by antibiotic-resistant E. coli in UK coastal water users: Environmental surveillance, exposure assessment, and epidemiological study (Beach Bum Survey). Environ Int 114, 326-333.

Levican, A., Alkeskas, A., Gunter, C., Forsythe, S.J. and Figueras, M.J. 2013. Adherence to and invasion of human intestinal cells by Arcobacter species and their virulence genotypes. Appl Environ Microbiol 79(16), 4951-4957.

Lewis, D.J., Voeller, D., Saitone, T.L. and Tate, K.W. 2019. Management Scale Assessment of Practices to Mitigate Cattle Microbial Water Quality Impairments of Coastal Waters. Sustainability 11(19).

Li, D., Van De Werfhorst, L.C., Steets, B., Ervin, J., Murray, J.L.S., Blackwell, A., Devarajan, N. and Holden, P.A. 2021. Sources of Low Level Human Fecal Markers in Recreational Waters of Two Santa Barbara, CA Beaches: Roles of WWTP Outfalls and Swimmers. Water Res 202, 117378.

Li, N., Dong, K., Jiang, G., Tang, J., Xu, Q., Li, X., Kang, Z., Zou, S., Chen, X., Adams, J.M. and Zhao, H. 2020. Stochastic processes dominate marine free-living Vibrio community assembly in a subtropical gulf. FEMS Microbiol Ecol 96(11).

Li, R., Carmichael, W.W., Brittain, S., Eaglesham, G.K., Shaw, G.R., Liu, Y. and Watanabe, M.M. 2001. FIRST REPORT OF THE CYANOTOXINS CYLINDROSPERMOPSIN AND DEOXYCYLINDROSPERMOPSIN FROM RAPHIDIOPSIS CURVATA (CYANOBACTERIA). J. Phycol. 37(6), 1121-1126.

Liang, H., Yu, Z., Wang, B., Ndayisenga, F., Liu, R., Zhang, H. and Wu, G. 2021. Synergistic Application of Molecular Markers and Community-Based Microbial Source Tracking Methods for Identification of Fecal Pollution in River Water During Dry and Wet Seasons. Front Microbiol 12, 660368.

Liang, J., Liu, J., Wang, X., Lin, H., Liu, J., Zhou, S., Sun, H. and Zhang, X.-H. 2019. Spatiotemporal Dynamics of Free-Living and Particle-Associated Vibrio Communities in the Northern Chinese Marginal Seas. Applied and environmental microbiology 85(9).

Lima, F.P. and Wethey, D.S. 2012. Three decades of high-resolution coastal sea surface temperatures reveal more than warming. Nat Commun 3, 704.

Lombardo, M.N., N, G.D., Wright, D.L. and Anderson, A.C. 2016. Crystal Structures of Trimethoprim-Resistant DfrA1 Rationalize Potent Inhibition by Propargyl-Linked Antifolates. ACS Infect Dis 2(2), 149-156.

Lu, S., Lee, J.R., Ryu, S.H., Chung, B.S., Choe, W.S. and Jeon, C.O. 2007. Runella defluvii sp. nov., isolated from a domestic wastewater treatment plant. Int J Syst Evol Microbiol 57(Pt 11), 2600-2603.

Madakumbura, G.D., Thackeray, C.W., Norris, J., Goldenson, N. and Hall, A. 2021. Anthropogenic influence on extreme precipitation over global land areas seen in multiple observational datasets. Nat Commun 12(1), 3944.

Magoc, T. and Salzberg, S.L. 2011. FLASH: fast length adjustment of short reads to improve genome assemblies. Bioinformatics 27(21), 2957-2963.

Martin, M. 2011. Cutadapt removes adapter sequences from high-throughput sequencing reads. EMBnet.journal 17(1), 10.

Martinez Arbizu, P. 2020 pairwiseAdonis: Pairwise multilevel comparison using adonis.

Martinez-Urtaza, J., Huapaya, B., Gavilan, R.G., Blanco-Abad, V., Ansede-Bermejo, J., Cadarso-Suarez, C., Figueiras, A. and Trinanes, J. 2008. Emergence of Asiatic

Vibrio diseases in South America in phase with El Nino. Epidemiology 19(6), 829-837.

Mazel, D., Dychinco, B., Webb, V.A. and Davies, J. 2000. Antibiotic Resistance in the ECOR Collection: Integrons and Identification of a Novel aad Gene. Antimicrobial Agents and Chemotherapy 44(6), 1568-1574.

McLellan, S.L., Fisher, J.C. and Newton, R.J. 2015. The microbiome of urban waters. Int Microbiol 18(3), 141-149.

McLellan, S.L., Newton, R.J., Vandewalle, J.L., Shanks, O.C., Huse, S.M., Eren, A.M. and Sogin, M.L. 2013. Sewage reflects the distribution of human faecal Lachnospiraceae. Environ Microbiol 15(8), 2213-2227.

McLellan, S.L. and Roguet, A. 2019. The unexpected habitat in sewer pipes for the propagation of microbial communities and their imprint on urban waters. Curr Opin Biotechnol 57, 34-41.

McSweeney, S.L., Kennedy, D.M., Rutherfurd, I.D. and Stout, J.C. 2017. Intermittently closed/open lakes and lagoons; their global distribution and boundary conditions. Geomorphology (Amsterdam, Netherlands) 292, 142-152.

Michael, I., Rizzo, L., McArdell, C.S., Manaia, C.M., Merlin, C., Schwartz, T., Dagot, C. and Fatta-Kassinos, D. 2013. Urban wastewater treatment plants as hotspots for the release of antibiotics in the environment: a review. Water Res 47(3), 957-995.

Millar, J.A. and Raghavan, R. 2017. Accumulation and expression of multiple antibiotic resistance genes in Arcobacter cryaerophilus that thrives in sewage. PeerJ 5, e3269.

Mills, K., Pershing, A., Brown, C., Chen, Y., Chiang, F.-S., Holland, D., Lehuta, S., Nye, J., Sun, J., Thomas, A. and Wahle, R. 2013. Fisheries Management in a Changing Climate: Lessons From the 2012 Ocean Heat Wave in the Northwest Atlantic. Oceanography 26(2).

Mobaraki, S., Aghazadeh, M., Soroush Barhaghi, M.H., Yousef Memar, M., Goli, H.R., Gholizadeh, P. and Samadi Kafil, H. 2018. Prevalence of integrons 1, 2, 3 associated with antibiotic resistance in Pseudomonas aeruginosa isolates from Northwest of Iran. Biomedicine (Taipei) 8(1), 2.

Mobsby, D. and Curtotti, R. 2018 Australian fisheries and aquaculture statistics, ABARES.

Mokracka, J., Koczura, R. and Kaznowski, A. 2012. Multiresistant Enterobacteriaceae with class 1 and class 2 integrons in a municipal wastewater treatment plant. Water Res 46(10), 3353-3363.

Murray, C.J.L., Ikuta, K.S., Sharara, F., Swetschinski, L., Aguilar, G.R., Gray, A., Han, C., Bisignano, C., Rao, P., Wool, E., Johnson, S.C., Browne, A.J., Chipeta, M.G., Fell, F., Hackett, S., Haines-Woodhouse, G., Hamadani, B.H.K., Kumaran, E.A.P., McManigal, B., Agarwal, R., Akech, S., Albertson, S., Amuasi, J., Andrews, J., Aravkin, A., Ashley, E., Bailey, F., Baker, S., Basnyat, B., Bekker, A., Bender, R., Bethou, A., Bielicki, J., Boonkasidecha, S., Bukosia, J., Carvalheiro, C., Castaneda-Orjuela, C., Chansamouth, V., Chaurasia, S., Chiurchiu, S., Chowdhury, F., Cook, A.J., Cooper, B., Cressey, T.R., Criollo-Mora, E., Cunningham, M., Darboe, S., Day, N.P.J., De Luca, M., Dokova, K., Dramowski, A., Dunachie, S.J., Eckmanns, T., Eibach, D., Emami, A., Feasey, N., Fisher-Pearson, N., Forrest, K., Garrett, D., Gastmeier, P., Giref, A.Z., Greer, R.C., Gupta, V., Haller, S., Haselbeck, A., Hay, S.I., Holm, M., Hopkins, S., Iregbu, K.C., Jacobs, J., Jarovsky, D., Javanmardi, F.,

Khorana, M., Kissoon, N., Kobeissi, E., Kostyanev, T., Krapp, F., Krumkamp, R., Kumar, A., Kyu, H.H., Lim, C., Limmathurotsakul, D., Loftus, M.J., Lunn, M., Ma, J., Mturi, N., Munera-Huertas, T., Musicha, P., Mussi-Pinhata, M.M., Nakamura, T., Nanavati, R., Nangia, S., Newton, P., Ngoun, C., Novotney, A., Nwakanma, D., Obiero, C.W., Olivas-Martinez, A., Olliaro, P., Ooko, E., Ortiz-Brizuela, E., Peleg, A.Y., Perrone, C., Plakkal, N., Ponce-de-Leon, A., Raad, M., Ramdin, T., Riddell, A., Roberts, T., VictoriaRobotham, J., Roca, A., Rudd, K.E., Russell, N., Schnall, J., Scott, J.A.G., Shivamallappa, M., Sifuentes-Osornio, J., Steenkeste, N., Stewardson, A.J., Stoeva, T., Tasak, N., Thaiprakong, A., Thwaites, G., Turner, C., Turner, P., van Doorn, H.R., Velaphi, S., Vongpradith, A., Vu, H., Walsh, T., Waner, S., Wangrangsimakul, T., Wozniak, T., Zheng, P., Sartorius, B., Lopez, A.D., Stergachis, A., Moore, C., Dolecek, C., Naghavi, M. and Antimicrobial Resistance, C. 2022. Global burden of bacterial antimicrobial resistance in 2019: a systematic analysis. Lancet 399(10325), 629-655.

Neave, M., Luter, H., Padovan, A., Townsend, S., Schobben, X. and Gibb, K. 2014. Multiple approaches to microbial source tracking in tropical northern Australia. Microbiologyopen 3(6), 860-874.

Needham, D.M., Sachdeva, R. and Fuhrman, J.A. 2017. Ecological dynamics and co-occurrence among marine phytoplankton, bacteria and myoviruses shows microdiversity matters. ISME J 11(7), 1614-1629.

Nevers, M.B., Byappanahalli, M.N., Shively, D., Buszka, P.M., Jackson, P.R. and Phanikumar, M.S. 2018. Identifying and Eliminating Sources of Recreational Water Quality Degradation along an Urban Coast. J Environ Qual 47(5), 1042-1050.

Newton, A., Brito, A.C., Icely, J.D., Derolez, V., Clara, I., Angus, S., Schernewski, G., Inácio, M., Lillebø, A.I., Sousa, A.I., Béjaoui, B., Solidoro, C., Tosic, M., Cañedo-Argüelles, M., Yamamuro, M., Reizopoulou, S., Tseng, H.-C., Canu, D., Roselli, L., Maanan, M., Cristina, S., Ruiz-Fernández, A.C., Lima, R.F.d., Kjerfve, B., Rubio-Cisneros, N., Pérez-Ruzafa, A., Marcos, C., Pastres, R., Pranovi, F., Snoussi, M., Turpie, J., Tuchkovenko, Y., Dyack, B., Brookes, J., Povilanskas, R. and Khokhlov, V. 2018. Assessing, quantifying and valuing the ecosystem services of coastal lagoons. Journal for Nature Conservation 44, 50-65.

Newton, R.J., Bootsma, M.J., Morrison, H.G., Sogin, M.L. and McLellan, S.L. 2013. A microbial signature approach to identify fecal pollution in the waters off an urbanized coast of Lake Michigan. Microb Ecol 65(4), 1011-1023.

Newton, R.J., McLellan, S.L., Dila, D.K., Vineis, J.H., Morrison, H.G., Eren, A.M. and Sogin, M.L. 2015. Sewage reflects the microbiomes of human populations. mBio 6(2), e02574.

Nguyen, K.H., Senay, C., Young, S., Nayak, B., Lobos, A., Conrad, J. and Harwood, V.J. 2018. Determination of wild animal sources of fecal indicator bacteria by microbial source tracking (MST) influences regulatory decisions. Water Res 144, 424-434.

Nigro, O.D., Hou, A., Vithanage, G., Fujioka, R.S. and Steward, G.F. 2011. Temporal and spatial variability in culturable pathogenic Vibrio spp. in Lake Pontchartrain, Louisiana, following hurricanes Katrina and Rita. Appl Environ Microbiol 77(15), 5384-5393.

Nyholm, S.V. and McFall-Ngai, M.J. 2021. A lasting symbiosis: how the Hawaiian bobtail squid finds and keeps its bioluminescent bacterial partner. Nat Rev Microbiol 19(10), 666-679.

O'Neil, J.M., Davis, T.W., Burford, M.A. and Gobler, C.J. 2012. The rise of harmful cyanobacteria blooms: The potential roles of eutrophication and climate change. Harmful Algae 14, 313-334.

O'Brien, D. and Eddie, I. 2013 Benchmarking global best practice: Innovation and leadership in surf city tourism and industry development.

O'Brien, J., McParland, E.L., Bramucci, A.R., Siboni, N., Ostrowski, M., Kahlke, T., Levine, N.M., Brown, M.V., van de Kamp, J., Bodrossy, L., Messer, L.F., Petrou, K. and Seymour, J.R. 2022. Biogeographical and seasonal dynamics of the marine Roseobacter community and ecological links to DMSP-producing phytoplankton. ISME Communications 2(1).

Oberbeckmann, S., Fuchs, B.M., Meiners, M., Wichels, A., Wiltshire, K.H. and Gerdts, G. 2012. Seasonal dynamics and modeling of a Vibrio community in coastal waters of the North Sea. Microb Ecol 63(3), 543-551.

OEH 2018 State of the beaches 2017-2018.

Okabe, S. and Shimazu, Y. 2007. Persistence of host-specific Bacteroides-Prevotella 16S rRNA genetic markers in environmental waters: effects of temperature and salinity. Applied microbiology and biotechnology 76(4), 935-944.

Olds, H.T., Corsi, S.R., Dila, D.K., Halmo, K.M., Bootsma, M.J. and McLellan, S.L. 2018. High levels of sewage contamination released from urban areas after storm events: A quantitative survey with sewage specific bacterial indicators. PLoS Med 15(7), e1002614.

Oliver, E.C.J., Donat, M.G., Burrows, M.T., Moore, P.J., Smale, D.A., Alexander, L.V., Benthuysen, J.A., Feng, M., Sen Gupta, A., Hobday, A.J., Holbrook, N.J., Perkins-Kirkpatrick, S.E., Scannell, H.A., Straub, S.C. and Wernberg, T. 2018. Longer and more frequent marine heatwaves over the past century. Nature Communications 9(1).

Ortega-Paredes, D., Haro, M., Leoro-Garzon, P., Barba, P., Loaiza, K., Mora, F., Fors, M., Vinueza-Burgos, C. and Fernandez-Moreira, E. 2019. Multidrug-resistant Escherichia coli isolated from canine faeces in a public park in Quito, Ecuador. J Glob Antimicrob Resist 18, 263-268.

Paaijmans, K.P., Takken, W., Githeko, A.K. and Jacobs, A.F. 2008. The effect of water turbidity on the near-surface water temperature of larval habitats of the malaria mosquito Anopheles gambiae. Int J Biometeorol 52(8), 747-753.

Padovan, A., Siboni, N., Kaestli, M., King, W.L., Seymour, J.R. and Gibb, K. 2021. Occurrence and dynamics of potentially pathogenic vibrios in the wet-dry tropics of northern Australia. Mar Environ Res 169, 105405.

Paerl, H.W., Gardner, W.S., Havens, K.E., Joyner, A.R., McCarthy, M.J., Newell, S.E., Qin, B. and Scott, J.T. 2016. Mitigating cyanobacterial harmful algal blooms in aquatic ecosystems impacted by climate change and anthropogenic nutrients. Harmful algae 54, 213-222.

Paerl, H.W., Hall, N.S. and Calandrino, E.S. 2011. Controlling harmful cyanobacterial blooms in a world experiencing anthropogenic and climatic-induced change. The Science of the total environment 409(10), 1739-1745.

Paoli, L., Ruscheweyh, H.J., Forneris, C.C., Hubrich, F., Kautsar, S., Bhushan, A., Lotti, A., Clayssen, Q., Salazar, G., Milanese, A., Carlstrom, C.I., Papadopoulou, C., Gehrig, D., Karasikov, M., Mustafa, H., Larralde, M., Carroll, L.M., Sanchez, P., Zayed, A.A., Cronin, D.R., Acinas, S.G., Bork, P., Bowler, C., Delmont, T.O., Gasol, J.M., Gossert, A.D., Kahles, A., Sullivan, M.B., Wincker, P., Zeller, G., Robinson, S.L., Piel, J. and Sunagawa, S. 2022. Biosynthetic potential of the global ocean microbiome. Nature 607(7917), 111-118.

Parker, J.K., McIntyre, D. and Noble, R.T. 2010. Characterizing fecal contamination in stormwater runoff in coastal North Carolina, USA. Water Res 44(14), 4186-4194.

Parker, J.L. and Shaw, J.G. 2011. Aeromonas spp. clinical microbiology and disease. J Infect 62(2), 109-118.

Pascual-Benito, M., Balleste, E., Monleon-Getino, T., Urmeneta, J., Blanch, A.R., Garcia-Aljaro, C. and Lucena, F. 2020. Impact of treated sewage effluent on the bacterial community composition in an intermittent mediterranean stream. Environ Pollut 266(Pt 1), 115254.

Paulus, G.K., Hornstra, L.M., Alygizakis, N., Slobodnik, J., Thomaidis, N. and Medema, G. 2019. The impact of on-site hospital wastewater treatment on the downstream communal wastewater system in terms of antibiotics and antibiotic resistance genes. Int J Hyg Environ Health 222(4), 635-644.

Paz, S., Bisharat, N., Paz, E., Kidar, O. and Cohen, D. 2007. Climate change and the emergence of Vibrio vulnificus disease in Israel. Environ Res 103(3), 390-396.

Pearman, J.K., Afandi, F., Hong, P. and Carvalho, S. 2018. Plankton community assessment in anthropogenic-impacted oligotrophic coastal regions. Environ Sci Pollut Res Int 25(31), 31017-31030.

Pei, R., Kim, S.C., Carlson, K.H. and Pruden, A. 2006. Effect of river landscape on the sediment concentrations of antibiotics and corresponding antibiotic resistance genes (ARG). Water Res 40(12), 2427-2435.

Perez-Cataluna, A., Salas-Masso, N., Dieguez, A.L., Balboa, S., Lema, A., Romalde, J.L. and Figueras, M.J. 2018. Revisiting the Taxonomy of the Genus Arcobacter: Getting Order From the Chaos. Front Microbiol 9, 2077.

Pianka, E.R. 1966. Latitudinal Gradients in Species Diversity: A Review of Concepts. The American naturalist 100(910), 33-46.

Pichler, M., Coskun, O.K., Ortega-Arbulu, A.S., Conci, N., Worheide, G., Vargas, S. and Orsi, W.D. 2018. A 16S rRNA gene sequencing and analysis protocol for the Illumina MiniSeq platform. Microbiologyopen 7(6), e00611.

Polak, O. and Shashar, N. 2013. Economic value of biological attributes of artificial coral reefs. ICES J. Mar. Sci. 70(4), 904-912.

Pommier, T., Canback, B., Riemann, L., Bostrom, K.H., Simu, K., Lundberg, P., Tunlid, A. and Hagstrom, A. 2007. Global patterns of diversity and community structure in marine bacterioplankton. Mol Ecol 16(4), 867-880.

Raes, E.J., Bodrossy, L., van de Kamp, J., Bissett, A. and Waite, A.M. 2018. Marine bacterial richness increases towards higher latitudes in the eastern Indian Ocean. Limnology and oceanography letters 3(1), 10-19.

Ralston, E.P., Kite-Powell, H. and Beet, A. 2011. An estimate of the cost of acute health effects from food- and water-borne marine pathogens and toxins in the USA. Journal of Water and Health 9(4), 680-694.

Randa, M.A., Polz, M.F. and Lim, E. 2004. Effects of temperature and salinity on Vibrio vulnificus population dynamics as assessed by quantitative PCR. Appl Environ Microbiol 70(9), 5469-5476.

Rasmussen-Ivey, C.R., Figueras, M.J., McGarey, D. and Liles, M.R. 2016. Virulence Factors of Aeromonas hydrophila: In the Wake of Reclassification. Front Microbiol 7, 1337.

Reischer, G.H., Kasper, D.C., Steinborn, R., Mach, R.L. and Farnleitner, A.H. 2006. Quantitative PCR Method for Sensitive Detection of Ruminant Fecal Pollution in Freshwater and Evaluation of This Method in Alpine Karstic Regions. Applied and Environmental Microbiology 72(8), 5610-5614.

Rich, A. and Keller, E.A. 2013. A hydrologic and geomorphic model of estuary breaching and closure. Geomorphology 191, 64-74.

Rippey, S.R. 1994. Infectious diseases associated with molluscan shellfish consumption. Clinical microbiology reviews 7(4), 419-425.

Rizvi, A.V. and Bej, A.K. 2010. Multiplexed real-time PCR amplification of tlh, tdh and trh genes in Vibrio parahaemolyticus and its rapid detection in shellfish and Gulf of Mexico water. Antonie Van Leeuwenhoek 98(3), 279-290.

Rognes, T., Flouri, T., Nichols, B., Quince, C. and Mahe, F. 2016. VSEARCH: a versatile open source tool for metagenomics. PeerJ 4, e2584.

Rothenheber, D. and Jones, S. 2018. Enterococcal Concentrations in a Coastal Ecosystem Are a Function of Fecal Source Input, Environmental Conditions, and Environmental Sources. Appl Environ Microbiol 84(17).

Roy, K., Jablonski, D., Valentine, J.W. and Rosenberg, G. 1998. Marine Latitudinal Diversity Gradients: Tests of Causal Hypotheses. Proceedings of the National Academy of Sciences - PNAS 95(7), 3699-3702.

Ryan, D.E. and Campbell, L. 2016. Identification and phylogeny of putative PEPC genes in three toxin-producing Karenia (Dinophyta) species. J. Phycol. 52(4), 618-625.

Sadat-Noori, M., Santos, I.R., Tait, D.R., McMahon, A., Kadel, S. and Maher, D.T. 2016. Intermittently Closed and Open Lakes and/or Lagoons (ICOLLs) as groundwater-dominated coastal systems: Evidence from seasonal radon observations. Journal of hydrology (Amsterdam) 535, 612-624.

Sala, E., Mayorga, J., Bradley, D., Cabral, R.B., Atwood, T.B., Auber, A., Cheung, W., Costello, C., Ferretti, F., Friedlander, A.M., Gaines, S.D., Garilao, C., Goodell, W., Halpern, B.S., Hinson, A., Kaschner, K., Kesner-Reyes, K., Leprieur, F., McGowan, J., Morgan, L.E., Mouillot, D., Palacios-Abrantes, J., Possingham, H.P., Rechberger, K.D., Worm, B. and Lubchenco, J. 2021. Protecting the global ocean for biodiversity, food and climate. Nature 592(7854), 397-402.

Sarmah, A.K., Meyer, M.T. and Boxall, A.B. 2006. A global perspective on the use, sales, exposure pathways, occurrence, fate and effects of veterinary antibiotics (VAs) in the environment. Chemosphere 65(5), 725-759.

Sarmiento, J.L. and Gruber, N. (2007) Ocean Biogeochemical Dynamics Ocean Biogeochemical Dynamics.

Sauer, E.P., Vandewalle, J.L., Bootsma, M.J. and McLellan, S.L. 2011. Detection of the human specific Bacteroides genetic marker provides evidence of widespread sewage contamination of stormwater in the urban environment. Water Res 45(14), 4081-4091.

Savio, D., Sinclair, L., Ijaz, U.Z., Parajka, J., Reischer, G.H., Stadler, P., Blaschke, A.P., Bloschl, G., Mach, R.L., Kirschner, A.K., Farnleitner, A.H. and Eiler, A. 2015. Bacterial diversity along a 2600 km river continuum. Environ Microbiol 17(12), 4994-5007.

Scallan, E., Hoekstra, R.M., Angulo, F.J., Tauxe, R.V., Widdowson, M.-A., Roy, S.L., Jones, J.L. and Griffin, P.M. 2011. Foodborne illness acquired in the United States-Major pathogens. Emerging infectious diseases 17(1), 7-15.

Scanes, E., Scanes, P.R. and Ross, P.M. 2020a. Climate change rapidly warms and acidifies Australian estuaries. Nature communications 11(1), 1803-1803.

Scanes, P.R., Ferguson, A. and Potts, J. 2020b. Catastrophic events and estuarine connectivity influence presence of aquatic macrophytes and trophic status of intermittently-open coastal lagoons in eastern Australia. Estuarine, coastal and shelf science 238, 106732.

Schallenberg, M., Larned, S.T., Hayward, S. and Arbuckle, C. 2010. Contrasting effects of managed opening regimes on water quality in two intermittently closed and open coastal lakes. Estuarine, coastal and shelf science 86(4), 587-597.

Schloss, P.D., Westcott, S.L., Ryabin, T., Hall, J.R., Hartmann, M., Hollister, E.B., Lesniewski, R.A., Oakley, B.B., Parks, D.H., Robinson, C.J., Sahl, J.W., Stres, B., Thallinger, G.G., Van Horn, D.J. and Weber, C.F. 2009. Introducing mothur: open-source, platform-independent, community-supported software for describing and comparing microbial communities. Appl Environ Microbiol 75(23), 7537-7541.

Scott, L.C., Wilson, M.J., Esser, S.M., Lee, N.L., Wheeler, M.E., Aubee, A. and Aw, T.G. 2021. Assessing visitor use impact on antibiotic resistant bacteria and antibiotic resistance genes in soil and water environments of Rocky Mountain National Park. Sci Total Environ 785, 147122.

Sehein, T., Richlen, M.L., Nagai, S., Yasuike, M., Nakamura, Y. and Anderson, D.M. 2016. Characterization of 17 new microsatellite markers for the dinoflagellate Alexandrium fundyense (Dinophyceae), a harmful algal bloom species. Journal of Applied Phycology 28(3), 1677-1681.

Semenza, J.C., Trinanes, J., Lohr, W., Sudre, B., Lofdahl, M., Martinez-Urtaza, J., Nichols, G.L. and Rocklov, J. 2017. Environmental Suitability of Vibrio Infections in a Warming Climate: An Early Warning System. Environ Health Perspect 125(10), 107004.

Sercu, B., Van De Werfhorst, L.C., Murray, J.L. and Holden, P.A. 2011. Sewage exfiltration as a source of storm drain contamination during dry weather in urban watersheds. Environ Sci Technol 45(17), 7151-7157.

Sercu, B., Werfhorst, L.C.V.D., Murray, J. and Holden, P.A. 2009. Storm Drains are Sources of Human Fecal Pollution during Dry Weather in Three Urban Southern California Watersheds. Environmental science & technology 43(2), 293-298.

Seymour, J., Williams, N.L.R. and Siboni, N. 2020a. Microbial source-tracking to assess the spatial extent and temporal persistence of water quality issues at Terrigal Beach.

Seymour, J., Williams, N.L.R. and Siboni, N. 2020b. Microbial source-tracking to assess water quality issues at Rose Bay.

Seymour, J., Williams, N.L.R. and Siboni, N. 2021. Microbial source-tracking to assess water quality in Central Coast Lagoons.

Shaheen, B.W., Oyarzabal, O.A. and Boothe, D.M. 2010. The role of class 1 and 2 integrons in mediating antimicrobial resistance among canine and feline clinical E. coli isolates from the US. Vet Microbiol 144(3-4), 363-370.

Shanks, O.C., Atikovic, E., Blackwood, A.D., Lu, J., Noble, R.T., Domingo, J.S., Seifring, S., Sivaganesan, M. and Haugland, R.A. 2008. Quantitative PCR for Detection and Enumeration of Genetic Markers of Bovine Fecal Pollution. Applied and Environmental Microbiology 74(3), 745-752.

Shanks, O.C., Newton, R.J., Kelty, C.A., Huse, S.M., Sogin, M.L. and McLellan, S.L. 2013. Comparison of the microbial community structures of untreated wastewaters from different geographic locales. Appl Environ Microbiol 79(9), 2906-2913.

Shrestha, R.G., Tanaka, Y., Malla, B., Tandukar, S., Bhandari, D., Inoue, D., Sei, K., Sherchand, J.B. and Haramoto, E. 2018. Development of a Quantitative PCR Assay for Arcobacter spp. and its Application to Environmental Water Samples. Microbes Environ 33(3), 309-316.

Shuval, H. 2003. Estimating the global burden of thalassogenic diseases: human infectious diseases caused by wastewater pollution of the marine environment. Journal of water and health 1(2), 53-64.

Siboni, N., Balaraju, V., Carney, R., Labbate, M. and Seymour, J.R. 2016. Spatiotemporal Dynamics of Vibrio spp. within the Sydney Harbour Estuary. Front Microbiol 7, 460.

SjÖStedt, J., Koch-Schmidt, P., Pontarp, M., CanbÄCk, B., Tunlid, A., Lundberg, P., HagstrÖM, A. and Riemann, L. 2012. Recruitment of Members from the Rare Biosphere of Marine Bacterioplankton Communities after an Environmental Disturbance. Applied and Environmental Microbiology 78(5), 1361-1369.

Skarzynska, M., Zaja, C.M., Bomba, A., Bocian, L., Kozdrun, W., Polak, M., Wia Cek, J. and Wasyl, D. 2021. Antimicrobial Resistance Glides in the Sky-Free-Living Birds as a Reservoir of Resistant Escherichia coli With Zoonotic Potential. Front Microbiol 12, 656223.

Smith, F.M.J., Wood, S.A., van Ginkel, R., Broady, P.A. and Gaw, S. 2011. First report of saxitoxin production by a species of the freshwater benthic cyanobacterium, Scytonema Agardh. Toxicon (Oxford) 57(4), 566-573.

Sobsey, M., Khatib, L., Hill, V., Alocilja, E. and Pillai, S. 2011. Pathogens In Animal Wastes And The Impacts Of Waste Management Practices On Their Survival, Transport And Fate M. Anim. Agric. Environ., 1-5.

Staley, C., Gould, T.J., Wang, P., Phillips, J., Cotner, J.B. and Sadowsky, M.J. 2015. Species sorting and seasonal dynamics primarily shape bacterial communities in the Upper Mississippi River. Sci Total Environ 505, 435-445.

Steele, J.A., Countway, P.D., Xia, L., Vigil, P.D., Beman, J.M., Kim, D.Y., Chow, C.E., Sachdeva, R., Jones, A.C., Schwalbach, M.S., Rose, J.M., Hewson, I., Patel, A., Sun, F., Caron, D.A. and Fuhrman, J.A. 2011. Marine bacterial, archaeal and protistan association networks reveal ecological linkages. ISME J 5(9), 1414-1425.

Steinbakk, M., Lingaas, E., Carlstedt-Duke, B., Høverstad, T., Midtvedt, A.C., Norin, K.E. and Midtvedt, T. 1992. Faecal Concentration of Ten Antibiotics and Influence on Some Microflora-Associated Characteristics (MACs). Microbial Ecology in Health and Disease 5(5), 269-276.

Strubbia, S., Phan, M.V.T., Schaeffer, J., Koopmans, M., Cotten, M. and Le Guyader, F.S. 2019. Characterization of Norovirus and Other Human Enteric Viruses in Sewage and Stool Samples Through Next-Generation Sequencing. Food Environ Virol 11(4), 400-409.

Sunday, J.M., Bates, A.E. and Dulvy, N.K. 2012. Thermal tolerance and the global redistribution of animals. Nature Climate Change 2(9), 686-690.

Suzuki, M.T., Taylor, L.T. and DeLong, E.F. 2000. Quantitative Analysis of Small-Subunit rRNA Genes in Mixed Microbial Populations via 5′-Nuclease Assays. Applied and Environmental Microbiology 66(11), 4605-4614.

Takahashi, S., Tomita, J., Nishioka, K., Hisada, T. and Nishijima, M. 2014. Development of a prokaryotic universal primer for simultaneous analysis of Bacteria and Archaea using next-generation sequencing. PLoS One 9(8), e105592.

Takemura, A.F., Chien, D.M. and Polz, M.F. 2014. Associations and dynamics of Vibrionaceae in the environment, from the genus to the population level. Front Microbiol 5, 38.

Tallon, P., Magajna, B., Lofranco, C. and Kam, T.L. 2005. Microbial indicators of faecal contamination in water: A current perspective. Water, air, and soil pollution 166(1-4), 139-166.

Tan, L., Li, L., Ashbolt, N., Wang, X., Cui, Y., Zhu, X., Xu, Y., Yang, Y., Mao, D. and Luo, Y. 2018. Arctic antibiotic resistance gene contamination, a result of anthropogenic activities and natural origin. Sci Total Environ 621, 1176-1184.

Tang, K.F.J. and Bondad-Reantaso, M.G. 2019. Impacts of acute hepatopancreatic necrosis disease on commercial shrimp aquaculture. Rev Sci Tech 38(2), 477-490.

Teeling, H., Fuchs, B.M., Becher, D., Klockow, C., Gardebrecht, A., Bennke, C.M., Kassabgy, M., Huang, S., Mann, A.J., Waldmann, J., Weber, M., Klindworth, A., Otto, A., Lange, J., Bernhardt, J., Reinsch, C., Hecker, M., Peplies, J., Bockelmann, F.D., Callies, U., Gerdts, G., Wichels, A., Wiltshire, K.H., Glöckner, F.O., Schweder, T. and Amann, R. 2012. Substrate-Controlled Succession of Marine Bacterioplankton Populations Induced by a Phytoplankton Bloom. Science 336(6081), 608-611.

Templar, H.A., Dila, D.K., Bootsma, M.J., Corsi, S.R. and McLellan, S.L. 2016. Quantification of human-associated fecal indicators reveal sewage from urban watersheds as a source of pollution to Lake Michigan. Water Res 100, 556-567.

Testa, J.M., Brady, D.C., Di Toro, D.M., Boynton, W.R., Cornwell, J.C. and Kemp, W.M. 2013. Sediment flux modeling: Simulating nitrogen, phosphorus, and silica cycles. Estuarine, Coastal and Shelf Science 131, 245-263.

Thompson, F.L., Iida, T. and Swings, J. 2004. Biodiversity of vibrios. Microbiol Mol Biol Rev 68(3), 403-431, table of contents.

Thurstan, R.H., Brittain, Z., Jones, D.S., Cameron, E., Dearnaley, J. and Bellgrove, A. 2018. Aboriginal uses of seaweeds in temperate Australia: an archival assessment. Journal of Applied Phycology 30(3), 1821-1832.

Tiwari, S. and Nanda, M. 2019. Bacteremia caused by Comamonas testosteroni an unusual pathogen. J Lab Physicians 11(1), 87-90.

Topalcengiz, Z., Spanninger, P.M., Jeamsripong, S., Persad, A.K., Buchanan, R.L., Saha, J., LeJeune, J., Jay-Russell, M.T., Kniel, K.E. and Danyluk, M.D. 2020. Survival of Salmonella in Various Wild Animal Feces That May Contaminate Produce. J. Food Prot. 83(4), 651-660.

TourismAustralia 2019 ANNUAL REPORT 2018-19.

Trinanes, J. and Martinez-Urtaza, J. 2021. Future scenarios of risk of Vibrio infections in a warming planet: a global mapping study. The Lancet Planetary Health 5(7), e426-e435.

Tsihrintzis, V.A. and Hamid, R. 1997. Modeling and management of urban stormwater runoff quality: A review. Water resources management 11(2), 136-164.

Turner, A. 2000. Trace metal contamination in sediments from UK estuaries: An empirical evaluation of the role of hydrous iron and manganese oxides. Estuar. Coast. Shelf Sci. 50(3), 355-371.

Turner, J.W., Good, B., Cole, D. and Lipp, E.K. 2009. Plankton composition and environmental factors contribute to Vibrio seasonality. ISME J 3(9), 1082-1092.

Vezzulli, L., Baker-Austin, C., Kirschner, A., Pruzzo, C. and Martinez-Urtaza, J. 2020. Global emergence of environmental non-O1/O139 Vibrio cholerae infections linked with climate change: a neglected research field? Environmental microbiology 22(10), 4342-4355.

Vezzulli, L., Colwell, R.R. and Pruzzo, C. 2013. Ocean warming and spread of pathogenic vibrios in the aquatic environment. Microb Ecol 65(4), 817-825.

Vredenburg, J., Varela, A.R., Hasan, B., Bertilsson, S., Olsen, B., Narciso-da-Rocha, C., Bonnedahl, J., Stedt, J., Da Costa, P.M. and Manaia, C.M. 2014. Quinolone-resistant Escherichia coli isolated from birds of prey in Portugal are genetically distinct from those isolated from water environments and gulls in Portugal, Spain and Sweden. Environ Microbiol 16(4), 995-1004.

Wang, H., Huang, B. and Hong, H. 1997. Size-fractionated productivity and nutrient dynamics of phytoplankton in subtropical coastal environments. Hydrobiologia 352, 97–106.

Weidhaas, J. and Lipscomb, E. 2013. A new method for tracking poultry litter in the Potomac Basin headwaters of West Virginia. Journal of Applied Microbiology 115(2), 445-454.

Wen, Y., Schoups, G. and van de Giesen, N. 2017. Organic pollution of rivers: Combined threats of urbanization, livestock farming and global climate change. Sci Rep 7, 43289.

Wetz, J.J., Blackwood, A.D., Fries, J.S., Williams, Z.F. and Noble, R.T. 2008. Trends in total Vibrio spp. and Vibrio vulnificus concentrations in the eutrophic Neuse River Estuary, North Carolina, during storm events. Aquat. Microb. Ecol. 53, 141-149.

Wexler, H.M. 2007. Bacteroides: the good, the bad, and the nitty-gritty. Clin Microbiol Rev 20(4), 593-621.

Whitaker, D. and Christman, M. 2010 Package 'clustsig', version 1.0;.

White, S.D., Rosychuk, R.A.W., Rienke, S.I. and Paradis, M. 1992. Use of tetracycline and niacinamide for treatment of autoimmune skin disease in 31 dogs. Journal of the American Veterinary Medical Association 200(10), 1497-1500.

WHO 2016 Weekly epidemiological record, pp. 421-428, World Health Organization.

WHO 2021 Guidelines on Recreational Water Quality.

Williams, N.L.R., Siboni, N., McLellan, S.L., Potts, J., Scanes, P., Johnson, C., James, M., McCann, V. and Seymour, J.R. 2022a. Rainfall leads to elevated levels of antibiotic resistance genes within seawater at an Australian beach. Environ Pollut 307, 119456.

Williams, N.L.R., Siboni, N., Potts, J., Campey, M., Johnson, C., Rao, S., Bramucci, A., Scanes, P. and Seymour, J.R. 2022b. Molecular microbiological approaches reduce ambiguity about the sources of faecal pollution and identify microbial hazards within an urbanised coastal environment. Water Research 218.

Wong, Y.Y., Lee, C.W., Bong, C.W., Lim, J.H., Narayanan, K. and Sim, E.U.H. 2019. Environmental control of Vibrio spp. abundance and community structure in tropical waters. FEMS Microbiol Ecol 95(11).

Xu, D., Liu, S., Chen, Q. and Ni, J. 2017. Microbial community compositions in different functional zones of Carrousel oxidation ditch system for domestic wastewater treatment. AMB Express 7(1), 40.

Yan, T., Li, X.D., Tan, Z.J., Yu, R.C. and Zou, J.Z. 2022. Toxic effects, mechanisms, and ecological impacts of harmful algal blooms in China. Harmful Algae 111.

Yang, Y.Y. and Toor, G.S. 2018. Stormwater runoff driven phosphorus transport in an urban residential catchment: Implications for protecting water quality in urban watersheds. Sci Rep 8(1), 11681.

Yasir, M. 2020. Analysis of Microbial Communities and Pathogen Detection in Domestic Sewage Using Metagenomic Sequencing. Diversity 13(1).

Yuri, K., Nakata, K., Katae, H., Tsukamoto, T. and Hasegawa, A. 1999. Serotypes and virulence factors of Escherichia coli strains isolated from dogs and cats. J. Vet. Med. Sci. 61(1), 37-40.

Zhang, W., Bougouffa, S., Wang, Y., Lee, O.O., Yang, J., Chan, C., Song, X. and Qian, P.Y. 2014. Toward understanding the dynamics of microbial communities in an estuarine system. PLoS One 9(4), e94449.

Zhang, X., Lin, H., Wang, X. and Austin, B. 2018. Significance of Vibrio species in the marine organic carbon cycle—A review. Science China Earth Sciences 61(10), 1357-1368.

Zhang, X.X., Zhang, T., Zhang, M., Fang, H.H. and Cheng, S.P. 2009. Characterization and quantification of class 1 integrons and associated gene cassettes in sewage treatment plants. Appl Microbiol Biotechnol 82(6), 1169-1177.

Zhu, Y.G., Zhao, Y., Li, B., Huang, C.L., Zhang, S.Y., Yu, S., Chen, Y.S., Zhang, T., Gillings, M.R. and Su, J.Q. 2017. Continental-scale pollution of estuaries with antibiotic resistance genes. Nat Microbiol 2, 16270.